Damping System Designs using Nonlinear Frequency Analysis Approach

By

Pengfei Guo

THESIS

Submitted for the degree of

DOCTOR OF PHILOSOPHY

in the

Department of Automatic Control and Systems Engineering,

Faculty of Engineering, University of Sheffield

Feb, 2012

To My Parents

Mr. Bao-Rui Guo and Mrs. Rui-Xia Gu

Abstract

The main purpose of this thesis focuses on the investigation of the frequency domain analysis and design approaches for nonlinear damping systems. With the development of modern mechanical and civil engineering structures, the vibration control has become a more and more important problem for the structural system protection. As typical energy dissipation equipments for the structural vibration control purpose, damping devices have been designed and fitted in many modern structural systems. Traditional frequency domain design methods for linear damping devices have been widely studied by engineers and applied in engineering practice, where the system output frequency response is equal to the input spectrum multiplied by the system frequency response function.

Recently, nonlinear damping devices have received more and more attentions and been applied in practical engineering systems to overcome the limitations of linear damping devices in the system vibration control. The analysis and design of nonlinear systems, however, are far more complicated than the design of linear systems. The frequency domain design methods for linear systems cannot easily be extended to the nonlinear cases. Traditional frequency domain analysis and design methods for nonlinear systems involve complicated computations, and are, consequently, difficult to be applied in practice. Therefore, more effective frequency domain analysis and design approaches should be developed to facilitate the design of nonlinear damping devices and to satisfy the demand for better vibration performance in practical engineering structural systems. Motivated by this requirement, several new frequency domain analysis and design approaches have been proposed for the analysis of the performance and the design of the characteristic parameters of nonlinear viscous damping devices. The main contributions of the research work can be summarized as follows.

(1) Based on the Ritz-Galerkin method, a new method for the evaluation of the transmissibility of nonlinear SDOF viscously damped vibration systems under general harmonic excitations is derived. The effects of damping characteristic parameters on the system transmissibility are investigated. The results reveal that properly designed nonlinear fluid viscous dampers can produce more ideal vibration control over a wide frequency range.

(2) The Output Frequency Response Function (OFRF) is a concept recently proposed at Sheffield for the analysis and design of nonlinear systems in the frequency domain. Based on the OFRF, a frequency domain analysis and design approach has been developed to study the impact of additional nonlinear viscous damping devices on the vibration isolation behaviours of MDOF viscously damped vibration systems, and to design the characteristic parameters of additional damping devices for a desired system vibration performance.

(3) Based on the OFRF, a new concept called Vibration Power Loss Factor (VPLF) is proposed to evaluate the effects of additional fluid viscous dampers on the vibration control of structural systems subjected to general loading excitations. A novel VPLF and OFRF based approach is then proposed for the design of additional fluid viscous dampers to achieve a desired vibration performance when the structural systems are subject to general loading excitations. The advantages of using different types of additional fluid viscous dampers in structural systems for the vibration control purpose are also investigated.

(4) Using the Finite Element (FE) model analyses, the effectiveness of the application of the proposed OFRF and VPLF based frequency domain design approaches in the design of additional fluid viscous dampers for the vibration control in more complicated structural systems has been verified.

The frequency domain analysis and design approaches proposed in this thesis provide a significant basis and important guidelines for the analysis and design of a wide class of nonlinear viscously damped engineering structural systems. The results reveal the advantages of additional nonlinear viscous damping devices in the system vibration control and have considerable significance for the design of the damping characteristic parameters to achieve a desired system vibration performance.

Acknowledgements

I would like to express my most sincere gratitude to Dr. Zi-Qiang Lang, my supervisor, for his excellent supervision, constructive suggestions and encouragement in my research and writing. He has provided lots of support in numerous ways in my studying and living in Sheffield throughout the period of this project. I also want to express my sincere thankfulness to the research and work staff of the department for their kind help and valuable suggestions on my research.

I want to acknowledge for the scholarship from the Engineering and Physical Science Research Council (EPSRC) in the UK. This thesis would not have been conducted without the financial support.

I also love to acknowledge Dr. Zhi-Ke Peng for his great help and useful discussions and advices. Particular thanks to Dr. Hatim Laalej, Dr. Shu Wang, Dr. Ling-Zhong Guo, Dr. Yu-Zhu Guo, Xue-Yan Zhao, Jing-Jing Luo, Xi-Liang Zhang, Da-Zhi Jiang and all other friends in Sheffield for their great help.

Finally, I would like to dedicate this thesis to my parents for their love, encouragement and support.

Contents

List of Figures

List of Tables

List of Acronyms

AMD Active Mass Damper

AVD Active Viscous Damper

DVI Displacement Vibration Isolation

DVIS Displacement Vibration Isolation System

FE Finite Element

FEA Finite Element Analysis

FEM Finite Element Method

FRF Frequency Response Function

FT Fourier Transform

FVI Force Vibration Isolation

FVIS Force Vibration Isolation System

GFRF Generalized Frequency Response Function

MDOF Multi-Degree of Freedom

MIMO Multi-Input-Multi-Output

MR Magnetorheological

NDE Nonlinear Differential Equation

OFRF Output Frequency Response Function

SDOF Single Degree of Freedom

SISO Single-Input-Single-Output

TMD Tuned Mass Damper

TLCD Tuned Liquid Column Damper

Chapter 1

Introduction

1.1 Background

1.1.1 Damping system design

Vibration control of systems is a generic problem which is fundamental in vibration suppression, noise attenuation, and control system designs [1-4]. With the development of modern mechanical and civil engineering systems, the safety and reliability related issues have become more and more important. In order to reduce unwanted structural vibration to an acceptable level, many vibration control approaches have been studied and applied in practical mechanical and civil engineering systems. Traditional vibration control methods are to increase the structure stiffness by adding sub-structures and new materials or to increase the system mass in the original design. However, these methods increase the construction cost and change the frequency domain characteristics of original structural systems, so that, in some special cases, the system vibration may even become worse [5]. Comparatively, there is a more effective approach to improve structural system safety and reliability against strong excitations [6], which is to supplement vibration control devices having suitable dynamic characteristics into structural systems to suppress the vibration and dissipate the energy. Especially for the existing mechanical and civil engineering systems, where the extra sub-structures and new materials are difficult and even impossible to apply, additional vibration control devices are much easier to operate with lower construction cost. The application of additional vibration control devices can significantly improve structures' performance under seismic, wind, blast and

other types of loading excitations. Their effectiveness in vibration control and energy dissipation has been verified by many theoretical analyses and experimental tests [5].

As one of the most typical vibration control devices, damping devices are a kind of energy dissipation equipments and often installed inside mechanical and civil engineering structural systems for vibration control purpose. Because of great vibration control effect that damping devices can achieve, adding additional damping has received special attentions by engineers and played an important role in the design of modern vibration control systems.

In order to maximize energy dissipation and vibration control effects of damping devices in vibration systems, many different kinds of damping devices have been studied and applied in practical engineering applications, such as multi-storey buildings, long-span bridges, towers and vehicles, etc.. The commonly used damping devices can be classified into either active or passive damping devices. Active damping devices suppress the structural vibration by using an appropriate feedback control system, while passive damping devices suppress the structural vibration by the inherent energy dissipation characteristics of dampers. For examples, an active controlled tuned mass damper with an 800T steel ball was applied in the 101 storey Taipei Financial Centre to suppress the structural vibration induced by wind and seismic excitations [7]; The engineering designers installed two passive tuned liquid column dampers on the top of the One Wall Centre Hotel and tested the building’s vibrations induced by wind loading excitations. Their results revealed that additional damping devices are quite efficient in the vibration control and take up less space [8].

As one of the most commonly used passive damping devices, fluid viscous damper has significant advantages in the vibration control design of practical

engineering systems. It has been intensively studied and proved to be the most cost-effective and least space-intensive vibration control device. It has almost no effect on the original system's mass and stiffness and its effectiveness in vibration control and energy dissipation has been verified by a lot of theoretical studies and practical applications [9-12]. Because linear fluid viscous dampers have been shown to have some disadvantages and limitations in the vibration control system design, nonlinear fluid viscous dampers have been used to provide a better solution of vibration control in many practical engineering systems [3, 5, 13].

Damping design is one of the most significant and challenging problems in the modern mechanical and civil engineering system design [9, 12, 14]. However, the analysis and design of nonlinearly damped vibrating systems are generally difficult. This is because there are no adequate generic techniques for the nonlinear system analysis and design [15], An effective analysis and design methodology for nonlinear structural systems is yet to be developed.

1.1.2 Analysis and design of linear and nonlinear systems in the time and frequency domains

With appropriate mathematical models or function descriptions, the system studies can often be transformed into the investigation on the characteristics of system models [16], and the studies can be conducted in either the time or the frequency domain.

The time domain analysis is a natural analysis method for most practical systems. The input and output signals of systems are all physical variables changing with time. The state-space, differential and difference equations are extensively used as the time domain models of systems.

Besides the time domain analysis, there are also many transform domain analysis methods for system studies. The frequency domain analysis is a special case of transform domain methods where the Fourier transform is used to represent the systems' behaviours and characteristics by using the functions of frequency variables. The specifications and criteria for the system design are usually expressed by the frequency domain concepts such as, e.g., the system transmissibility and phase delay etc.. Compared with the time domain analysis, the frequency domain analysis can provide more physically meaningful insights into system dynamic behaviors such as the stability and resonance, etc. [17]. Consequently, extensive theoretical and applied research studies have been conducted on the system frequency domain analysis and design in system, control, and relevant subject areas [18, 19].

Linear systems have been intensively studied in both the time and frequency domains [17, 20-22]. For linear systems, it is possible to use the responses to a small set of inputs to predict the response to any possible input [23]. Linear systems' time-domain output to a general input can be numerically and theoretically calculated from the system model. Linear systems' output frequency response can be obtained by multiplying the input spectrum and the linear system's frequency response function, which is referred to as FRF [21]. This simple linear systems' frequency domain relationship analytically describes the effects of system properties on the output frequency response [24]. In the early days, researchers focused on the linear damping system designs [17, 20, 25] because linear system models in terms of differential and difference equations are easy to solve and most weakly nonlinear systems can be approximated by equivalent linear systems under certain conditions which is known as linearization [22, 26].

However, many practical engineering systems cannot easily be described by a simple linear model or mathematical function. The relationship between the

input and output spectrum of nonlinear systems is much more complicated. The nonlinearities in systems can make the output response sensitive to the initial conditions and computational errors, and can lead to complex phenomena such as chaos, bifurcation, harmonics and inter-modulation [27-30]. Conventional linear systems' analysis and design approaches in the time and frequency domains cannot be directly extended to nonlinear systems. In order to describe and analyze nonlinear systems, many studies have been conducted in the time domain with results relating to the Volterra series, NARMAX (Nonlinear AutoRegressive Moving Average with eXogenous input) models, neural networks and fuzzy systems. Many typical nonlinear system equations, such as Duffing equation and Van Der Pol equation, etc. [31, 32], have been studied. The transient and steady-state characteristics of nonlinear systems have been discussed by the time domain analysis approaches in many literatures [5, 28, 33-35] and significant progress towards understanding nonlinear systems' characteristics has been made.

The frequency domain characteristics of different nonlinear system mathematical models and function descriptions have also been widely studied, which involve NDE (Nonlinear Differential Equations), NARX (Nonlinear Auto-Regressive model with eXogenous input), TDDE (Time Delayed Differential Equations) and so on. In order to study the relationship between nonlinear systems' input spectrum and output frequency response [36], many nonlinear frequency domain analysis approaches have been proposed, such as describing function [3], perturbation and averaging methods [37], Ritz-Galerkin method [38], harmonic balance method [39] and GFRF (Generalized Frequency Response Function) concept [40]. The results provided important guidelines in the analysis and design of practical engineering systems. Recently, based on the Volterra series expression and GFRF concept of nonlinear systems, some researchers [41-43] focused on the study to extend the well known linear systems' frequency domain relationship to nonlinear systems [44]. By using

GFRF concept, the behaviours of a nonlinear system subjected to a general input can be studied through its GFRF expressions and output spectrum [16]. Many literatures have focused on the estimation and computation of the GFRFs of nonlinear systems from the system model parameters or input-output data. These results provide an important foundation for the frequency domain analysis and design of nonlinear systems.

Conventional nonlinear frequency domain analysis approaches involve a large amount of algebra and symbolic computations and are often difficult to be applied in practice. In order to tackle this problem, the OFRF (Output Frequency Response Function) concept was proposed in [24]. Focusing on the effects of the system's nonlinear characteristic parameters on the output frequency response, the OFRF concept extends the well known frequency domain input-output relationship of linear systems to nonlinear systems and provides an explicit analytical description for the relationship between the output frequency response and parameters that define system nonlinearity. The application of the OFRF concept can considerably facilitate the frequency domain analysis and design of nonlinear systems in engineering practice.

Although the studies on nonlinear systems have been carried out by researchers for several decades, many significant problems still remain unsolved, such as the stability analysis, parameters optimal design and sensitivity analysis. Nonlinear system analysis and design approaches are far from being fully developed in both theoretical studies and practical applications.

1.2 Research achievements

The main achievements of this thesis are to investigate the important issue of the application of nonlinear damping for the vibration control of mechanical and

civil engineering structural systems and to develop effective frequency domain analysis and design approaches for nonlinear damping devices. The studies focus on the analysis of the effects of nonlinear viscous damping on the system vibration response under both harmonic and general excitations and the design of damping characteristic parameters to achieve a desired system performance.

Although nonlinear fluid viscous dampers have been considered as a better solution for the vibration control purpose and some practical applications have been studied [11, 45, 46], the effects of fluid viscous dampers on the system frequency domain responses under different loading excitations have not received enough attention. The main issues involve how to evaluate the effects of fluid viscous dampers on the system output frequency response and how to design the damping characteristic parameters for a specific vibration control purpose. In order to answer these questions, the vibration transmissibility of SDOF nonlinear structural systems are theoretically evaluated for different fluid viscous dampers and under more general harmonic excitations. Based on the results, a nonlinear damping system design procedure is proposed to facilitate the design of nonlinear damping characteristic parameters for a desired vibration control performance. These studies further confirm the advantages of nonlinear fluid viscous dampers in vibration control and provide useful guidelines for the design of nonlinear fluid viscous dampers in practical engineering applications.

Obviously, the link between the output frequency response of a vibrating system and the characteristic parameters of dampers fitted in the system is important for the system analysis and design. Due to a lack of this link, conventional damping analysis and design approaches involve a large amount of complicated computations and are, therefore, difficult to be used in practice [5, 9, 47]. The OFRF concept was recently proposed in [24] to provide an analytical relationship between the system output frequency response and parameters which define the system nonlinearity. Motivated by this progress, the OFRF

expressions of viscously damped vibration systems are derived in the present study to represent the relationship between the system output frequency response and nonlinear viscous damping parameters. The results reveal, for the first time, an explicit analytical relationship between the system output frequency response and nonlinear damping characteristic parameters. This provides a really significant foundation for nonlinear damping system designs, which has never been available before.

Based on the OFRF concept, the analysis and design of nonlinear damping devices for structural systems subjected to harmonic or general loading excitations can be performed in the frequency domain. In practice, loading excitations can be classified into harmonic loadings such as those induced by rotary machines and general excitations such as wind loadings. Motivated by the need to deal with different loading excitations in different practical applications, the criteria and procedures for the design of nonlinear damping devices for structural systems subject to harmonic and general excitations are developed, respectively, where the OFRF concept is applied in the design to achieve a desired vibration control performance. In order to further verify the effectiveness of the new nonlinear damping analysis and design approaches, the studies are also extended to more complicated situations where the Finite Element (FE) models are used to represent the structural systems under different loading excitations, such as earthquake and wind loading. These results have significant implications for the analysis and design of nonlinear damping devices for the vibration control of structural systems in a wide range of practical applications.

1.3Layout of this thesis

This thesis consists of eight chapters. Chapter 1 is the introductory chapter

which shows the background, research achievements and layout of this thesis. Chapter 2 introduces the commonly used vibration control approaches and typical damping devices in mechanical and civil engineering systems. Chapter 3 introduces the time and frequency domain representations of linear and nonlinear systems and reviews the development of the nonlinear system analysis in the frequency domain. The OFRF concept is also introduced in detail in Chapter 3 as the theoretical foundation of the studies in this thesis. Chapters 4-7 describe the main work of the present studies on the damping system design using nonlinear frequency analysis approach. Finally in Chapter 8, the results introduced in previous chapters are summarized and suggestions for the further research studies are proposed. In the following, a more detailed introduction of what is presented in Chapters 2-7 of this thesis is provided.

Chapter 2 introduces the commonly used vibration control approaches, which include active and passive damping devices. The advantages and disadvantages of typical damping devices in vibration control of mechanical and civil engineering systems are discussed. As the most cost-effective and least space-intensive vibration control devices, fluid viscous dampers have significant advantages in vibration control and energy dissipation. Moreover, compared with linear fluid viscous damper, nonlinear fluid viscous damper has been considered as a better solution in the vibration control of practical engineering systems.

Chapter 3 firstly introduces the time and frequency domain representations of linear and nonlinear systems. Then the commonly used nonlinear system frequency domain analysis approaches are reviewed and the GFRF concept is discussed in details. Finally, the important OFRF concept, which reveals an explicit analytical relationship between the nonlinear system characteristic parameters and the system output frequency response is introduced as the theoretical foundation of many studies in this thesis.

In **Chapter 4**, focusing on different types of viscous damping and loading conditions, a general mathematical model is firstly derived for SDOF viscously damped vibration isolation systems subject to a harmonic excitation with amplitude proportional to the driving frequency raised to an arbitrary power. Then the Ritz-Galerkin method is applied to theoretically evaluate the system displacement and force transmissibility and determine the effects of nonlinear viscous damping on the system vibration isolation. The results reveal that the Ritz-Galerkin method based solutions have an excellent agreement with numerical integration solutions using Runge-Kutta method. After that, a three-step design procedure is proposed to facilitate the design of nonlinear damping characteristic parameters for a desired system vibration isolation performance. Two case studies are finally given to demonstrate how to implement the proposed design procedure in practical applications.

Chapter 5 extends the OFRF concept to the cases of nonlinearly damped vibration systems described by an antisymmetric differential equation model, and reveals an explicit polynomial relationship between the system output frequency response and the nonlinear damping coefficient and exponent. The transmissibility of the SDOF and MDOF displacement vibration isolation system (DVIS) and force vibration isolation system (FVIS) with fitted nonlinear fluid viscous dampers are analyzed, respectively, to show the effects of nonlinear fluid viscous dampers on the system vibration isolation under harmonic loading conditions. The comparisons between numerical simulation results and the OFRF based estimates show that the OFRF concept can be used as a powerful frequency analysis approach to significantly facilitate the design of damping parameters of additional nonlinear fluid viscous dampers to achieve a desired vibration performance. A case study is provided to demonstrate how to apply an OFRF based four-step procedure to conduct nonlinear fluid viscous damper designs in practice.

Chapter 6 first proposes a concept called Vibration Power Loss Factor (VPLF) to evaluate the vibration control effects of additionally fitted fluid viscous dampers on civil structures subject to seismic and wind loading excitations. Based on the OFRF concept, an explicit polynomial relationship between the VPLF of civil structural systems and the damping coefficient of additionally fitted nonlinear fluid viscous dampers is then derived to facilitate the damper design. After that, the design idea is applied to the design of additional damping devices for a 7-Storey civil building structure subject to seismic and wind loading excitations respectively. The structural vibration responses under different loading excitations are then investigated to show the advantages and disadvantages of the application of different types of fluid viscous dampers in improving the structural vibration performance.

In **Chapter 7**, the OFRF concept is firstly applied to estimate the displacement and force vibration transmissibility of the FE models of multi-storey civil structures under harmonic excitations. The results demonstrate the effectiveness of the use of the OFRF based approach in the analysis of more complicated engineering structural systems. Then the OFRF approach and the VPLF concept are used for the design of additional viscous damping devices for a German offshore wind energy research platform based on the platform's FE model. Wind loading excitations are considered in the design to determine the damping coefficient of additional nonlinear viscous damping devices and their installation locations along the structure for vibration control purpose. The results demonstrate the effectiveness of the proposed design approaches and reveal that, compared with linear viscous damping devices, equivalent nonlinear viscous damping devices can achieve the same vibration control under the loading condition considered in the design but much better vibration control under the loading conditions which are either milder or severer than the considered design condition.

Finally, in **Chapter 8**, main conclusions reached and contributions achieved by the studies in this thesis are summarized. Suggestions for the further research work and potential application areas are also proposed.

Chapter 2

Damping Systems Design

2.1 Vibration control using damping devices

Vibration, which refers to the system oscillations about an equilibrium point, is a common physical phenomenon in practical mechanical and civil engineering systems. Sometimes, vibration is useful and some vibration related industrial productions have been designed, which include, for example, vibratory plate compactors and vibrating griddles. But sometimes, vibration is harmful and even dangerous for the safety of engineering systems and structures. These cases include, for example, the motions of bridges and buildings in earthquakes or strong winds, and the shaking of washing machines [48].

With the development of modern mechanical and civil engineering systems, the safety and reliability related issues have become more and more important, especially when engineering systems and structures are working in some extreme loading conditions such as in offshore wind farms and high-speed rotating machineries. Vibrations caused by internal or external excitations have a potential threat on not only engineering systems' normal operations but also on human lives. The tragic consequences of recent earthquakes in China (2008), Haiti (2010), Chile (2010) and New Zealand (2011) have shown the tremendous importance of vibration control for the protection of infrastructures, such as buildings and bridges etc..

In order to suppress unwanted vibrations to an acceptable level, many traditional vibration control methods have been studied and applied in engineering system

designs. The structural engineers often focus their efforts on the designs of structural stiffness and mass to suppress vibrations and protect structural systems [49]. But these methods can increase the construction cost and change the frequency domain characteristics of the original structural systems, so that, in some special cases, the vibration may even become worse [5]. Recently, there has been a trend towards utilizing supplemental control algorithms and vibration isolators to improve the structural systems' safety and reliability against strong loading excitations [6]. This method inserts vibration control devices having suitable dynamic characteristics into the structural systems requiring protection [50]. Compared with the traditional stiffness-and-mass design methodology, the application of additional vibration isolators has been considered to be a more effective method for the vibration control purpose. The effects of this method on the vibration energy dissipation and vibration control have been verified by many theoretical analyses and experimental tests [5].

Damping is a phenomenon by which mechanical energy is dissipated from system dynamic actions [51]. It is a typical vibration control method, which enables practical vibration systems to achieve optimal dynamic performance when subjected to seismic, wind, blast or other types of transient shocks and disturbances [10]. Damping devices are a kind of energy dissipation equipments, which are often installed inside mechanical and civil engineering structural systems such as buildings, towers and bridges etc. for vibration control purpose. They are often used as replaceable/disposable components, which are added to engineering systems to damp out the mechanical energy induced by loading excitations [12]. In modern structural system designs, damping devices have played an important role in mechanical and civil engineering applications [52]. The knowledge about damping and damping devices is very important in the analysis and design of complex structural systems [51].

The damping devices design has received special attentions [5, 10, 46, 53]

because of the great performance that damping devices can achieve in vibration control and energy dissipation. The issue of vibration control using damping devices has become one of the most challenging problems faced by technical analysts and engineering designers [49], and has significant implications for the engineering design of vibration systems in a wide range of practical applications.

2.2 Damping based vibration control approaches

In order to maximize energy dissipative properties and vibration control effects of damping devices in vibration systems, many different kinds of damping devices have been studied and applied in practical engineering applications to improve systems' dynamic performance. The corresponding optimal design approaches for these damping systems have also be proposed [5]. The adoption of supplemental damping devices offers an important way to improve systems' dynamic performance against unacceptable vibrations. The commonly used damping devices can be classified into two categories of active and passive damping devices.

2.2.1 Active damping devices

Based on the feedback control theory, active damping devices dissipate the vibration energy of systems using additional actuators [54], which act based on the displacements, velocities, or accelerations, etc. measured by corresponding sensors from the vibrating systems. Based on the sensor measurements, a closed loop feedback control approach is applied to drive the actuators to reduce the system vibration as required [54, 55]. An active damping device requires fast sensing equipment, stable control algorithm and responsive actuator technology [56]. According to whether the damping devices provide additional energy into

systems, practical active damping devices can be classified as fully active and semi-active damping devices. Fully active damping devices exert an independent force to improve the system characteristics and semi-active damping devices only change the damping characteristic parameters of the devices. Typical fully active damping devices include Active Mass Damper (AMD) [56], parts of Active Viscous Dampers (AVD) [57] and so on; Typical semi-active damping devices include parts of Active Viscous Dampers (AVD) [57], Magnetorheological (MR) Damper [6] and so on.

AMD is a typical active mass damper containing a lumped mass, a spring, and a feedback control circuit which usually consists of a piezoelectric accelerometer, a controller, and an electromagnetic transducer as the actuator. The accelerations of the system vibrations are measured by additional piezoelectric accelerometer; the controller uses a control algorithm to generate a feedback control force to counter the system vibrations. The advantage of AMD is that it just needs an appropriate additional actuator and, apart from the weight of the actuator, doesn’t induce any major intrusion into the controlled structural system.

Different from AMD, AVD generates the feedback force in the form of damping force, which means that it depends on the relative velocity of vibrating systems and it can be used as either the fully active or semi-active damping devices. The active viscous dampers usually generate the damping force by utilizing the viscous effect of viscous fluids to dissipate the vibration energy. This method has little effect on the system mass and stiffness, but needs complicated control algorithms and accurate measurements in practical applications.

MR damper is a damper filled with MR fluid, which is usually controlled by an electromagnet field. MR damper has many attractive features, including high yield strength, low viscosity and stable hysteretic behaviour over a broad temperature range. Compared with other kinds of active damping devices, MR

damper provides a convenient and effective method to generate the desired resisting force by a magnetic control. Moreover, MR damper can become a passive damping device and still dissipate vibration energy even when the control hardware is broken down.

Although many active damping devices and corresponding control theories have been successfully applied in practical engineering systems to suppress vibrations, many significant challenges have to be addressed before active damping controls can gain general acceptance in industry. The main challenges include the costs, system maintenance, power consumption, and reliability and robustness in different loading conditions [6].

2.2.2 Passive damping devices

Different from active damping devices, passive damping devices dissipate the vibration energy by their inherent damping characteristics without needing sensors, external power sources or actuators. So they need less construction and maintenance cost and are easier to operate in the mechanical and civil engineering systems. Some typical passive damping devices include Base Isolation [58, 59], Tuned Mass Damper (TMD) [60, 61], Tuned Liquid Column Damper (TLCD) [62, 63], Viscous Damper [64-66], Viscoelastic Damper [67], Metallic Damper [68] and so on.

2.2.2.1 Base Isolation

Base isolation is one of the most powerful approaches in the earthquake engineering pertaining to the passive structural vibration control technologies. It is usually used to reinforce structural systems to survive from the seismic destruction. Proper initial designs and subsequent modifications are needed to

achieve this objective. In the design for base isolation, additional devices are often fitted between a structural system to be protected, and the shaking foundation. The objective is to reduce the system fundamental frequency and absorb the vibration energy to protect the structural integrity [69]. Most base isolation devices utilize the friction effect and deformation of rubber or metal materials to isolate the protected structural systems from vibration sources. Because this technique is usually applied in civil engineering systems such as civil buildings and bridges to improve these systems' dynamic performance under seismic excitations, it is also known as seismic isolation. The design of base isolation, including various types of energy absorbing materials to achieve energy dissipation, has been the main subject of many studies [5]. With the development of the base isolation technologies, many different types of base isolation devices have been studied and applied in practical applications, such as the lead rubber bearing, high damping rubber bearing and friction pendulum bearing as shown in Fig.2.1(a)-(c). However, some inherent problems in the base isolation methods limit their wide applications in practical engineering systems. For examples, the lead core in the bearing is toxic for the environment; the material ageing and abrasion of the rubber and metal in the bearing make the maintenance of these base isolation devices important; base isolation method should be considered in the system design stage and the construction cost is significantly high when this technology is applied in existing mechanical or civil engineering systems.

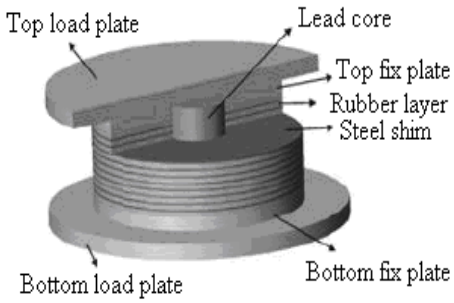

(a) Lead rubber bearing

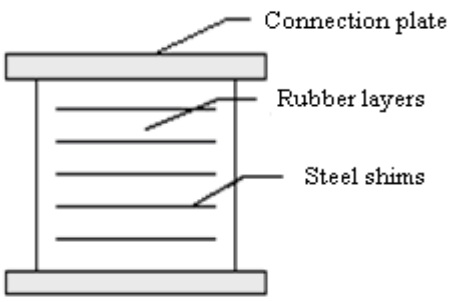

(b) High damping rubber bearing

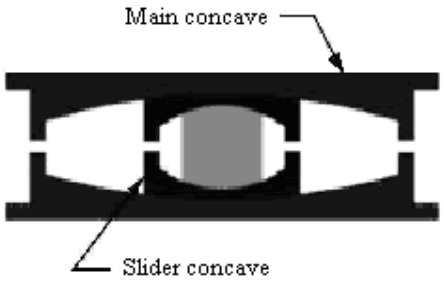

(c) Friction pendulum bearing

Fig.2.1 Base isolation devices [59]

The applications of base isolation devices in the foundation of mechanical and civil engineering systems as a mean of seismic design have attracted considerable attentions in recent years [58]. Many numerical and experimental simulations and theoretical studies have been reported in literatures [58, 59]. In order to study the effectiveness of different base isolation devices on a simplified SDOF vibration system, Su et al. [58] evaluated the system vibration induced by two earthquake records and compared the peak displacement in a variety of loading conditions. Their results revealed that, under appropriate design, most base isolation devices can significantly reduce the effects of the earthquake excitations on the system vibration. Moreover, a new design procedure for a friction base isolator was developed and its effectiveness in practical applications was also studied; Abrishambaf and Ozay [59] assessed the effects of several types of bases isolation devices on the seismic protection of 3, 6 and 9-storey buildings. Through comparing the transmitted acceleration and horizontal displacement of the vibration systems, the optimal designs of different base isolators were studied in order to reduce the construction cost of civil buildings; Kelly [70] reviewed the development history of base isolation approaches and summarized their applications in practical engineering systems. Focusing on the vibration isolation of civil buildings and bridges subjected to earthquakes, several system vibration simulations were provided to show the advantages and disadvantages of these base isolation devices in the vibration control and energy dissipation.

2.2.2.2 Tuned Mass Damper (TMD)

TMD is a passive vibration control approach which attaches an additional mass m_d to a practical vibration system via spring and damping devices as shown in Fig.2.2. The vibration energy of the original system is absorbed and dissipated by the attached mass, spring and damper. By tuning the natural frequency of the additional mass-spring-damper system to close to that of the original vibration system, the frequency domain characteristic of the improved vibration system will be obviously changed: the single peak of the original vibration system without TMD at the resonant frequency divides into two peaks at two nearby frequencies and the original peak is tuned approximately to near zero as shown in Fig.2.3, where the parameters ξ are in direct proportion to the damping coefficient c_d in TMD. TMD can provide good vibration control effect when the motion of the vibration system is governed by the fundamental mode to which the TMD is tuned [71]. A typical practical example is the TMD system applied in the Taipei Financial Centre to reduce the motions of the building induced by wind loadings as shown in Fig. 2.4. The main design problem of TMD is to optimize the parameters of the mass, spring and damper for the vibration system in different loading conditions. Although TMD has been widely applied in many practical engineering branches, such as seismic protection of civil buildings, offshore industry and railway projects, the adoption of TMD in the structures will obviously increase these systems' mass [72] and the two peaks phenomenon indicates that TMD becomes not effective in reducing the vibration in non-resonant frequency regions and, on the contrary, it may enhance the vibration over these frequency ranges [71]. Compared with other passive vibration control methods, TMD requires more physical installation space and is more expensive to operate.

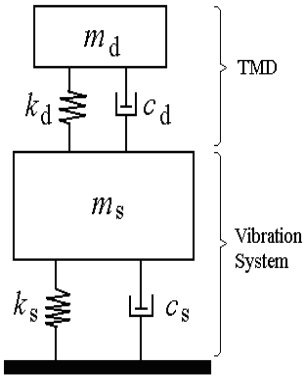

Fig.2.2 SDOF vibration system and the additional TMD [73]

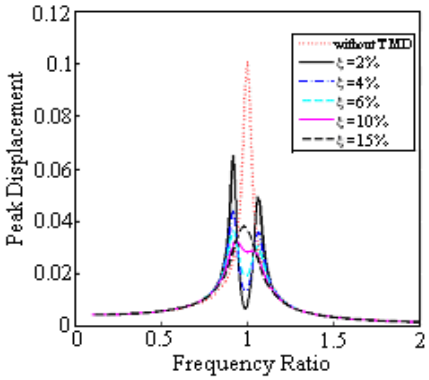

Fig.2.3 Peak displacement induced by unit sinusoidal base excitation with and without TMD [71]

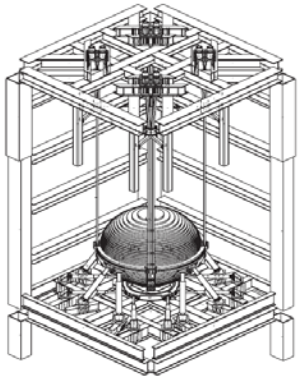

Fig.2.4 Schematic of the TMD system in Taipei Financial Centre [74]

After the pioneering work on the optimal design of TMD for a SDOF mass-spring-damper system by Den Hartog in 1956 [75], there has been a lot of subsequent theoretical studies and practical applications in the system vibration control using TMD approach. Kitamura et al. [76] reviewed the design and vibration analysis of a steel tower with TMD and studied the effects of the additional TMD on the structure vibration in earthquakes; Rana and Soong [77] summarized the effects of TMD parameters on the performance of vibration control and studied the vibration control of a general MDOF system with TMD using steady-state and time-history analysis methods; Lin et al. [78] proposed a new TMD model to suppress both the vertical and torsional vibration responses of long-span bridges and to enhance the structures' stability under wind loadings. Based on their parametric analysis, the design procedure of the new TMD for wind-excited bridges was also proposed; Lee et al. [79] developed an optimal

design theory for the additional TMD in a MDOF vibration system. The optimal design parameters of TMD were systematically determined by an efficient numerical procedure which minimizes the mean square value of the structural responses in the frequency domain; Using the numerical searching technique, Bakre and Jangid [73] proposed an explicit formula to optimize the TMD parameters to suppress the system vibration under various combinations of loadings, which can be readily used in the practical applications.

2.2.2.3 Tuned Liquid Column Damper (TLCD)

TLCD replaces the attached lumped mass in TMD by water or other liquids in a tube-like container tank which is specifically designed and tuned to the natural frequency of a vibration system [80] as shown in Fig.2.5. The vibration energy of the structural system with a fitted TLCD device is dissipated by the moving liquids and the turbulent damping force induced by the built-in orifice plate in TLCD. The geometry of the liquid container is determined by theoretical analysis to give a desired natural frequency of oscillation of the liquid in TLCD. A sluice gate or other similar device is often used to dissipate the energy in the moving liquid. The frequency domain characteristic of vibration systems with a fitted TLCD, which is shown in Fig.2.6, is similar to what can be achieved by using TMD approach, which is shown in Fig.2.3. Fig.2.7 shows the 3D rendering of the Comcast Centre’s TLCD tank, which is the largest TLCD in the world with 1300 tons water. Compared with TMD approach, TLCD method increases less additional mass and is more efficient in heavy loading conditions [80]. Moreover, TLCD approach is easy to accommodate in practical structures even in retrofit of existing buildings and needs little maintenance. Therefore, It’s a preferable energy absorbing method for the low frequency vibration control of high-rise buildings, long span bridges and offshore structures subjected to earthquakes, wind and waves [81].

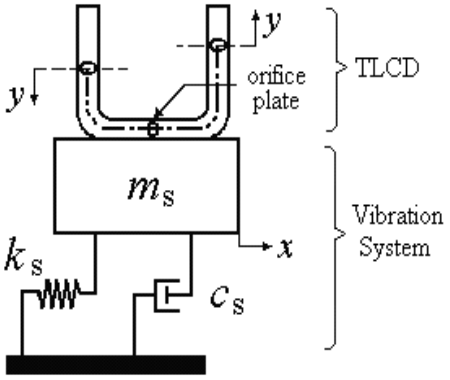

Fig.2.5 Model of SDOF vibration system and the additional TLCD [82]

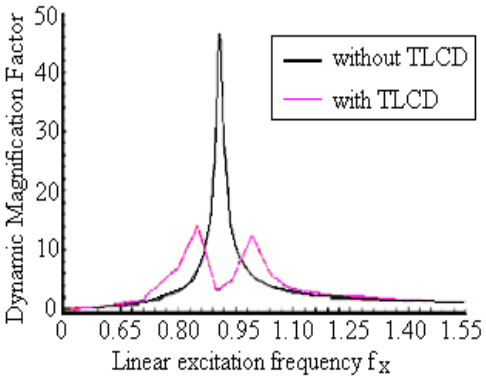

Fig.2.6 Dynamic magnification factor under harmonic excitations [81]

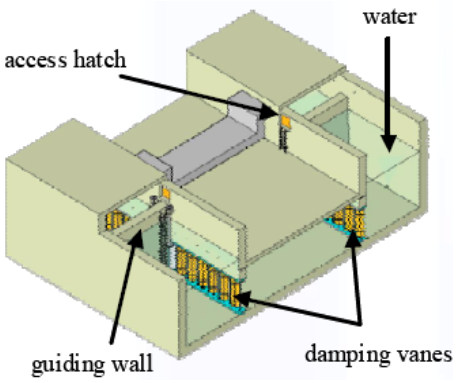

Fig.2.7 3D rendering of the Comcast Centre's TLCD tank

TLCD was firstly proposed by Sakai et al. [1] as a means of suppressing vibrations within structures. Up to now, it has been implemented in many civil buildings such as Hotel Cosima [83], Hyatt Hotel and Ichida Building in Osaka [84]. Its effectiveness on the vibration control of practical engineering structures has been studied by many researchers [81, 85, 86]. Vandiver and Mitome [85] investigated the effects of liquid storage tanks containing glycol on the vibration of offshore structures and concluded that the appropriate selection of the geometry of storage tanks would result in obvious suppression of dynamic response at the fundamental flexural natural frequency of structures; Xu and Kwok [86] studied the applications of TLCD in reducing the along-wind response of tall structures. By numerical examples, the effectiveness of TLCD on the vibration control was compared with the traditional TMD approach and the advantages of TLCD were also summarized; Reiterer and Ziegler [81]

investigated the vibration control effects of different parameters of TLCD on a SDOF shear frame under combined horizontal and vertical excitations and studied the stability of TLCD's dynamic performance; Colwell and Basu [80] simulated the structural responses of an offshore wind turbine with a TLCD under wind and wave loading excitations. The fatigue analysis was also carried out to show the effect of TLCD on enhancing the fatigue life and reducing bending moments of offshore structures.

2.2.2.4 Viscous Damper

Viscous damping devices having appropriate dynamic characteristics are usually installed in vibration systems to dissipate the energy and protect the system safety under different loading conditions. Their applications in the mechanical and civil engineering systems have a long history and they have been widely recognized as an effective means of reducing the effects of wind, earthquakes and other loadings on the system vibration. As one of the most commonly used viscous damping devices, a typical viscous damper is shown in Fig.2.8. Fig.2.9 shows a practical application of viscous dampers installed in a parking garage in USA to protect the structure as a seismic strengthening method. Viscous damper suppresses the system vibration by its damping force resisting on the relative motion between different components of the system where the damper is installed. The system's vibration kinetic energy is dissipated by transforming to thermal energy inside the damper. Compared with other passive vibration control approaches, viscous dampers in vibration systems are easier to install and have almost no effect on the system mass and stiffness [87]. Moreover, the construction cost for structural vibration control can be significantly reduced by applying reasonably designed viscous dampers.

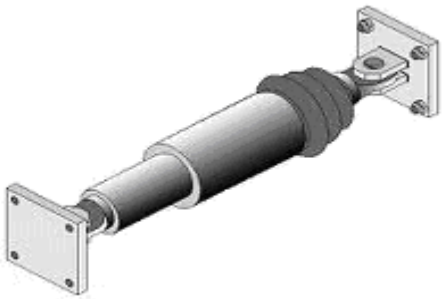

Fig.2.8 A typical viscous damper [88]

Fig.2.9 Viscous dampers in a parking garage [89]

Originated from military and aerospace applications, viscous dampers have been widely used in a lot of practical vibration systems to protect structures against wind, blast and earthquakes excitations [9]. The adoption of supplemental viscous dampers offers an important way to upgrade structures' dynamic characteristic and suppress the vibration. Many theoretical and experimental studies have been performed to show the contribution of viscous dampers on the system vibration control. Symans and Constantinou [65] discussed the practical applications of several kinds of viscous dampers in seismic protections of civil buildings and bridges. They demonstrated the effectiveness of viscous dampers in absorbing seismic energy through experimental simulations of a 3-storey building frame; Ravindra and Mallik [90-92] studied the effects of different kinds of viscous dampers on the performance of vibration systems under harmonic loadings. They observed bifurcations, chaos and strange attractors due to the presence of nonlinearity in springs and dampers in vibration isolators. Their results concluded that suitable designs of nonlinear viscous dampers could entirely eliminate the sub-harmonics and chaotic motions and thus provided an effective passive control method to suppress various instabilities occurring in nonlinear vibration systems; In order to evaluate the damping effect achieved by additional viscous dampers on the vibration of civil structures, Occhiuzzi [12] proposed a numerical methodology to calculate modal damping ratios of vibration structures with viscous dampers and applied it to analyze many practical engineering applications of supplemental viscous dampers in the protection of civil buildings.

2.2.2.5 Viscoelastic Damper

Similar to viscous dampers, viscoelastic dampers utilize both viscous and elastic behaviours of viscoelastic materials such as rubber to suppress the system vibration and dissipate the energy. Fig.2.10 shows the diagram of a typical viscoelastic damper. In this damper, the viscoelastic material is filled between layers of steel to reduce the vibration between two ends of the damper. A practical viscoelastic damper installed in a civil building for the seismic protection is shown in Fig.2.11. Different from viscous dampers, viscoelastic dampers' dynamic characteristics are influenced by many parameters such as temperature, dynamic strain rate, static pre-load and so on. Although viscoelastic dampers have been installed in some civil buildings to reduce the drifts between floors induced by wind or earthquakes, their vibration control effects on the mechanical and civil engineering systems are still not satisfactory because of their sensitiveness to the environment and strict dependence on the viscoelastic materials.

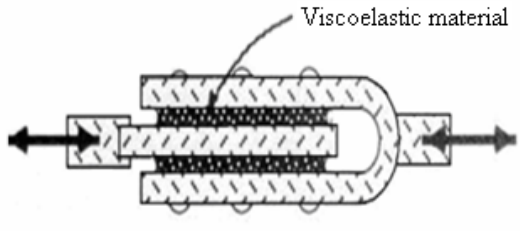

Fig.2.10Diagram of viscoelastic damper[93] Fig.2.11Viscoelastic damper in a civil building [94]

Since the first installation in World Trade Centre in USA in 1969, viscoelastic dampers have been successfully incorporated in a number of tall buildings as viable energy dissipating devices to suppress wind- and earthquake-induced motion of building structures [95]. With the development of material science, viscoelastic dampers have received more and more attentions and their effectiveness on vibration control have been demonstrated by both analytical

and experimental studies. Tsai and Lee [96] considered the effect of environment temperature on viscoelastic dampers' dynamic characteristic. They investigated the energy absorbing capacities of different viscoelastic dampers and their vibration control effects on the structures during earthquakes. Focusing on the vibration behaviour of a 10-storey building equipped with viscoelastic dampers under seismic excitations, both analytical and experimental studies were performed to show the effectiveness of viscoelastic dampers in high-rise buildings on improving their seismic resistance; Samali and Kwok [95] reviewed the successful applications of viscoelastic dampers in a number of major tall buildings in USA and Japan and summarized the research results. Some guidelines for the optimal design of viscoelastic dampers in the practical engineering applications were also provided; Chang et al. [97] studied the seismic behaviour of a viscoelastically damped structure under mild and strong earthquake excitations at room temperature. Analytical studies were carried out to predict the equivalent damping ratios and the seismic response of the structure. Numerical and experimental results revealed that viscoelastic dampers were effective in attenuating structural seismic response.

2.2.2.6 Metallic Damper

Metallic damper utilizes the inelastic bending or torsion deformation of metal material to absorb mechanical energy as shown in Fig.2.12. Fig.2.13 shows a experimental test for investigating the vibration control effects of metallic dampers on a two-storey platform. The adoption of metallic dampers can also help to increase the stiffness of structures to reduce the vibration. It's usually applied in the seismic retrofit and reinforce of structures which are found to be deficient. Metallic dampers are easy to manufacture and integrate into practical structures. They have shown stable energy absorbing property in earthquakes and other loading excitations, moreover almost no environmental factors can

affect their performance [98]. Because metallic dampers can not repeatedly perform their effects on system vibration control in heavy loading conditions, they should be replaced after earthquake or according to the maintenance plan.

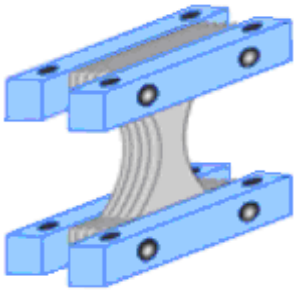

Fig.2.12 X-shaped Metallic damper [99]

Fig.2.13 Metallic damper in an experimental platform [68]

Using steel plates for absorbing and dissipating vibration energy was first used exclusively in nuclear installation [100]. Because of its effectiveness on the energy dissipation in vibration systems, it has been more and more widely used in the vibration control designs of new generation of mechanical and civil engineering systems. Many experimental tests and analytical analysis have been conducted by researchers to study the energy absorbing capabilities of different shapes of metallic dampers. Stiemer et al. [101] tested the vibration control effect of X-shaped metallic dampers on a 3-storey building under seismic excitations. Their test results confirmed that the metallic dampers were extremely effective in reducing pipe stresses in regions of ductile support; Li et al. [68] performed the quasi-static and shaking-table tests for the single round-hole metallic damper and double X-shape metallic damper. Their results revealed that these metallic dampers not only provided additional structural stiffness, but also had good seismic energy dissipation capabilities; Chen and Eads [102] summarized the commonly used metallic dampers and tested their fatigue properties under irregular loading and earthquake loading. Based on these results, the seismic retrofit and reinforce design procedure with metallic

dampers was outlined and applied into the seismic protection of an existing highway bridge.

2.3 Fluid viscous damper for vibration systems

As one of the most commonly used passive damping devices, fluid viscous damper was firstly utilized to attenuate the recoil of 75mm French artillery rifle in 1897 [11]. It became widespread within armies and navies of most countries in the 1900-1945 periods, however it was not widely publicized because of its secretive nature [87]. At that time, most fluid viscous dampers operated by the viscous effect between metal plates immerged in the fluid inside the damper as shown in Fig.2.14. Because the damping effects depended on the viscosity of the fluid, which changed significantly with temperature, these early fluid viscous dampers were sensitive to the working environment and temperature. With the end of the Cold War in the late 1980's, the fully developed viscous damping technology was declassified and became available for the general public [10]. The high capacity fluid viscous dampers found a lot of commercial applications in civil buildings and bridges subjected to seismic and wind excitations [11]. In 1994, a modern fluid viscous damper was proposed by Soong and Constantinou [103] and widely applied in the protection of mechanical and civil engineering structures as shown in Fig.2.15. This kind of fluid viscous dampers dissipated the vibration energy by forcing the compressible silicone fluid to flow through orifices and causing a pressure difference to produce the resistance force. This change of the damping principle of modern fluid viscous dampers significantly reduced the damping devices' volume and improved their stability in complex working environment, which accelerated the development and applications of fluid viscous dampers in practical mechanical and civil engineering systems.

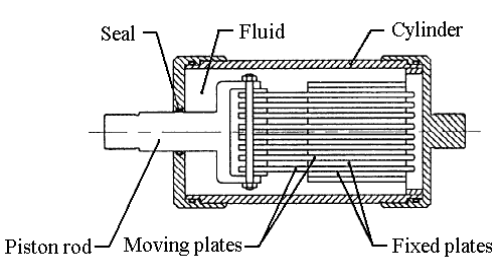

Fig.2.14 Early fluid viscous damper [103]

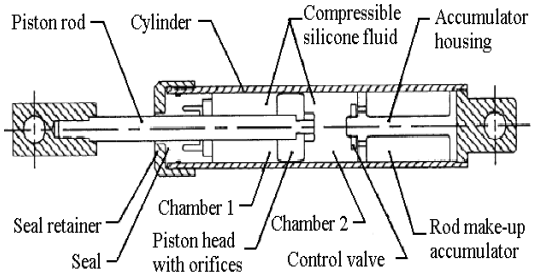

Fig.2.15 Modern fluid viscous damper [103]

Up to now, through a lot of theoretical and experimental studies, fluid viscous dampers have been proved to be the most cost-effective and least space-intensive in the system vibration control design [10]. Compared with other types of vibration control devices, fluid viscous dampers have several inherent and significant advantages [87]:

1. The damping force is essentially out of phase with primary bending and shear stresses in a structure, which implies that a fluid viscous damper can be used to reduce both internal shear forces and deflections in the structure.
2. Fluid viscous dampers are self-contained, no auxiliary equipment or power is required.
3. Modern fluid viscous dampers operate at a fluid pressure level of significant magnitude, which makes the dampers small, compact and easy to install.
4. Fluid viscous dampers are generally less expensive, easier to install and less maintain than other passive damping devices, which are helpful to reduce the overall cost of a practical structure.
5. The effectiveness of passive fluid viscous dampers has been proved by the test of time, with over 100 years of large scale successful use, in the most severe environments by the military and aerospace industries.

Fluid viscous dampers for the protection of commercial and public structures

under seismic and wind loadings were widely used since 1990s and witnessed significant developments due to pressing demands for the protection of structural installations, nuclear reactors, mechanical components, and sensitive instruments from earthquake ground motion, shocks and impact loads [5]. The engineers and physicists have also developed many different types of installation modes for fluid viscous damping devices to satisfy these demands as shown in Fig.2.16.

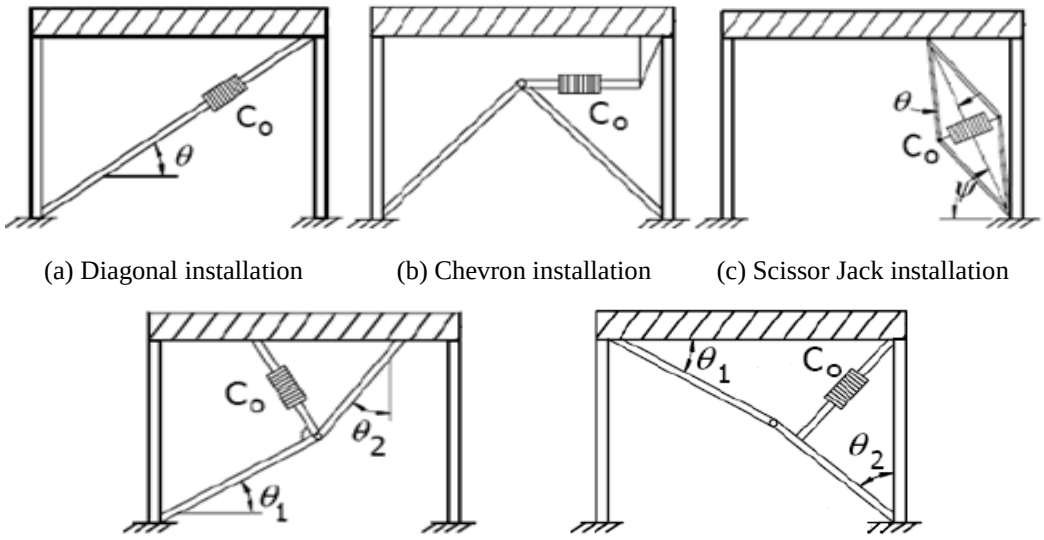

(a) Diagonal installation (b) Chevron installation (c) Scissor Jack installation

(d) Upper toggle installation (e) Reverse toggle installation

Fig.2.16 Typical installation modes of fluid viscous damping devices [104]

In practical engineering applications, the Arrowhead Regional Medical Centre in USA was the first application of fluid viscous dampers in the seismic protection field. The five buildings of this complex used a total of 186 dampers, which were installed in systems parallel with rubber base isolation bearings to dissipate the seismic energy [10]. After the Loma Prieta earthquake, the California department of transportation used considerable full scale nonlinear fluid viscous dampers to control the deformation of the suspended trusses on Vincent Thomas Bridge [105]. In the Rion-Antirion Bridge project in Greece, nonlinear fluid viscous dampers with lower-than-one power damping characteristic parameter were installed to reduce the deformation induced by the seismic ground motion [106]. Many researchers and engineers have also done a lot of studies and

presented many results. McNamara et al. [107] focused on the vibration isolation of a 39-storey office building subjected to wind loadings and compared the effectiveness of different vibration isolation devices. Finally, the fluid viscous dampers were proved to be the most cost-effective and least space-intensive on the office building and were installed in the form of diagonal and toggle braces in several floors. Their results revealed that the fluid viscous dampers could give the building additional inherent damping and improve the building's dynamic behaviours from 20% to 30%. Hwang and Tseng [14] proposed a new design procedure for supplemental fluid viscous dampers in practical bridge structures and applied it to the vibration control design of a three-span bridge under seismic excitations. In 2008, LORD Corporation adopted several fluid viscous dampers in a typical wind turbine to reduce the structure vibration, the results revealed that these additional fluid viscous dampers can bleed off more than 50% of the wind and wave loadings [108].

In theoretical analysis, the resistive damping force F_{D} produced by a pure fluid viscous damper can be described by $F_{\mathrm{D}} = C_a \left|\dot{u}_r\right|^a \operatorname{sign}(\dot{u}_r)$, where C_a and a are the damping coefficient and exponent, $\dot{u}_r$ is the relative velocity between the two ends of the damper [46, 65, 103]. The relationship between the damping force and the relative velocity of typical fluid viscous dampers under different values of a is shown in Fig.2.17. When the damping exponent $a = 1$, the damper's dynamic characteristic is linear, otherwise the damper's dynamic characteristic is nonlinear. Because a fluid viscous damper's damping force acts in the opposite direction to that of the relative velocity between two ends of the damper itself, it is an ideal energy dissipation device in the structural vibration control [46].

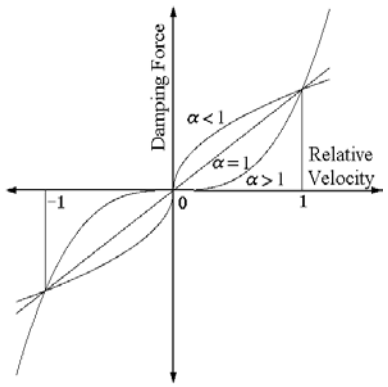

Fig.2.17 Damping characteristic of fluid viscous dampers under different values of exponent a [46]

The viscous damping coefficient and exponent can be modified by filling with different viscous fluids and modifying the configuration of the chambers inside the damper. So the practical fluid viscous dampers' dynamic characteristic can be either linear or nonlinear according to the design requirement. The conventional designs of viscously damped vibration isolators are often concerned with the determination of the stiffness and damping characteristic parameters in a linear SDOF vibration isolator model. Linear fluid viscous dampers' dynamic characteristics have been widely studied and many methods and techniques [53, 60-62] have been developed to cope with the analysis and design of linear viscously damped systems in practice, where the design criteria and indices can explicitly be related to the design parameters [17, 20, 25]. But it's well known that there are still some unsolved problems in the vibration control design of the systems with linear fluid viscous dampers. For example, there is a dilemma for the frequency domain analysis of SDOF viscously damped vibration system as shown in Fig.2.18. In this typical SDOF vibration system, a harmonic force $F \cdot \sin(\omega t)$ is imposed on the lumped mass M and the movement of the lumped mass is isolated by a spring with stiffness k and a linear damping with the coefficient c associated with the spring. F_{out} is the resulting force transmitted to the foundation by the spring and damping. Tao and Mak [52] reviewed the effects of linear fluid viscous damping on the force

transmissibility in order to isolate the force transmitted to the ground. The important result as shown in Fig.2.19 revealed that the increase of damping ratio, which is directly proportional to the damping coefficient c, not only reduces the peak transmissibility at resonance frequency Ω_0 where the frequency ratio is equal to 1, but also increases the force transmissibility over the frequency ratio region $\Omega/\Omega_0 \geq \sqrt{2}$ which was commonly called "isolation region". Therefore, the operating frequency range of linear fluid viscous damper based vibration isolation systems was limited [5], it was beneficial at resonance and non-beneficial in higher frequency region.

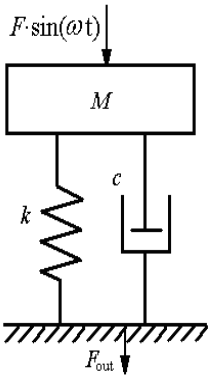

Fig.2.18 SDOF viscously damped system [52]

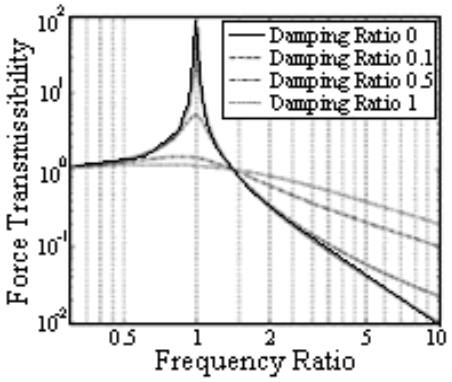

Fig.2.19 Force transmissibility for SDOF viscously damped system [52]

In order to overcome the limitations with using linear fluid viscous dampers in vibration system design, many techniques and devices, such as fully active and semi-active vibration isolators [109, 110] and "skyhook" dampers etc., have been studied and developed, although these isolation devices implies higher costs and more system maintenance.

Up to now, nonlinear passive fluid viscous dampers have been considered as a better solution in practical applications and many researchers have conducted studies applying nonlinear fluid viscous dampers in the vibration control of structural systems [33, 48, 111, 112]. Earlier activities include the work of Ruzicka and Derby [48] who applied the equivalent linear damping concept to

SDOF vibration systems with a velocity-pth power damper and showed the effect of nonlinear damping on suppressing the system force and displacement transmissibility. Ravindra and Mallik [33] used the harmonic balance method to examine the response of nonlinear vibration system subjected to force and displacement excitations, respectively. They studied the effects of nonlinear damping and stiffness on the system transmissibility. Recently, Yang [111] developed a mathematical model for a complex nonlinear coupling SDOF isolator for attenuating vibration which coupled quadratic, linear viscous, Coulomb dampers and nonlinear springs. The absolute acceleration transmissibility was evaluated by combining Fourier transforms and the harmonic balance method to illustrate the dynamic performance of the isolator. Mario [112] proposed a statistical linearization technique to evaluate the equivalent damping ratios of nonlinear fluid viscous dampers and applied a nonlinear fluid viscous damper with a lower-than-one exponent in a one-story shear-type building to reduce the structural vibration response caused by the seismic excitation. In 2008, Ibrahim [5] made a comprehensive assessment of recent developments of nonlinear vibration isolators which covered the traditional and non-traditional systems and proposed the recommendations for future research directions of the nonlinear vibration system design. Focusing on the dilemma revealed in frequency domain analysis of linear viscously damped vibration systems, Lang et al. [43, 47, 113] studied the potential of the application of cubic nonlinear fluid viscous dampers to improve the structural systems' vibration performance. Fig.2.20 shows the cubic nonlinearly damped system considered in the studies. Compared with the SDOF vibration system in Fig.2.18, this improved system introduced a cubic nonlinear fluid viscous damper between the lumped mass and foundation to suppress the system vibration. Fig 2.21 shows the force transmissibility of this system under different values of the cubic nonlinear damping characteristic parameter ξ_3. Clearly, compared with the case of the SDOF vibrating system with a fitted

linear fluid viscous damper in Fig.2.9, a much better vibration control performance can be achieved by introducing a cubic nonlinear fluid viscous damper. The nonlinear damping produces a significant vibration isolation over resonant frequencies but doesn't have the same detrimental effects in the isolation region as what can be observed in the linear damping case as shown in Fig.2.19.

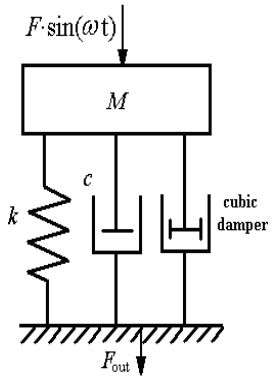

Fig.2.20 SDOF vibration with a fitted cubic nonlinear damper [47]

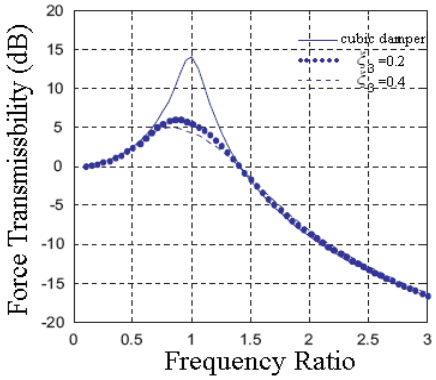

Fig.2.21 Force transmissibility for SDOF vibration system with a fitted cubic nonlinear damper [47]

2.4 Conclusions

In this chapter, the commonly used vibration control approaches in mechanical and civil engineering systems are introduced. The vibration control effects of typical damping devices on mechanical and civil engineering systems are discussed.

Fully active and semi-active damping devices, such as AMD, AVD and MR damper, suppress the system vibration by additional actuators. The automatic control theory and technology are often needed to design and implement an active control for the system; Passive damping devices, such as base isolation devices, TMD, TLCD, viscous damper, viscoelastic damper and metallic damper, reduce the system vibration and dissipate the energy by inherent damping

characteristics and need relatively less additional equipments and maintenance.

As one of the most commonly used passive damping devices, fluid viscous dampers have been introduced in detail. Compared with other damping devices, fluid viscous damper has been proved to be the most cost-effective and least space-intensive vibration control device. It has almost no effect on the original system's mass and stiffness and has significant advantages in vibration control and energy dissipation. In practice, the available range of the damping exponent of fluid viscous dampers is subject to the constraints determined by the devices' manufacturing process [9]. In such cases, fully active or semi-active damping devices such as those implemented using MR dampers can be used as solutions [114].

In order to overcome the limitations of linear fluid viscous dampers in vibration system designs, nonlinear fluid viscous dampers have been considered as a better solution in practical applications and many studies have demonstrated the effectiveness of nonlinear damping on vibration control and energy dissipation. However, nonlinear systems are generally complicated and there are no adequate generic techniques for nonlinear system analysis and design. In the next chapter, currently available theories and methods for the analysis and design of nonlinear damping in engineering systems will be discussed. These will be the basis of a series of new nonlinear damping research studies that will be reported in the later chapters of the thesis.

Chapter 3

Analysis and Design of Linear and Nonlinear Systems

3.1 Time and frequency domain representations of linear and nonlinear systems

3.1.1 Linear systems

In automatic control theory [19, 21], signal processing [115-117] and telecommunications [118], etc., the physical relationship between signals can usually be considered as systems and described by different mathematical models. A general deterministic system can be described by a mathematical operator H that maps an input signal $u(t)$ to an output signal $y(t)$ in the time domain as

$$y(t) = H\big(u(t)\big) \tag{3.1}$$

As the most basic systems, linear systems' performance characteristics can be simply described by mathematical models using linear operators [16] and they satisfy the properties of superposition and scaling [21] as follows:

Given two valid time domain inputs $u_1(t)$, $u_2(t)$ and the corresponding outputs $y_1(t)$, $y_2(t)$ of a linear system, which can be described by

$$\begin{cases} y_1(t) = H\big(u_1(t)\big) \\ y_2(t) = H\big(u_2(t)\big) \end{cases} \tag{3.2}$$

for any scalar values α and β, the system satisfies the following relationship

$$\alpha y_1(t) + \beta y_2(t) = H\left(\alpha u_1(t) + \beta u_2(t)\right) \tag{3.3}$$

This means that if a complicated input of a linear system can be represented by a sum of simpler inputs, then this linear system's output response to these simpler inputs can be calculated separately and then added to obtain the system output response to the complicated input [115].

Considering a linear, stable, causal and single-input-single-output (SISO) system in the time domain, the system output $y(t)$ subjected to a general input $u(t)$ can be represented by the convolution integral as [119]

$$y(t) = \int_{-\infty}^{\infty} h(\sigma)u(t-\sigma)d\sigma \tag{3.4}$$

where $h(\sigma)$ is the impulse response of the system, which is called "kernel". The physical meaning of $h(\sigma)$ is the output response of the system, initially at rest, to a unitary impulse applied at time $t = 0$.

In the frequency domain, when a stable time-invariant linear system is subject to an input whose the Fourier Transform (FT) exists, the output frequency response of this linear system can be expressed by [21]

$$Y(j\omega) = H(j\omega)U(j\omega) \tag{3.5}$$

where $U(j\omega)$ and $Y(j\omega)$ are the system input and output spectrum which are the Fourier transforms of the system's time domain input $u(t)$ and output $y(t)$, respectively. $H(j\omega)$ is the linear system's Frequency Response Function (FRF). This simple linear frequency domain relationship explicitly shows how the linear system affects on the input spectrum to produce the output frequency response at any frequency ω of interest. Eq.(3.5) has been widely applied in control engineering for the system analysis and controller design, in electronics and communications for the synthesis of analogue and digital filters, and in mechanical and civil engineering systems for the analysis of vibrations [24].

For linear systems, the steady-state output response to a periodic input excitation is periodic with the same frequency, but not necessarily in phase due to, for example, the energy dissipation by the damping term which causes the output to lag the input [120]. The proportional change in the amplitude of a vibration signal $T(\omega) = |Y(j\omega)| / |U(j\omega)| = |H(j\omega)|$ as it passes through a structural system from the input to the output is the system gain at frequency ω, which is also called "system transmissibility" [121]. For different system inputs and outputs, the system transmissibility can be defined by displacement transmissibility, force transmissibility, etc. [121, 122]. The phase delay $\varphi(\omega) = \angle Y(j\omega) - \angle U(j\omega) = \angle H(j\omega)$ represents the degree by which the output lags the input as a consequence of passage through the system in the frequency domain. The plots of the system transmissibility $T(\omega)$ and the phase delay $\varphi(\omega)$ are usually given together as they specify all properties of the system output response to a harmonic input at different frequencies, which is called "Bode plot". Another commonly used plot to present the information is "Nyquist plot" [123], which shows both system transmissibility $T(\omega)$ and phase delay $\varphi(\omega)$ on a single plot using frequency ω as a parameter in the complex plane.

3.1.2 Nonlinear systems

Compared with linear systems, nonlinear systems don't satisfy the properties of superposition and scaling in Eq.(3.3). They usually have complicated output characteristics and dynamic behaviours in both the time and frequency domains, such as chaos [27], bifurcation [28], fraction frequency and double frequency [34], etc.. These phenomena complicate the study on nonlinear systems. Although some nonlinear systems can be approximated by equivalent linear systems under certain conditions which is known as linearization [22, 26], there are no adequate generic techniques for the nonlinear system analysis and design

[15].

Nonlinear system studies have significance in engineering design [124], signal processing [4, 125], system identification [126] and so on, because most practical systems are inherently nonlinear. The most common types of nonlinearity encountered in practical systems are due to nonlinear stiffness and damping, clearances, impacts, friction and saturation effects, etc., whose dynamic characteristics are usually amplitude, velocity and frequency dependent [120].

Practical nonlinear systems are extremely diverse, and the analysis and design methods are problem dependent. There are no generic methods to deal with the problems with nonlinearity by either theoretical analysis or experimental simulation. The time and frequency domain relationships between linear systems' input-output and system characteristic parameters in Eqs.(3.4) and (3.5) can not be easily extended to nonlinear cases.

Recently, many studies [24, 44, 119, 127-129] have focused on the nonlinear systems which can be described by the Volterra series. Volterra series is a widely used mathematical description of the input-output relationship for nonlinear systems [127]. It is based on a functional power series expansion and derived by Volterra in 1900s for general functional relationships [128]. It is a generalization of power series and is ideal for representing frequency-dependent small nonlinearities [130]. Many literatures [44, 127, 130] have conducted the applications of the Volterra series in practical mechanical and civil engineering systems. For a nonlinear system which is stable at zero equilibrium point, the input-output relationship under certain conditions can be approximated by a truncated Volterra series [24, 44] as

$$y(t) = \sum_{n=1}^{N} \int_{-\infty}^{\infty} \cdots \int_{-\infty}^{\infty} h_n(\tau_1, \cdots, \tau_n) \prod_{i=1}^{n} u(t-\tau_i)\, \mathrm{d}\tau_i \tag{3.6}$$

where $h_n(\tau_1,\cdots,\tau_n)$, $1 \le n \le N$ is known as the n^{th} order Volterra kernel [124], which is the extension of the linear impulse response function $h(\sigma)$ in Eq.(3.4) to the nonlinear case, and N denotes the maximum order of the system nonlinearity. The Volterra series representation of nonlinear systems can also be expressed as

$$y(t) = \sum_{n=1}^{N} y_n(t) \tag{3.7}$$

where

$$y_n(t) = \int_{-\infty}^{\infty} \cdots \int_{-\infty}^{\infty} h_n(\tau_1,\cdots,\tau_n) \prod_{i=1}^{n} u(t-\tau_i) d\tau_i \tag{3.8}$$

is the contribution of the nth order system nonlinearity to the output response $y(t)$. It's simply an extension of the linear convolution integral to the higher order cases. The multidimensional Fourier transform of the Volterra kernel $h_n(\tau_1,\cdots,\tau_n)$ yields nth order frequency response function (FRF) or Generalised Frequency Response Functions (GFRFs) [120]

$$H_n(j\omega_1,\cdots,j\omega_n) = \int_{-\infty}^{\infty} \cdots \int_{-\infty}^{\infty} h_n(\tau_1,\cdots,\tau_n) \times e^{-(\omega_1\tau_1+\cdots+\omega_n\tau_n)j} \, \mathrm{d}\tau_1 \cdots \mathrm{d}\tau_n \tag{3.9}$$

Based on the GFRF, Eq. (3.8) can be written as [129]

$$y_n(t) = \frac{1}{(2\pi)^n} \int_{-\infty}^{\infty} \cdots \int_{-\infty}^{\infty} H_n(j\omega_1,\cdots,j\omega_n) \prod_{i=1}^{n} U(j\omega_i) e^{j(\omega_1+\cdots+\omega_n)t} d\omega_i \tag{3.10}$$

The GFRF concept provides useful insights into the harmonic and inter-modulation effects commonly associated with nonlinear system behaviours and Eqs.(3.7-3.10) can be used to show how the output frequency response of nonlinear systems are generated by a combination of these effects [131].

Volterra series provides an important theoretical foundation for the nonlinear system analysis and design. It is a powerful tool that can deal with a wide class of nonlinear systems [124, 132] and can provide a straightforward theoretical

explanation to the appearance of many nonlinear phenomena including the generation of super-harmonics and the appearance of sub-harmonic resonances [133]. The Volterra series has been widely studied and applied in modeling [119, 134], identification [135], control [136] and signal processing [137] for different deterministic and stochastic nonlinear systems [138].

3.2 Nonlinear system analysis in the frequency domain

Frequency domain analysis converts system signals from the time to the frequency domain using the Fourier transform [16]. Compared with the time domain analysis, the frequency domain analysis can provide more physically meaningful insights into the system dynamic behaviours [139], such as the stability [140] and resonance [17], which are easier for engineers to understand in most cases [41]. Consequently, the frequency domain approaches have been extensively applied in the analysis and design of practical engineering systems.

One of the main objectives of the system frequency domain analysis is to study the relationship between the system input spectrum and output frequency response [36]. The linear system's FRF in Eq.(3.5) has been widely used in many engineering fields to investigate linear systems' characteristics in the frequency domain [17, 20-22], where the output frequency response can be explicitly related to the input spectrum and system characteristic parameters in the time domain model. For example, Fridman and Gil [141] analysed the stability of linear systems with uncertain time-varying delays and studied the relationship between the system stability and the constant values of the delays. Soliman and Ismailzadeh [20] presented theoretical expressions for the system transmissibility, the optimum values of mass, stiffness and damping ratios of linear vibration systems, and consequently related these parameters to the systems' resonant characteristics.

However, nonlinear system analysis and design in the frequency domain are far more complicated. It's well known that nonlinear systems are often observed to have harmonics and complex inter-modulation phenomena [29, 30], which can transfer the signal energy from the frequency components of input to produce outputs at quite different frequency components. Moreover, the chaos and bifurcation [27] phenomena are also encountered in nonlinear systems. All of these complicate the study on nonlinear systems' behaviors. According to the Volterra series theory of nonlinear systems, the relationship between the nonlinear system's input and output spectrum involves complex multi-dimensional integration known as the association of variables and a summation with a possibly infinite number of terms [124]. An explicit analytical description for the relationship between the system characteristics and output frequency response can not be obtained easily as in the linear system case. Therefore, the analysis and design theories and methods of nonlinear systems in the frequency domain are far from being fully developed [41].

Although nonlinear systems are much complicated than linear systems, many kinds of nonlinear systems have been investigated in the literatures [27, 28, 34, 119, 120] using different analysis and design methods and applied in a lot of branches of science and practical engineering [16, 41]. The results have provided important theoretical foundations for nonlinear systems modelling, identification, analysis and design. In order to describe nonlinear systems, many mathematical models have been used, including Nonlinear AutoRegresive Moving Average with eXogenous input (NARMAX) models [142], Nonlinear Differential Equations (NDE) model [129], Nonlinear Auto-Regressive model with eXogenous input (NARX), Time Delayed Differential Equations (TDDE) model [143] and so on. Many typical nonlinear system equations, such as Duffing equation [31], Van Der Pol equation [32] and Lorenz equation [13], etc., have been studied. Some nonlinear system frequency analysis approaches and technologies, such as describing function, averaging method and harmonic

balance method, etc., have also been developed. For the nonlinear system analysis and design in the frequency domain, the describing function [3], perturbation and averaging methods [37] have ever taken an important role. The describing function method is an approximate procedure for analyzing certain nonlinear control problems based on the quasi-linearization concept [144]. It provides a powerful mathematical approach for the design of systems with a single nonlinear component [3]. Perturbation and averaging methods [145, 146] are always used to obtain an approximate solution such that the approximation error is small and the approximate solution is expressed in terms of equations simpler than the original equation. Although these methods have their limitations, errors or assumptions, some effective practical applications have been extensively reported [145, 147, 148]. In addition to perturbation and averaging methods, other approximate solution methods for the nonlinear system analysis were established and developed, including Ritz-Galerkin method and harmonic balance method [39]. Ritz-Galerkin method [38] transfers the problem of solving nonlinear differential equations into the solution of a group of new equations. Compared with describing function and perturbation methods, Ritz-Galerkin method follows a different idea, which is to find a solution that can minimize the error energy so that a higher accuracy can be achieved by taking the effect of higher order harmonics into account in the solution. The harmonic balance method is also a well established method. This method assumes that a Fourier series can represent a nonlinear system's steady state solution and can be used to deal with complicated problems in nonlinear systems such as sub-harmonics and jump behaviors [149, 150].

Based on the nonlinear system analysis methods and techniques, significant progresses towards understanding nonlinear systems have been achieved [103, 151-155]. Suzuki and Hedrick [156] developed an Interactive Inverse Random Input Describing Function method to find an approximate nonlinear function from the given data and applied it to the analysis and design of a second order

servo system with actuator saturation. Their results showed the advantages of nonlinear controllers and were verified by the Monte-Carlo simulations. Based on the describing function method, Aracil and Gordillo [157] analyzed the stability of nonlinear PD and PI fuzzy controllers and provided the formulation for a simplified version of these controllers. Chandra et al. [158] combined the straightforward perturbation method with Laplace transform to determine the transient response of a SDOF nonlinear vibration system and proposed an approximated solution, which can be used to directly evaluate the nonlinear system's transient response. Emadi [159] proposed a generalized state-space averaging method to investigate the negative impedance instability in hybrid ac and dc distribution systems and presented the stable region for these typical nonlinear systems. Based on the harmonic balance method, Braindra and Mallik [90] studied the effects of nonlinear damping on the steady-state, harmonic response and the transmissibility of a vibration system with combined Coulomb damper, viscous damper and a cubic nonlinear spring. They also presented the stability analysis of these solutions with a parametric study on the effects of different types of damping [160].

Recently, more and more studies have focused on the nonlinear system analysis and design in the frequency domain using the GFRF concept [40]. Based on the theory of Volterra series expansion, the study of nonlinear system frequency domain characteristics was initiated by the introduction of the GFRF concept by George in 1959 [40]. GFRF concept extends the linear FRF in Eq.(3.5) to nonlinear cases for a wide class of nonlinear systems that can be described by Volterra series [44, 119] in Eq.(3.6). The GFRF concept provides an important theoretical basis for the frequency domain analysis of nonlinear systems. For nonlinear systems, based on the GFRF concept, Lang and Billings [36] derived an analytical expression for the system output frequency response to a general input in 1996. The result is given by

$$\begin{cases} Y(j\omega) = \sum_{n=1}^{N} Y_n(j\omega) \quad \text{for } \forall\, \omega \\ Y_n(j\omega) = \dfrac{1/\sqrt{n}}{(2\pi)^{n-1}} \int_{\omega_1+\cdots+\omega_n=\omega} H_n(j\omega_1,\cdots,j\omega_n) \times \prod_{i=1}^{n} U(j\omega_i)\, \mathrm{d}\sigma_\omega \end{cases} \tag{3.11}$$

where $Y_n(j\omega)$ represents the n[th] order output frequency response of the nonlinear system. The term $\int_{\omega_1+\cdots+\omega_n=\omega} H_n(j\omega_1,\cdots,j\omega_n)\prod_{i=1}^{n} U(j\omega_i)\,\mathrm{d}\sigma_\omega$ denotes the integration of $H_n(j\omega_1,\cdots,j\omega_n)\prod_{i=1}^{n} U(j\omega_i)$ over the n-dimensional hyper-plane $\omega_1+\cdots+\omega_n=\omega$ [24] and $\mathrm{d}\sigma_\omega$ is the integral factor in this hyper-plane. Eq.(3.11) is a natural extension of the well known relationship Eq.(3.5) of linear systems to nonlinear systems and reveals how the nonlinear mechanisms operate on the input spectrum to produce the output frequency response [24].

In linear systems, the FRF concept shows that the possible output frequencies are the same as the input frequencies. But in nonlinear systems, which can be described by the Volterra series in Eq.(3.6), the possible output frequencies at the steady state are generally given by

$$f_Y = \bigcup_{n=1}^{N} f_{Y_n} \tag{3.12}$$

where f_Y is the non-negative frequency range of the nonlinear system output and f_{Y_n} represents the non-negative frequency range produced by the n[th] order system nonlinearity. In 1997, Lang and Billings [42] derived an explicit expression of the output frequency range f_Y for nonlinear systems subjected to a general input with a spectrum given by

$$U(j\omega) = \begin{cases} U(j\omega) & \text{when } |\omega| \in (a,b) \\ 0 & \text{otherwise} \end{cases} \tag{3.13}$$

where $b > a \geq 0$. The result is given by

$$\begin{cases} f_Y = f_{Y_N} \bigcup f_{Y_{N-(2p^*-1)}} \\ f_{Y_n} = \begin{cases} \bigcup_{k=0}^{i^*-1} I_k & \text{when } \dfrac{nb}{(a+b)} - \left[\dfrac{na}{(a+b)} \right] < 1, \\ \bigcup_{k=0}^{i^*} I_k & \text{when } \dfrac{nb}{(a+b)} - \left[\dfrac{na}{(a+b)} \right] \geq 1, \end{cases} \\ I_k = (na - k(a+b),\ nb - k(a+b)) \quad \text{for } k = 0, \cdots, i^* - 1 \\ I_{i^*} = (0, nb - i^*(a+b)) \end{cases} \tag{3.14}$$

where $i^* = \left[\dfrac{na}{(a+b)} \right] + 1$, the operator $[.]$ means to take the integer part, p^* could be taken as $1,2,\cdots,[N/2]$. Eq.(3.14) is a significant analytical description for the output frequencies of nonlinear systems and a natural extension for the well known concept about the linear system's output frequency range to the nonlinear case.

Up to now, many nonlinear system studies in the frequency domain have focused on the determination of the GFRFs [16, 131, 161, 162] and significant results relating to the estimation and computation of the GFRF expressions for practical nonlinear systems have been achieved [18, 35, 163]. Initially, the GFRFs of nonlinear systems were estimated from measured signals by extending the classical Fast Fourier Transform (FFT), windowing and smoothing techniques to many dimensions [164, 165]. Then, Bendat [166] developed a least square routine to estimate the GFRFs of nonlinear systems from the random data. Later on, Bedrosian and Rice [167] proposed the harmonic probing method to derive higher order GFRFs of nonlinear systems from the system differential equation representations. After that, Billings and Tsang [168] extended the harmonic probing approach to the discrete time nonlinear systems. Based on the recursive expressions of GFRF for the nonlinear systems which can be described by Nonlinear Differential Equations (NDE), Nonlinear Auto-Regressive model with eXogenous input (NARX) or Time Delayed Differential Equations (TDDE) [143], a more effective and

straightforward algorithm for computing the higher order GFRF of NDE, NARX and TDDE models was developed by Peyton-Jones [129] to simplify the involved computations. All of these provide important theoretical foundations for the study on nonlinear systems in the frequency domain.

Consider continuous time nonlinear systems which can be described by a Nonlinear Differential Equation (NDE)

$$\sum_{m=1}^{M}\sum_{\substack{p=0\\p+q=m}}^{m}\sum_{l_1,\cdots,l_{p+q}=0}^{L} c_{pq}(l_1,\cdots,l_{p+q})\prod_{i=1}^{p} D^{l_i}y(t)\times\prod_{i=p+1}^{p+q} D^{l_i}u(t)=0 \tag{3.15}$$

where the operator D is defined by $D^l x(t)=\mathrm{d}^l x(t)/\mathrm{d}t^l$, M and L are the maximum degree of nonlinearity in terms of $y(t)$ and $u(t)$, and the maximum order of derivative, respectively, $c_{pq}(l_1,\cdots,l_{p+q})$ represent the system model coefficients. If a nonlinear system described by the NDE model (3.15) satisfies the following assumptions:

(i) The system is stable at zero equilibrium.

(ii) The system can equivalently be described by the Volterra series model with $N \geq M$ over a regime around the equilibrium.

It was shown in [169] that the GFRFs of nonlinear systems can be determined from the model parameters as follows

$$H_n(j\omega_1,\cdots,j\omega_n)=-\frac{H_{nu}(j\omega_1,\cdots,j\omega_n)+H_{nuy}(j\omega_1,\cdots,j\omega_n)+H_{ny}(j\omega_1,\cdots,j\omega_n)}{\sum_{l_1=0}^{L}c_{10}(l_1)(j\omega_1+\cdots+j\omega_n)^{l_1}} \tag{3.16}$$

where

$$H_{nu}(j\omega_1,\cdots,j\omega_n)=\sum_{l_1,l_n=0}^{L} c_{0n}(l_1,\cdots,l_n)\prod_{i=1}^{n}(j\omega_i)^{l_i} \tag{3.17}$$

$$H_{nuy}(j\omega_1,\cdots,j\omega_n)=\sum_{q=1}^{n-1}\sum_{p=1}^{n-q}\sum_{l_1,l_n=0}^{L} c_{pq}(l_1,\cdots,l_{p+q})H_{n-q,p}(j\omega_1,\cdots,j\omega_{n-p})\prod_{i=n-q+1}^{p+q}(j\omega_i)^{l_i} \tag{3.18}$$

$$H_{ny}(j\omega_1,\cdots,j\omega_n)=\sum_{p=2}^{n}\sum_{l_1,l_p=0}^{L}c_{p0}(l_1,\cdots,l_p)H_{np}(j\omega_1,\cdots,j\omega_n) \tag{3.19}$$

and $H_{np}(j\omega_1,\cdots,j\omega_n)$ can be determined by the recursive expressions as follows [169]

$$H_{np}(j\omega_1,\cdots,j\omega_n)=\sum_{i=1}^{n-p+1}H_i(j\omega_1,\cdots,j\omega_i)H_{n-i,p-1}(j\omega_{i+1},\cdots,j\omega_n)\times(j\omega_1+\cdots+j\omega_i)^{l_p} \tag{3.20}$$

with

$$H_{n1}(j\omega_1,\cdots,j\omega_n)=H_n(j\omega_1,\cdots,j\omega_n)(j\omega_1+\cdots+j\omega_n)^{l_1} \tag{3.21}$$

The results in Eqs.(3.16)-(3.21) can considerably facilitate the numerical evaluation of the GFRFs of nonlinear systems described by Eq.(3.15) and can determine the GFRF expression up to any order of interest [169].

In 2001, Swain and Billings [170] extended the above recursive results to the Multi-Input-Multi-Output (MIMO) nonlinear systems. However, the recursive expressions in Eqs.(3.20-3.21) for the determination of GFRFs in Eq.(3.16) can't readily be used to explicitly show how the coefficients in the NDE model affect the system GFRFs. The evaluation of higher order GFRFs becomes more difficult [41]. In order to solve this problem, Peyton Jones [129] developed a simplified expression of $H_{np}(j\omega_1,\cdots,j\omega_n)$ as

$$H_{np}(j\omega_1,\cdots,j\omega_n)=\sum_{\substack{\text{all combs }(\gamma_1,\cdots,\gamma_p)\\ \text{taken from }(1\cdots N)\\ \text{with repetition}\\ \left|\sum\gamma_i=n\right.}}\left(H_{\gamma_1}(jw_{\gamma_1})\cdots H_{\gamma_p}(jw_{\gamma_p})\right)f_y(w_{\gamma_1},\cdots,w_{\gamma_p}) \tag{3.22}$$

where $f_y(\cdot)$ represents the remaining terms as

$$f_y(w_{\gamma_1},\cdots,w_{\gamma_p})=\left(\sum_{\substack{\text{all permutations}\\ \text{of }(\gamma_1,\cdots,\gamma_p)}}\prod_{i=1}^{p}\left(j\sum w_{\gamma_i}\right)^{l_i}\right)\qquad\text{for NDE model} \tag{3.23}$$

$$f_y(w_{\gamma_1},\cdots,w_{\gamma_p})=\left(\sum_{\substack{\text{all permutations}\\ \text{of }(\gamma_1,\cdots,\gamma_p)}}\prod_{i=1}^{p}\exp\left(-j\left(\sum w_{\gamma_i}\right)k_i\right)\right)\quad\text{for NARX model} \tag{3.24}$$

$$f_y(w_{\gamma_1},\cdots,w_{\gamma_p}) = \left(\sum_{\substack{\text{all permutations} \\ \text{of } (\gamma_1,\cdots,\gamma_p)}} \prod_{i=1}^{p} \left(j\sum w_{\gamma_i}\right)^{l_i} \exp\left(-j\left(\sum w_{\gamma_i}\right)k_i\right) \right) \quad \text{for TDDE model (3.25)}$$

Based on the GFRF concept and the above results for the determination of GFRF expressions, further studies on the frequency domain behaviors of nonlinear systems have been carried out and many important results have been achieved. Billings and Lang [171] studied the energy transfer characteristics of nonlinear systems, which had been observed in many practical systems in electronic, mechanical, civil and materials engineering. Swain et al. [172] used the n^{th} order GFRF expression and proposed a new approach to identify the parameters of both continuous and discrete nonlinear systems in the frequency domain. Boaghe et al. [173] combined time and frequency domain identification approaches to analyse the dynamic characteristics of a NARMAX model, which represented a gas turbine engine. In their studies, the GFRFs revealed the nonlinear couplings between the input harmonic components taking place at low frequencies and having much richer frequency components in the output. Energy release and energy storage phenomena were also detected from the GFRF plots.

Although many important progresses towards understanding nonlinear systems in the frequency domain have been made by using the GFRF concept, the limitation of the GFRF based approach is also obvious. This is because the GFRFs are a sequence of multivariable functions defined in a high dimensional frequency space. The evaluation of the values of higher order GFRFs is difficult due to the large amount of algebra and symbolic computations that are involved. The GFRF concept itself can't provide an explicit analytical relationship between the system time domain model parameters and the system output frequency response function to reveal how the system output frequency response depends on the system parameters.

3.3 Output Frequency Response Function (OFRF)

Because of the lack of an explicit analytical description for the relationship between nonlinear system parameters and the system output frequency response, the nonlinear system analysis and design in the frequency domain are much more complicated than that in the linear case. In order to circumvent complicated algebra and symbolic computations involved in the GFRF based nonlinear system analysis and design, Lang and Billings et al [24, 42, 139, 171] have conducted a series of research studies and derived an explicit analytical relationship between the output frequency response and the time domain model coefficients for a wide class of nonlinear systems that can be described by NDE models. The result is referred to the OFRF concept.

Consider a nonlinear system which can be described by the NDE model Eq.(3.15) and satisfies the assumptions (i) and (ii). Based on the Volterra series theory of nonlinear systems and the GFRF concept, the system output frequency response under a general input can be given by Eq.(3.11), and the possible output frequencies can be described by Eq.(3.14). However, because of the complicated integration computations involved in the multi-dimensional hyper-plane, Eq.(3.11) is difficult to be used in the nonlinear system analysis and design. In order to solve this problem, using the recursive nth order GFRF expressions for the NDE model in Eqs.(3.16-3.21), Lang and Billings et al [24] proved, for the first time, that when the parameters in the 1st order GFRF $H_1(.)$ of the nonlinear system and frequency variables $\omega_1,\cdots,\omega_n$ are given, the nth order GFRF $H_n(j\omega_1,\cdots,j\omega_n)$ of nonlinear systems can be expressed as follows

$$H_n(j\omega_1,\cdots,j\omega_n)=\sum_{(j_1,\cdots j_{s_n})\in J_n}\Theta^{(n:j_1\cdots j_{s_n})}_{\lambda_1\cdots\lambda_{s_n}}(j\omega_1,\cdots,j\omega_n)\lambda_1^{j_1}\cdots\lambda_{s_n}^{j_{s_n}} \tag{3.26}$$

which is a polynomial function of the system parameters in a set given by

$$C_2^n = C_2 \bigcup C_3 \bigcup \cdots \bigcup C_n \tag{3.27}$$

where C_n, $n \geq 2$, is composed of the parameters of the NDE model in Eq.(3.15) as follows

$$C_n = \left\{ \begin{array}{ll} c_{0n}(l_1, \cdots, l_n), & l_i = 0, \cdots, L; i = 1, \cdots, n \\ c_{pq}(l_1, \cdots, l_{p+q}), & l_i = 0, \cdots, L; i = 1, \cdots, p+q, \\ & q = 1; p = 1, \cdots, n-1, \\ & q = 2; p = 1, \cdots, n-2, , \\ & \cdots \quad \cdots \quad \cdots \\ & q = n-1; p = 1 \\ c_{p0}(l_1, \cdots, l_p), & l_i = 0, \cdots, L; i = 1, \cdots, p, \\ & p = 2, \cdots, n \end{array} \right\} \tag{3.28}$$

$\lambda_1, \cdots, \lambda_{s_n}$ are the elements in C_2^n; $\Theta_{\lambda_1 \cdots \lambda_{s_n}}^{(n: j_1 \cdots j_{s_n})}(j\omega_1, \cdots, j\omega_n)$ represents a function of $\omega_1, \cdots, \omega_n$ and the parameters in $H_1(.)$, and J_n is a set of s_n dimensional non-negative integer vectors which contain the exponents of those monomials $\lambda_1^{j_1} \cdots \lambda_{s_n}^{j_{s_n}}$.

For example, consider the differential equation model of a well-known mechanical system, described by [174]

$$m\ddot{y}(t) + ky(t) + a_1 \dot{y}(t) + a_2 \dot{y}^2(t) + a_3 \dot{y}^3(t) = u(t) \tag{3.29}$$

The 1st to 3rd order GFRFs of this mechanical system can be determined recursively from Eqs.(3.16-3.21) to produce the results below

$$H_1(j\omega) = \frac{1}{\beta(j\omega)} \tag{3.30}$$

$$H_2(j\omega_1, j\omega_2) = \frac{\omega_1 \omega_2}{\beta(j\omega_1)\beta(j\omega_2)\beta(j\omega_1 + j\omega_2)} \cdot a_2 \tag{3.31}$$

$$H_3(j\omega_1, j\omega_2, j\omega_3) = \frac{\omega_1\omega_2\omega_3\left[\dfrac{(\omega_2+\omega_3)}{\beta(j\omega_2+j\omega_3)} + \dfrac{(\omega_1+\omega_2)}{\beta(j\omega_1+j\omega_2)}\right]}{\beta(j\omega_1)\beta(j\omega_2)\beta(j\omega_3)\beta(j\omega_1+j\omega_2+j\omega_3)} \cdot a_2^2 + \frac{j\omega_1\omega_2\omega_3}{\beta(j\omega_1)\beta(j\omega_2)\beta(j\omega_3)\beta(j\omega_1+j\omega_2+j\omega_3)} \cdot a_3 \quad (3.32)$$

where $\beta(j\omega) = m(j\omega)^2 + a_1(j\omega) + k$, $\beta(j\omega_1 + j\omega_2) = m(j\omega_1 + j\omega_2)^2 + a_1(j\omega_1 + j\omega_2) + k$ and $\beta(j\omega_1 + j\omega_2 + j\omega_3) = m(j\omega_1 + j\omega_2 + j\omega_3)^2 + a_1(j\omega_1 + j\omega_2 + j\omega_3) + k$. Obviously, these are polynomial functions of system parameters a_2 and a_3.

When a nonlinear system can be approximated by a Volterra series with order N in the neighbour of its zero equilibrium, substituting the GFRF expressions in Eq.(3.26) into the description for the system output frequency response Eq.(3.11) yields

$$Y(j\omega) = \sum_{(j_1,\cdots,j_{s_N})\in J} \gamma_{j_1\cdots j_{s_N}}(\omega) x_1^{j_1}\cdots x_{s_N}^{j_{s_N}} \quad (3.33)$$

where $x_1,\cdots,x_{s_N}$ are the elements in C_2^N, J is a set of s_N dimensional non-negative integer vectors which contain the exponents of those monomials $x_1^{j_1}\cdots x_{s_N}^{j_{s_N}}$. $\gamma_{j_1\cdots j_{s_N}}(\omega)$ represents the coefficient of the term $x_1^{j_1}\cdots x_{s_N}^{j_{s_N}}$, which is a function of the frequency variable ω and also depends on the parameters in the 1st order GFRF $H_1(.)$ of the nonlinear system. Eq.(3.33) was defined by Lang et al in [24] as the Output Frequency Response Function (OFRF) of nonlinear systems.

For example, consider the mechanical system described by Eq.(3.29) again. The OFRF of this nonlinear system can be obtained as [24]

$$Y(j\omega) = P_{11}(j\omega) + a_2P_{21}(j\omega) + a_3P_{31}(j\omega) + a_2^2P_{42}(j\omega) + a_2a_3P_{41}(j\omega) + a_3^2P_{32}(j\omega) \quad (3.34)$$

when the system nonlinearity up to 4th order is taken into account. In (3.34), $P_{i_1i_2}(j\omega)$, $i_1 = 1,2,3,4$, $i_2 = 1,2$, are the functions of the frequency variable ω and the system parameters m, a_1 and k. The values of $P_{i_1i_2}(j\omega)$ can be

determined directly from the simulation or experimental test data as introduced as follows.

Consider the general nonlinear system OFRF representation

$$Y(j\omega) = \sum_{(j_1,\cdots,j_{s_N})\in J} \gamma_{j_1\cdots j_{s_N}}(\omega) x_1^{j_1}\cdots x_{s_N}^{j_{s_N}} = \sum_{j_1=0}^{m_1}\sum_{j_2=0}^{m_2}\cdots\sum_{j_{s_N}}^{m_{s_N}} \gamma_{j_1\cdots j_{s_N}}(\omega) x_1^{j_1}\cdots x_{s_N}^{j_{s_N}} \tag{3.35}$$

where m_i are the maximum power of x_i, $i = 1,2,\cdots,s_N$, in the OFRF expression. It was shown in [24] that the functions $\gamma_{j_1\cdots j_{s_N}}(\omega)$, $j_i = 0,\cdots,m_i$, can be determined from the system simulation or experimental data by the least square method as

$$\begin{bmatrix} \gamma_{\underbrace{0,\cdots,0}_{s_N}}(\omega) \\ \vdots \\ \gamma_{m_1,\cdots,m_{s_N}}(\omega) \end{bmatrix} = \left(X_{\overline{M}}^T X_{\overline{M}}\right)^{-1} \cdot X_{\overline{M}}^T \begin{bmatrix} Y^1(j\omega) \\ \vdots \\ Y^{\overline{M}}(j\omega) \end{bmatrix} \tag{3.36}$$

where $\overline{M} \geq (m_1+1)(m_2+1)\cdots(m_{s_N}+1)$

$$X_{\overline{M}} = \begin{bmatrix} (x_{11}^0\cdots x_{s_N1}^0) & \cdots & \cdots & (x_{11}^{m_1}\cdots x_{s_N1}^{m_{s_N}}) \\ \vdots & \vdots & \vdots & \vdots \\ \vdots & \vdots & \vdots & \vdots \\ (x_{1\overline{M}}^0\cdots x_{s_N\overline{M}}^0) & \cdots & \cdots & (x_{1\overline{M}}^{m_1}\cdots x_{s_N\overline{M}}^{m_{s_N}}) \end{bmatrix} \tag{3.37}$$

and $Y^w(j\omega)$ is the system output spectrum when system parameters are taken as $x_{1w},\cdots,x_{s_Nw}$ with $w = 1,\cdots,\overline{M}$ and $x_{iw} \in \{x_i(1),\cdots,x_i(m_i+1)\}$. $(x_{1r},\cdots,x_{s_Nr}) \neq (x_{1q},\cdots,x_{s_Nq})$ when $r \neq q$. $x_i(1),\cdots,x_i(m_i+1)$ are m_i+1 different values that can be taken by the system parameter x_i. For the practical applications of OFRF concept in the analysis and design of nonlinear systems, the system output spectrum $Y^w(j\omega)$ can be evaluated from the system output responses obtained from the simulation analysis or experimental tests.

In Peng et al. [175], the OFRF concept and the above least square method were

applied to the analysis of nonlinearly damped MDOF structural systems. The results have significant implication for the design of additional nonlinear damping devices in MDOF systems for vibration control purpose.

In [24], simulation studies were conducted to verify the theoretical derivations of the OFRF, and to demonstrate the effectiveness of the method proposed for the determination of the OFRF from simulation or experimental data. A comparison between the output spectrum obtained via performing the FFT analysis of the simulated system output data and the results evaluated using the OFRF expression was also made. The result indicates that a very good match can be achieved.

The OFRF concept extends the well-known linear system relationship in Eq.(3.5) to the nonlinear case and reveals a link between the system time domain model parameters and the system output frequency response. This can be used to considerably facilitate the nonlinear system analysis and design in the frequency domain [24]. Although nonlinear systems which exhibit sub-harmonics and chaos can not be analyzed using the OFRF based approach, because the basis of the OFRF concept is the Volterra series theory of nonlinear systems which occupies the middle ground in generality and applicability of the theories of nonlinear systems, the OFRF concept has considerable significance for the systematic applications of the nonlinear system analysis and design in engineering practice [24].

For the practical analysis and design of nonlinear systems, Lang et al [2, 24, 36, 43, 47, 113, 114, 139] have conducted considerable studies and made significant progress. For example, in [139], a general procedure was proposed to determinate the OFRF for a given NDE or NARX model and the potential practical applications of the OFRF-based analysis were discussed. The analysis of a nonlinear spring-damping system was used to illustrate the effectiveness of

the OFRF based approach in the study of nonlinear vibration control systems; In [2], the OFRF expression of a closed-loop nonlinear system was derived, which shows the relationship between the system output frequency response and controller parameters and provides an important basis for the nonlinear feedback controller analysis and design. The results revealed that, compared with a linear damping based control, the performance of a vibration system can be improved by properly introducing a simple nonlinear damping device; In [47], the study focused on the applications of the OFRF concept in the analysis of SDOF vibration systems and the effects of nonlinear viscous damping parameters on the vibration control were analysed. The results revealed that the OFRF concept is helpful for the analysis and exploitation of the potential advantages of nonlinear fluid viscous dampers in vibration control. In [43], an effective algorithm was proposed to determine the monomials in the OFRF representation of nonlinear systems, the effects of the characteristic parameters of a nonlinear engine mount on the system output frequency behaviours were studied to facilitate the nonlinear vibration system design. In [113], the OFRF concept was applied to theoretically investigate the force transmissibility of SDOF passive vibration isolators, the results indicated that nonlinear vibration isolators with an antisymmetric damping characteristic have great potential to overcome the problems encountered in the linear passive vibration isolators design. The results were also verified by simulation studies. In [114], the OFRF concept was applied to analyze the effects of the damping characteristics parameters and the current in an MR damper on the output frequency response of SDOF vibration system subject to a harmonic excitation. The results allow engineers to directly control the current of a commercially available MR damper to achieve a desired system response without a feedback control system.

3.4 Conclusions

In this chapter, the time and frequency domain representations of linear and nonlinear systems are introduced and the commonly used frequency domain approaches for nonlinear system analysis and design are reviewed.

Compared with linear systems, the characteristics of nonlinear systems are much more complicated. The conventional nonlinear frequency domain analysis approaches and design technologies, such as describing function, perturbation and averaging methods, Ritz-Galerkin method, harmonic balance method and GFRF concept, can not provide an explicit analytical description for the relationship between the system characteristic parameters and output frequency response.

In order to circumvent complicated mathematical computations and facilitate the nonlinear system analysis and design in the frequency domain, the OFRF concept of nonlinear systems was introduced based on the Volterra series theory and the GFRF concept of nonlinear systems. The OFRF concept extends the well known frequency domain input-output relationship of linear systems to nonlinear systems and reveals the significant link between the system output frequency response and parameters that define system nonlinearity. It provides important foundation for the nonlinear system analysis and design in the frequency domain and is also the basis of most results that will be presented in later chapters.

Chapter 4

Analysis and Design of the Transmissibility of SDOF Viscously Damped Vibration Systems

For the purpose of nonlinear damping designs, the evaluation of transmissibility of SDOF viscously damped vibration systems is studied in this chapter. A general mathematical model is firstly derived for the cases where the systems are subject to harmonic loadings. Then the Ritz-Galerkin method is applied to theoretically evaluate the system displacement and force vibration transmissibility. The effects of nonlinear viscous damping parameters on the system vibration control at different frequencies are discussed. A three-step procedure for the nonlinear damping system design is finally proposed to facilitate the design of nonlinear viscous damping parameters for a desired steady-state vibration performance. Two case studies are also provided to demonstrate how to implement the proposed nonlinear damping design procedure in practical applications.

4.1 Introduction

Transmissibility is a commonly used concept in the field of shock and vibration control [17] to describe the transmission of unwanted force and motion from the excitation source to a mechanical or civil engineering system [176]. It’s defined in the frequency domain as the ratio of the steady-state output amplitude to the harmonic input amplitude in a vibration system. Two major types of system transmissibility are force transmissibility and displacement transmissibility. As an important evaluation criterion for the effectiveness of vibration control

devices, system transmissibility has been widely studied and applied in the analysis and design of practical engineering systems. Many important results have been reported in literatures [52, 113, 176, 177].

As introduced in Chapter 2, there is a dilemma associated with the design of linear fluid viscous dampers, that is, introducing a considerable linear viscous damping in a vibration system to reduce the force transmissibility at the resonant frequency could lead to deterioration to the force transmissibility over higher frequency region [113]. In order to tackle this problem, nonlinear fluid viscous dampers were initially studied and their potential to achieve better vibration control was demonstrated in 1971 [50]. Milovanovic et al. [177] investigated the influence of system characteristic parameters on the relative and absolute displacement transmissibility of a SDOF viscously damped vibration system. The effects of linear and nonlinear fluid viscous dampers on the system vibration control were evaluated and compared to highlight the beneficial effects of nonlinear fluid viscous dampers; Lang et al. [47] and Peng et al. [113] applied the frequency domain analysis approach to theoretically investigate the force transmissibility of SDOF vibration isolators with nonlinear damping characteristics. Their results rigorously proved that nonlinear isolators can be applied to overcome the dilemma encountered in the design of linear fluid viscous dampers.

This chapter is concerned with the analysis and design of the force and displacement transmissibility of nonlinear fluid viscous dampers based vibration systems. The objectives are to extend nonlinear damping study to more general harmonic loading conditions, and to propose an effective procedure to facilitate the design of nonlinear viscous damping in practical applications. For these purposes, a general mathematical model is first derived for SDOF viscously damped vibration system subject to a harmonic input with amplitude proportional to the driving frequency raised to an arbitrary power. Then the

Ritz-Galerkin method is applied to theoretically evaluate and analyse the system displacement and/or force transmissibility. After that, a three-step procedure for the nonlinear damping system design is proposed using the Ritz-Galerkin method based analysis to facilitate the design of nonlinear damping parameters for a desired vibration performance. The results reveal that, if appropriately designed, nonlinear fluid viscous dampers are more effective than linear fluid viscous dampers in vibration control at both the resonant and higher frequencies and can significantly improve the system vibration performance in different loading conditions. These provide important guidelines for the nonlinear fluid viscous damper design and have implications for the engineering designs of vibration systems for a wide range of practical applications.

4.2 SDOF vibration isolators with a nonlinear viscous damping device

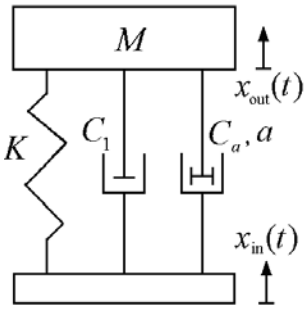

Fig.4.1 Displacement Vibration Isolation System (DVIS)

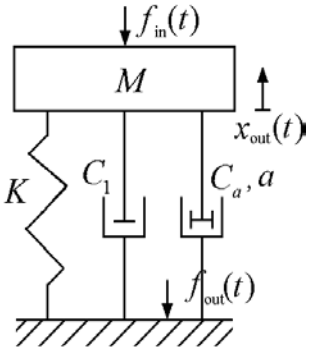

Fig.4.2 Force Vibration Isolation System (FVIS)

Consider the SDOF displacement and force vibration isolation systems shown in Figs.4.1 and 4.2, respectively, where a nonlinear fluid viscous damper is used as the energy dissipation device. In the case of DVIS, the foundation moves due to a general harmonic displacement excitation

$$x_{\text{in}}(t) = H\Omega^n \sin(\Omega t) \tag{4.1}$$

where n denotes the exponent of the input excitation. The movement of the

lumped mass M is isolated by a spring with stiffness K and a fluid viscous damper with power damping characteristic parameter a and damping coefficient C_a; C_1 is the linear damping coefficient associated with the spring. In the case of FVIS, a general harmonic force

$$f_{\text{in}}(t) = H\Omega^n \sin(\Omega t) \tag{4.2}$$

is imposed on the lumped mass and the same spring-damper mechanism is used between the lumped mass and foundation.

The fluid viscous damper in DVIS and FVIS is a typical damping device as introduced in Chapter 2. The damping force is described by

$$F_{\text{D}} = C_a \left|\dot{u}_r\right|^a \text{sign}(\dot{u}_r) \tag{4.3}$$

where $\dot{u}_r$ is the relative velocity between the two ends of the damper [33, 46, 50].

For DVIS and FVIS, the system equations can be described by:

$$\begin{aligned} M\ddot{x}_{\text{out}}(t) = {} & K\left(x_{\text{in}}(t) - x_{\text{out}}(t)\right) + C_1\left(\dot{x}_{\text{in}}(t) - \dot{x}_{\text{out}}(t)\right) \\ & + C_a\left|\dot{x}_{\text{in}}(t) - \dot{x}_{\text{out}}(t)\right|^a \cdot \text{sign}\left(\dot{x}_{\text{in}}(t) - \dot{x}_{\text{out}}(t)\right) \end{aligned} \quad \text{for DVIS} \tag{4.4}$$

and

$$\begin{cases} M\ddot{x}_{out}(t) + Kx_{out}(t) + C_1\dot{x}_{out}(t) + C_a\left|\dot{x}_{out}(t)\right|^a \cdot \text{sign}\left(\dot{x}_{out}(t)\right) = f_{\text{in}}(t) \\ f_{\text{out}}(t) = Kx_{out}(t) + C_1\dot{x}_{out}(t) + C_a\left|\dot{x}_{out}(t)\right|^a \cdot \text{sign}\left(\dot{x}_{out}(t)\right) = f_{\text{in}}(t) - M\ddot{x}_{out}(t) \end{cases} \quad \text{for FVIS} \tag{4.5}$$

respectively.

The SDOF DVIS and FVIS with a fluid viscous damper subject to the general harmonic input $x_{\text{in}}(t)$ or $f_{\text{in}}(t)$ represent a range of practical vibration control systems. For example, when $n = 0$, the model of DVIS can represent the building's displacement vibrations in earthquake; When $n = 0$, the model of FVIS can be used to evaluate the force transmission in structures subject to loads from wind or water wave; When $n = 2$ for FVIS, the input can represent

the force excitation from a rotating machine with an eccentric mass such as washing machine and automobile engine, and the model can describe the effects of the eccentric mass on the system's vibrating behaviors.

The study on the effects of nonlinear damping characteristic parameters C_a and a on the system vibration transmissibility is significant for achieving desired vibration performance. The results can also provide important guidelines for the future research on the analysis and design of vibration isolators for more complicated structures such as civil buildings, towers and bridges.

4.3 Evaluation of the force and displacement transmissibility of the SDOF DVIS and FVIS with a nonlinear viscous damping device

4.3.1 The force and displacement transmissibility

The objective of the adoption of a nonlinear viscous damping device in a vibration system is to isolate unwanted vibrations so that the adverse effects of vibrations can be kept within an acceptable level. Specifically speaking, for a DVIS, the displacement of the lumped mass $x_{\text{out}}(t)$ is to be reduced; while for FVIS, either the force transmitted to the foundation $f_{\text{out}}(t)$ or the displacement of the lumped mass $x_{\text{out}}(t)$ is to be suppressed according to the design requirement. According to the pioneering studies on the effects of nonlinear damping devices on the vibration system behaviours [50, 178], the system vibrations at the excitation frequency have the most significant effect and the higher harmonics can be neglected. Consequently, the force and displacement transmissibility of the SDOF DVIS and FVIS subject to the harmonic inputs in Eq.(4.1) and Eq.(4.2), respectively can be defined as

$$DD(\Omega)=\frac{\left|X_{\text{out}}(j\Omega)\right|}{\left|X_{\text{in}}(j\Omega)\right|}=\frac{\left|X_{\text{out}}(j\Omega)\right|}{H\Omega^{n}} \quad \text{in DVIS} \tag{4.6}$$

$$FD(\Omega)=\frac{\left|X_{\text{out}}(j\Omega)\right|}{\left|F_{\text{in}}(j\Omega)\right|}=\frac{\left|X_{\text{out}}(j\Omega)\right|}{H\Omega^{n}} \quad \text{in FVIS} \tag{4.7}$$

$$FF(\Omega)=\frac{\left|F_{\text{out}}(j\Omega)\right|}{\left|F_{\text{in}}(j\Omega)\right|}=\frac{\left|F_{\text{out}}(j\Omega)\right|}{H\Omega^{n}} \quad \text{in FVIS} \tag{4.8}$$

respectively. In Eqs.(4.6) to (4.8), $X_{\text{in}}(j\Omega)$, $F_{\text{in}}(j\Omega)$, $X_{\text{out}}(j\Omega)$, and $F_{\text{out}}(j\Omega)$ are the Fourier Transforms of $x_{\text{in}}(t)$, $f_{\text{in}}(t)$, $x_{\text{out}}(t)$ and $f_{\text{out}}(t)$ respectively. $DD(\Omega)$ denotes the displacement-displacement transmissibility of DVIS; $FD(\Omega)$ and $FF(\Omega)$ represent the force-displacement transmissibility and force-force transmissibility of FVIS, respectively.

4.3.2 The Ritz-Galerkin method

As introduced in Chapter 2, the Ritz-Galerkin method [38] is a powerful technique for solving nonlinear differential equations. Consider a nonlinear differential equation with the general form:

$$F(D,x,t)=0 \tag{4.9}$$

where $D=\mathrm{d}/\mathrm{d}t$ is the differential operator, $F(D,x,t)$ is a nonlinear function of D, x and t.

Obviously, for the exact solution $x(t)$ of Eq.(4.9), $F(D,x(t),t)=0$. Assume that $X(t)$ is an approximate solution to the differential equation, then

$$\varepsilon(t)=F(D,X(t),t) \tag{4.10}$$

is the approximating error due to $X(t)\neq x(t)$, and $X(t)$ can be described as the sum of a finite number n^* of harmonics, i.e.,

$$X(t)=\sum_{i=1}^{n^*}c_i\sin(i\omega t-a_i) \tag{4.11}$$

The basic idea of the Ritz-Galerkin method is to find an approximate solution $X(t)$ to Eq.(4.9) such that the integrated error over a variation scope $t \in [a,b]$ as defined by

$$J = \int_a^b \varepsilon^2(t)\,\mathrm{d}t \tag{4.12}$$

reaches a minimum value. The solution can then be obtained by solving the group equation

$$\begin{cases} \dfrac{\partial J}{\partial c_1} = \int_a^b 2\varepsilon(t)\dfrac{\partial \varepsilon(t)}{\partial c_1}dt = 0 \\ \cdots \\ \dfrac{\partial J}{\partial c_n} = \int_a^b 2\varepsilon(t)\dfrac{\partial \varepsilon(t)}{\partial c_n}dt = 0 \\ \dfrac{\partial J}{\partial a_1} = \int_a^b 2\varepsilon(t)\dfrac{\partial \varepsilon(t)}{\partial a_1}dt = 0 \\ \cdots \\ \dfrac{\partial J}{\partial a_n} = \int_a^b 2\varepsilon(t)\dfrac{\partial \varepsilon(t)}{\partial a_n}dt = 0 \end{cases} \tag{4.13}$$

4.3.3 Evaluation of the transmissibility

Rewrite Eqs.(4.4) and (4.5) in a dimensionless format as follows:

$$\ddot{f}(\tau) + f(\tau) + \xi_1 \dot{f}(\tau) + \xi_a \left|\dot{f}(\tau)\right|^a \cdot \mathrm{sign}\left(\dot{f}(\tau)\right) = \overline{\Omega}^{n+2}\sin(\overline{\Omega}\tau) \quad \text{for DVIS} \tag{4.14}$$

$$\ddot{g}(\tau) + g(\tau) + \xi_1 \dot{g}(\tau) + \xi_a \left|\dot{g}(\tau)\right|^a \cdot \mathrm{sign}\left(\dot{g}(\tau)\right) = \overline{\Omega}^{n}\sin(\overline{\Omega}\tau) \quad \text{for FVIS} \tag{4.15}$$

where $\tau = \Omega_0 t$, $\Omega_0 = \sqrt{K/M}$, $\overline{\Omega} = \Omega/\Omega_0$, $f(\tau) = y(\tau) - x(\tau)$,

$x(\tau) = Kx_{\mathrm{in}}(\tau/\Omega_0)/(MH\Omega_0^{n+2})$, $y(\tau) = Kx_{\mathrm{out}}(\tau/\Omega_0)/(MH\Omega_0^{n+2})$,

$g(\tau) = Kx(\tau/\Omega_0)/(H\Omega_0^{n})$, $f_{\mathrm{out}}(\tau) = \overline{\Omega}^n\sin(\overline{\Omega}\tau) - \ddot{g}(\tau)$, $\xi_1 = \dfrac{C_1}{\sqrt{MK}}$,

$\xi_a = \dfrac{C_a\left(MH\Omega_0^{n+2}\right)^{a-1}}{\sqrt{(MK)^a}}$ for DVIS, and $\xi_a = \dfrac{C_a(H\Omega_0^n)^{a-1}}{\sqrt{(MK)^a}}$ for FVIS.

For the convenience of analysis, rewrite Eqs.(4.14) and (4.15) uniformly as follows

$$\ddot{e}(\tau)+e(\tau)+\xi_1\dot{e}(\tau)+\xi_a\left|\dot{e}(\tau)\right|^a\cdot\operatorname{sign}\left(\dot{e}(\tau)\right)=\overline{\Omega}^m\sin(\overline{\Omega}\tau) \tag{4.16}$$

where $e(\tau)=f(\tau)$, $m=n+2$ for DVIS, and $e(\tau)=g(\tau)$, $m=n$ for FVIS.

A Ritz-Galerkin method based procedure for determining the transmissibility of nonlinear vibration systems can be summarized as follows:

(i) Choose an approximate solution to the system nonlinear differential equation description as given in Eq.(4.11).

(ii) Substitute the approximate solution into Eq.(4.10) to obtain an explicit analytical expression for the approximating error.

(iii) Determine the parameters c_i and a_i, $i=1,\cdots,n$, in the approximate solution by solving group Eq.(4.13).

(iv) Evaluate the transmissibility of the nonlinear vibration system using the obtained approximate solution.

The transmissibility of the SDOF DVIS and FIVS that can be determined using the above procedure for systems (4.16) is summarized in the following proposition:

Proposition 1. For the SDOF DVIS and FVIS with a nonlinear viscous damping device which can uniformly be described by the dimensionless Eq.(4.16), the force and displacement transmissibility as defined in Section 4.3.1 can be evaluated as

$$DD(\overline{\Omega})=\sqrt{\overline{\Omega}^{2m}+x^2\overline{\Omega}^4+2xy\overline{\Omega}^{m+2}}\Big/\overline{\Omega}^m \quad \text{for DVIS} \tag{4.17}$$

$$FD(\overline{\Omega})=x\Big/\left(K\overline{\Omega}^m\right) \quad \text{for FVIS} \tag{4.18}$$

$$FF(\overline{\Omega})=\sqrt{\overline{\Omega}^{2m}+x^2\overline{\Omega}^4+2xy\overline{\Omega}^{m+2}}\Big/\overline{\Omega}^m \quad \text{for FVIS} \tag{4.19}$$

where x and y are the solutions to the following equations:

$$\begin{cases} \left(\left(1-\overline{\Omega}^2\right)^2+\xi_1^2\overline{\Omega}^2\right)x-\overline{\Omega}^m\left(1-\overline{\Omega}^2\right)y+\xi_1\overline{\Omega}^{m+1}z \\ +\xi_a\xi_1(a+1)\overline{\Omega}^{a+1}J(a+1)x^a+a\xi_a^2\overline{\Omega}^{2a}J(2a)x^{2a-1}+a\xi_a\overline{\Omega}^{a+m}J(a+1)x^{a-1}z=0 \\ \left(\overline{\Omega}^m\left(1-\overline{\Omega}^2\right)z+\xi_1\overline{\Omega}^{m+1}y\right) \\ +\xi_a\overline{\Omega}^a\left(1-\overline{\Omega}^2\right)\left((a+1)J(a+1)-aJ(a-1)\right)x^a+a\xi_a\overline{\Omega}^{a+m}\left(J(a-1)-J(a+1)\right)x^{a-1}y=0 \\ y^2+z^2=0 \end{cases} \tag{4.20}$$

when $a \geq 1$ or

$$\begin{cases} \left(\left(1-\overline{\Omega}^2\right)^2+\xi_1^2\overline{\Omega}^2\right)x-\overline{\Omega}^m\left(1-\overline{\Omega}^2\right)y+\xi_1\overline{\Omega}^{m+1}z \\ +\xi_a\xi_1(a+1)\overline{\Omega}^{a+1}J(a+1)x^a+a\xi_a^2\overline{\Omega}^{2a}J(2a)x^{2a-1}+a\xi_a\overline{\Omega}^{a+m}J(a+1)x^{a-1}z=0 \\ -\left(1-\overline{\Omega}^2\right)x+\overline{\Omega}^m y=0 \\ y^2+z^2=0 \end{cases} \tag{4.21}$$

when $0 \leq a < 1$ where $J(a)=\dfrac{4}{\pi}\cdot\int_0^{\pi/2}\cos^a x dx$.

Proof of Proposition 1:

For Eq.(4.16), define the approximate solution as:

$$\hat{e}(\tau)=A\sin(\overline{\Omega}\tau+\beta),\quad A>0 \tag{4.22}$$

to describe the transmissibility of the dimensionless system as

$$DD(\overline{\Omega})=\frac{\left\|A\sin(\overline{\Omega}\tau+\beta)+\overline{\Omega}^{m-2}\sin(\overline{\Omega}\tau)\right\|}{\overline{\Omega}^{m-2}}=\sqrt{\overline{\Omega}^{2m}+A^2\overline{\Omega}^4+2A\cos\beta\overline{\Omega}^{m+2}}\Big/\overline{\Omega}^m \tag{4.23}$$

$$FD(\overline{\Omega})=A/\left(K\overline{\Omega}^m\right) \tag{4.24}$$

$$FF(\overline{\Omega})=\frac{\left\|A\overline{\Omega}^2\sin(\overline{\Omega}\tau+\beta)+\overline{\Omega}^m\sin(\overline{\Omega}\tau)\right\|}{\overline{\Omega}^m}=\sqrt{\overline{\Omega}^{2m}+A^2\overline{\Omega}^4+2A\cos\beta\overline{\Omega}^{m+2}}\Big/\overline{\Omega}^m \tag{4.25}$$

where the sign $\|\ \|$ represents the vibration amplitude.

Consequently, the approximating error due to $\hat{e}(\tau)\neq e(\tau)$ can be obtained as

$$\begin{aligned}\varepsilon(\tau)=&A\left(1-\overline{\Omega}^2\right)\sin(\overline{\Omega}\tau+\beta)+\xi_1\overline{\Omega}A\cos(\overline{\Omega}\tau+\beta) \\ &+\xi_a\overline{\Omega}^aA^a\left|\cos(\overline{\Omega}\tau+\beta)\right|^a\cdot\operatorname{sign}\left(\cos(\overline{\Omega}\tau+\beta)\right)-\overline{\Omega}^m\sin(\overline{\Omega}\tau)\end{aligned} \tag{4.26}$$

Define an auxiliary function

$$E(\overline{\Omega}\tau,\beta,a)=\left|\cos(\overline{\Omega}\tau+\beta)\right|^{a}\cdot\operatorname{sign}\left(\cos(\overline{\Omega}\tau+\beta)\right) \tag{4.27}$$

to rewrite Eq.(4.26) as

$$\begin{aligned}\varepsilon(\tau)=&A\left(1-\overline{\Omega}^{2}\right)\sin(\overline{\Omega}\tau+\beta)+\xi_1\overline{\Omega}A\cos(\overline{\Omega}\tau+\beta)\\&+\xi_a\overline{\Omega}^{a}A^{a}E(\overline{\Omega}\tau,\beta,a)-\overline{\Omega}^{m}\sin(\overline{\Omega}\tau)\end{aligned} \tag{4.28}$$

The integral error of the approximating solution over an interval $[a,b]$ is given by

$$J=\int_a^b\varepsilon^{2}(\tau)d\tau \tag{4.29}$$

Then A and β in Eq.(4.22) can be determined from the following equations

$$\begin{cases}\dfrac{\partial J}{\partial A}=\displaystyle\int_a^b 2\varepsilon(\tau)\cdot\frac{\partial\varepsilon}{\partial A}d\tau=0\\[2ex]\dfrac{\partial J}{\partial\beta}=\displaystyle\int_a^b 2\varepsilon(\tau)\cdot\frac{\partial\varepsilon}{\partial\beta}d\tau=0\end{cases} \tag{4.30}$$

Because a harmonic excitation is considered, choose $a=0$ and $b=2\pi$, and rewrite Eq.(4.30) as

$$\begin{cases}\dfrac{\partial J}{\partial A}=2\displaystyle\int_0^{2\pi}\left[A\left(1-\overline{\Omega}^{2}\right)\sin(\overline{\Omega}\tau+\beta)+\xi_1\overline{\Omega}A\cos(\overline{\Omega}\tau+\beta)+\xi_a\overline{\Omega}^{a}A^{a}E(\overline{\Omega}\tau,\beta,a)-\overline{\Omega}^{m}\sin(\overline{\Omega}\tau)\right]\times\\\qquad\left[\left(1-\overline{\Omega}^{2}\right)\sin(\overline{\Omega}\tau+\beta)+\xi_1\overline{\Omega}\cos(\overline{\Omega}\tau+\beta)+\xi_a\overline{\Omega}^{a}(a)A^{a-1}E(\overline{\Omega}\tau,\beta,a)\right]d\left(\overline{\Omega}\tau+\beta\right)=0\\[2ex]\dfrac{\partial J}{\partial\beta}=2\displaystyle\int_0^{2\pi}\left[A\left(1-\overline{\Omega}^{2}\right)\sin(\overline{\Omega}\tau+\beta)+\xi_1\overline{\Omega}A\cos(\overline{\Omega}\tau+\beta)+\xi_a\overline{\Omega}^{a}A^{a}E(\overline{\Omega}\tau,\beta,a)-\overline{\Omega}^{m}\sin(\overline{\Omega}\tau)\right]\times\\\qquad\left[A\left(1-\overline{\Omega}^{2}\right)\cos(\overline{\Omega}\tau+\beta)-\xi_1\overline{\Omega}A\sin(\overline{\Omega}\tau+\beta)+\xi_a\overline{\Omega}^{a}A^{a}\dfrac{\partial E(\overline{\Omega}\tau,\beta,a)}{\partial\beta}\right]d\left(\overline{\Omega}\tau+\beta\right)=0\end{cases} \tag{4.31}$$

After some simplifying manipulations, Eq.(4.31) can further be written as

$$\begin{aligned}&\pi A\left(1-\overline{\Omega}^2\right)^2-\overline{\Omega}^m\left(1-\overline{\Omega}^2\right)\pi\cos\beta+\xi_1^2\overline{\Omega}^2A\pi+\xi_1\overline{\Omega}^{m+1}\pi\sin\beta\\&+\xi_a\int_0^{2\pi}\begin{bmatrix}(a+1)\overline{\Omega}^aA^a\left(1-\overline{\Omega}^2\right)E(\overline{\Omega}\tau,\beta,a)\sin(\overline{\Omega}\tau+\beta)\\+\xi_1(a+1)\overline{\Omega}^{a+1}A^aE(\overline{\Omega}\tau,\beta,a)\cos(\overline{\Omega}\tau+\beta)\\+\xi_a\overline{\Omega}^{2a}(a)A^{2a-1}E^2(\overline{\Omega}\tau,\beta,a)\\-\overline{\Omega}^{a+m}(a)A^{a-1}E(\overline{\Omega}\tau,\beta,a)\sin(\overline{\Omega}\tau)\end{bmatrix}d\left(\overline{\Omega}\tau+\beta\right)=0\end{aligned}\tag{4.32}$$

and

$$\begin{aligned}&\overline{\Omega}^m\left(1-\overline{\Omega}^2\right)A\pi\sin\beta+\xi_1\overline{\Omega}^{m+1}A\pi\cos\beta\\&+\xi_a\int_0^{2\pi}\begin{bmatrix}\overline{\Omega}^a\left(1-\overline{\Omega}^2\right)A^{a+1}E(\overline{\Omega}\tau,\beta,a)\cos(\overline{\Omega}\tau+\beta)\\-\xi_1\overline{\Omega}^{a+1}A^{a+1}E(\overline{\Omega}\tau,\beta,a)\sin(\overline{\Omega}\tau+\beta)\\+\overline{\Omega}^a\left(1-\overline{\Omega}^2\right)A^{a+1}\dfrac{\partial E(\overline{\Omega}\tau,\beta,a)}{\partial\beta}\sin(\overline{\Omega}\tau+\beta)\\+\xi_1\overline{\Omega}^{a+1}A^{a+1}\dfrac{\partial E(\overline{\Omega}\tau,\beta,a)}{\partial\beta}\cos(\overline{\Omega}\tau+\beta)\\+\xi_a\overline{\Omega}^{2a}A^{2a}\dfrac{\partial E(\overline{\Omega}\tau,\beta,a)}{\partial\beta}E(\overline{\Omega}\tau,\beta,a)\\-\overline{\Omega}^{a+m}A^a\dfrac{\partial E(\overline{\Omega}\tau,\beta,a)}{\partial\beta}\sin(\overline{\Omega}\tau)\end{bmatrix}d\left(\overline{\Omega}\tau+\beta\right)=0\end{aligned}\tag{4.33}$$

which can be further reduced to

$$\begin{cases}\left(\left(1-\overline{\Omega}^2\right)^2+\xi_1^2\overline{\Omega}^2\right)A-\overline{\Omega}^m\left(1-\overline{\Omega}^2\right)\cos\beta+\xi_1\overline{\Omega}^{m+1}\sin\beta\\+\xi_a\xi_1(a+1)\overline{\Omega}^{a+1}A^aJ(a+1)+a\xi_a^2\overline{\Omega}^{2a}A^{2a-1}J(2a)+a\xi_a\overline{\Omega}^{a+m}A^{a-1}\sin\beta J(a+1)=0\\\left(\overline{\Omega}^m\left(1-\overline{\Omega}^2\right)\sin\beta+\xi_1\overline{\Omega}^{m+1}\cos\beta\right)\\+\xi_a\overline{\Omega}^a\left(1-\overline{\Omega}^2\right)A^a\left((a+1)J(a+1)-aJ(a-1)\right)+a\xi_a\cos\beta\overline{\Omega}^{a+m}A^{a-1}\left(J(a-1)-J(a+1)\right)=0\end{cases}\tag{4.34}$$

where $J(a)=\dfrac{4}{\pi}\cdot\int_0^{\pi/2}\cos^a x\,dx$.

Define $x=A>0$, $y=\cos\beta$ and $z=\sin\beta$. Substituting $A=x$, $\cos\beta=y$ and $\sin\beta=z$ into Eq.(4.34) yields

$$\begin{cases} \left(\left(1-\overline{\Omega}^2\right)^2+\xi_1^2\overline{\Omega}^2\right)x-\overline{\Omega}^m\left(1-\overline{\Omega}^2\right)y+\xi_1\overline{\Omega}^{m+1}z \\ +\xi_a\xi_1(a+1)\overline{\Omega}^{a+1}J(a+1)x^a+a\xi_a^2\overline{\Omega}^{2a}J(2a)x^{2a-1}+a\xi_a\overline{\Omega}^{a+m}J(a+1)x^{a-1}z=0 \\ \left(\overline{\Omega}^m\left(1-\overline{\Omega}^2\right)z+\xi_1\overline{\Omega}^{m+1}y\right)+\xi_a\overline{\Omega}^a\left(1-\overline{\Omega}^2\right)\left((a+1)J(a+1)-aJ(a-1)\right)x^a \\ +a\xi_a\overline{\Omega}^{a+m}\left(J(a-1)-J(a+1)\right)x^{a-1}y=0 \\ y^2+z^2=1 \end{cases} \tag{4.35}$$

When $a\geq 1$, Eq.(4.35) becomes

$$\begin{cases} \left(\left(1-\overline{\Omega}^2\right)^2+\xi_1^2\overline{\Omega}^2\right)x-\overline{\Omega}^m\left(1-\overline{\Omega}^2\right)y+\xi_1\overline{\Omega}^{m+1}z \\ +\xi_a\xi_1(a+1)\overline{\Omega}^{a+1}J(a+1)x^a+a\xi_a^2\overline{\Omega}^{2a}J(2a)x^{2a-1}+a\xi_a\overline{\Omega}^{a+m}J(a+1)x^{a-1}z=0 \\ \left(\overline{\Omega}^m\left(1-\overline{\Omega}^2\right)z+\xi_1\overline{\Omega}^{m+1}y\right)+\xi_a\overline{\Omega}^a\left(1-\overline{\Omega}^2\right)\left((a+1)J(a+1)-aJ(a-1)\right)x^a \\ +a\xi_a\overline{\Omega}^{a+m}\left(J(a-1)-J(a+1)\right)x^{a-1}y=0 \\ y^2+z^2=1 \end{cases} \tag{4.36}$$

When $0\leq a<1$, because $J(a-1)=\dfrac{4}{\pi}\cdot\int_0^{\pi/2}\dfrac{1}{\cos^{1-a}x}dx\to+\infty$, Eq.(4.35) can be written as

$$\begin{cases} \left(\left(1-\overline{\Omega}^2\right)^2+\xi_1^2\overline{\Omega}^2\right)x-\overline{\Omega}^m\left(1-\overline{\Omega}^2\right)y+\xi_1\overline{\Omega}^{m+1}z \\ +\xi_a\xi_1(a+1)\overline{\Omega}^{a+1}J(a+1)x^a+a\xi_a^2\overline{\Omega}^{2a}J(2a)x^{2a-1}+a\xi_a\overline{\Omega}^{a+m}J(a+1)x^{a-1}z=0 \\ -\left(1-\overline{\Omega}^2\right)x+\overline{\Omega}^m y=0 \\ y^2+z^2=1 \end{cases} \tag{4.37}$$

Therefore,

$$DD(\overline{\Omega})=\sqrt{\overline{\Omega}^{2m}+A^2\overline{\Omega}^4+2A\cos\beta\overline{\Omega}^{m+2}}\Big/\overline{\Omega}^m=\sqrt{\overline{\Omega}^{2m}+x^2\overline{\Omega}^4+2xy\overline{\Omega}^{m+2}}\Big/\overline{\Omega}^m \tag{4.38}$$

$$FD(\overline{\Omega})=A/\left(K\overline{\Omega}^m\right)=x/\left(K\overline{\Omega}^m\right) \tag{4.39}$$

$$FF(\overline{\Omega})=\sqrt{\overline{\Omega}^{2m}+A^2\overline{\Omega}^4+2A\cos\beta\overline{\Omega}^{m+2}}\Big/\overline{\Omega}^m=\sqrt{\overline{\Omega}^{2m}+x^2\overline{\Omega}^4+2xy\overline{\Omega}^{m+2}}\Big/\overline{\Omega}^m \tag{4.40}$$

where x and y can be determined from Eq.(4.36) or Eq.(4.37). Thus **Proposition 1** is proved.

From **Proposition 1**, the transmissibility of the SDOF vibration systems at any frequency of concern can be determined from system time domain model parameters. Eqs.(4.20) and (4.21) are both typical transcendental equations whose solutions can be found using graphical or numerical methods such as Bisection, Newton-Raphson, and Regula Falsi methods. In the present study, the "solve" command in the Matlab software is used to find x and y from Eqs.(4.20) and (4.21). Obviously, the Ritz-Galerkin method based procedure can readily be applied to evaluate the system force and/or displacement transmissibility so as to facilitate the analysis and design of the effects of nonlinear damping characteristic parameters on the performance of the vibration systems.

4.3.4 Verification of the transmissibility evaluation

In order to verify the effectiveness of the Ritz-Galerkin based transmissibility evaluation method for the DVIS and FVIS given by **Proposition 1**, comparisons were made between the numerically evaluated DVIS and FVIS transmissibility and the results analytically determined from **Proposition 1** for the cases where $M = 10\,\text{kg}$, $K = 4000\,\text{N/m}$, $n = 0$, linear damping coefficient $C_1 = 20\,\text{Ns/m}$ ($\xi_1 = 0.1$) and the viscous damping characteristic parameters a and C_a are chosen over a range of values. The results are shown in Figs.4.3 and 4.4, for the transmissibility of DVIS and FVIS, respectively.

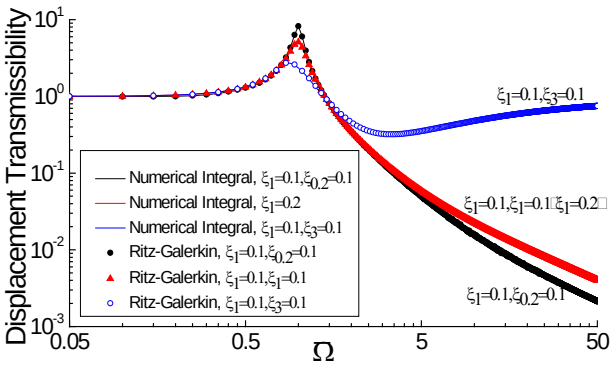

Fig.4.3 Comparisons between the numerically and analytically evaluated displacement transmissibility of a DVIS with a fluid viscous damper

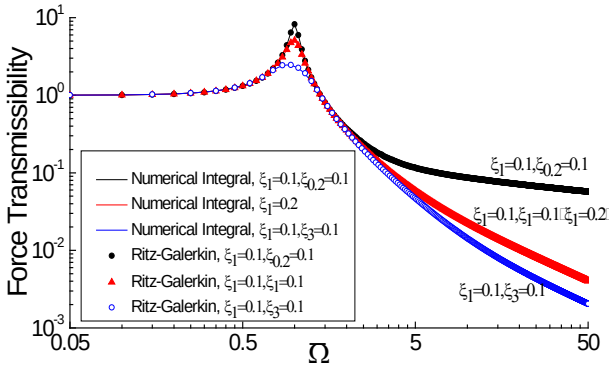

Fig.4.4 Comparisons between the numerically and analytically evaluated force transmissibility of a FVIS with a fluid viscous damper

These results clearly indicate an excellent agreement between the results obtained by the two different techniques, and therefore demonstrate the effectiveness of the Ritz-Galerkin method based analytical solutions in **Proposition 1**.

4.3.5 The effects of nonlinear viscous damping on the force and displacement transmissibility

In order to study the effects of different linear and nonlinear viscous damping characteristic parameters on the force and displacement transmissibility of SDOF vibration isolation systems that can be uniformly described by Eq.(4.16), the displacement-displacement transmissibility $DD(\overline{\Omega})$ in DVIS and force-force transmissibility $FF(\overline{\Omega})$ in FVIS in the case of $n=0$ are evaluated using **Proposition 1** for different types of fluid viscous dampers over the frequency region from $\overline{\Omega}=0.05$ to $\overline{\Omega}=50$. The results are shown in Figs.4.5-4.8. Figs.4.5 and 4.6 show the effects of linear viscous damping characteristics on the system displacement and force transmissibility. Figs.4.7 and 4.8 show the effects of different nonlinear viscous damping characteristics on the system transmissibility. In addition, for the harmonic excitations at the frequencies of $\overline{\Omega}=1$ (the resonance frequency) and $\overline{\Omega}=50$ (a higher

frequency), the displacement and/or force transmissibility in DVIS and FVIS are evaluated under different system damping characteristic parameters and loading conditions. These results are shown in Figs.4.9-4.17.

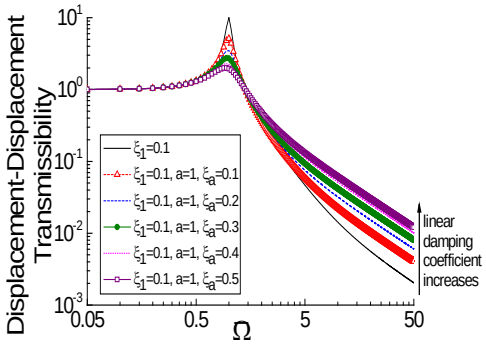

Fig.4.5 Effects of linear viscous damping characteristics on $DD(\overline{\Omega})$ in DVIS when $n=0$

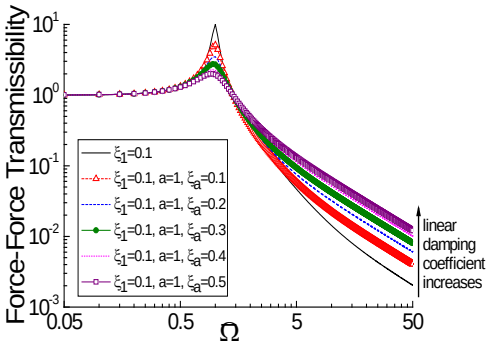

Fig.4.6 Effects of linear viscous damping characteristics on $FF(\overline{\Omega})$ in FVIS when $n=0$

The results in Figs.4.5 and 4.6 reveal a dilemma associated with the design of linear viscously damped vibration systems: the increase of linear viscous damping reduces the system transmissibility at the resonance frequency $\overline{\Omega}=1$, but increases the system transmissibility over the high frequency region, which is detrimental for the system vibration performance.

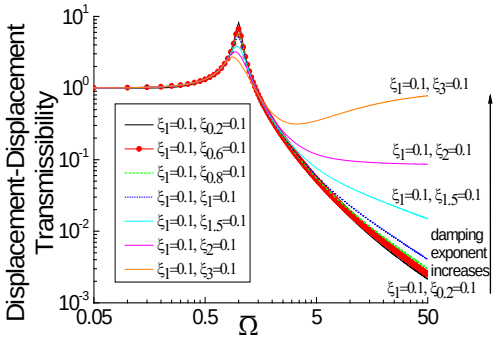

Fig.4.7 Effects of nonlinear viscous damping characteristics on $DD(\overline{\Omega})$ in DVIS when $n=0$

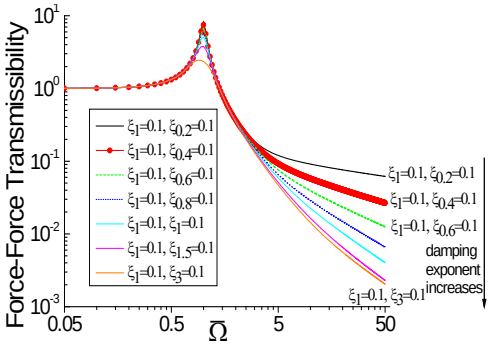

Fig.4.8 Effects of nonlinear viscous damping characteristics on $FF(\overline{\Omega})$ in FVIS when $n=0$

It can be observed from Figs.4.7 and 4.8 that the effects of the damping coefficient ξ_a of different types of nonlinear fluid viscous dampers on the

displacement-displacement transmissibility $DD(\overline{\Omega})$ in DVIS and force-force transmissibility $FF(\overline{\Omega})$ in FVIS are different. Comparing with the linear fluid viscous damper case, for the displacement vibration isolation in DVIS, a more ideal damping effect can be achieved when $a<1$, that is, when a lower-than-one power damping parameter is used. But, in this case, a viscous damping device with its power damping characteristic parameter $a>1$ is detrimental over higher frequency ranges. However the situations are completely different for the force vibration isolation in FVIS. In the FVIS case, a more ideal damping effect can be achieved when $a>1$, that is, when a higher-than-one power damping parameter is used, but a viscous damping device with power damping characteristic parameter $a<1$ is detrimental over higher frequency ranges. By an ideal damping effect performance, we mean in here that the damping only reduces the system transmissibility over the range of the system resonance frequency without a detrimental effect over other frequencies.

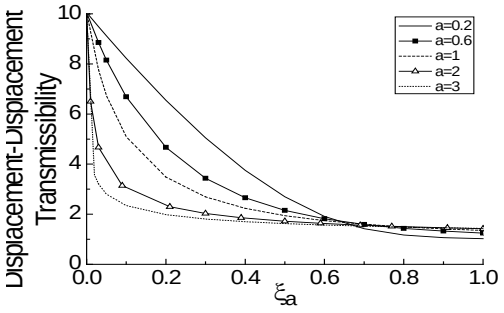

Fig.4.9 Effects of nonlinear damping parameters a and ξ_a on $DD(\overline{\Omega})$ in DVIS at $\overline{\Omega}=1$ when $n=0$

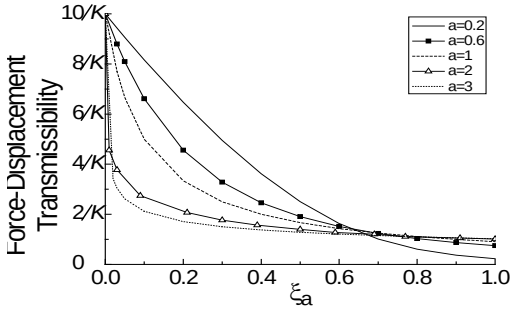

Fig.4.10 Effects of nonlinear damping parameters a and ξ_a on $FD(\overline{\Omega})$ in FVIS at $\overline{\Omega}=1$ when $n=0$

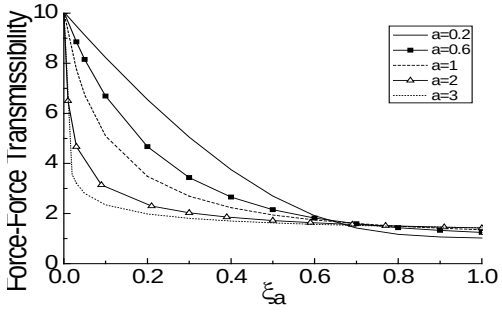

Fig.4.11 Effects of nonlinear damping parameters a and ξ_a on $FF(\overline{\Omega})$ in FVIS at $\overline{\Omega}=1$ when $n=0$

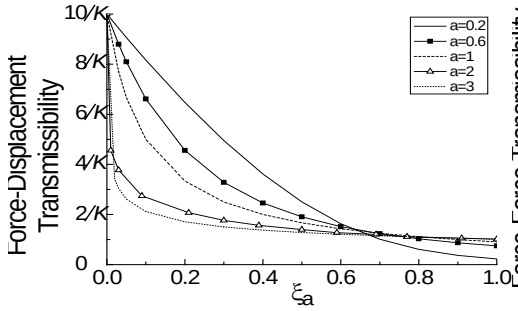

Fig.4.12 Effects of nonlinear damping parameters a and ξ_a on $FD(\overline{\Omega})$ in FVIS at $\overline{\Omega}=1$ when $n=2$

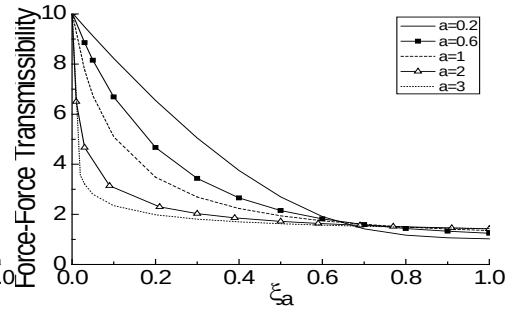

Fig.4.13 Effects of nonlinear damping parameters a and ξ_a on $FF(\overline{\Omega})$ in FVIS at $\overline{\Omega}=1$ when $n=2$

From the results in Figs.4.9-4.13, the effects of different types of fluid viscous dampers ($a<1$, $a=1$ and $a>1$) on the system vibration performance can further be observed. Basically, at the system resonance frequency ($\overline{\Omega}=1$), the displacement-displacement transmissibility in DVIS, and the force-force and force-displacement transmissibility in FVIS can significantly be reduced by an increase in the viscous damping coefficient ξ_a. The transmissibility can also be reduced by an increase in the power damping characteristic parameter a provided that $\xi_a \le 0.65$. However, over the region of higher frequencies (around $\overline{\Omega}=50$), the effects of ξ_a and a on the system transmissibility are much more complicated. These can be observed from Figs.4.14-4.17. It is worth pointing out that the effects of additional fluid viscous dampers on the system transmissibility between the resonant and higher frequencies are much more complicated and not considered in this thesis. Although these analysis results depend on the amplitude of the excitation, which is due to the nonlinear system characteristics, these results and conclusions have considerable significance and provide important guidelines for the analysis and design of nonlinear fluid viscous dampers to achieve a desired system vibration performance.

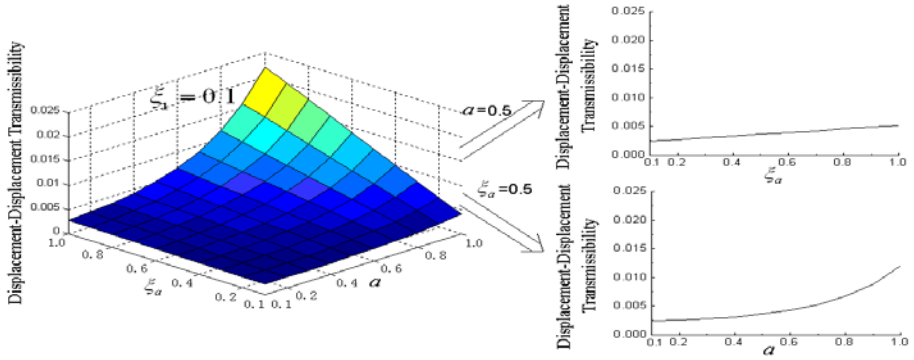

Fig.4.14 Effects of nonlinear damping parameters $a \in (0,1]$ and ξ_a on $DD(\overline{\Omega})$ in DVIS at $\overline{\Omega} = 50$ when $n = 0$

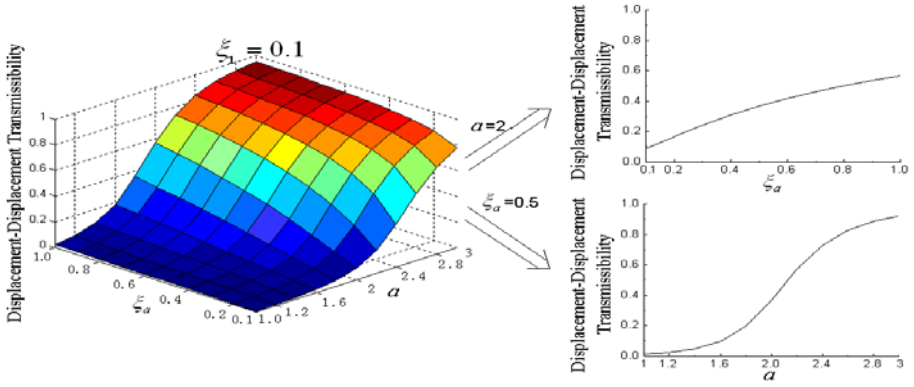

Fig.4.15 Effects of nonlinear damping parameters $a \in [1,3]$ and ξ_a on $DD(\overline{\Omega})$ in DVIS at $\overline{\Omega} = 50$ when $n = 0$

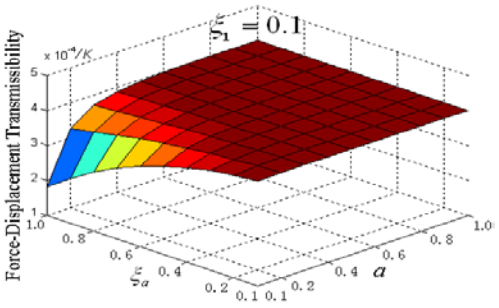

(a) when $a \in (0,1]$ and $n = 0$

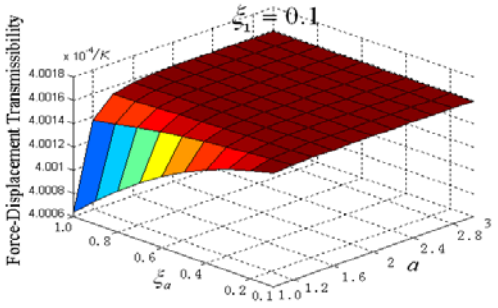

(b) when $a \in [1,3]$ and $n = 0$

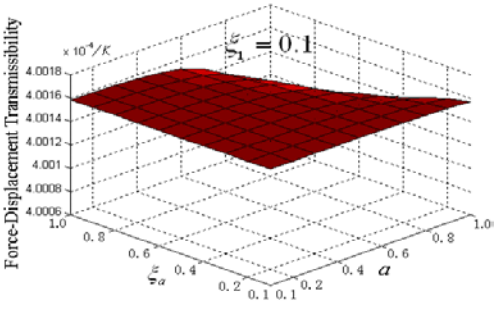

(c) when $a \in (0,1]$ and $n = 2$

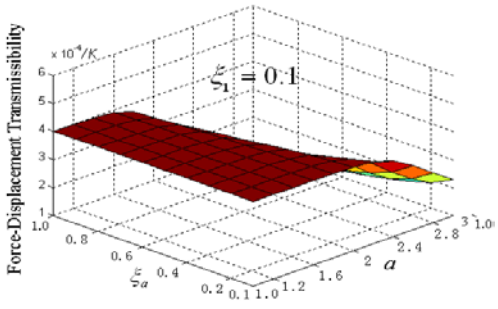

(d) when $a \in [1,3]$ and $n = 2$

Fig.4.16 Effects of nonlinear damping parameters a and ξ_a on $FD(\overline{\Omega})$ in FVIS at $\overline{\Omega} = 50$

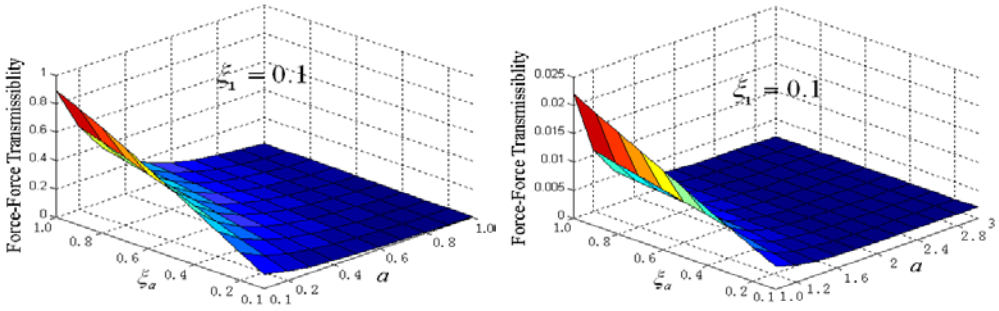

(a) when $a \in (0,1]$ and $n = 0$

(b) when $a \in [1,3]$ and $n = 0$

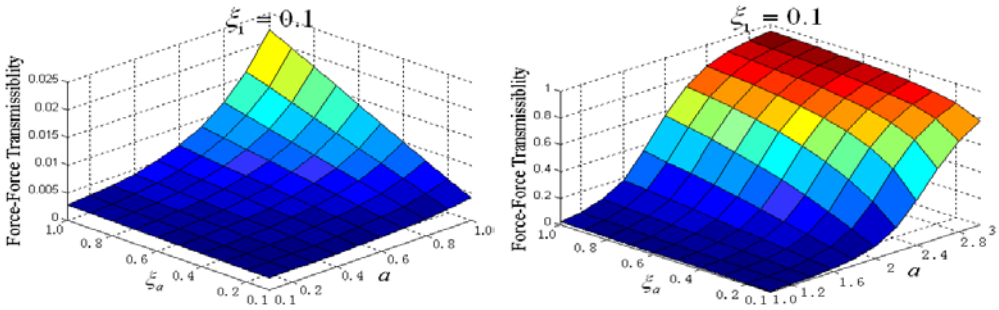

(c) when $a \in (0,1]$ and $n = 2$

(d) when $a \in [1,3]$ and $n = 2$

Fig.4.17 Effects of nonlinear damping parameters a and ξ_a on $FF(\overline{\Omega})$ in FVIS at $\overline{\Omega} = 50$

The results in Figs.4.14, 4.15, 4.16(a,b) and 4.17(a,b) indicate that:

- In the case of $n = 0$, for DVIS, when $a < 1$, an increase in the viscous damping coefficient ξ_a almost doesn't affect the system displacement-displacement transmissibility $DD(\overline{\Omega})$ at a higher frequency ($\overline{\Omega} = 50$).
- In the case of $n = 0$, for FVIS, when $a > 1$, an increase in ξ_a has almost no effect on the system force-displacement transmissibility $FD(\overline{\Omega})$ and force-force transmissibility $FF(\overline{\Omega})$ at a higher frequency ($\overline{\Omega} = 50$).
- In the case of $n = 0$, for FVIS, a nonlinear fluid viscous damper with the power damping characteristic parameter $a \le 0.3$ can reduce the system force-displacement transmissibility $FD(\overline{\Omega})$ at a higher frequency ($\overline{\Omega} = 50$) but will increase the force-force transmissibility $FF(\overline{\Omega})$ at the same frequency.

Figs.4.18-4.20 provide a much clearer 2-d illustration of these observations. From these results, it can be concluded that, over the whole frequency range, a nonlinear fluid viscous damper with $a \le 0.3$ is ideal for both the displacement-displacement transmissibility $DD(\overline{\Omega})$ of DVIS and the force-displacement $FD(\overline{\Omega})$ of FVIS in the case of $n = 0$; and a nonlinear fluid viscous damper with $a > 1$ is ideal for the force-force transmissibility $FF(\overline{\Omega})$ of FVIS in the case of $n = 0$ These results are all consistent with the conclusions achieved previously in [43, 47, 50, 177].

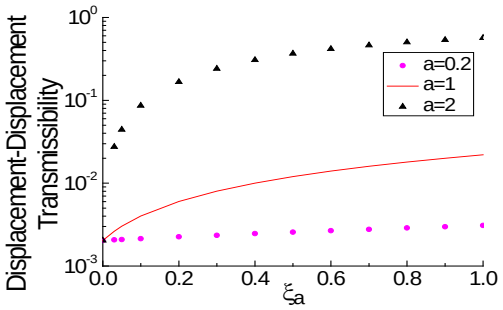

Fig.4.18 2-d illustration of effects of nonlinear damping parameters a and ξ_a on $DD(\overline{\Omega})$ in DVIS at $\overline{\Omega} = 50$ when $n = 0$

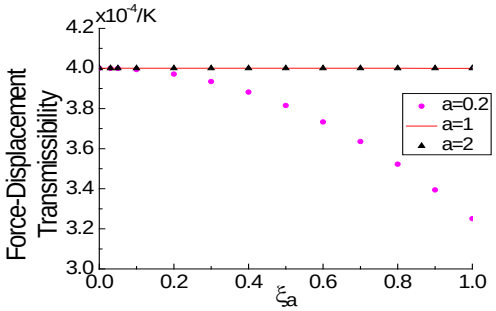

Fig.4.19 2-d illustration of effects of nonlinear damping parameters a and ξ_a on $FD(\overline{\Omega})$ in FVIS at $\overline{\Omega} = 50$ when $n = 0$

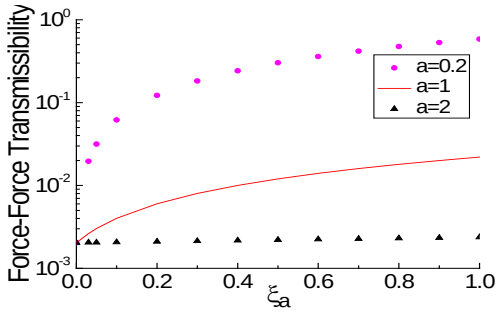

Fig.4.20 2-d illustration of effects of nonlinear damping parameters a and ξ_a on $FF(\overline{\Omega})$ in FVIS at $\overline{\Omega} = 50$ when $n = 0$

For the case of $n = 2$ in FVIS, Figs.4.16(c,d) and 4.17(c,d) indicate that:

- When $a \le 0.3$, an increase in the viscous damping coefficient ξ_a has almost no effect on the force-displacement transmissibility $FD(\overline{\Omega})$

and force-force transmissibility $FF(\overline{\Omega})$ at a higher frequency ($\overline{\Omega}=50$).

- When $a>1$, an increase in the viscous damping coefficient ξ_a will reduce the force-displacement transmissibility $FD(\overline{\Omega})$ but increase the force-force transmissibility $FF(\overline{\Omega})$ at a higher frequency ($\overline{\Omega}=50$).

Much clearer 2-d illustrations of these observations are shown in Figs.4.21 and 4.22. These results indicate that the power damping characteristic parameter a needs to be properly designed for the case of $n=2$ in FVIS to achieve desired vibration isolation. This is important for the reduction of vibrations induced by high-speed rotating machines such as washing machines and automobile engines etc..

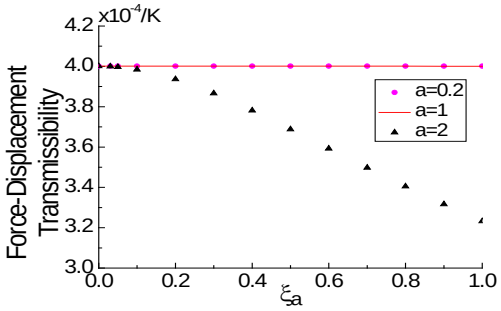

Fig.4.21 2-d illustration of effects of nonlinear damping parameters a and ξ_a on $FD(\overline{\Omega})$ in FVIS at $\overline{\Omega}=50$ when $n=2$

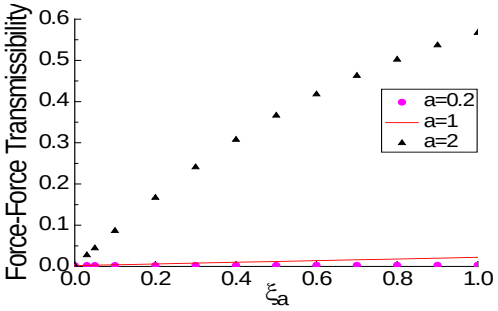

Fig.4.22 2-d illustration of effects of nonlinear damping parameters a and ξ_a on $FF(\overline{\Omega})$ in FVIS at $\overline{\Omega}=50$ when $n=2$

4.4 Design of nonlinear viscous damping parameters

Based on **Proposition 1**, a design procedure for nonlinear damping characteristic parameters in the SDOF DVIS and FVIS can be proposed as follows.

(i) Choose the range of the power damping characteristic parameter a to avoid obvious force or displacement transmissibility change over the range of higher frequencies according to the analysis in Section 4.3.5.

(ii) Rewrite the system equation in the dimensionless format as given in Eq.(4.16) and evaluate the effects of the damping characteristic parameters a and ξ_a on the system force and/or displacement transmissibility over the resonant and higher frequency regions using **Proposition 1**.

(iii) Find the appropriate values for the damping characteristic parameters a and ξ_a from the results in Step (ii) such that a design requirement for the system performance over both resonant and higher frequency regions can be met.

Two examples are provided below to demonstrate the practical applications and effectiveness of the above design procedure.

Example 1:

Consider a SDOF DVIS as shown in Fig.4.1, where $M = 10\,\text{kg}$, $K = 4000\,\text{N/m}$, $\xi_1 = 0.1$, the system resonant frequency $\omega_0 = \sqrt{K/M} = 20\,\text{rad/s}$. Without a nonlinear viscous damping device in the system, the displacement-displacement transmissibility at the resonant frequency ($\overline{\Omega} = 1$) and a higher frequency ($\overline{\Omega} = 50$) can be evaluated as $DD(1) = 10.05$ and $DD(50) = 2.04 \times 10^{-3}$, respectively. Consider the vibration isolation effects that can be achieved by additional fluid viscous dampers by numerical simulations, the design objective is defined as $DD(1) = DD^*(1) \le 3$ and $DD(50) = DD^*(50) \le 4 \times 10^{-3}$. This design objective can reduce the displacement-displacement transmissibility at the resonant frequency without significant increase at the higher frequency. Then a nonlinear fluid viscous damper can be designed as follows.

Following the design procedure, first, determine the range of the power damping

characteristic parameter a as $a<1$ because the displacement-displacement transmissibility of DVIS is to be suppressed in this case. Second, solve Eq.(4.21) to evaluate the system displacement-displacement transmissibility at $\overline{\Omega}=1$ and $\overline{\Omega}=50$ over a range of the damping characteristic parameters a and ξ_a such that $a\in[0.1,1]$ and $\xi_a\in[0,1]$ with $\xi_1=0.1$. The results are shown in Figs.4.23 and 4.24.

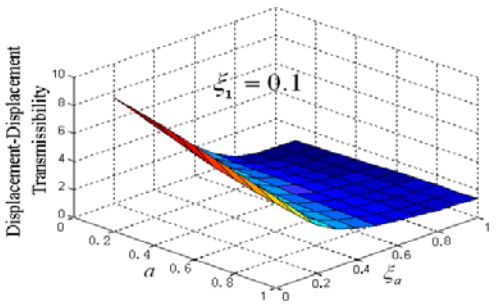

Fig.4.23 The effects of damping characteristic parameters a and ξ_a on $DD(\overline{\Omega})$ at the resonance frequency $\overline{\Omega}=1$ in Example 1

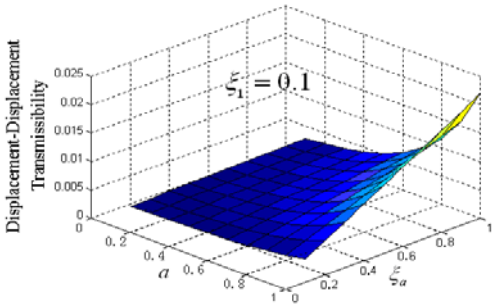

Fig.4.24 The effects of damping characteristic parameters a and ξ_a on $DD(\overline{\Omega})$ at a higher frequency $\overline{\Omega}=50$ in Example 1

From the results in Figs.4.23 and 4.24, the appropriate values of a and ξ_a which satisfy the design requirements $DD^*(1)\le 3$ and $DD^*(50)\le 4\times10^{-3}$ can be found. The results are shown in Fig.4.25. Consequently, $a=0.4$ and $\xi_a=0.5$ are determined as the final design. The system transmissibility under this design is $DD(1)=2.3$ and $DD(50)=3.1\times10^{-3}$, which clearly satisfies the design requirements. A comparison of the displacement-displacement transmissibility of the system with and without the designed nonlinear fluid viscous damper is shown in Fig.4.26. Notice that when a linear fluid viscous damper is used to achieve the same design requirement of $DD(1)=2.3$, $a=1$, the linear damping coefficient should be designed as $\xi_a=0.483$ using **Proposition 1**. In this case, the system transmissibility at the higher frequency of $\overline{\Omega}=50$ is $DD(50)=9.67\times10^{-3}$, which is clearly larger than the transmissibility value that can be achieved by the nonlinear fluid viscous damper

designed above.

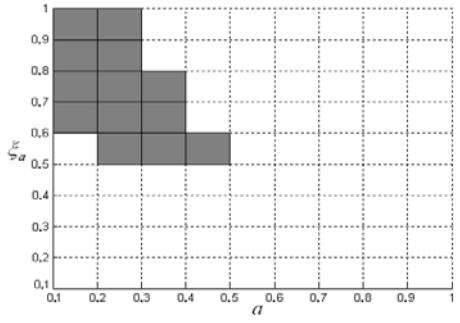

Fig.4.25 a and ξ_a which satisfy the design requirements in the case of Example 1

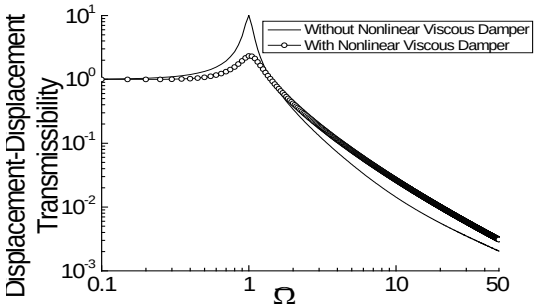

Fig.4.26 A comparison of $DD(\overline{\Omega})$ of the systems with and without a designed nonlinear fluid viscous damper in the case of Example 1

Example 2:

Consider the SDOF engine vibration suspension system in [179] and replace the semi-active control device with a nonlinear fluid viscous damper in this case study. The engine vibration suspension system can obviously be described by the SDOF FVIS model in Fig.4.2. The system equation can be written as:

$$M\ddot{x}(t) + Kx(t) + C_1\dot{x}(t) + C_a\left|\dot{x}(t)\right|^a \cdot \mathrm{sign}\left(\dot{x}(t)\right) = m_e r\omega^2 \sin(\omega t) \qquad (4.41)$$

where $M = 50\,\mathrm{kg}$ is the mass of the engine and platform, $K = 83300\,\mathrm{N/m}$ is the equivalent spring stiffness, $C_1 = 204\,\mathrm{Ns/m}$ ($\xi_1 = 0.1$) is the linear damping coefficient associated with the spring, $m_e = 1\mathrm{kg}$ is the eccentric mass of the engine, $r = 0.05\,\mathrm{m}$ is the eccentric radius. Without a nonlinear viscous damping device, the force-displacement and force-force transmissibility of the system at the resonance frequency ($\overline{\Omega} = 1$) and a higher frequency ($\overline{\Omega} = 50$) are $FD(1) = 10/K$, $FD(50) = 4.0016\times10^{-4}/K$, $FF(1) = 10.05$ and

$FF(50) = 2.04 \times 10^{-3}$ respectively. A nonlinear fluid viscous damper is designed for the system in order to achieve a desired vibration performance in terms of the suppression of both displacement and force vibrations. Consider the vibration isolation effects that can be achieved by additional fluid viscous dampers by numerical simulations, the design objectives are specified as

$FD^*(1) \le 4/K$, $FD^*(50) \le 4.1 \times 10^{-4}/K$, $FF^*(1) \le 4$ and $FF^*(50) \le 2.6 \times 10^{-3}$

Firstly, from the analysis results for the case of $n = 2$ in FVIS, it is known that when both the force-displacement and force-force transmissibility is to be considered, the range of power damping characteristic parameter a that should be used is $a \le 0.3$. This range of a can avoid a significant increase of the displacement and force vibration amplitude over higher frequencies. Secondly, solve Eq.(4.21) to evaluate the force-displacement and force-force transmissibility at $\overline{\Omega} = 1$ and $\overline{\Omega} = 50$ over a range of the damping characteristic parameters a and ξ_a such that $a \in [0.05, 0.3]$ and $\xi_a \in [0.1, 1]$ with $\xi_1 = 0.1$. The results are shown in Figs.4.27 to 4.30.

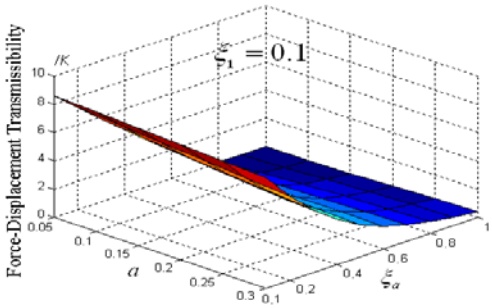

Fig.4.27 The effects of damping characteristic parameters a and ξ_a on $FD(\overline{\Omega})$ at the resonance frequency $\overline{\Omega} = 1$ in Example 2

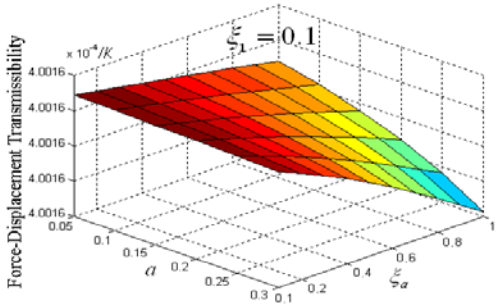

Fig.4.28 The effects of damping characteristic parameters a and ξ_a on $FD(\overline{\Omega})$ at a higher frequency $\overline{\Omega} = 50$ in Example 2

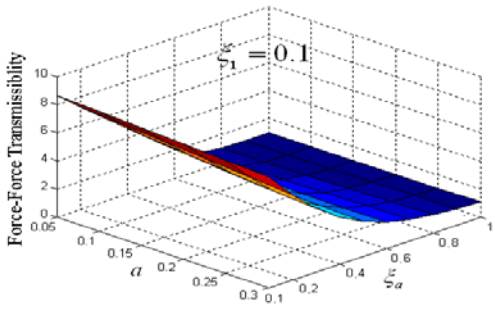

Fig.4.29 The effects of damping characteristic parameters a and ξ_a on $FF(\overline{\Omega})$ at the resonance frequency $\overline{\Omega}=1$ in Example 2

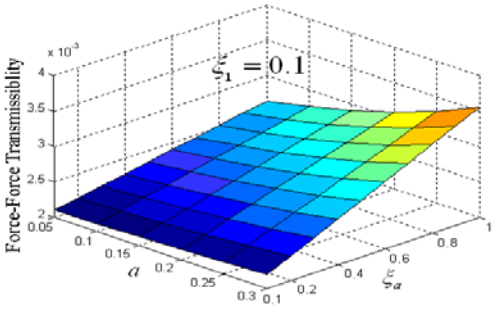

Fig.4.30 The effects of damping characteristic parameters a and ξ_a on $FF(\overline{\Omega})$ at a higher frequency $\overline{\Omega}=50$ in Example 2

From the evaluation results, it can be found that a smaller a makes less effect on the force-force transmissibility at the higher frequency $\overline{\Omega}=50$. Consider to meet the design objectives for both the force-displacement and force-force transmissibility, $a=0.2$ and $\xi_a=0.4$ are eventually chosen as the final design.

The system transmissibility under this design is $FD(1)=3.6/K$, $FD(50)=4\times10^{-4}/K$, $FF(1)=3.8$ and $FF(50)=2.5\times10^{-3}$. A comparison of the force-displacement and force-force transmissibility of the systems with and without the designed nonlinear fluid viscous damper is shown in Figs.4.31 and 4.32, respectively.

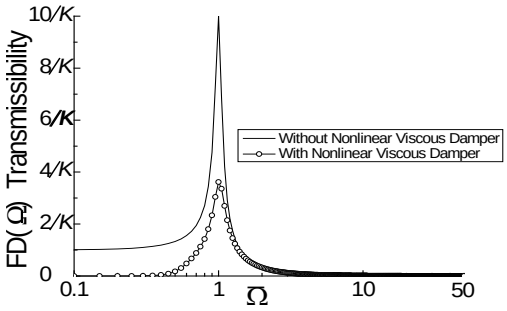

Fig.4.31 Comparison of $FD(\overline{\Omega})$ of the systems with and without a designed nonlinear fluid viscous damper in Example 2

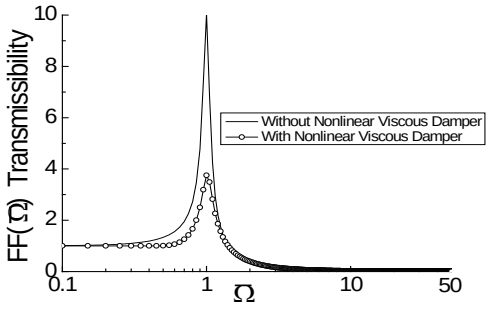

Fig.4.32 Comparison of $FF(\overline{\Omega})$ of the systems with and without a designed nonlinear fluid viscous damper in Example 2

When a linear fluid viscous damper is used to achieve the same design requirement of $FF(1)=3.8$. It is known that $a=1$ and the linear damping coefficient can be determined as $\xi_a=0.173$. In this case, the other system transmissibility results are $FD(1)=3.66/K$, $FD(50)=4\times10^{-4}/K$, $FF(50)=5.48\times10^{-3}$ indicating that the overall performance of the system is obviously worse than what can be achieved by the above designed nonlinear fluid viscous damper.

Figs.4.26, 4.31 and 4.32 and the comparisons between the overall performances that can be achieved by a nonlinear damper design and an equivalent linear damper design clearly show that an appropriately designed nonlinear fluid viscous damper can reduce the system transmissibility around the resonant frequency without a significant increase in the transmissibility over the higher frequency region. Therefore, the three step design procedure proposed in this chapter can be applied to effectively achieve such desired design objectives.

4.5 Conclusions

In this chapter, the force and displacement transmissibility of nonlinear fluid viscous damper based SDOF vibration systems have been studied using the Ritz-Galerkin method. General harmonic loading conditions have been considered such that the loading amplitude is proportional to the driving frequency raised to an arbitrary power. This covers a range of practical loading conditions. The results reveal that:

- For SDOF DVIS, when the exponent parameter of the input excitation $n=0$, the power damping characteristic parameter $a\le0.3$ is more effective for the suppression of the displacement transmissibility at both the resonant and higher frequencies;
- For SDOF FVIS, when $n=0$, an ideal damping effect in terms of

suppressing the system force transmissibility can be achieved when choosing $a > 1$; For the reduction of the displacement vibration, a fluid viscous damper with the parameter $a \leq 0.3$ should be used;

- For SDOF FVIS, when $n = 2$, $a > 1$ is more ideal to suppress the displacement vibration at both the resonant and higher frequencies; For the reduction of the force vibration transmitted to the foundation, a fluid viscous damper with the parameter $a \leq 0.3$ should be used.

These conclusions significantly extend the results in previous nonlinear damping studies as reported in [43, 47, 50]. Based on these new analyses, a design procedure for nonlinear damping characteristic parameters has been proposed, which provides an important guideline for the nonlinear fluid viscous damper type selection and parameters design in engineering practice. These results have significant implications for the analysis and design of vibration control systems in a wide range of practical applications.

Although only the SDOF DVIS and FVIS with a viscous damping device are considered in this chapter, the principle of the Ritz-Galerkin method based evaluation and analysis approach can be applied to the analysis and design of more general nonlinearly damped structural systems including automotive engine suspension systems, washing machines, civil buildings, and tower structures. In order to extend the analysis and design principle to complicated structural systems, the issue of more involved computations has to be addressed.

The results in this chapter reveal the potential of nonlinear fluid viscous dampers in the system vibration control and demonstrate that nonlinear fluid viscous dampers can perform better vibration control effects than linear fluid viscous dampers. However, nonlinear damping designs are much more difficult for more complicated structural systems in engineering practice where a large amount of complicated computations are involved if the technique proposed in

this chapter is directly applied. To solve this problem, the relationship between the structural system vibration response and characteristic parameters of additionally fitted nonlinear dampers will be studied in following chapters when the systems are in different loading conditions. Nonlinear frequency analysis and design approaches that have recently been developed at Sheffield [24, 43, 47] will be applied to conduct the analysis and design for the system vibration control purpose.

Chapter 5

Output Frequency Response Function (OFRF) of Viscously Damped Vibration Systems

In this chapter, the Output Frequency Response Function (OFRF) concept is applied to the analysis and design of viscously damped vibration systems which can be described by an anti-symmetric nonlinear differential equation model. The explicit analytical OFRF expression for the relationship between the system output frequency response and nonlinear viscous damping parameters is derived. The effectiveness of the OFRF representation is verified by numerical simulations of a 2DOF force vibration system. Using the OFRF representation, the effects of damping characteristic parameters of fluid viscous dampers on the transmissibility of viscously damped vibration systems are discussed. Based on these results, an OFRF based approach for the fluid viscous dampers design is proposed to achieve desired system vibration control performance and the effectiveness of this approach is verified by a case study.

5.1 Introduction

The analysis and design of damping devices for linear vibration systems have been widely studied in literatures [17, 20, 25, 163] and the results reveal that the design criteria and indices can be explicitly related to the linear damping characteristic parameters [5]. However, because of the limitations of linear damping in the vibration control of engineering systems as introduced in Chapter 2, more and more researchers [5, 111, 150] have recognized the necessity and feasibility of using nonlinear damping in vibration systems as introduced in Chapter 3. These results have proved that properly designed

nonlinear damping devices can provide more ideal suppression effects on the system vibration responses. Therefore, the analysis and design of characteristic parameters of nonlinear damping devices have been a significant problem for the system vibration control purpose in recent years [5].

However, the analysis and design of nonlinearly damped systems are far more complicated than that in the linear systems. The frequency domain analysis and design approaches of linear systems cannot easily be extended to nonlinear cases [24]. Traditional analysis and design approaches for nonlinear systems involve complicated computations [103, 151-155]. In order to resolve these problems, many analysis and design approaches for nonlinear systems have been proposed as introduced in Chapter 3. As a recently proposed frequency analysis approach for nonlinear systems by Lang et al. [24, 42, 47, 113, 114], the OFRF concept provides an explicit analytical expression for the relationship between the system output frequency response and the parameters which define the system nonlinearity. Its effectiveness has been verified by both numerical simulations and experimental tests [114, 180]. Different from other nonlinear system analysis approaches, the OFRF concept shows how the system output frequency response can be analytically related to the nonlinear system parameters [24]. This can considerably facilitate the design of these parameters to achieve a desired system performance.

This chapter focuses on the development of a new OFRF based nonlinear fluid viscous damper design approach. For this purpose, the OFRF representation of the output frequency response of a class of nonlinear viscously damped vibration systems is derived; both the viscous damping coefficient and exponent are considered as the system parameters to be designed. The effectiveness of the OFRF representation is then verified by numerical simulation studies on a SDOF force vibration system. After that, the effects of damping characteristic parameters of nonlinear fluid viscous dampers on the transmissibility of

nonlinearly damped MDOF Displacement Vibration Isolation System (DVIS) and Force Vibration Isolation System (FVIS) are investigated using the OFRF based method. Finally, a four-step procedure is proposed based on the OFRF concept to facilitate the design of nonlinear damping parameters for a desired system vibration performance. These results have significant implications and provide an important basis for the analysis and design of nonlinear damping characteristic parameters for a wide class of vibration control applications.

5.2 The OFRF of viscously damped vibration systems

5.2.1 Viscously damped vibration systems

Consider the class of nonlinear systems which can be described by a polynomial form, anti-symmetric nonlinear differential equation such that

$$\sum_{m=1}^{\bar{M}}\sum_{\substack{p=0\\p+q=m}}^{m}\sum_{l_1^{(p,q)},\cdots,l_{p+q}^{(p,q)}=0}^{\bar{L}}\bar{c}_{pq}(l_1^{(p,q)},\cdots,l_{p+q}^{(p,q)};g_1^{(p,q,l)},\cdots,g_{p+q}^{(p,q,l)}) \times\prod_{i=1}^{p}\left|D^{l_i^{(p,q)}}y(t)\right|^{g_i^{(p,q,l)}}\cdot\operatorname{sign}\left(D^{l_i^{(p,q)}}y(t)\right)\cdot\prod_{j=p+1}^{p+q}\left|D^{l_j^{(p,q)}}u(t)\right|^{g_j^{(p,q,l)}}\cdot\operatorname{sign}\left(D^{l_j^{(p,q)}}u(t)\right)=0 \tag{5.1}$$

where the operator D is defined by $D^l x(t)=\mathrm{d}^l x(t)/\mathrm{d}t^l$; $\bar{M}$ and $\bar{L}$ are the maximum degree of nonlinearity in terms of the system output $y(t)$ and input $u(t)$, and the maximum order of derivative, respectively; The coefficients $\bar{c}_{pq}(l_1^{(p,q)},\cdots,l_{p+q}^{(p,q)};g_1^{(p,q,l)},\cdots,g_{p+q}^{(p,q,l)})$, where $l=(l_1^{(p,q)},\cdots,l_{p+q}^{(p,q)})$, represents the parameters of the system, $g_i^{(p,q,l)}\geq 0$ and $g_j^{(p,q,l)}\geq 0$ are the exponents of $\left|D^{l_i^{(p,q)}}y(t)\right|$ and $\left|D^{l_j^{(p,q)}}u(t)\right|$, respectively. Note that an different (p,q) and an associated $l=(l_1^{(p,q)},\cdots,l_{p+q}^{(p,q)})$ identify a differential term in Eq.(5.1). When $p=1,q=0,l_1=1$ or $p=0,q=1,l_1^{(0,1)}=1$, for example, the general term in Eq.(5.1) becomes

$$\bar{c}_{1,0}(1; g_1^{(1,0,1)}) \cdot \left| D^1 y(t) \right|^{g_1^{(1,0,1)}} \cdot \text{sign}\left(D^1 y(t) \right) \tag{5.2}$$

or

$$\bar{c}_{0,1}(1; g_1^{(0,1,1)}) \cdot \left| D^1 u(t) \right|^{g_1^{(0,1,1)}} \cdot \text{sign}\left(D^1 u(t) \right) \tag{5.3}$$

Clearly, Eqs.(5.2) or (5.3) can represent the damping force

$$F_{\text{D}} = C_a \left| \dot{u}_r \right|^a \text{sign}(\dot{u}_r) \tag{5.4}$$

produced by a viscous damping device, where C_a and a are the viscous damping coefficient and exponent, respectively. $\dot{u}_r$ is the relative velocity between the two ends of the damping device [46, 65, 103]. In these cases, Eq.(5.1) can be used to represent vibration systems with nonlinear viscous damping devices that have been widely used in practical engineering systems [5, 9, 12].

For example, two widely used mechanical systems with nonlinear fluid viscous dampers can be represented by

$$m\ddot{y}(t) + ky(t) + c_1 \dot{y}(t) + c_3 \dot{y}^3(t) = u(t) \tag{5.5}$$

and

$$m\ddot{y}(t) + ky(t) + c_1 \dot{y}(t) + c_{0.5} \left| \dot{y}(t) \right|^{0.5} \cdot \text{sign}\left(\dot{y}(t) \right) = u(t) \tag{5.6}$$

Obviously, Eq.(5.5) is a specific case of Eq.(5.1) where $\bar{c}_{0,1}(0;1) = -1$, $\bar{c}_{1,0}(2;1) = m$, $\bar{c}_{1,0}(0;1) = k$, $\bar{c}_{1,0}(1;1) = c_1$, $\bar{c}_{1,0}(1;3) = c_3$, else $\bar{c}_{pq}(\cdot) = 0$. Eq.(5.6) is another specific case of (5.1) where $\bar{c}_{0,1}(0;1) = -1$, $\bar{c}_{1,0}(2;1) = m$, $\bar{c}_{1,0}(0;1) = k$, $\bar{c}_{1,0}(1;1) = c_1$, $\bar{c}_{1,0}(1;0.5) = c_{0.5}$, else $\bar{c}_{pq}(\cdot) = 0$.

In the system presented by Eq.(5.5), the nonlinear fluid viscous damper has a higher-than-one exponent ($a = 3 > 1$) which can produce a larger damping force ($c_3 \dot{y}^3(t)$) to control the system vibration when $\dot{y}(t)$ is significant (higher vibration velocity). This kind of viscous damping devices has been widely used

in high-speed rotating machines such as washing machines and automobile engines etc. [5, 178]. In the system presented by Eq.(5.6), the nonlinear fluid viscous damper has a lower-than-one exponent ($a = 0.5 < 1$) which can produce a larger damping force ($c_{0.5}\left|\dot{y}(t)\right|^{0.5}\text{sign}\left(\dot{y}(t)\right)$) to control the system vibration when $\dot{y}(t)$ is less significant (lower vibration velocity). This kind of viscous damping devices has been widely used in the seismic protection of civil structures and in low-speed machines [46, 65, 87].

5.2.2 The OFRF representation of nonlinear viscously damped vibration systems

In order to apply the OFRF concept to the analysis and design of nonlinear viscously damped vibration systems that can generally be described by Eq.(5.1), the OFRF expression for the relationship between the system output frequency response and nonlinear damping characteristic parameters should be firstly derived.

When $g_i^{(p,q,l)}$ and $g_j^{(p,q,l)}$ in Eq.(5.1) are all fixed, the general term

$$\prod_{i=1}^{p}\left|D^{l_i^{(p,q)}}y(t)\right|^{g_i^{(p,q,l)}}\cdot\text{sign}\left(D^{l_i^{(p,q)}}y(t)\right)\cdot\prod_{j=p+1}^{p+q}\left|D^{l_j^{(p,q)}}u(t)\right|^{g_j^{(p,q,l)}}\cdot\text{sign}\left(D^{l_j^{(p,q)}}u(t)\right)$$

is a continuous function of the derivative terms $D^{l_i^{(p,q)}}y(t)$ and $D^{l_j^{(p,q)}}u(t)$, which, based on the Weierstrass approximation theorem [181], can be arbitrarily well approximated by a finite order polynomial function of $D^{l_i^{(p,q)}}y(t)$ and $D^{l_j^{(p,q)}}u(t)$ such that

$$\begin{aligned}&\prod_{i=1}^{p}\left|D^{l_i^{(p,q)}}y(t)\right|^{g_i^{(p,q,l)}}\cdot\text{sign}\left(D^{l_i^{(p,q)}}y(t)\right)\cdot\prod_{j=p+1}^{p+q}\left|D^{l_j^{(p,q)}}u(t)\right|^{g_j^{(p,q,l)}}\cdot\text{sign}\left(D^{l_j^{(p,q)}}u(t)\right)\\&=\sum_{m=1}^{\hat{M}}\sum_{\substack{p=0\\p+q=m}}^{m}\sum_{l_1^{(p,q)},\cdots,l_{p+q}^{(p,q)}=0}^{\hat{L}}\hat{c}_{pq}(l_1^{(p,q)},\cdots,l_{p+q}^{(p,q)})\prod_{i=1}^{p}D^{l_i^{(p,q)}}y(t)\times\prod_{j=p+1}^{p+q}D^{l_j^{(p,q)}}u(t)\end{aligned}\tag{5.7}$$

where $\hat{M}$ and $\hat{L}$ are the maximum degree of nonlinearity in terms of $y(t)$ and $u(t)$ (or the derivatives of $y(t)$ and $u(t)$) and the maximum order of derivative in the Weierstrass approximation expression. $\hat{c}_{pq}(l_1^{(p,q)},\cdots,l_{p+q}^{(p,q)})$ are the coefficients of the approximating polynomial.

Therefore, the anti-symmetric differential equation (5.1) can be arbitrarily well approximated by a NDE model such that

$$\begin{aligned}
&\sum_{m=1}^{\bar{M}}\sum_{\substack{p=0\\p+q=m}}^{m}\sum_{l_1^{(p,q)},\cdots,l_{p+q}^{(p,q)}=0}^{\bar{L}}\bar{c}_{pq}(l_1^{(p,q)},\cdots,l_{p+q}^{(p,q)};g_1^{(p,q,l)},\cdots,g_{p+q}^{(p,q,l)})\\
&\quad\times\prod_{i=1}^{p}\left|D^{l_i^{(p,q)}}y(t)\right|^{g_i^{(p,q,l)}}\cdot\operatorname{sign}\left(D^{l_i^{(p,q)}}y(t)\right)\cdot\prod_{j=p+1}^{p+q}\left|D^{l_j^{(p,q)}}u(t)\right|^{g_j^{(p,q,l)}}\cdot\operatorname{sign}\left(D^{l_j^{(p,q)}}u(t)\right)\\
&=\sum_{m=1}^{\bar{M}}\sum_{\substack{p=0\\p+q=m}}^{m}\sum_{l_1^{(p,q)},\cdots,l_{p+q}^{(p,q)}=0}^{\bar{L}}\bar{c}_{pq}(l_1^{(p,q)},\cdots,l_{p+q}^{(p,q)};g_1^{(p,q,l)},\cdots,g_{p+q}^{(p,q,l)})\\
&\quad\times\left[\sum_{m=1}^{\hat{M}}\sum_{\substack{p=0\\p+q=m}}^{m}\sum_{l_1^{(p,q)},\cdots,l_{p+q}^{(p,q)}=0}^{\hat{L}}\hat{c}_{pq}(l_1,\cdots,l_{p+q})\prod_{i=1}^{p}D^{l_i^{(p,q)}}y(t)\times\prod_{j=p+1}^{p+q}D^{l_j^{(p,q)}}u(t)\right]\\
&=\sum_{m=1}^{\tilde{M}}\sum_{\substack{p=0\\p+q=m}}^{m}\sum_{l_1^{(p,q)},\cdots,l_{p+q}^{(p,q)}=0}^{\tilde{L}}\tilde{c}_{pq}(l_1^{(p,q)},\cdots,l_{p+q}^{(p,q)})\prod_{i=1}^{p}D^{l_i^{(p,q)}}y(t)\times\prod_{j=p+1}^{p+q}D^{l_j^{(p,q)}}u(t)
\end{aligned}\tag{5.8}$$

where the parameter $\tilde{c}_{pq}(l_1^{(p,q)},\cdots,l_{p+q}^{(p,q)})$ is proportionally related to the coefficient $\bar{c}_{pq}(l_1^{(p,q)},\cdots,l_{p+q}^{(p,q)};g_1^{(p,q,l)},\cdots,g_{p+q}^{(p,q,l)})$. $\tilde{M}$ and $\tilde{L}$ are the maximum degree of nonlinearity in terms of $y(t)$ and $u(t)$ (or the derivatives of $y(t)$ and $u(t)$) and the maximum order of derivative in the NDE model.

Based on the OFRF concept for NDE models as introduced in Chapter 3, when the coefficients in Eq.(5.1) are all fixed apart from $\xi=\bar{c}_{p^*q^*}(l_1^{(p^*,q^*)},\cdots,l_{p^*+q^*}^{(p^*,q^*)};g_1^{(p^*,q^*,l^*)},\cdots,g_{p^*+q^*}^{(p^*,q^*,l^*)})$ with $p^*+q^*\geq 1$ and $l^*=(l_1^{(p^*,q^*)},\cdots,l_{p^*+q^*}^{(p^*,q^*)})$, the system output frequency response $Y(j\omega)$ to a general input can be expressed as

$$Y(j\omega)=P_0(j\omega)+\xi P_1(j\omega)+\xi^2P_2(j\omega)+\cdots+\xi^{\hat{N}}P_{\hat{N}}(j\omega)\tag{5.9}$$

where $\hat{N}$ depends on the highest order used for the Volterra series representation of the system output. $P_i(j\omega)$, $i = 0, 1, \cdots, \hat{N}$, are the functions of the system input spectrum, the frequency ω of interest and depend on all the system parameters apart from ξ.

Now consider the case where all system parameters in Eq (5.1) are fixed apart from $p^* = 1$, $q^* = 0$, $l_1^{(1,0)} = 1$ and $g_1^{(1,0,1)} = s$, $\bar{c}_{1,0}(1; g_1^{(1,0,1)}) \neq 0$. In this case, Eq.(5.1) can be rearranged as

$$\begin{aligned}\bar{c}_{1,0}(1; g_1^{(1,0,1)}) \cdot \left|D^1 y(t)\right|^{g_1^{(1,0,1)}} \cdot \operatorname{sign}\left(D^1 y(t)\right) = -\sum_{m=1}^{\bar{M}} \sum_{\substack{p=0 \\ p+q=m}}^{m} \sum_{\substack{l_1^{(p,q)},\cdots,l_{p+q}^{(p,q)}=0 \\ \text{except } \bar{c}_{1,0}(1; g_1^{(1,0,1)})}}^{\bar{L}} \bar{c}_{pq}(l_1^{(p,q)}, \cdots, l_{p+q}^{(p,q)}; g_1^{(p,q,l)}, \cdots, g_{p+q}^{(p,q,l)}) \\ \times \prod_{i=1}^{p} \left|D^{l_i^{(p,q)}} y(t)\right|^{g_i^{(p,q,l)}} \cdot \operatorname{sign}\left(D^{l_i^{(p,q)}} y(t)\right) \cdot \prod_{j=p+1}^{p+q} \left|D^{l_j^{(p,q)}} u(t)\right|^{g_j^{(p,q,l)}} \cdot \operatorname{sign}\left(D^{l_j^{(p,q)}} u(t)\right)\end{aligned} \tag{5.10}$$

Then

$$\begin{aligned}\left|Dy(t)\right|^{g_1^{(1,0,1)}} \cdot \operatorname{sign}\left(Dy(t)\right) = -\frac{1}{\bar{c}_{1,0}(1; g_1^{(1,0,1)})} \cdot \sum_{m=1}^{\bar{M}} \sum_{\substack{p=0 \\ p+q=m}}^{m} \sum_{\substack{l_1^{(p,q)},\cdots,l_{p+q}^{(p,q)}=0 \\ \text{except } \bar{c}_{1,0}(1; g_1^{(1,0,1)})}}^{\bar{L}} \bar{c}_{pq}(l_1^{(p,q)}, \cdots, l_{p+q}^{(p,q)}; g_1^{(p,q,l)}, \cdots, g_{p+q}^{(p,q,l)}) \\ \times \prod_{i=1}^{p} \left|D^{l_i^{(p,q)}} y(t)\right|^{g_i^{(p,q,l)}} \cdot \operatorname{sign}\left(D^{l_i^{(p,q)}} y(t)\right) \cdot \prod_{j=p+1}^{p+q} \left|D^{l_j^{(p,q)}} u(t)\right|^{g_j^{(p,q,l)}} \cdot \operatorname{sign}\left(D^{l_j^{(p,q)}} u(t)\right)\end{aligned} \tag{5.11}$$

Taking the absolute value and then logarithm on both sides of Eq.(5.11) yields

$$\begin{aligned}&g_1^{(1,0,1)} \cdot \ln\left(\left|Dy(t)\right|\right) = \\ &\ln\left(\left|\begin{aligned}&\frac{1}{\bar{c}_{1,0}(1; g_1^{(1,0,1)})} \cdot \sum_{m=1}^{\bar{M}} \sum_{\substack{p=0 \\ p+q=m}}^{m} \sum_{\substack{l_1^{(p,q)},\cdots,l_{p+q}^{(p,q)}=0 \\ \text{except } \bar{c}_{1,0}(1; g_1^{(1,0,1)})}}^{\bar{L}} \bar{c}_{pq}(l_1^{(p,q)}, \cdots, l_{p+q}^{(p,q)}; g_1^{(p,q,l)}, \cdots, g_{p+q}^{(p,q,l)}) \\ &\times \prod_{i=1}^{p} \left|D^{l_i^{(p,q)}} y(t)\right|^{g_i^{(p,q,l)}} \cdot \operatorname{sign}\left(D^{l_i^{(p,q)}} y(t)\right) \cdot \prod_{j=p+1}^{p+q} \left|D^{l_j^{(p,q)}} u(t)\right|^{g_j^{(p,q,l)}} \cdot \operatorname{sign}\left(D^{l_j^{(p,q)}} u(t)\right)\end{aligned}\right|\right)\end{aligned} \tag{5.12}$$

Because the terms on both sides of Eq (5.12) are continuous functions, they can both be approximated arbitrarily well by a finite order polynomial function with coefficients proportional to $g_1^{(1,0,1)} = s$. Therefore, based on the OFRF concept, the system output frequency response $Y(j\omega)$ to a general input can, in this

case, be expressed as

$$Y(j\omega) = P_0^*(j\omega) + sP_1^*(j\omega) + s^2P_2^*(j\omega) + \cdots + s^{\breve{N}}P_{\breve{N}}^*(j\omega) \qquad (5.13)$$

where $\breve{N}$ depends on the highest order used for the Volterra series representation of the system output. $P_j^*(j\omega)$, $j = 0, 1, \cdots, \breve{N}$, are the functions of the system input spectrum, the frequency ω of interest and depend on all the system parameters apart from $g_1^{(1,0,1)} = s$. Similarly, the OFRF representation for the system output frequency response in terms of viscous damping exponent $g_1^{(0,1,1)} = s$, when $p^* = 0$, $q^* = 1$ and $l_1^{(0,1)} = 1$, can be derived.

Consider a nonlinear viscously damped vibration system with the damping characteristic described by Eq.(5.4). Denote $a = s$ and $C_a = \xi$. Based on the OFRF representations of Eqs.(5.9) and (5.13), the system output frequency responses for $s = 0, 1, \cdots, \breve{N}$ can be expressed as

$$\begin{bmatrix} Y(j\omega)|_{s=0,} \\ Y(j\omega)|_{s=1} \\ \vdots \\ Y(j\omega)|_{s=\breve{N}} \end{bmatrix} = \begin{bmatrix} 1 & 0^1 & \cdots & 0^{\breve{N}} \\ 1 & 1^1 & \ddots & 1^{\breve{N}} \\ \vdots & \ddots & \ddots & \vdots \\ 1 & \breve{N}^1 & \cdots & \breve{N}^{\breve{N}} \end{bmatrix} \cdot \begin{bmatrix} P_0^*(j\omega) \\ P_1^*(j\omega) \\ \vdots \\ P_{\breve{N}}^*(j\omega) \end{bmatrix} = \begin{bmatrix} P_0(j\omega)|_{s=0} & P_1(j\omega)|_{s=0} & \cdots & P_{\hat{N}}(j\omega)|_{s=0} \\ P_0(j\omega)|_{s=1} & P_1(j\omega)|_{s=1} & \ddots & P_{\hat{N}}(j\omega)|_{s=1} \\ \vdots & \ddots & \ddots & \vdots \\ P_0(j\omega)|_{s=\breve{N}} & P_1(j\omega)|_{s=\breve{N}} & \cdots & P_{\hat{N}}(j\omega)|_{s=\breve{N}} \end{bmatrix} \cdot \begin{bmatrix} 1 \\ \xi^1 \\ \vdots \\ \xi^{\hat{N}} \end{bmatrix} \qquad (5.14)$$

Define

$$\mathbf{P}(j\omega) = \begin{bmatrix} P_{0,0}(j\omega) & P_{0,1}(j\omega) & \cdots & P_{0,\hat{N}}(j\omega) \\ P_{1,0}(j\omega) & P_{1,1}(j\omega) & \ddots & P_{1,\hat{N}}(j\omega) \\ \vdots & \ddots & \ddots & \vdots \\ P_{\breve{N},0}(j\omega) & P_{\breve{N},1}(j\omega) & \cdots & P_{\breve{N},\hat{N}}(j\omega) \end{bmatrix} = \begin{bmatrix} 1 & 0^1 & \cdots & 0^{\breve{N}} \\ 1 & 1^1 & \ddots & 1^{\breve{N}} \\ \vdots & \ddots & \ddots & \vdots \\ 1 & \breve{N}^1 & \cdots & \breve{N}^{\breve{N}} \end{bmatrix}^{-1} \cdot \begin{bmatrix} P_0(j\omega)|_{s=0} & P_1(j\omega)|_{s=0} & \cdots & P_{\hat{N}}(j\omega)|_{s=0} \\ P_0(j\omega)|_{s=1} & P_1(j\omega)|_{s=1} & \ddots & P_{\hat{N}}(j\omega)|_{s=1} \\ \vdots & \ddots & \ddots & \vdots \\ P_0(j\omega)|_{s=\breve{N}} & P_1(j\omega)|_{s=\breve{N}} & \cdots & P_{\hat{N}}(j\omega)|_{s=\breve{N}} \end{bmatrix} \qquad (5.15)$$

Then Eq.(5.14) can be rewritten as

$$\begin{bmatrix} P_0^*(j\omega) \\ P_1^*(j\omega) \\ \vdots \\ P_{\breve{N}}^*(j\omega) \end{bmatrix} = \begin{bmatrix} P_{0,0}(j\omega) & P_{0,1}(j\omega) & \cdots & P_{0,\hat{N}}(j\omega) \\ P_{1,0}(j\omega) & P_{1,1}(j\omega) & \ddots & P_{1,\hat{N}}(j\omega) \\ \vdots & \ddots & \ddots & \vdots \\ P_{\breve{N},0}(j\omega) & P_{\breve{N},1}(j\omega) & \cdots & P_{\breve{N},\hat{N}}(j\omega) \end{bmatrix} \cdot \begin{bmatrix} 1 \\ \xi^1 \\ \vdots \\ \xi^{\hat{N}} \end{bmatrix} \tag{5.16}$$

Note that $P_{m,n}(j\omega)$ in Eq.(5.16), where $m = 0, 1, \cdots, \breve{N}$ and $n = 0, 1, \cdots, \hat{N}$, are the functions of the system input spectrum, the frequency of interest ω and all the system parameters apart from the viscous damping coefficient ξ and exponent s.

Substituting Eq.(5.16) into Eq.(5.13) yields

$$\begin{aligned} Y(j\omega) = & P_{0,0}(j\omega) + \xi^1 P_{0,1}(j\omega) + \cdots + \xi^{\hat{N}} P_{0,\hat{N}}(j\omega) + \\ & s\left[P_{1,0}(j\omega) + \xi^1 P_{1,1}(j\omega) + \cdots + \xi^{\hat{N}} P_{1,\hat{N}}(j\omega)\right] + \cdots + \\ & s^{\breve{N}}\left[P_{\breve{N},0}(j\omega) + \xi^1 P_{\breve{N},1}(j\omega) + \cdots + \xi^{\hat{N}} P_{\breve{N},\hat{N}}(j\omega)\right] \\ = & \sum_{p=0}^{\breve{N}} \sum_{q=0}^{\hat{N}} P_{p,q}(j\omega) s^p \xi^q \end{aligned} \tag{5.17}$$

Eq (5.17) is the OFRF representation of nonlinear viscously damped vibration systems with both the nonlinear viscous damping coefficient and exponent being taken into account. The result reveals that there exists a simple polynomial relationship between the system output frequency response and nonlinear viscous damping coefficient ξ and exponent s, which obviously has significant implication for the analysis and design of the effects of nonlinear damping characteristic parameters on the vibration system performance.

5.2.3 Determination of the OFRF

In order to apply the OFRF representation Eq.(5.17) in the system analysis and

design, $P_{p,q}(j\omega)$ in the equation has to be determined. Following the idea proposed in [24], this can be achieved using the system simulation or experimental data as follows.

Denote $\breve{N} = N_1$ and $\hat{N} = N_2$, then Eq (5.17) can be written as

$$Y(j\omega) = \sum_{p=0}^{N_1} \sum_{q=0}^{N_2} P_{p,q}(j\omega) s^p \xi^q \tag{5.18}$$

Denote $\psi_i(j\omega)$, $i = 1, 2, \cdots, m$, as the output frequency responses of the system under m different combinations of the viscous damping coefficient ξ and exponent s represented by $\{\xi_i, s_i\}, i = 1,..., m$.

It is known from Eq.(5.18) that given $\psi_i(j\omega)$, ξ_i and s_i, provided that $m \geq (N_1 + 1)(N_2 + 1)$ and $\{\xi_i, s_i\} \neq \{\xi_k, s_k\}$ when $i \neq k$, the coefficients $P_{p,q}(j\omega)$, $p = 0, 1, \cdots, N_1$ and $q = 0, 1, \cdots, N_2$, can be determined by the least square method as

$$\mathbf{P}(j\omega) = \left([X]^T \cdot [X] \right)^{-1} \cdot \left([X]^T \cdot [Y] \right) \tag{5.19}$$

where

$$[X] = \begin{bmatrix} 1 & s_1 & \xi_1 & \cdots & s_1^{N_1} \xi_1^{N_2} \\ 1 & s_2 & \xi_2 & \ddots & s_2^{N_1} \xi_2^{N_2} \\ \vdots & \ddots & \ddots & \ddots & \vdots \\ 1 & s_m & \xi_m & \cdots & s_m^{N_1} \xi_m^{N_2} \end{bmatrix}, \quad [Y] = \begin{bmatrix} \psi_1(j\omega) \\ \psi_2(j\omega) \\ \vdots \\ \psi_m(j\omega) \end{bmatrix}$$

One issue that needs to be considered when using this method to determine the OFRF expression is how to determine N_1 and N_2. There is no general solution to this problem. Generally, larger values of N_1 and N_2 can produce more accurate results but the computation will be more complicated and more simulation or experimental data are needed.

5.2.4 Verification of the OFRF representation

In order to verify the effectiveness of the OFRF representation derived in Section 5.2.3 above, consider the SDOF FVIS shown in Fig.5.1

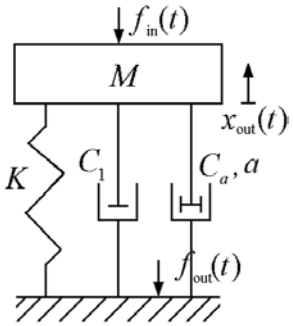

Fig.5.1 SDOF FVIS

In the SDOF FVIS, a general harmonic force

$$f_{\text{in}}(t) = H\Omega^n \sin(\Omega t) \quad \text{and} \quad n = 0 \tag{5.20}$$

is applied on the lumped mass. The movement of the lumped mass M is isolated by a spring with stiffness K and a fluid viscous damper with power damping characteristic parameter a and damping coefficient C_a; C_1 is the linear damping coefficient associated with the spring. $f_{\text{out}}(t)$ represents the force transmitted to the foundation, which is the system vibration output. The fluid viscous damper is a typical viscous damping device which can be described by Eq.(5.4). The system dynamic equation can be described by

$$\begin{cases} M\ddot{x}(t) + Kx(t) + C_1\dot{x}(t) + C_a\left|\dot{x}(t)\right|^a \cdot \text{sign}\left(\dot{x}(t)\right) = f_{\text{in}}(t) \\ f_{\text{out}}(t) = Kx(t) + C_1\dot{x}(t) + C_a\left|\dot{x}(t)\right|^a \cdot \text{sign}\left(\dot{x}(t)\right) = f_{\text{in}}(t) - M\ddot{x}(t) \end{cases} \tag{5.21}$$

which can be described in a dimensionless form as

$$\ddot{g}(\tau) + g(\tau) + \xi_1\dot{g}(\tau) + \xi_a\left|\dot{g}(\tau)\right|^a \cdot \text{sign}\left(\dot{g}(\tau)\right) = \sin(\overline{\Omega}\tau) \tag{5.22}$$

where $\tau = \Omega_0 t$, $\Omega_0 = \sqrt{K/M}$, $\overline{\Omega} = \Omega/\Omega_0$, $x(\tau) = Kx_{\text{in}}(\tau/\Omega_0)/(MH\Omega_0^2)$,

$g(\tau) = Kx(\tau/\Omega_0)/H$, $f_{\text{out}}(\tau) = \sin(\overline{\Omega}\tau) - \ddot{g}(\tau)$

$\xi_1 = \dfrac{C_1}{\sqrt{MK}}$, $\xi_a = \dfrac{C_a H^{a-1}}{\sqrt{(MK)^a}}$.

As introduced in Chapter 4, the force transmissibility $FF(\Omega)$ of the SDOF FVIS under harmonic excitations is defined as the ratio between the amplitude of the system output frequency response and the input excitation at the frequency of interest Ω

$$FF(\Omega) = \left|Y(j\Omega)\right| / H \tag{5.23}$$

where the system output frequency response $Y(j\Omega) = F_{\text{out}}(j\Omega)$ can be calculated by the FFT of $f_{\text{out}}(t)$ from the simulation or experimental data. Therefore the force transmissibility of the SDOF FVIS can be studied by investigating the system output frequency response $Y(j\Omega)$.

When the system mass, stiffness, linear damping coefficient and the amplitude of harmonic force excitation are given as $M = 10\,\text{kg}$, $K = 4000\,\text{N/m}$, $C_1 = 50\,\text{N/m}$ and $H = 100\,\text{N}$, the force transmissibility of the SDOF FVIS at the system resonant frequency ($\overline{\Omega} = 1$) were first evaluated by numerical simulations using MATLAB. Then an OFRF based representation of the force transmissibility was determined. The OFRF takes the form of a 3rd order polynomial as follows

$$Y(j\omega) = \sum_{m=0}^{3}\sum_{n=0}^{3} P_{m,n}(j\Omega) a^m C_a^n \tag{5.24}$$

where $P_{m,n}(j\Omega)$, $m, n = 0, 1, 2, 3$, were obtained from $(3+1)\cdot(3+1) = 16$ numerical simulation studies on the system. In the 16 simulation studies, the system was excited by the same harmonic excitation but the system parameters C_a and a took 16 different sets of values as below.

$C_{a_1} = 0,\ a_1 = 1;\ C_{a_2} = 0,\ a_2 = 4;\ C_{a_3} = 60,\ a_3 = 1.6;\ C_{a_4} = 60,\ a_4 = 3.2;$

$C_{a_5} = 100,\ a_5 = 2;\ C_{a_6} = 100,\ a_6 = 2.8;\ C_{a_7} = 140,\ a_7 = 1;\ C_{a_8} = 140,\ a_8 = 2.4;$

$C_{a_9} = 140,\ a_9 = 4;\ C_{a_{10}} = 180,\ a_{10} = 2;\ C_{a_{11}} = 180,\ a_{11} = 2.8;\ C_{a_{12}} = 220,\ a_{12} = 1.6;$

$C_{a_{13}} = 220,\ a_{13} = 3.2;\ C_{a_{14}} = 300,\ a_{14} = 1;\ C_{a_{15}} = 300,\ a_{15} = 2.4;\ C_{a_{16}} = 300,\ a_{16} = 4.$

The output frequency response $Y(j\omega)$ of the system were evaluated from the 16 numerically simulated system outputs to yield the results $Y_1(j\Omega),\cdots,Y_{16}(j\Omega)$

$$Y_1(j\Omega) = -400.04 - 99.4\mathrm{i}; \quad Y_2(j\Omega) = -400.04 - 99.4\mathrm{i};$$

$$Y_3(j\Omega) = -194.11 - 98.91\mathrm{i}; \quad Y_4(j\Omega) = -206.44 - 96.34\mathrm{i};$$

$$Y_5(j\Omega) = -166.19 - 97.97\mathrm{i}; \quad Y_6(j\Omega) = -178.48 - 96.39\mathrm{i};$$

$$Y_7(j\Omega) = -105.31 - 99.4\mathrm{i}; \quad Y_8(j\Omega) = -155.41 - 96.87\mathrm{i};$$

$$Y_9(j\Omega) = -176.08 - 93.63\mathrm{i}; \quad Y_{10}(j\Omega) = -132.58 - 97.62\mathrm{i};$$

$$Y_{11}(j\Omega) = -151.01 - 95.73\mathrm{i}; \quad Y_{12}(j\Omega) = -107.43 - 98.5\mathrm{i};$$

$$Y_{13}(j\Omega) = -149.47 - 94.63\mathrm{i}; \quad Y_{14}(j\Omega) = -57.19 - 99.4\mathrm{i};$$

$$Y_{15}(j\Omega) = -119.89 - 96.31\mathrm{i}; \quad Y_{16}(j\Omega) = -149.92 - 92.57\mathrm{i}.$$

From these results, $P_{m,n}(j\Omega)$, $m,n = 0,1,2,3$ in Eq.(5.24) were obtained by the least square method in Eq.(5.19). After this, the force transmissibility of the SDOF FVIS in Fig.5.1 at the system resonant frequency ($\overline{\Omega} = 1$) was evaluated using the determined system OFRF as

$$FF(\Omega) = \left|Y(j\Omega)\right| \Big/ H = \left|\sum_{m=0}^{3}\sum_{n=0}^{3} P_{m,n}(j\Omega) a^m C_a^n\right| \Big/ H \tag{5.25}$$

Figs 5.2 and 5.3 show the system force transmissibility evaluated from the OFRF representation Eq.(5.25) and numerical simulation studies, respectively, over the range of damping characteristic parameters $C_a \in [0, 320]$ and $a \in [1, 4.4]$ to compare the results evaluated using both conventional numerical simulation and the new OFRF based approaches. Note that, in Figs 5.2 and 5.3, some values of the damping parameters C_a and a are outside the range of $C_a \in [0, 300]$ and $a \in [1, 4]$ where the OFRF representation Eq.(5.25) was determined. This is to demonstrate the performance of the OFRF over a wider range of values of the damping characteristic parameters. Fig.5.4 shows the

difference between the results that have been obtained by the two methods.

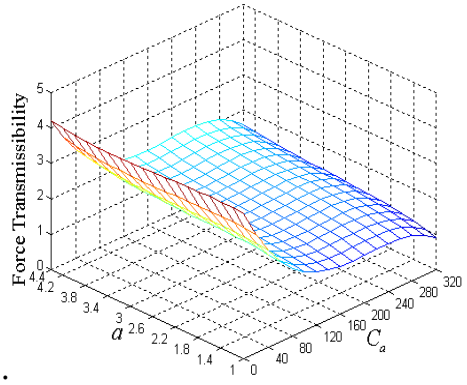

Fig.5.2 Force transmissibility at the resonant frequency of the SDOF FVIS evaluated from the OFRF (5.25)

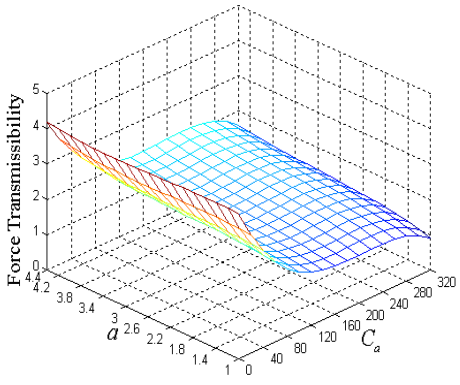

Fig.5.3 Force transmissibility at the resonant frequency of the SDOF FVIS obtained from numerical simulations

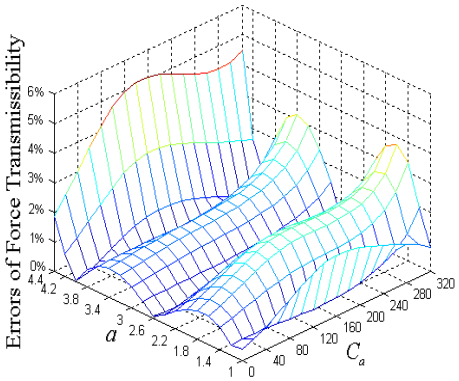

Fig.5.4 Errors with the force transmissibility determined by the OFRF (5.25)

Clearly, the data curves in Figs.5.2 to 5.4 reveal that the errors from the OFRF expression in Eq.(5.25) are less than 5%. These results demonstrate the effectiveness of the OFRF concept and its evaluation method described in Section 5.2.3. It is worth pointing out that the error with the OFFR representation is mainly due to the fact that the OFRF (5.24) only takes a 3rd order polynomial function of the nonlinear damping characteristic parameters a and C_a to approximate the system output frequency response. Basically, the lower order of the OFRF, the less accurate the OFRF representation will be. For example, if the OFRF takes a 2nd order polynomial function of a and C_a to approximate the system output frequency response, $N_1 = N_2 = 2$ in Eq.(5.18). The system transmissibility evaluated by the corresponding OFRF and the errors

with the OFRF representation are shown in Figs. 5.5 and 5.6 respectively. Clearly, the errors with the 2nd order OFRF representation are more significant, which raise up to 8%. Generally, higher order polynomial function of OFRF can produce more accurate results but the computation will be more complicated and more simulation or experimental data are needed.

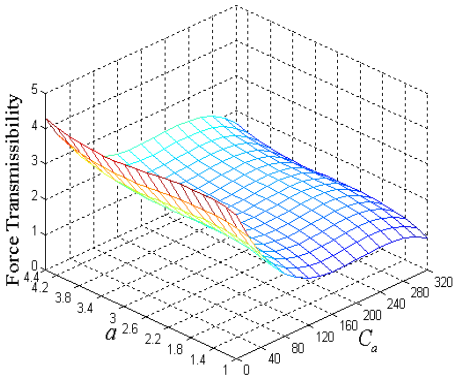

Fig.5.5 Force transmissibility at the resonant frequency of the SDOF FVIS determined by a 2nd order OFRF

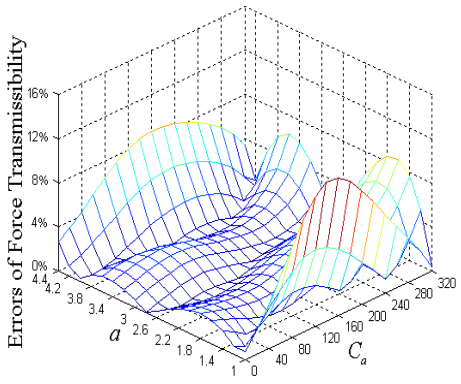

Fig 5.6 Errors with the 2nd order OFRF representation

5.3 Effects of nonlinear damper location and characteristic parameters on the vibration transmissibility of MDOF systems

In this section, the OFRF based method will be applied to the analysis of MDOF nonlinear viscously damped vibration systems. The objective is to study the effects of nonlinear damper location and damping characteristic parameters on the system vibration transmissibility under harmonic excitations.

5.3.1 MDOF DVIS and FVIS

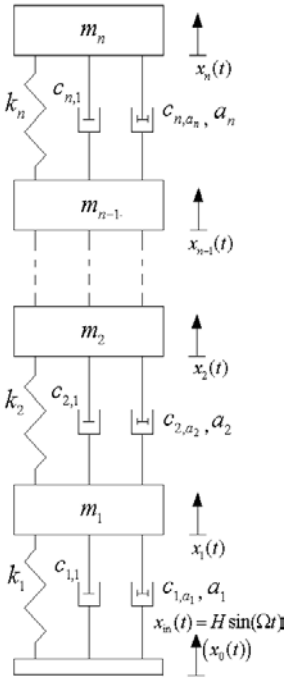

Fig.5.7 MDOF DVIS

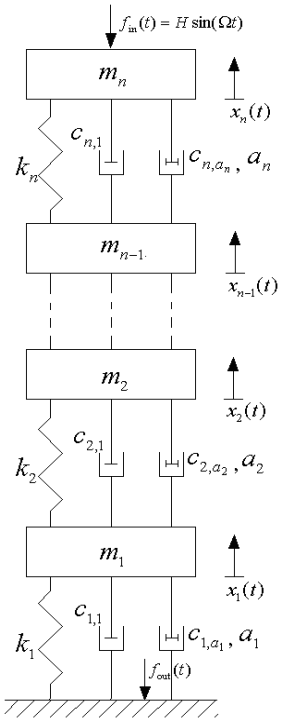

Fig.5.8 MDOF FVIS

Consider the MDOF DVIS and FVIS as shown in Figs.5.7 and 5.8, respectively. The MODOF DVIS can be used to present the mechanical and civil engineering system subject to base excitation, such as the earthquake; The MDOF FVIS can be used to study the vibrations of civil buildings or towers subject to external loading excitations, such as the wind. In the case of MDOF DVIS, the foundation moves due to a harmonic displacement excitation

$$x_0(t) = x_{\text{in}}(t) = H\sin(\Omega t) \tag{5.26}$$

The movement x_i of the lumped mass m_i, $i = 1,2,\cdots,n$, are isolated by the springs with stiffness k_i and fluid viscous dampers with damping coefficient C_{i,a_i} and exponent a_i. $C_{i,1}$ are the linear damping coefficients associated with the springs. The displacement transmissibility $DD_i(\Omega)$ are defined as the amplitude ratio between the system displacement vibration frequency response $Y_i(j\Omega)$ at the i^{th} storey ($x_i(t)$) and the input excitation amplitude H, that is,

$$DD_i(\Omega) = \left|Y_i(j\Omega)\right| / H \tag{5.27}$$

In the case of MDOF FVIS, a harmonic force excitation

$$f_{\text{in}}(t) = H\sin(\Omega t) \tag{5.28}$$

is imposed on the top lumped mass m_n and the same spring-damper mechanisms are used between each storey. The force transmissibility $FF(\Omega)$ is defined as the amplitude ratio between the frequency response $Y(j\Omega)$ of the force transmitted to the foundation ($f_{\text{out}}(t)$) and the input excitation

$$FF(\Omega) = \left|Y(j\Omega)\right| \big/ H \tag{5.29}$$

Nonlinear viscous damping devices whose damping force F_{D} can be described by

$$F_{\text{D}} = C_{i,a_i}\left|\dot{u}_r\right|^{a_i}\text{sign}(\dot{u}_r) \tag{5.30}$$

are fitted at each storey to reduce the vibration responses of MDOF DVIS and MDOF FVIS under harmonic excitations. In (5.30), C_{i,a_i} and a_i represent the viscous damping coefficients and exponent of the fluid viscous damper fitted at the i^{th} storey.

The dynamic equations of MDOF DVIS and FVIS can be described by

$$\text{M}\ddot{\text{X}} + \text{C}\dot{\text{X}} + \text{KX} + \text{F}_{\text{N}} = \text{F} \tag{5.31}$$

where M , C and K are the system mass, linear damping, and stiffness matrices given by

$$\text{M} = \begin{bmatrix} m_1 & 0 & \cdots & 0 \\ 0 & m_2 & \ddots & 0 \\ \vdots & \ddots & \ddots & \vdots \\ 0 & 0 & \cdots & m_n \end{bmatrix},$$

$$\text{C} = \begin{bmatrix} c_{1,1}+c_{2,1} & -c_{2,1} & \cdots & 0 & 0 \\ -c_{2,1} & c_{2,1}+c_{3,1} & \ddots & \ddots & 0 \\ \vdots & \ddots & \ddots & -c_{n-1,1} & 0 \\ 0 & \ddots & -c_{n-1,1} & c_{n-1,1}+c_{n,1} & -c_{n,1} \\ 0 & \cdots & 0 & -c_{n,1} & c_{n,1} \end{bmatrix},$$

$$K=\begin{bmatrix} k_1+k_2 & -k_2 & \cdots & 0 & 0 \\ -k_2 & k_2+k_3 & \ddots & \ddots & 0 \\ \vdots & \ddots & \ddots & -k_{n-1} & 0 \\ 0 & \ddots & -k_{n-1} & k_{n-1}+k_n & -k_n \\ 0 & \cdots & 0 & -k_n & k_n \end{bmatrix},$$

$\mathrm{X}=\left(x_1, x_2, \cdots, x_n\right)^{\mathrm{T}}$ is the system displacement vector,

$$\mathrm{F}=\left(c_{1,1}\dot{x}_0+k_1x_0, 0, \cdots, 0, 0\right)^{\mathrm{T}} \quad \text{for MDOF DVIS} \tag{5.32}$$

and

$$\mathrm{F}=\left(0, 0, \cdots, 0, -f_{\mathrm{in}}(t)\right)^{\mathrm{T}} \quad \text{for MDOF FVIS} \tag{5.33}$$

$\mathrm{F_N}$ is the vector of damping force produced by fitted fluid viscous dampers given by

$$\mathrm{F_N}=\begin{bmatrix} c_{1,a_1}\cdot\left|\dot{x}_1-\dot{x}_0\right|^{a_1}\cdot\mathrm{sign}\left(\dot{x}_1-\dot{x}_0\right)-c_{2,a_2}\cdot\left|\dot{x}_2-\dot{x}_1\right|^{a_2}\cdot\mathrm{sign}\left(\dot{x}_2-\dot{x}_1\right) \\ c_{2,a_2}\cdot\left|\dot{x}_2-\dot{x}_1\right|^{a_2}\cdot\mathrm{sign}\left(\dot{x}_2-\dot{x}_1\right)-c_{3,a_3}\cdot\left|\dot{x}_3-\dot{x}_2\right|^{a_3}\cdot\mathrm{sign}\left(\dot{x}_3-\dot{x}_2\right) \\ \vdots \\ c_{n,a_n}\cdot\left|\dot{x}_n-\dot{x}_{n-1}\right|^{a_n}\cdot\mathrm{sign}\left(\dot{x}_n-\dot{x}_{n-1}\right) \end{bmatrix}.$$

The force transmitted to the foundation in MDOF FVIS can be described by

$$f_{\mathrm{out}}(t)=k_1x_1(t)+c_{1,1}\dot{x}_1(t)+c_{1,a_1}\cdot\left|\dot{x}_1(t)\right|^{a_1}\cdot\mathrm{sign}\left(\dot{x}_1(t)\right) \tag{5.34}$$

When the fitted fluid viscous dampers in the MDOF DVIS and FVIS are all linear dampers, these systems are linear systems. The displacement transmissibility $DD_i(\Omega)$, $i=1, 2, \cdots, n$, of linear MDOF DVIS can be evaluated from the system parameters as

$$\left[DD_1(\Omega)\ DD_2(\Omega)\cdots DD_n(\Omega)\right]^{\mathrm{T}}=\left[\left|s_1(\Omega)\right|\left|s_2(\Omega)\right|\cdots\left|s_n(\Omega)\right|\right]^{\mathrm{T}} \tag{5.35}$$

where

$$\begin{bmatrix} s_1(\Omega) \\ s_2(\Omega) \\ \vdots \\ s_n(\Omega) \end{bmatrix} = \begin{bmatrix} \begin{pmatrix} -m_1\Omega^2 + (k_1+k_2) \\ +(c_1+c_2)\Omega j \end{pmatrix} & -c_2\Omega j - k_2 & 0 & \cdots & 0 \\ -c_2\Omega j - k_2 & \begin{pmatrix} -m_2\Omega^2 + (k_2+k_3) \\ +(c_2+c_3)\Omega j \end{pmatrix} & -c_3\Omega j - k_3 & \ddots & 0 \\ 0 & -c_3\Omega j - k_3 & \ddots & \ddots & \vdots \\ \vdots & \ddots & \ddots & \ddots & -c_n\Omega j - k_n \\ 0 & \cdots & \cdots & -c_n\Omega j - k_n & \left(-m_n\Omega^2 + k_n + c_n\Omega j\right) \end{bmatrix}^{-1} \cdot \begin{bmatrix} c_1\Omega j + k_1 \\ 0 \\ 0 \\ \vdots \\ 0 \end{bmatrix} \quad (5.36)$$

Similarly, the force transmissibility $FF(\Omega)$ of linear MDOF FVIS can be evaluated from the system parameters as

$$FF(\Omega) = \left|\left(c_1\Omega j + k_1\right) \cdot s_1(\Omega)\right| \quad (5.37)$$

where

$$\begin{bmatrix} s_1(\Omega) \\ s_2(\Omega) \\ \vdots \\ s_n(\Omega) \end{bmatrix} = \begin{bmatrix} \begin{pmatrix} -m_1\Omega^2 + (k_1+k_2) \\ +(c_1+c_2)\Omega j \end{pmatrix} & -c_2\Omega j - k_2 & 0 & \cdots & 0 \\ -c_2\Omega j - k_2 & \begin{pmatrix} -m_2\Omega^2 + (k_2+k_3) \\ +(c_2+c_3)\Omega j \end{pmatrix} & -c_3\Omega j - k_3 & \ddots & 0 \\ 0 & -c_3\Omega j - k_3 & \ddots & \ddots & \vdots \\ \vdots & \ddots & \ddots & \ddots & -c_n\Omega j - k_n \\ 0 & \cdots & \cdots & -c_n\Omega j - k_n & \left(-m_n\Omega^2 + k_n + c_n\Omega j\right) \end{bmatrix}^{-1} \cdot \begin{bmatrix} 0 \\ 0 \\ \vdots \\ 0 \\ -1 \end{bmatrix} \quad (5.38)$$

5.3.2 Effects of nonlinear damper location and damping characteristic parameters on the transmissibility of MDOF DVIS and FVIS

Consider n-DOF DVIS and FVIS as shown in Figs.5.7 and 5.8 where $m_i = 10\,\text{kg}$, $k_i = 4000\,\text{N/m}$, $c_{i,1} = 50\,\text{Ns/m}$, $i = 1, 2, \cdots, n$, $H = 10^{-3}\,\text{m}$ for the n-DOF DVIS and $H = 100\,\text{N}$ for the n-DOF FVIS. Without additionally fitted fluid viscous dampers, the DVIS and FVIS systems' natural frequencies can be evaluated [182] as $\omega_{1,2,3} = [8.9, 24.9, 36]\,\text{rad/s}$ and the displacement transmissibility of n-DOF DVIS and force transmissibility of n-DOF FVIS can be evaluated by Eqs.(5.35)-(5.38). The results are shown in Figs.5.9 and 5.10 for the cases of $n = 1, 2, 3$.

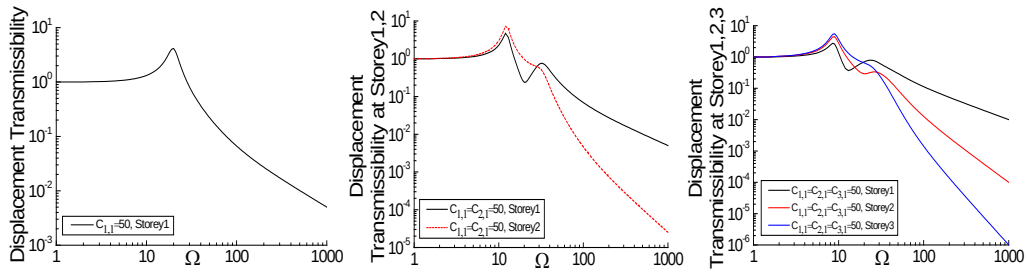

(a)1-DOF DVIS (b) 2-DOF DVIS (c) 3-DOF DVIS

Fig.5.9 Displacement transmissibility of n-DOF DVIS

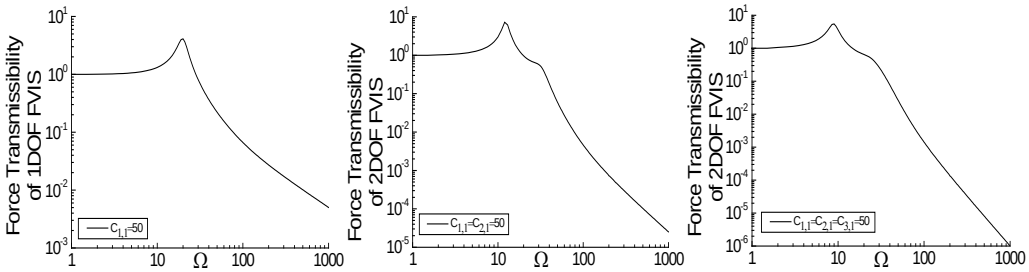

(a)1-DOF FVIS (b) 2-DOF FVIS (c) 3-DOF FVIS

Fig.5.10 Force transmissibility of n-DOF FVIS

In order to suppress the vibration over a wide frequency region, additional fluid viscous dampers are often fitted into the structural systems to achieve a better system vibration control performance.

Although the effects of linear fluid viscous dampers on the system transmissibility can be evaluated by Eqs.(5.35)-(5.38), the effects of nonlinear fluid viscous dampers on the system transmissibility can not be evaluated directly. Therefore, the OFRF concept is applied to evaluate the displacement transmissibility $DD_i(\Omega)$, $i=1,...,n$ for the DVIS and the force transmissibility $FF(\Omega)$ for the FVIS in the following.

The OFRF representations are first determined for the system output frequency response $Y_i(j\Omega)$ of the n-DOF DVIS, and $Y(j\Omega)$ of the n-DOF FVIS, respectively. This can be achieved in a way similar to what has been described in Section 5.2.4.

To illustrate the process, consider a simple case where the effect of damping

characteristic parameters C_{2,a_2} and a_2 of a nonlinear fluid viscous damper on the displacement transmissibility $DD_1(\Omega)$ of a 3-DOF DVIS is to be investigated. Because, in this case, $DD_1(\Omega) = |Y_1(j\Omega)| / H$ as defined in Eq.(5.27), the displacement transmissibility can be evaluated from the system output frequency response $Y_1(j\Omega)$. The OFRF expression of the system output frequency response $Y_1(j\Omega)$ used in this case takes the form of

$$Y_1(j\omega) = \sum_{m=0}^{2}\sum_{n=0}^{2} P_{m,n}(j\Omega) a_2^m C_{2,a_2}^n \tag{5.39}$$

In order to work out $P_{m,n}(j\Omega)$, $m,n = 0,1,2,3$ to determine the OFRF representation (5.39). $(2+1)\cdot(2+1) = 9$ simulation studies were conducted where the system was excited by the same harmonic excitation with the damping characteristic parameters C_{2,a_2} and a_2 taking 9 different sets of values as follows

$C_{2,a_2,1} = 5, a_{2,1} = 0.5$; $C_{2,a_2,2} = 10, a_{2,2} = 0.5$; $C_{2,a_2,3} = 50, a_{2,3} = 0.8$;

$C_{2,a_2,4} = 100, a_{2,4} = 0.8$; $C_{2,a_2,5} = 5, a_{2,5} = 1.5$; $C_{2,a_2,6} = 100, a_{2,6} = 1.5$;

$C_{2,a_2,7} = 1\text{E}3, a_{2,7} = 2.5$; $C_{2,a_2,8} = 3\text{E}3, a_{2,8} = 2.5$; $C_{2,a_2,9} = 1\text{E}4\ a_{2,9} = 2.5$;

The output frequency response $Y_1(j\Omega)$ of the system were evaluated from the 9 simulated system outputs to yield the results $Y_{1,1}(j\Omega), \cdots, Y_{1,9}(j\Omega)$. Then $P_{m,n}(j\Omega)$, $m,n = 0,1,2,3$ in Eq.(5.39) can be obtained by the least square method in Eq.(5.19).

After an OFRF has been determined to represent the analytical relationship between the system output frequency response and the characteristic parameters of fitted additional dampers, the system displacement and force transmissibility $DD_i(\Omega)$ and $FF(\Omega)$ can be evaluated using the determined OFRF

representations. Figs.5.11 to 5.19 show the results in different cases that were obtained using corresponding OFRF representations, where a_i, $i=1,2,3$, represents the damping exponent of additional fluid viscous damper on the i^{th} storey and $C_{i,ai}$ represents the damping coefficient. From these results, it can be found that all types of fluid viscous dampers can suppress the system vibration at the system resonant frequencies. However, the effects of different types of fluid viscous dampers on the system transmissibility over the higher frequency region are more complicated.

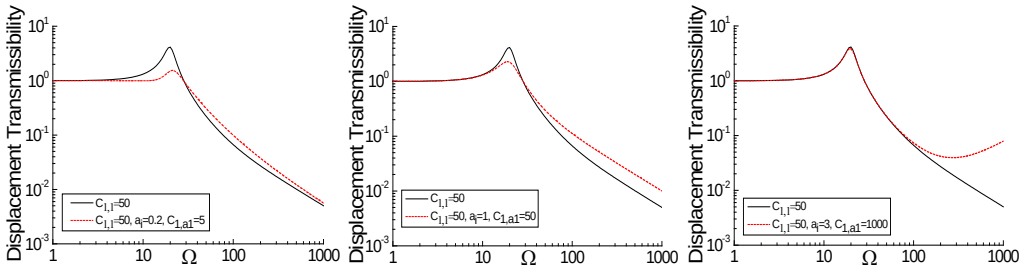

(a) $a_i=0.2<1$ (b) $a_i=1$ (c) $a_i=3>1$

Fig.5.11 Effects of damper location and damping characteristic parameters on $DD_1(\Omega)$ of 1DOF DVIS

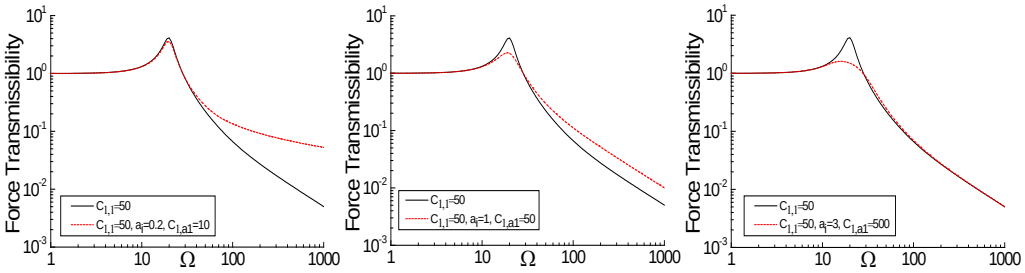

(a) $a_i=0.2<1$ (b) $a_i=1$ (c) $a=3>1$

Fig.5.12 Effects of damper location and damping characteristic parameters on $FF(\Omega)$ of 1DOF FVIS

It can be observed from Fig.5.11 that, in the case of 1DOF DVIS, a nonlinear fluid viscous damper with damping exponent $a_1 \geq 1$ will increase the displacement transmissibility over the higher frequency region, which is harmful and even dangerous for the system safety. In contrast, a nonlinear fluid viscous damper with damping exponent $a_1<1$ can perform more ideal vibration effect

on the displacement transmissibility at both the resonant and higher frequencies. However, the effects of fluid viscous dampers on the force transmissibility are completely different in 1DOF FVIS as shown in Fig.5.12, where a nonlinear fluid viscous damper with damping exponent $a_1 > 1$ can perform more ideal vibration effect on the force transmissibility at both the resonant and higher frequencies. These OFRF based evaluation results confirm the conclusions of the SDOF DVIS and FVIS reached in the analysis in Chapter 4.

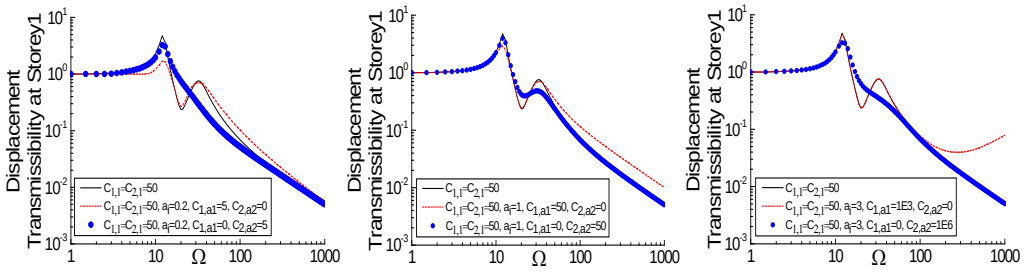

(a) $a_i = 0.2 < 1$ (b) $a_i = 1$ (c) $a_i = 3 > 1$

Fig.5.13 Effects of damper location and damping characteristic parameters on $DD_1(\Omega)$ of 2DOF DVIS

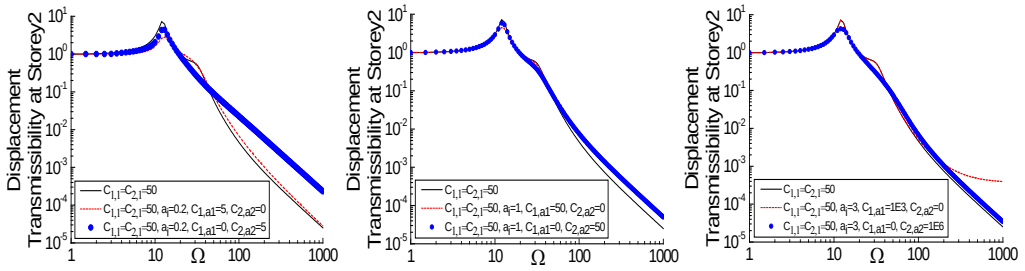

(a) $a_i = 0.2 < 1$ (b) $a_i = 1$ (c) $a_i = 3 > 1$

Fig.5.14 Effects of damper location and damping characteristic parameters on $DD_2(\Omega)$ of 2DOF DVIS

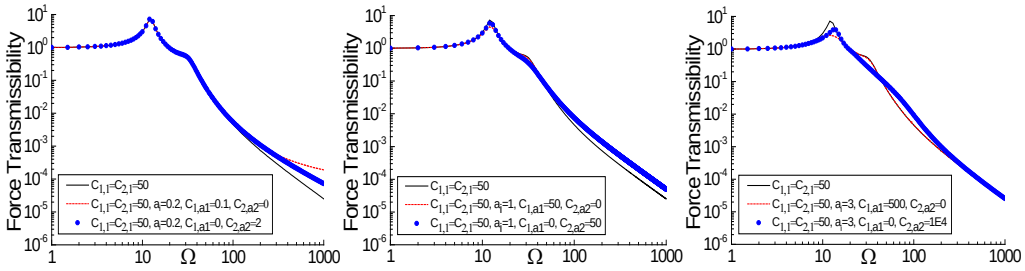

(a) $a_i = 0.2 < 1$ (b) $a_i = 1$ (c) $a_i = 3 > 1$

Fig.5.15 Effects of damper location and damping characteristic parameters on $FF(\Omega)$ of 2DOF FVIS

In the case of 2DOF DVIS, the results in Figs. 5.13 and 5.14 reveal that linear fluid viscous dampers ($a_1 = a_2 = 1$) installed in Storey1 and Storey2 will increase the displacement transmissibility at Storey1 and Storey2 over the higher frequency region. Therefore, linear fluid viscous dampers should be avoided to use in the systems when the vibrations at higher frequency should be considered and isolated. From the results in Figs.5.13 and 5.14, it can be found that an ideal approach of fitting fluid viscous dampers in the MDOF system should be to fit a nonlinear fluid viscous damper with damping exponent $a_1 < 1$ at Storey1 and to fit a nonlinear fluid viscous damper with damping exponent $a_2 > 1$ at Storey2. Such fittings can reduce the displacement transmissibility at Storey 1 and Storey 2 ($DD_1(\Omega)$ and $DD_2(\Omega)$) over the system 1st and 2nd resonant frequencies without detrimental effects on the transmissibility over the higher frequency region.

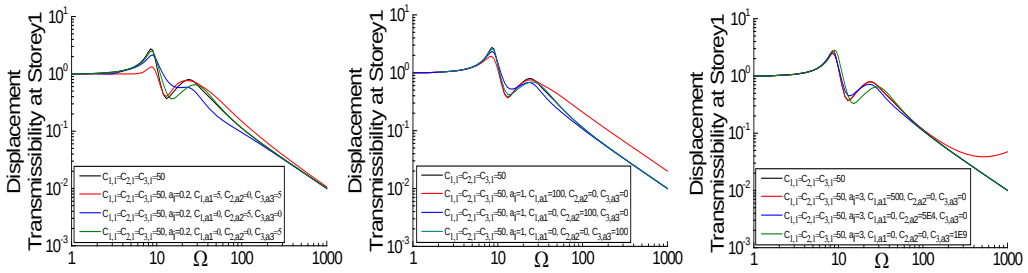

(a) $a_i = 0.2 < 1$ (b) $a_i = 1$ (c) $a_i = 3 > 1$

Fig.5.16 Effects of damper location and damping characteristic parameters on $DD_1(\Omega)$ of 3DOF DVIS

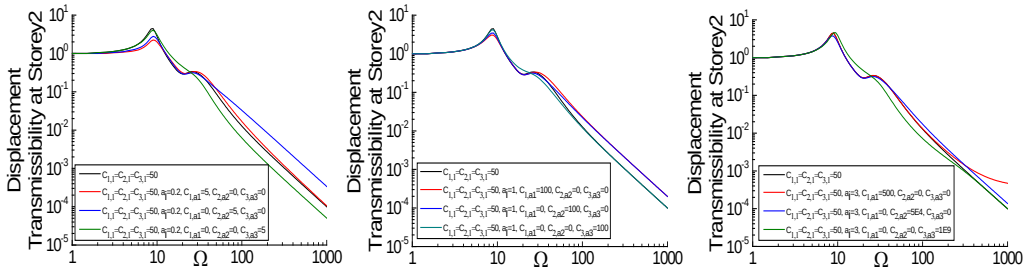

(a) $a_i = 0.2 < 1$ (b) $a_i = 1$ (c) $a_i = 3 > 1$

Fig.5.17 Effects of damper location and damping characteristic parameters on $DD_2(\Omega)$ of 3DOF DVIS

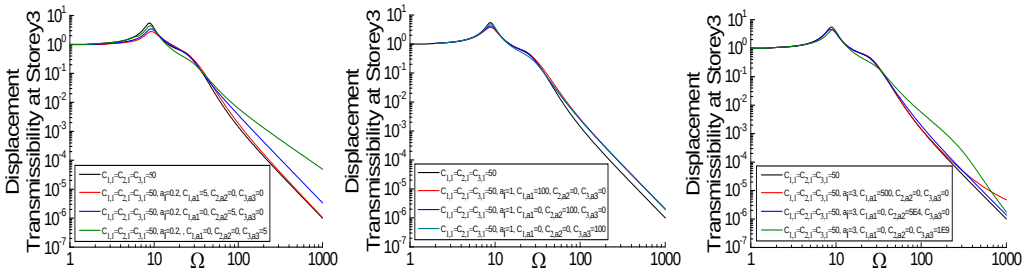

(a) $a_i = 0.2 < 1$ (b) $a_i = 1$ (c) $a_i = 3 > 1$

Fig.5.18 Effects of damper location and damping characteristic parameters on $DD_3(\Omega)$ of 3DOF DVIS

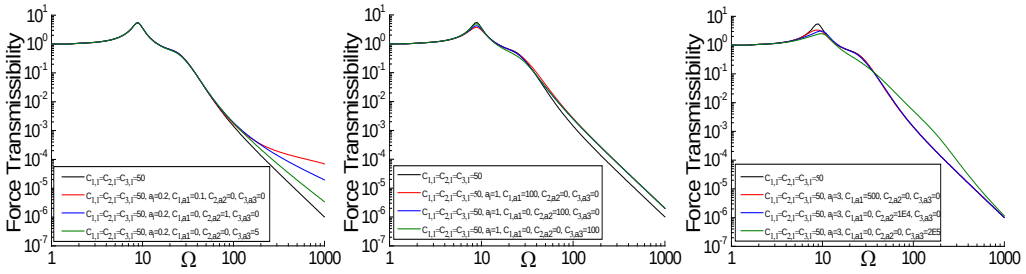

(a) $a_i = 0.2 < 1$ (b) $a_i = 1$ (c) $a_i = 3 > 1$

Fig.5.19 Effects of damper location and damping characteristic parameters on $FF(\Omega)$ of 3DOF FVIS

In the case of 3DOF DVIS, Figs.5.16 to 5.18 show that, the ideal approach of fitting fluid viscous dampers in the system should be to fit a nonlinear fluid viscous damper with a lower-than-one damping exponent at Storey1 ($a_1 < 1$) and nonlinear fluid viscous dampers with higher-than-one damping exponents at Storey 2 and 3 ($a_2 > 1$ and $a_3 > 1$). Otherwise, the fitted additional fluid viscous dampers will increase the system displacement transmissibility $DD_1(\Omega)$, $DD_2(\Omega)$ or $DD_3(\Omega)$ over the higher frequency region. For examples, a linear fluid viscous damper with damping exponent $a_1 = 1$ in Storey1 will increase $DD_1(\Omega)$, $DD_2(\Omega)$ and $DD_3(\Omega)$ over higher frequency region as shown in Figs. 5.16(b), 5.17(b) and 5.18(b); a nonlinear fluid viscous damper with damping exponent $a_2 = 0.2$ at Storey2 has little effect on $DD_1(\Omega)$ but will obviously increase $DD_2(\Omega)$ and $DD_3(\Omega)$ over higher frequency region as shown in Figs. 5.16(a), 5.17(a) and 5.18(a).

In the cases of 2DOF and 3DOF FVIS, from the results in Figs.5.15 and 5.19, it can be observed that fluid viscous dampers in each storey should be designed as having the damping exponent $a_i > 1$, $i = 1, 2, 3$. This kind of fluid viscous dampers design has ideal vibration control effects on the system force transmissibility at both the resonant and higher frequencies. More detailed effects of installation locations and damping characteristic parameters of fluid viscous dampers on the displacement and force transmissibility of 1, 2 and 3DOF DVIS and FVIS over higher frequency region are listed in Tables.5.1 to 5.6.

Table.5.1 Effects of fluid viscous dampers on $DD_1(\Omega)$ of 1DOF DVIS

Transmissibility	$a_1 = 0.2$	$a_1 = 1$	$a_1 = 3$
$DD_1(\Omega)$ over higher frequency	0	+	+

Table.5.2 Effects of fluid viscous dampers on $DD_1(\Omega)$ and $DD_2(\Omega)$ of 2DOF DVIS

Transmissibility	$a_1 = 0.2$	$a_2 = 0.2$	$a_1 = 1$	$a_2 = 1$	$a_1 = 3$	$a_2 = 3$
$DD_1(\Omega)$ over higher frequency	0	0	+	0	+	0
$DD_2(\Omega)$ over higher frequency	0	+	+	+	+	0

Table.5.3 Effects of fluid viscous dampers on $DD_1(\Omega)$, $DD_2(\Omega)$ and $DD_3(\Omega)$ of 3DOF DVIS

Transmissibility	$a_1 = 0.2$	$a_2 = 0.2$	$a_3 = 0.2$	$a_1 = 1$	$a_2 = 1$	$a_3 = 1$	$a_1 = 3$	$a_2 = 3$	$a_3 = 3$
$DD_1(\Omega)$ over higher frequency	0	0	0	+	0	0	+	0	0
$DD_2(\Omega)$ over higher frequency	0	+	-	+	+	0	+	0	0
$DD_3(\Omega)$ over higher frequency	0	+	+	+	+	+	+	0	0

Table.5.4 Effects of fluid viscous dampers on $FF(\Omega)$ of 1DOF FVIS

Transmissibility	$a_1 = 0.2$	$a_1 = 1$	$a_1 = 3$
$FF(\Omega)$ over higher frequency	+	+	0

Table.5.5 Effects of fluid viscous dampers on $FF(\Omega)$ of 2DOF FVIS

Transmissibility	$a_1 = 0.2$	$a_2 = 0.2$	$a_1 = 1$	$a_2 = 1$	$a_1 = 3$	$a_2 = 3$
$FF(\Omega)$ over higher frequency	+	+	+	+	0	0

Table.5.6 Effects of fluid viscous dampers on $FF(\Omega)$ of 3DOF FVIS

Transmissibility	$a_1 = 0.2$	$a_2 = 0.2$	$a_3 = 0.2$	$a_1 = 1$	$a_2 = 1$	$a_3 = 1$	$a_1 = 3$	$a_2 = 3$	$a_3 = 3$
$FF(\Omega)$ over higher frequency	+	+	+	+	+	+	0	0	0

In the tables, a_1, a_2 and a_3 represent the damping exponents of fluid viscous dampers installed at Storey1, 2 and 3, respectively. “0” means that the fluid viscous damper has little effect on the system transmissibility over the higher frequency region, “-” means that the fluid viscous damper will reduce the system transmissibility over the higher frequency region and “+” means that the fluid viscous damper will increase the system transmissibility over the higher frequency region. For example, when $DD_1(\Omega)$, $DD_2(\Omega)$ and $DD_3(\Omega)$ of 3DOF DVIS should be reduced at both the resonant and higher frequencies in the vibration isolation design, the type selection of additional fluid viscous dampers should be $a_1 = 0.2$, $a_2 = 3$ and $a_2 = 3$ as shown in Table.5.3; When $DD_1(\Omega)$ and $DD_2(\Omega)$ of 2DOF DVIS should be reduced at both the resonant and higher frequencies, the type selection of additional fluid viscous dampers should be $a_1 = 0.2$ and $a_2 = 3$ as shown in Table.5.2.

The above studies reveal how the nonlinear damping characteristic parameters affect the displacement and force transmissibility of MDOF systems over a wide frequency range. These results provide an important basis for the selection of the type of nonlinear dampers and the design of damping characteristic parameters in MDOF structural systems for different vibration control purposes.

5.4 Damping parameters design using the OFRF approach

Using the OFRF based evaluation method described in Eqs.(5.18) and (5.19), a procedure for the fluid viscous dampers design for the MDOF DVIS and FVIS can be proposed as follows.

(i) Choose appropriate fluid viscous damper type (damping exponent a) to avoid obvious change of the system displacement or force transmissibility over the higher frequency region according to the vibration control requirement and the analysis in Section 5.3.

(ii) Define an OFRF expression Eq.(5.18) according to the damping characteristic parameters to be designed.

(iii) Obtain the system output frequency responses by numerical simulations or experimental tests with different viscous damping parameters and determine the $P_{p,q}(j\omega)$ in Eq.(5.18) using the least square method in Eq.(5.19).

(iv) Find the desired damping characteristic parameters from the determined OFRF expression (5.18) to achieve a desired system vibration control performance.

An example is provided below to demonstrate the application and effectiveness of the above fluid viscous dampers design procedure.

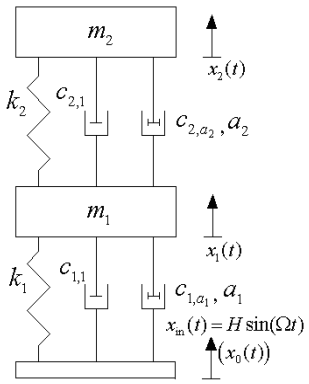

Fig.5.20 A 2DOF DVIS

Consider a 2DOF DVIS as shown in Fig.5.20, where the lumped masses are

$m_1 = m_2 = 10\,\text{kg}$, linear springs' stiffness coefficients are $k_1 = k_2 = 4000\,\text{N/m}$, linear damping coefficients associated with the springs are $c_{1,1} = c_{2,1} = 20\,\text{Ns/m}$, the amplitude of harmonic displacement excitation is $H = 10^{-3}\,\text{m}$. Without additionally fitted viscous damping devices in this vibration system, the displacement transmissibility $DD_1(\Omega)$ and $DD_2(\Omega)$ at Storey1 and Storey2 over the frequency region $\Omega \in [1, 1000]\,\text{rad/s}$ can be evaluated by Eqs.(5.35) and (5.36). The results are shown in Fig.5.21.

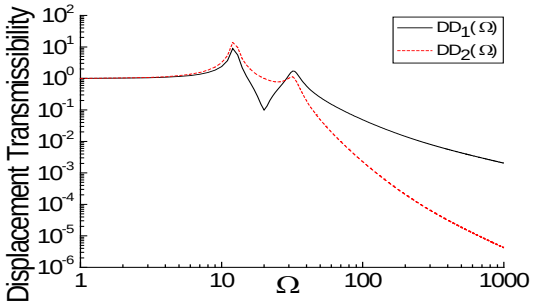

Fig.5.21 $DD_1(\Omega)$ and $DD_2(\Omega)$ of 2DOF without fluid viscous damper

This system's 1st and 2nd resonant frequencies are $\Omega_1 = 12.36\,\text{rad/s}$ and $\Omega_2 = 32.36\,\text{rad/s}$. The displacement transmissibility at these two resonant frequencies and a higher frequency $\Omega_3 = 1000\,\text{rad/s}$ are $DD_1(\Omega_1) = 11.7583$, $DD_1(\Omega_2) = 1.7384$, $DD_1(\Omega_3) = 2.04\text{E-}3$, $DD_2(\Omega_1) = 18.967$, $DD_2(\Omega_2) = 1.083$ and $DD_2(\Omega_3) = 4.165\text{E-}6$, respectively. In order to reduce the displacement transmissibility at the resonant frequencies Ω_1 and Ω_2 without significant increase at the higher frequency Ω_3 and consider the vibration isolation effects that can be achieved by additional fluid viscous dampers by numerical simulations, the design objective is defined as $DD_1^*(\Omega_1) \le 7$, $DD_1^*(\Omega_2) \le 1.3$, $DD_1^*(\Omega_3) \le 2.5\text{E}-3$, $DD_2^*(\Omega_1) \le 12$, $DD_2^*(\Omega_2) \le 0.9$ and $DD_2^*(\Omega_3) \le 5.5\text{E}-6$, a nonlinear fluid viscous damper with the damping characteristic parameters a_1 and C_{1,a_1} at Storey1 can be designed as follows.

Following the design procedure, firstly, determine the range of the damping characteristic parameter a_1 as $a_1 < 1$ because the displacement transmissibility of 2DOF DVIS is to be suppressed and the nonlinear fluid viscous damper is fitted at Storey1 in this case. Second, define the OFRF expressions of the system output frequency responses $Y_1(j\Omega)$ and $Y_2(j\Omega)$ at Storey1 and Storey2 as

$$Y_1(j\Omega) = \sum_{p=0}^{2}\sum_{q=0}^{2} P_{p,q}(j\Omega)\cdot a_1^p C_{1,a_1}^q \tag{5.40}$$

and

$$Y_2(\Omega) = \sum_{p=0}^{2}\sum_{q=0}^{2} Q_{p,q}(j\Omega)\cdot a_1^p C_{1,a_1}^q \tag{5.41}$$

respectively. The displacement transmissibility $DD_1(\Omega)$ and $DD_2(\Omega)$ at Storey1 and Storey2 can be described by

$$DD_1(\Omega) = \left|Y_1(j\Omega)\right| / H \tag{5.42}$$

and

$$DD_2(\Omega) = \left|Y_2(j\Omega)\right| / H \tag{5.43}$$

Using the Runge-Kutta integration method in MATLAB program, the system output frequency responses $Y_1(j\Omega)$ and $Y_2(j\Omega)$ and the corresponding displacement transmissibility $DD_1(\Omega)$ and $DD_2(\Omega)$ over the frequencies of Ω_1, Ω_2, and Ω_3 were evaluated. The results are shown in Table.5.7 and 5.8, respectively.

Table.5.7 Output frequency responses $Y_1(j\Omega)$ and $Y_2(j\Omega)$ of 2DOF DVIS under different damping characteristic parameters over three different frequencies

	$Y_1(j\Omega_1)$	$Y_1(j\Omega_2)$	$Y_1(j\Omega_3)$	$Y_2(j\Omega_1)$	$Y_2(j\Omega_2)$	$Y_2(j\Omega_3)$
$a_1 = 0.2$ $C_{1,a_1} = 1$	-0.0094-0.001i	-0.0015-0.0003i	-2.122E-6 +3.881E-7i	-0.0152 -0.001i	8.452E-4 +4.116E-4i	1.663E-9 +4.062E-9i
$a_1 = 0.2$ $C_{1,a_1} = 3$	-0.0055-0.0008i	-0.001-0.0005i	-2.364E-6 +3.883E-7i	-0.009-0.001i	5.338E-4 +4.786E-4i	1.743E-9 +4.545E-9i

$a_1 = 0.2$ $C_{1,a_1} = 5$	-0.0028-0.0007i	-6.486E-4 -6.94E-4i	-2.604E-6 +3.848E-7i	-0.0046 -0.001i	2.787E-4 +5.211E-4i	1.83E-9 +5.025E-9i
$a_1 = 0.4$ $C_{1,a_1} = 1$	-0.0102-0.001i	-0.0016-0.0002i	-2.117E-6 +3.875E-7i	-0.0166 -0.001i	9.243E-4 +3.922E-4i	1.655E-9 +4.051E-9i
$a_1 = 0.4$ $C_{1,a_1} = 3$	-0.0078-0.0009i	-0.0014-0.0004i	-2.345E-6 +3.837E-7i	-0.0126 -0.001i	7.544E-4 +4.338E-4i	1.736E-9 +4.51E-9i
$a_1 = 0.4$ $C_{1,a_1} = 5$	-0.0059-0.0009i	-0.0011-0.0005i	-2.574E-6 +3.854E-7i	-0.0095 -0.0011i	6.075E-4 +4.664E-4i	1.824E-9 +4.967E-9i
$a_1 = 0.6$ $C_{1,a_1} = 1$	-0.0108-0.001i	-0.0017-0.0002i	-2.112E-6 +3.894E-7i	-0.0174 -0.001i	9.666E-4 +3.811E-4i	1.652E-9 +4.037E-9i
$a_1 = 0.6$ $C_{1,a_1} = 3$	-0.0091-0.001i	-0.0015-0.0003i	-2.328E-6 +3.835E-7i	-0.0148 -0.001i	8.71E-4 +4.059E-4i	1.728E-9 +4.478E-9i
$a_1 = 0.6$ $C_{1,a_1} = 5$	-0.0078-0.001i	-0.0014-0.0003i	-2.547E-6 +3.856E-7i	-0.0126 -0.0011i	7.851E-4 +4.27E-4i	1.806E-9 +4.911E-9i

Table.5.8 Displacement transmissibility of 2DOF DVIS under different damping characteristic parameters over three different frequencies

	$DD_1(\Omega_1)$	$DD_1(\Omega_2)$	$DD_1(\Omega_3)$	$DD_2(\Omega_1)$	$DD_2(\Omega_2)$	$DD_2(\Omega_3)$
$a_1 = 0.2$ $C_{1,a_1} = 1$	9.47	1.5103	0.0022	15.275	0.9401	4.39E-6
$a_1 = 0.2$ $C_{1,a_1} = 3$	5.602	1.1523	0.0024	9.0362	0.7169	4.868E-6
$a_1 = 0.2$ $C_{1,a_1} = 5$	2.8999	0.9499	0.0026	4.6779	0.5909	5.348E-6
$a_1 = 0.4$ $C_{1,a_1} = 1$	10.2972	1.6127	0.0022	16.6093	1.0041	4.376E-6
$a_1 = 0.4$ $C_{1,a_1} = 3$	7.8382	1.3983	0.0024	12.6431	0.8703	4.832E-6
$a_1 = 0.4$ $C_{1,a_1} = 5$	5.9343	1.2310	0.0026	9.5723	0.7659	5.291E-6
$a_1 = 0.6$ $C_{1,a_1} = 1$	10.8090	1.6686	0.0021	17.4348	1.0390	4.362E-6
$a_1 = 0.6$ $C_{1,a_1} = 3$	9.1809	1.5436	0.0024	14.8089	0.9609	4.8E-6
$a_1 = 0.6$ $C_{1,a_1} = 5$	7.8539	1.4360	0.0026	12.6685	0.8937	5.232E-6

Using the method described in Section 5.2.3, $P_{p,q}(j\Omega)$ and $Q_{p,q}(j\Omega)$ in the OFRF expressions (5.40) and (5.41) at the frequencies of Ω_1, Ω_2 and Ω_3 can be determined from the system output frequency responses $Y_1(j\Omega)$ and $Y_2(j\Omega)$ in Table.5.7. Consequently, the system displacement transmissibility $DD_1(\Omega)$ and $DD_2(\Omega)$ at Ω_1, Ω_2 and Ω_3 and over the range of the nonlinear damping parameters $a_1 \in [0.2, 0.6]$ and $C_{a1} \in [1, 5]$ can be calculated by

$$DD_1(\Omega) = \left| \sum_{p=0}^{2} \sum_{q=0}^{2} P_{p,q}(j\Omega) \cdot a_1^p C_{1,a_1}^q \right| \Big/ H, \quad a_1 \in [0.2, 0.6] \text{ and } C_{a1} \in [1, 5] \quad (5.44)$$

and

$$DD_2(\Omega) = \left| \sum_{p=0}^{2} \sum_{q=0}^{2} Q_{p,q}(j\Omega) \cdot a_1^p C_{1,a_1}^q \right| \Big/ H, \quad a_1 \in [0.2, 0.6] \text{ and } C_{a1} \in [1, 5] \quad (5.45)$$

Consider a design requirement in terms of the system displacement transmissibility $DD_1(\Omega)$ and $DD_2(\Omega)$ at frequencies of Ω_1, Ω_2 and Ω_3 such that

$$DD_1^*(\Omega_1) \le 7 \; DD_1^*(\Omega_2) \le 1.3 \text{ and } DD_1^*(\Omega_3) \le 2.5\,\mathrm{E}-3;$$

$$DD_2^*(\Omega_1) \le 12, DD_2^*(\Omega_2) \le 0.9 \text{ and } DD_2^*(\Omega_3) \le 5.5\,\mathrm{E}-6.$$

The values of the damping characteristic parameters a_1 and C_{1,a_1} that can achieve the design requirement were found out from the results of $DD_1(\Omega)$ and $DD_2(\Omega)$ evaluated using Eqs.(5.44) and (5.45) at Ω_1, Ω_2 and Ω_3 and over the range of the damping characteristic parameters

$a_1 \in [0.2, 0.6]$ and $C_{a1} \in [1, 5]$

The results, which synthetically consider the design requirements on the system displacement transmissibility at different frequencies, are as shown by the darker area in Fig.5.22.

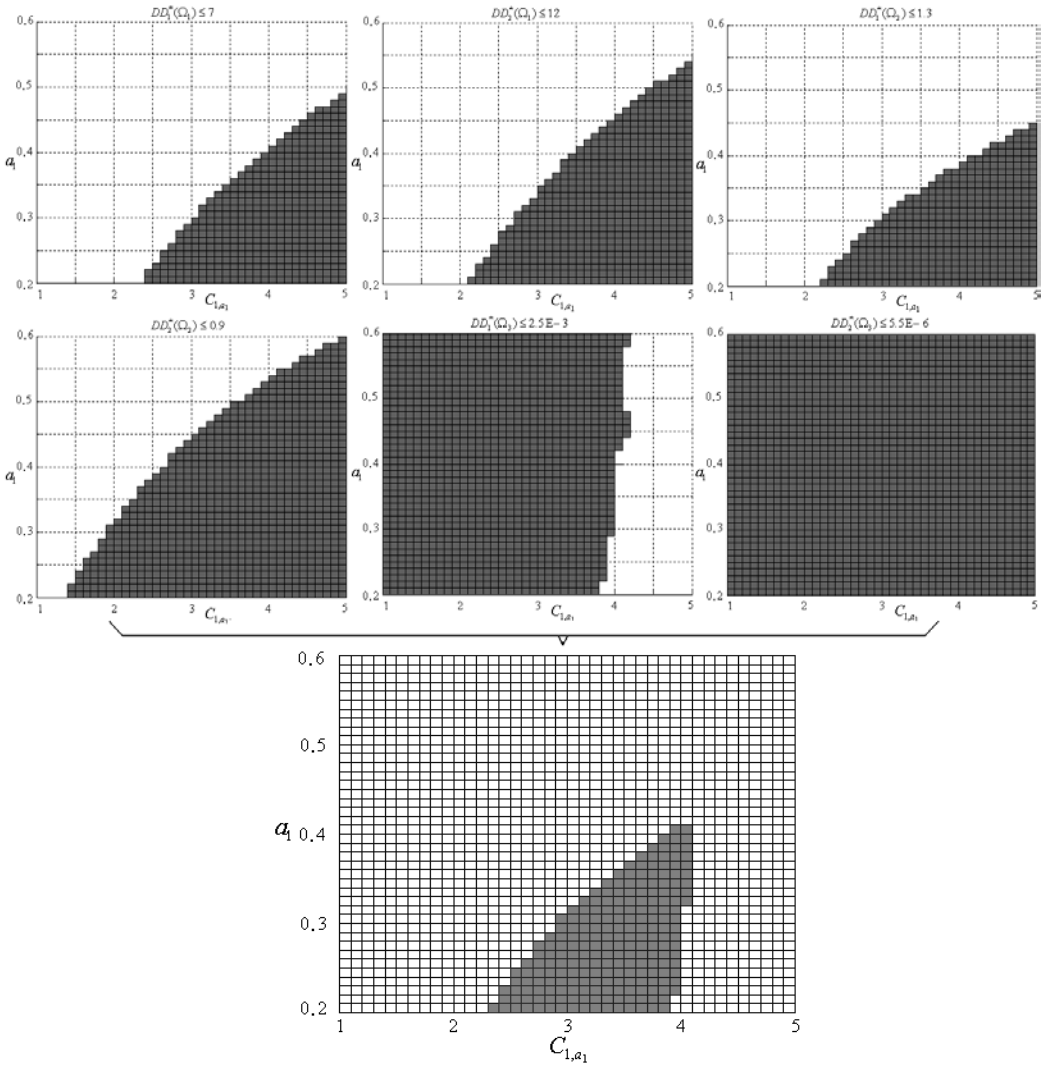

Fig.5.22 Viscous damping parameters a_1 and C_{1,a_1} which satisfy the design requirements

If, for example, $a_1 = 0.3$ and $C_{1,a_1} = 3.5$ are determined as the final design. The system displacement transmissibility $DD_1(\Omega)$ and $DD_2(\Omega)$ at Ω_1, Ω_2 and Ω_3 under this design are

$DD_1(\Omega_1) = 6.234$, $DD_1(\Omega_2) = 1.2339$ and $DD_1(\Omega_3) = 2.4436\text{E-}3$;

$DD_2(\Omega_1) = 10.0556$, $DD_2(\Omega_2) = 0.7678$ and $DD_2(\Omega_3) = 4.9646\text{E-}6$

which clearly satisfies the design requirement.

However, if a nonlinear fluid viscous damper with the parameters outside the optimal range in Fig.5.22 is fitted at Storey1, for example, $a_1 = 0.3$ and $C_{1,a_1} = 5$, the values of the system displacement transmissibility $DD_1(\Omega)$ and

$DD_2(\Omega)$ at the three frequencies become

$DD_1(\Omega_1) = 4.5937$, $DD_1(\Omega_2) = 1.0941$ and $DD_1(\Omega_3) = 2.6169\,\mathrm{E}-3$;

$DD_2(\Omega_1) = 7.4099$, $DD_2(\Omega_2) = 0.6806$ and $DD_2(\Omega_3) = 5.3122\,\mathrm{E}-6$

which doesn't satisfy the requirement of $DD_1^*(\Omega_3) \le 2.5\,\mathrm{E}-3$.

The comparisons of the displacement transmissibility $DD_1(\Omega)$ and $DD_2(\Omega)$ of the 2DOF DVIS with and without the designed nonlinear fluid viscous damper with $a_1 = 0.3$ and $C_{1,a_1} = 3.5$ fitted at Storey 1 are shown in Figs.5.23 and 5.24, respectively. The results clearly indicate that an appropriately designed nonlinear fluid viscous damper can reduce the system transmissibility around the system resonant frequencies without a significant increase over the higher frequency region.

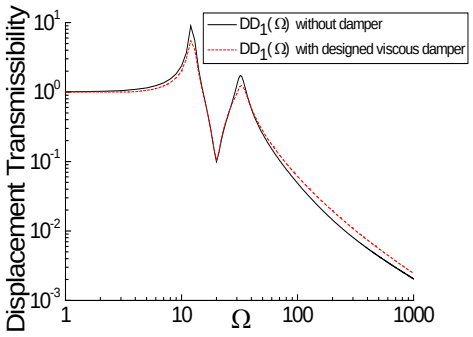

Fig.5.23 $DD_1(\Omega)$ of 2DOF DVIS with and without designed fluid viscous damper

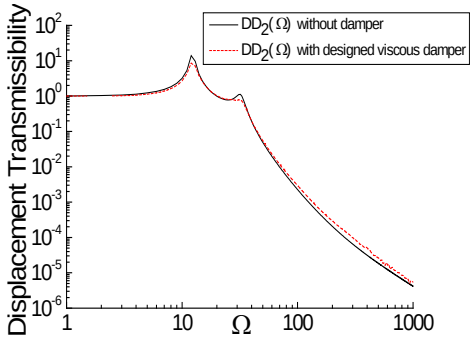

Fig.5.24 $DD_2(\Omega)$ of 2DOF DVIS with and without designed fluid viscous damper

It is worth mentioning that, if needed, the slight increase of the system transmissibility over the higher frequency region in Figs.5.23 and 5.24 can be further reduced by taking a damping exponent less than 0.3. However, in practice, the available range of the damping exponent of passive damping devices is subject to the constraints determined by the devices' manufacturing process [9]. In such cases, semi-active damping devices such as those implemented using MR dampers can be used as solutions [114].

5.5 Conclusions

In this chapter, the OFRF concept is applied to the analysis and design of MDOF viscously damped vibration systems. The explicit polynomial OFRF expression for the relationship between the system output frequency response and nonlinear damping characteristic parameters is derived. It shows how the system output frequency response can be analytically related to the nonlinear damping characteristic parameters. A comparison between the results from the OFRF based evaluation and numerical simulation has verified the effectiveness of the application of the OFRF based approach in the analysis of nonlinear viscously damped vibration systems. Moreover, based on the OFRF representation, the effects of damping characteristic parameters of nonlinear fluid viscous dampers on the displacement and force transmissibility of MDOF DVIS and FVIS are studied. The results reveal that

- For 1, 2 and 3DOF DVIS under harmonic displacement excitations, compared with other types of fluid viscous dampers, a nonlinear fluid viscous damper with damping exponent $a_1 < 1$ at Storey1 and nonlinear fluid viscous dampers with damping exponents $a_i > 1$, $i = 2, 3$, at the upper storeys (Storey2 and Storey3) can perform ideal control effect on the system displacement vibration. This approach of fitting additional fluid viscous dampers can reduce the displacement transmissibility around the system resonant frequencies but have less effect on the displacement transmissibility over higher frequency region.

- For 1, 2 and 3DOF FVIS under harmonic force excitations, compared with other types of fluid viscous dampers, nonlinear fluid viscous dampers with damping exponent $a_i > 1$, $i = 1, 2, 3$, at all storeys (Storey1 to Storey3) are more ideal for the suppression of the force transmissibility at both the resonant and higher frequencies.

Based on these analyses, an OFRF based design procedure for nonlinear viscously damped vibration systems is proposed to facilitate the design of nonlinear fluid viscous damper parameters for a desired system vibration suppression performance.

The studies in this chapter have applied the OFRF concept to the analysis and design of nonlinear MDOF viscously damped vibration systems. The results show the advantage of nonlinear viscous damping in the vibration control of MDOF viscously damped structural systems, and provide important guidelines for the design of nonlinear fluid viscous damper parameters for a desired system performance. The results have considerable significance for the practical applications of nonlinear viscous damping devices in a wide class of engineering structural systems.

Chapter 6

Design of Damping Devices for Structural Vibration Control

In order to design the damping devices for structural system vibration control, the concept of Vibration Power Loss Factor (VPLF) is firstly proposed in this chapter to evaluate the vibration reduction effects of additional fluid viscous dampers in engineering structural systems. An explicit analytical relationship between the VPLF and the damping coefficient of fluid viscous dampers additionally fitted into a structural system is then derived using the Output Frequency Response Function (OFRF) concept. After that, a novel nonlinear damping design approach is proposed based on the OFRF representation of the VPLF of viscously damped structural systems to achieve a desired vibration performance. Numerical simulation studies on a typical 7-storey building structure subject to seismic and wind loading excitations demonstrate the effectiveness of the proposed design approach. The results reveal that, compared with linear fluid viscous dampers, equivalent nonlinear fluid viscous dampers can achieve overall better vibration effects. These results have significant implications for the design and fitting of additional fluid viscous dampers in practical structural systems for vibration control purpose.

6.1 Introduction

The safety issues of modern engineering structural systems have received more and more attention because of tragic consequences of earthquakes and strong wind, which have shown tremendous importance of vibration control in civil buildings and bridges etc. infrastructures. In order to suppress vibrations and

protect structural systems, traditional vibration control methods often increase the system stiffness. But these methods will lead to the increase of system modal frequencies and even increase vibrations when the system is subjected to the seismic and wind loading excitations over the frequency ranges higher than the original system modal frequencies. In order to resolve this problem, many vibration control approaches and vibration control devices have been proposed and applied to increase the system safety and reliability against strong earthquake and wind. Recently, nonlinear fluid viscous dampers have been considered to be a more effective vibration control approach for practical engineering system designs [5, 103]. Many researchers have conducted studies considering the applications of nonlinear fluid viscous dampers in the vibration control of practical engineering systems as introduced in Chapter 2.

After nonlinear fluid viscous dampers have been introduced as additional devices into a vibration system, the most important issue to be addressed is how to design the dampers' damping characteristic parameters to achieve a desired vibration control performance. The solution partly depends on how to evaluate the vibration control effects of the additional fluid viscous dampers on the system output response. Currently, the concepts of maximum vibration offset and modal damping ratio have been widely used for this purpose [12]. However, it is difficult to relate a structural system's maximum vibration offset to the damping characteristic parameters so as to facilitate the system vibration control design. The equivalent modal damping ratio method was proposed by Soong and Constantinou [183] and Lee et al. [184] for the simple harmonic analyses. However the modal damping ratio is basically a linear system concept, which is difficult to be applied for the analysis and design of nonlinear vibration systems subject to complicated loadings such as earthquakes and winds [112].

This chapter is concerned with the development of a novel approach for the design of additional nonlinear fluid viscous dampers to achieve desired vibration

control in practical engineering systems. This new design will be based on the OFRF concept of nonlinear systems proposed by Lang et al. [24] and a new concept known as VPLF introduced in this study. By using the OFRF concept, an explicit analytical relationship between the system VPLF and damping coefficient of nonlinear fluid viscous dampers additionally fitted into a vibration system can be obtained. This explicit analytical relationship can significantly facilitate the parameter design of additional fluid viscous dampers so as to achieve a desired vibration performance in a wide range of loading conditions. Simulation studies are conducted to demonstrate the effectiveness of this new approach in the design of nonlinear fluid viscous dampers for the vibration control of a 7-storey building structure subject to seismic and wind loading excitations. These results have significant implications for the design and fitting of additional fluid viscous dampers in practical structural systems for vibration control purpose.

6.2 The VPLF of nonlinear viscously damped vibration systems

6.2.1 The Vibration Power Loss Factor (VPLF)

The energy and power are two frequently used vibration system characteristics. The energy of a mechanical and civil engineering system's vibration $y(t)$ can be determined as

$$E = \int_0^T |y(t)|^2 dt \tag{6.1}$$

where T is the total time period considered for the evaluation. The vibration power refers to the average of vibration energy over the time T and is given by

$$P = E/T = \frac{1}{T}\int_0^T |y(t)|^2 dt \tag{6.2}$$

The VPLF of a vibration system is defined by

$$\gamma = (1 - P/P_0) \times 100\% \tag{6.3}$$

where P_0 denotes the power of the original structural system vibration response; P represents the power of the structural system vibration response after a vibration control mechanism has been introduced. Therefore, the system VPLF indicates the reduction in the power of the system vibration response that can be achieved by the introduction of a vibration control mechanism.

A larger value of VPLF γ means that the vibration control mechanism can dissipate more significant vibration power, which should be the objective of the design of the vibration control mechanism. In the current study, different types of fluid viscous dampers refer to the dampers whose damping exponent parameters a are different. In order to compare the vibration control effects of different types of fluid viscous dampers, it is defined that different types of fluid viscous dampers have an equivalent vibration control effect on a structural system if the VPLF values of the system with these different dampers are the same, that is, $\gamma(C_a) = \gamma(C_b)$, where C_a and C_b present the coefficients of two different types of fluid viscous dampers.

6.2.2 The OFRF based representation of the system VPLF

Consider a vibration system with a fitted nonlinear fluid viscous damper with the damping characteristic as introduced in chapter 2

$$F_{\mathrm{D}} = C_a \left| \dot{u}_r \right|^a \operatorname{sign}(\dot{u}_r) \tag{6.4}$$

where F_{D} is the damping force produced by the damper, $\dot{u}_r$ is the relative velocity between the two ends of the damper, C_a and a are the damping coefficient and exponent, respectively.

Based on the OFRF concept, the relationship between the FT spectrum $Y(j\omega)$ of the system vibration response $y(t)$ and the viscous damping coefficient C_a can be described by the following polynomial function known as the system OFRF

$$Y(j\omega) = \overline{P}_0(j\omega) + \sum_{i=1}^{\overline{N}} C_a^i \overline{P}_i(j\omega) \tag{6.5}$$

where $\overline{P}_{i_1}(j\omega) = a_{i_1}(j\omega) + b_{i_1}(j\omega)j$, $i_1 = 0, 1, \cdots, \overline{N}$, are the functions of the system input spectrum and dependent on all the system parameters apart from C_a, $\overline{N}$ is determined by the highest order of system nonlinearity up to which the system output spectrum can be well represented by a Volterra series.

From Eq.(6.5), it can be obtained that

$$\begin{aligned} |Y(j\omega)|^2 &= \left| \overline{P}_0(j\omega) + \sum_{i=1}^{\overline{N}} C_a^i \overline{P}_i(j\omega) \right|^2 \\ &= \left| \left[a_0(j\omega) + b_0(j\omega)j \right] + \sum_{i=1}^{\overline{N}} \left\{ C_a^i \left[a_i(j\omega) + b_i(j\omega)j \right] \right\} \right|^2 \\ &= \sum_{i=0}^{2\overline{N}} C_a^i Q_i(j\omega) \end{aligned} \tag{6.6}$$

where $Q_{i_1}(j\omega)$, $i_1 = 0,\ 1, ...,\ 2\overline{N}$, are the functions of the same nature as $\overline{P}_{i_1}(j\omega)$, $i_1 = 0, 1, \cdots, \overline{N}$.

For example, when the OFRF expression for a vibration system's output spectrum $Y(j\omega)$ can be described by

$$Y(j\omega) = \overline{P}_0(j\omega) + C_a \overline{P}_1(j\omega) + C_a^2 \overline{P}_2(j\omega) \tag{6.7}$$

where $\overline{P}_{i_1}(j\omega) = a_{i_1}(j\omega) + b_{i_1}(j\omega)j$, $i_1 = 0, 1, 2$, then

$$\begin{aligned}
\left|Y(j\omega)\right|^2 &= \left|\bar{P}_0(j\omega)+C_a\bar{P}_1(j\omega)+C_a^2\bar{P}_2(j\omega)\right|^2 \\
&= \left|\left[a_0(j\omega)+b_0(j\omega)j\right]+C_a\left[a_1(j\omega)+b_1(j\omega)j\right]+C_a^2\left[a_2(j\omega)+b_2(j\omega)j\right]\right|^2 \\
&= \left[a_0^2(j\omega)+b_0^2(j\omega)\right]+C_a\left[2a_0(j\omega)a_1(j\omega)+2b_0(j\omega)b_1(j\omega)\right] \\
&\quad +C_a^2\left[a_1^2(j\omega)+b_1^2(j\omega)+2a_0(j\omega)a_2(j\omega)+2b_0(j\omega)b_2(j\omega)\right] \\
&\quad +C_a^3\left[2a_1(j\omega)a_2(j\omega)+2b_1(j\omega)b_2(j\omega)\right]+C_a^4\left[a_2^2(j\omega)+b_2^2(j\omega)\right] \\
&= Q_0(j\omega)+C_aQ_1(j\omega)+C_a^2Q_2(j\omega)+C_a^3Q_3(j\omega)+C_a^4Q_4(j\omega)
\end{aligned} \tag{6.8}$$

where

$$Q_0(j\omega) = a_0^2(j\omega)+b_0^2(j\omega),$$

$$Q_1(j\omega) = 2a_0(j\omega)a_1(j\omega)+2b_0(j\omega)b_1(j\omega),$$

$$Q_2(j\omega) = a_1^2(j\omega)+b_1^2(j\omega)+2a_0(j\omega)a_2(j\omega)+2b_0(j\omega)b_2(j\omega),$$

$$Q_3(j\omega) = 2a_1(j\omega)a_2(j\omega)+2b_1(j\omega)b_2(j\omega),$$

$$Q_4(j\omega) = a_2^2(j\omega)+b_2^2(j\omega).$$

According to the Parseval's theorem [185], the vibration power P of the system output response $y(t)$ can be determined as

$$P = \frac{1}{T}\int_0^T \left|y(t)\right|^2 dt = \int_{-\infty}^{\infty}\left|Y(j\omega)\right|^2 \frac{\mathrm{d}\omega}{2\pi T} \tag{6.9}$$

Substituting the expression of $\left|Y(j\omega)\right|^2$ in Eq.(6.6) into Eq.(6.9) yields

$$P = P_0 + \sum_{i=1}^{2\bar{N}} C_a^i P_i \tag{6.10}$$

where P_0 is the power of the system vibration response when no fluid viscous damper is fitted, and

$$P_i = \int_{-\infty}^{\infty} Q_i(j\omega)\frac{\mathrm{d}\omega}{2\pi T}, \quad i = 0, 1, \cdots, 2\bar{N} \tag{6.11}$$

Consequently, the system VPLF as defined in Eq.(6.3) can be described by a polynomial function of the viscous damping coefficient C_a as follows

$$\gamma(C_a) = \left(P_0 - P\right)/P_0 = \sum_{i=1}^{2\bar{N}} C_a^i \rho_i \tag{6.12}$$

where $\rho_i = -P_i/P_0$, $i = 1, 2, \cdots, 2\bar{N}$. Eq.(6.12) is the OFRF based representation of the VPLF of nonlinear viscously damped vibration systems, which provides a significant analytical relationship between the system VPLF and the damping coefficient C_a of additionally fitted nonlinear fluid viscous dampers.

6.2.3 Determination of the OFRF based representation of the system VPLF

The OFRF based representation of the system VPLF in Eq.(6.12) involves a set of coefficients ρ_i, $i = 1, 2, \cdots, 2\bar{N}$, which are constants depending on the system input spectrum and all the system parameters apart from C_a. In order to apply Eq.(6.12) in the vibration system analysis and design, these coefficients have to be determined.

Denote γ_i, $i = 1, 2, \cdots, m$, as the VPLF values of a nonlinear viscously damped vibration system under m different nonlinear damping coefficient $C_{a,i}$, $i = 1, 2, \cdots, m$. It is known from Eq.(6.12) that given γ_i and $C_{a,i}$, $i = 1, 2, \cdots, m$, provided that $m \geq 2\bar{N}$, the coefficients ρ_i, $i = 1, 2, \cdots, 2\bar{N}$, can be determined by the following least square method

$$[\rho_{1,} \cdots, \rho_{2\bar{N}}]^{\mathrm{T}} = \left(\left[x\right]^{\mathrm{T}} \cdot \left[x\right]\right)^{-1} \cdot \left(\left[x\right]^{\mathrm{T}} \cdot \left[Y\right]\right) \tag{6.13}$$

where

$$\left[x\right] = \begin{bmatrix} C_{a,1} & C_{a,1}^2 & C_{a,1}^3 & \cdots & C_{a,1}^{2\bar{N}} \\ C_{a,2} & C_{a,2}^2 & C_{a,2}^3 & \ddots & C_{a,2}^{2\bar{N}} \\ \vdots & \ddots & \ddots & \ddots & \vdots \\ C_{a,m} & C_{a,m}^2 & C_{a,m}^3 & \cdots & C_{a,m}^{2\bar{N}} \end{bmatrix}, \quad \left[Y\right] = \begin{bmatrix} \gamma_1 \\ \gamma_2 \\ \vdots \\ \gamma_m \end{bmatrix} \tag{6.14}$$

Because γ_i is the VPLF value of the system output response under an input excitation of interest when $C_a = C_{a,i}$, γ_i can be determined from the simulated or experimentally measured output response of the system to this input excitation when the nonlinear damping coefficient C_a is taken as $C_{a,i}$. Therefore, using Eq.(6.13), the OFRF based representation of the system VPLF can be determined directly from system simulation or experimental test data.

One issue that needs to be considered when using this approach is how to determine $\overline{N}$. There is no general theoretical solution to this problem. However, in practice, taking a value for $\overline{N}$ within the range of 2, 3, 4, 5 is often sufficient.

6.3 Nonlinear fluid viscous dampers design for vibration control of civil structures

On the basis of the OFRF based representation for the VPLF of a nonlinear viscously damped vibration system, given the damping exponent parameter a, the design of the system nonlinear damping coefficient C_a can be conducted using the following procedure:

(i) Conduct simulation study or experimental tests on the original vibration system where additional nonlinear fluid viscous damper/dampers are to be fitted for vibration control purpose. A specific input loading of concern for the design should be considered in the simulation or experimental tests. Evaluate the vibration power P_0 of the original system without additional fluid viscous damper/dampers from the simulated or experimentally measured system output responses.

(ii) Fit additional nonlinear fluid viscous damper/dampers in the vibration system and conduct the simulation studies or experimental tests again to evaluate the vibration power P of the system output response under different values of damping coefficients C_a.

(iii) Evaluate the VPLF value γ_i, $i = 1, 2, \cdots, m$, of the system output response under different values of the damping coefficient $C_{a,i}$ from Eq.(6.3) using the results obtained in step (ii).

(iv) Determine the coefficients ρ_i, $i = 1, 2, \cdots, 2\overline{N}$, to obtain the OFRF based representation of the system VPLF in Eq.(6.12) by substituting the results obtained in previous steps into Eq.(6.13).

(v) Conduct the design to achieve a desired VPLF value γ^* for the vibration system by solving equation $\gamma^* = \sum_{i=1}^{2\overline{N}} C_a^i \rho_i$ for C_a.

In the following section, numerical simulation studies on a 7-storey building structure subject to seismic and wind loading excitations will be conducted to show how to follow the above procedure to perform the design and to demonstrate the effectiveness of this new approach in nonlinear fluid viscous dampers design.

6.4 Simulation study of additional fluid viscous dampers design for a 7-storey building structure

6.4.1 7-storey building structure

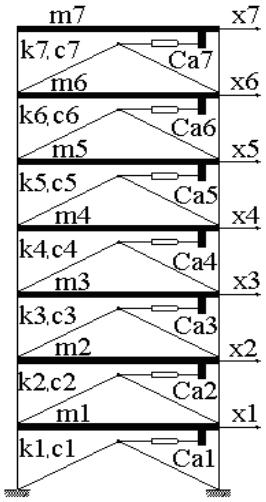

Fig.6.1 7-storey building structure with fitted additional fluid viscous dampers

Consider a 7-storey building structure as shown in Fig.6.1 where additional fluid viscous dampers are fitted in each floor to control the structure vibration induced by seismic or wind loading excitations. This structural system can be described by the following dynamic equilibrium equation

$$M\ddot{X}(t) + C\dot{X}(t) + KX(t) = F(t) + F_d(t) \tag{6.15}$$

where M, C and K are the system mass, damping and stiffness matrices, respectively. $X(t)$, $\dot{X}(t)$ and $\ddot{X}(t)$ are the system displacement, velocity and acceleration vectors, respectively. $F(t)$ is the force excitation on the structural system induced by seismic or wind loading excitations. $F_d(t)$ is the damping force produced by additional fluid viscous dampers fitted in each floor of the structure. The following system parameter values [57] are used in the simulation studies

$$M = 8.75\times10^4 I_{7\times7}(\text{kg}) \tag{6.16}$$

$$K = \begin{bmatrix} 29.28 & -14.64 & & & & & 0 \\ -14.64 & 31.59 & -16.95 & & & & \\ & -16.95 & 30.96 & -14.01 & & & \\ & & -14.01 & 28.02 & -14.01 & & \\ & & & -14.01 & 25.13 & -11.12 & \\ & & & & -11.12 & 22.24 & -11.12 \\ 0 & & & & & -11.12 & 11.12 \end{bmatrix} \times 10^7 (\text{N/m}) \tag{6.17}$$

An inherent structural damping ratio $\xi = 2\%$ is assumed for this structural system, the system damping matrix C can be described by [186]

$$C = 2\xi\omega_1 M \tag{6.18}$$

where ω_1 is the 1st natural frequency of the 7-storey building structure and the structural system's 1st to 7th natural frequencies can be evaluated as [182]

$$\omega_{1\sim7} = \text{sqrt}\left(\text{eig}\left(M^{-1}K\right)\right) = [8.54, 23.85, 38.94, 53.07, 62.06, 71.26, 80.49]\,\text{rad/s} \tag{6.19}$$

where sqrt(.) denotes to evaluate the square root and eig(.) represents to evaluate the eigen values of a matrix.

6.4.2 Seismic and wind loading excitations

6.4.2.1 Seismic excitations

In the simulation studies, the seismic and wind loading excitations are considered respectively to examine the vibration response of the 7-storey building structure.

EI-Centro S00E (1940) seismic excitation is a time history of acceleration recorded in EI Centro Terminal Substation Building in California. Because the qualitative aspects of the earthquake were well-recorded, it is often used in the design of earthquake-proof structures, particularly for the time history analysis. The time history data of the EI-Centro earthquake, including the acceleration, velocity and displacement, are shown in Fig.6.2 (a)-(c).

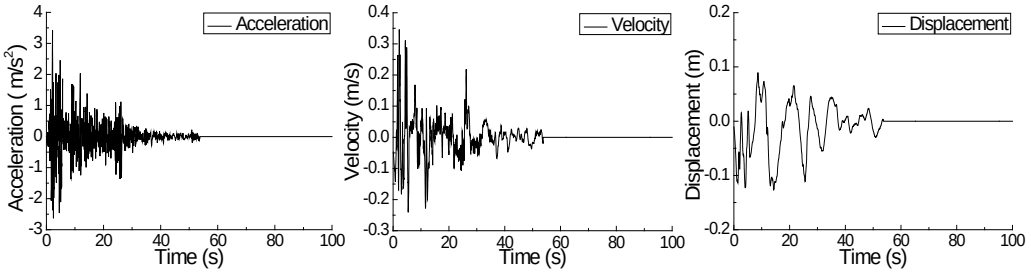

(a) Acceleration (b) Velocity (c) Displacement

Fig.6.2 EI-Centro seismic excitation

6.4.2.2 Wind loading excitations

The real wind speed $v(t)$ can be decomposed into a constant mean wind speed V_m and a turbulent wind speed. The mean wind speeds at different locations of structural systems are different. The following exponential model is usually used to describe the shear effect on the mean wind speed at a certain elevation [187]

$$V_m(z) = V_{m,r} \cdot \left(\frac{z}{z_r} \right)^{a_{\text{shear}}} \tag{6.20}$$

where $V_m(z)$ and $V_{m,r}$ are the mean wind speed at the height z and reference height z_r, respectively. $a_{shear} = 1/8.4$ is the power law coefficient. The real wind's turbulence has different forms and is usually represented in a Power Spectral Density (PSD) function. One typical PSD model is the Kaimal spectrum [188]

$$\frac{fS_{\text{Kaimal}}(f)}{\sigma^2} = \frac{4fL_v/V_m}{(1+6fL_v/V_m)^{5/3}} \tag{6.21}$$

where L_v is the length scale: $L_v = \begin{cases} 5.67z & z \le 60\,\text{m} \\ 340.2\,\text{m} & z > 60\,\text{m} \end{cases}$; z is the location height; f is the wind frequency; σ is the time varying wind speed standard deviation and a recommended value by an international standard [187] is

$$\sigma = 0.12\left[(15\,\text{m/s} + 3V_m)/4 + 1.84\,\text{m/s}\right] \tag{6.22}$$

Because wind speeds at different height z are correlative in practical engineering systems, this relationship is usually described by a coherence function, which is given by Davenport [189]

$$coh(j,k,f) = \exp\left(-\frac{a_d d_{j,k} f}{V_m} \right) \tag{6.23}$$

where $d_{j,k}$ is the spatial separation between nodes j and k. $a_d = 10$ is the decay factor.

Based on the coherence function in Eq.(6.23), the $n \times n$ cross power spectra density (CPSD) matrix $S(f)$ can be obtained by

$$S(f) = \begin{bmatrix} S_{11}(f) & S_{12}(f) & \cdots & S_{1n}(f) \\ S_{21}(f) & S_{22}(f) & \cdots & S_{1n}(f) \\ \cdots & \cdots & \cdots & \cdots \\ S_{n1}(f) & S_{n2}(f) & \cdots & S_{nn}(f) \end{bmatrix} \tag{6.24}$$

where the auto power spectra density $S_{jj}(f)$ can be determined by the Kaimal spectrum function in Eq.(6.21) and the CPSD function term $S_{jk}(f)$ is given as

$$S_{jk}(f) = \sqrt{S_{jj}(f) S_{kk}(f)} \cdot coh(j,k,f) \tag{6.25}$$

According to the Cholesky decomposition, the CPSD matrix $S(f)$ can be written as the product of a lower triangular matrix $H(f)$ and the transpose of its complex conjugate $\left[H^*(f)\right]^{\mathrm{T}}$ as

$$S(f) = H(f) \cdot \left[H^*(f)\right]^{\mathrm{T}} \tag{6.26}$$

Finally, the multi-point wind speed time histories $v_j(t)$ can be calculated by the Shinozuka method [190] as

$$v_j(t) = V_m + \sum_{m=1}^{j} \sum_{l=1}^{N} \sqrt{2\Delta f} \cdot \left| H_{jm}(f_l) \right| \cos(2\pi f_l t + \phi_{ml}), \quad j = 1,2,\cdots,p \tag{6.27}$$

where $f_l = l\Delta f$, $\Delta f = \dfrac{f_u}{N}$. p is the number of the wind speed to be numerically simulated at different locations. f_u is the considered maximum wind speed frequency, N is the considered discrete frequency number, V_m is the mean wind speed. ϕ_{ml} is the random phase between $[0,2\pi]$. The time length of the simulated wind speed series $T \le 1/\Delta f$ and the time interval $\Delta t \ge 1/(2 f_u)$.

The procedure to numerically simulate the wind speed time histories of

multi-point wind loading excitations can be summarized as:

(i) Define the height z_r and mean wind speed $V_{m,r}$ at a reference location and the maximum frequency f_u and incremental frequency Δf to be considered.

(ii) Evaluate the mean wind speed at different locations $V_m(z)$ to apply the wind loading excitations by Eq.(6.20).

(iii) Calculate the Kaimal spectrum $S_{\text{Kaimal}}(f)$ at different locations with the corresponding mean wind speed $V_m(z)$ by Eqs.(6.21) and (6.22).

(iv) Obtain the CPSD matrix $S(f)$ as shown in Eq.(6.24) by Eqs.(6.23) and (6.25).

(v) Decompose the CPSD matrix $S(f)$ to find the lower triangular matrix $H(f)$ as shown in Eq.(6.26).

(vi) Substitute the mean wind speed $V_m(z)$ at different locations and the lower triangular matrix $H(f)$ into Eq.(6.27) to calculate the multi-point wind speed time histories $v_j(t)$.

In this study, the wind loading excitation with mean wind speed $V_{m,r} = 20\,\text{m/s}$ at Storey1, maximum frequency $f_u = 10\,\text{Hz}$ and incremental frequency $\Delta f = 0.01\,\text{Hz}$, was considered and applied in the vibration response analysis of the 7-storey building structure. Following the above computational process, the along-wind speed time histories at each storey of the structure were calculated, one realization of the wind speed at Storey1 and its Power Spectral Density (PSD) are shown in Fig.6.3 as an example. The corresponding wind force excitation $F_{\text{storey}1}(t)$ on the structure can be evaluated from the formula recommended by American Petroleum Institute (API RP 2A) as

$$F_{\text{storey}1}(t) = \frac{1}{2}\rho C_s A v(t)^2 \tag{6.28}$$

where $\rho = 1.2\,\text{kg/m}^3$ is the density of the air flow, $C_s = 1.2$ is the shape coefficient of the 7-storey building structure, $A = 20\,\text{m}^2$ is the projected area of each storey, $v(t)$ is the time varying wind speed.

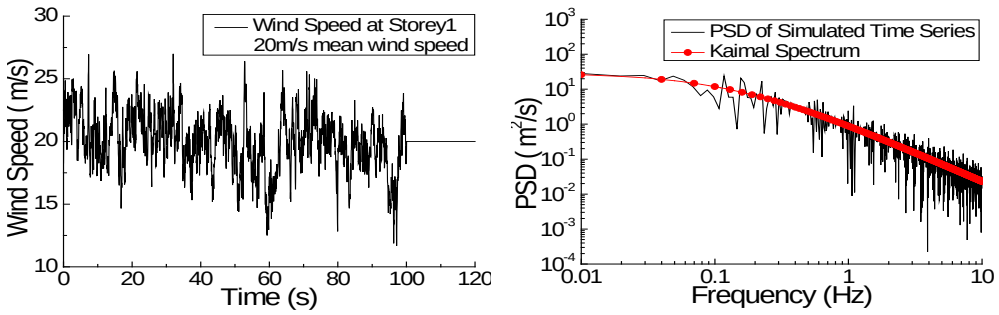

(a) Time varying wind speed at Storey1 (b) PSD of the simulated wind speed

Fig.6.3 An example of wind speed at Storey1 under $V_{m,r}(z) = 20\,\text{m/s}$

6.4.3 The effect of system stiffness on the vibration control

Before the design of additional fluid viscous dampers for the 7-storey building structure, the effect of system stiffness on the vibration control is firstly studied. Because the increase of system stiffness will lead to the increase of system modal frequencies, according to the FRF concept introduced in Chapter 2, linear systems' output frequency response can even increase when the main frequency region of input excitation is higher than the original system's modal frequencies.

For the 7-storey building structure subjected to seismic and wind excitations as introduced in Section 6.4.2, when the system stiffness matrix $K^* = kK$, the effects of k on the vibration power of the structural displacement at Storey7 were studied by numerical simulations and the results are shown in Fig.6.4 for the EI-Centro earthquake excitation and in Fig.6.5 for $20\,\text{m/s}$ mean wind speed excitation.

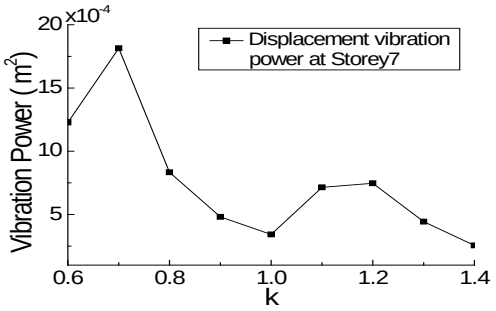

Fig.6.4 Displacement vibration power at Storey7 under EI-Centro earthquake

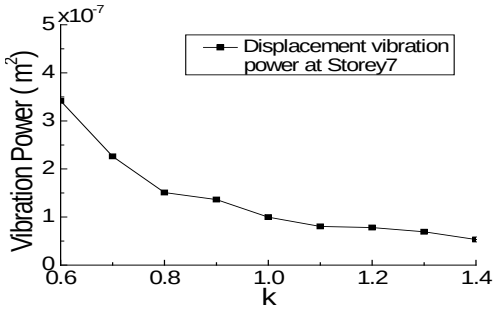

Fig.6.5 Displacement vibration power at Storey7 under $20\,\mathrm{m/s}$ mean wind speed excitation

The time varying displacement vibration at Storey7 with two different system stiffness matrices K^* $(K^* = kK)$ under seismic and wind loading excitations are shown in Fig.6.6 and Fig.6.7, respectively.

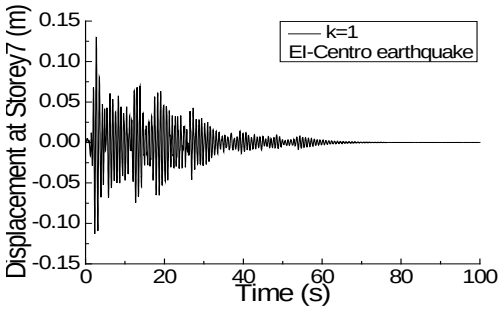

(a) Displacement at Storey7 with $k = 1$

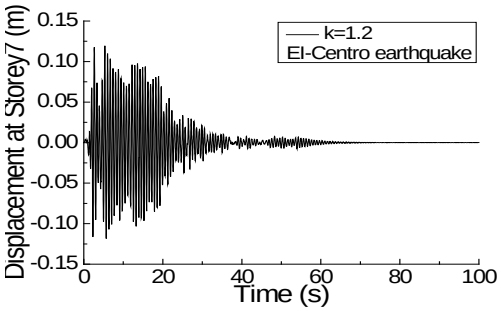

(b) Displacement at Storey7 with $k = 1.2$

Fig.6.6 Displacement at Storey7 with two different system stiffness under EI-Centro earthquake

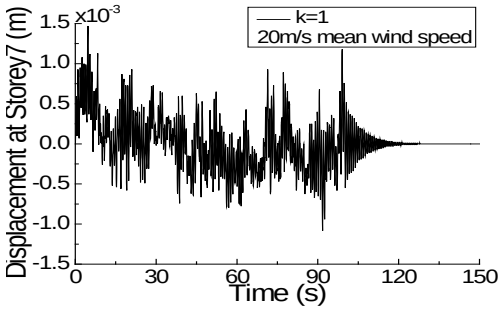

(a) Displacement at Storey7 with $k = 1$

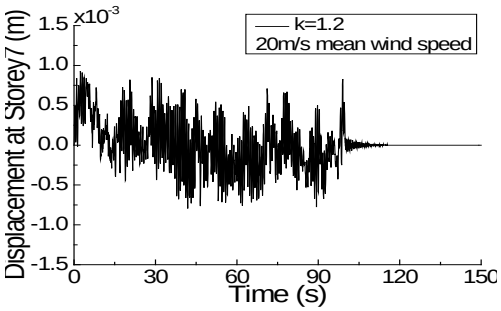

(b) Displacement at Storey7 with $k = 1.2$

Fig.6.7 Displacement at Storey7 with two different system stiffness under $20\,\mathrm{m/s}$ mean wind speed excitation

As shown in Fig.6.4, the increase of system stiffness can lead to the increase of displacement vibration power, which should be avoided in the system vibration

control design. Moreover, by increasing the system stiffness, although the maximum displacements vibration offset can be decreased as indicated in Fig.6.6(b) and Fig.6.7(b), the displacement vibrations during 0-20s in Fig.6.6(b) and 30-60s in Fig.6.7(b) are more violent than the original system's output vibration responses shown in Fig.6.6(a) and Fig.6.7(a), which is harmful and even dangerous for the building structure. These results also reveal the limitation of the maximum vibration offset method in the vibration control design of practical structural systems.

6.4.4 Additional fluid viscous dampers design

6.4.4.1 Determination of vibration power of the 7-storey building structure without fitted fluid viscous dampers

Consider the seismic and wind loading excitations as introduced in Section 6.4.2 as input excitations to the 7-storey building structure, respectively. The vibration response of the system without fitted fluid viscous dampers can be numerically simulated using the Runge-Kutta integration method. The system output displacement vibration at Storey 7 and its FT are shown in Fig.6.8 under EI-Centro earthquake excitation and in Fig.6.9 under 20 m/s mean wind speed excitation.

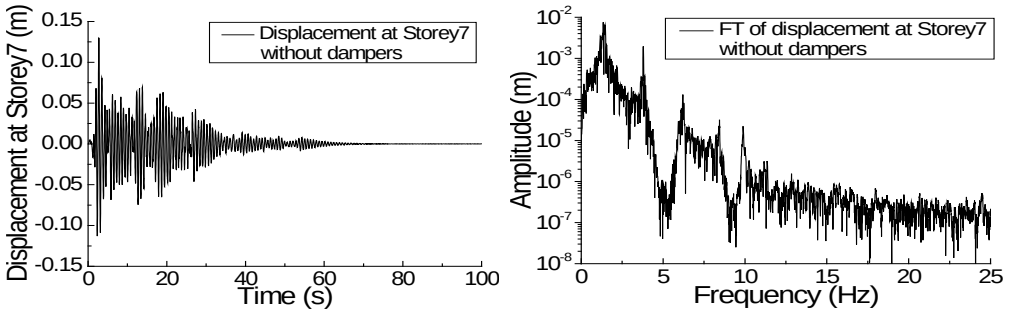

(a) Displacement vibration at Storey7 (b) FT of displacement at Storey7

Fig.6.8 Displacement vibration at Storey7 and its FT under EI-Centro earthquake

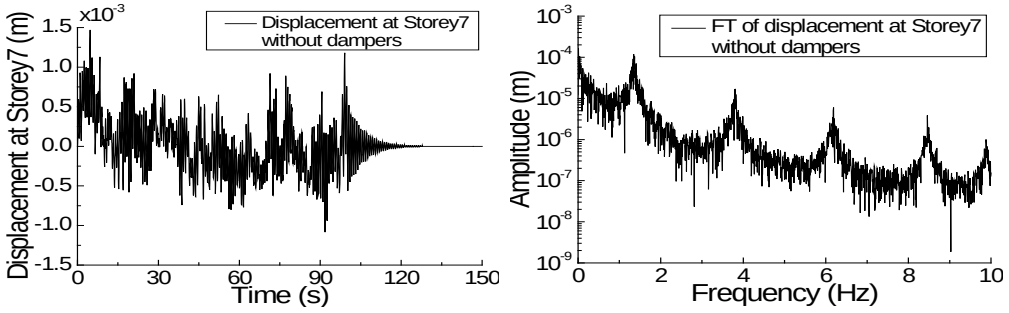

(a) Displacement vibration at Storey7 (b) FT of displacement at Storey7

Fig.6.9 Displacement vibration at Storey7 and its FT under 20 m/s mean wind speed excitation

The vibration powers of the displacement at Storey7 of the 7-storey building structure without fitted fluid viscous dampers can be evaluated as $P_{\mathrm{EI}} = 3.4257\mathrm{E}-4\mathrm{m}^2$ under EI-Centro earthquake excitation and $P_{\mathrm{wind}} = 9.983\mathrm{E}-8\mathrm{m}^2$ under 20 m/s mean wind speed excitation.

6.4.4.2 Design of the damping coefficient of additional fluid viscous dampers

From Section 6.4.4.1, it is known that when no additional fluid viscous dampers are fitted, the vibration powers of the system displacement at Storey7 are $P_{\mathrm{EI}} = 3.4257\mathrm{E}-4\mathrm{m}^2$ under EI-Centro earthquake and $P_{\mathrm{wind}} = 9.983\mathrm{E}-8\mathrm{m}^2$ under 20 m/s mean wind speed excitation. Consider the cases of additional fluid viscous dampers fitted between each storey of the structure to dissipate the vibration energy. In order to simplify the dampers design, all the fitted fluid viscous dampers are defined to have the same damping characteristics parameters, and the OFRF based representation for the system VPLF γ takes the following form

$$\gamma(C_a) = \rho_1 C_a + \rho_2 C_a^2 + \rho_3 C_a^3 + \rho_4 C_a^4 \tag{6.29}$$

In order to work out ρ_i, $i = 1, 2, 3, 4$, to determine Eq.(6.29), 4 simulation

studies were conducted where the 7-storey building structure was excited by the same input excitation, and the damping coefficients C_a of additional fluid viscous dampers took 4 different values for each damping exponent a as shown in Table.6.1 under EI-Centro earthquake excitation, and in Table.6.2 under 20 m/s mean wind speed excitation.

Table.6.1 Damping characteristic parameters, vibration power and VPLF at Storey7 under EI-Centro earthquake

Exponent a	Coefficient C_a	$P_{\mathrm{EI}}(\mathrm{m}^2)$	γ
0.2	1E4	3.1345E-4	8.5%
0.2	5E4	2.3935E-4	30.1%
0.2	1E5	1.8728E-4	45.3%
0.2	5E5	4.2469E-5	87.6%
1	1E5	3.1334E-4	8.5%
1	5E5	2.4552E-4	28.3%
1	1E6	1.9402E-4	43.4%
1	3E6	9.7836E-5	71.4%
3	1E7	3.1701E-4	7.5%
3	1E8	2.4323E-4	29.0%
3	3E8	1.7569E-4	48.7%
3	1E9	1.0693E-4	68.8%

Table.6.2 Damping characteristic parameters, vibration power and VPLF at Storey7 under 20 m/s mean wind speed excitation

Exponent a	Coefficient C_a	$P_{\mathrm{wind}}(\mathrm{m}^2)$	γ
0.2	1E4	5.6077E-8	43.8%
0.2	2E4	5.0687E-8	49.2%
0.2	3E4	4.435E-8	55.6%

0.2	4E4	3.918E-8	60.8%
1	5E6	5.9731E-8	40.2%
1	1E7	5.6397E-8	43.5%
1	4E7	5.0363E-8	49.6%
1	7E7	4.6827E-8	53.1%
3	1E14	5.962E-8	40.3%
3	1E15	5.4633E-8	45.3%
3	1E16	4.991E-8	50.0%
3	5E16	4.5321E-8	54.6%

Substituting the results in Tables.6.1 and 6.2 into Eq.(6.13), the OFRF based representation of the VPLF of the system displacement vibration at Storey 7 can be obtained for the cases where three different types of additional fluid viscous dampers ($a = 0.2,1,\text{and}\,3$) are fitted in the structural system, respectively. The results are:

$$\gamma(a=0.2,\text{EI}-\text{Centro},C_a)=(9.3302\text{E-}6)\cdot C_a+(-8.7539\text{E-}11)\cdot C_a^2+(4.5802\text{E-}16)\cdot C_a^3+(-6.2651\text{e-}22)\cdot C_a^4 \tag{6.30}$$

$$\gamma(a=1,\text{EI}-\text{Centro},C_a)=(9.5318\text{E-}7)\cdot C_a+(-1.1035\text{E-}12)\cdot C_a^2+(7.3233\text{E-}19)\cdot C_a^3+(-1.4798\text{E-}25)\cdot C_a^4 \tag{6.31}$$

$$\gamma(a=3,\text{EI}-\text{Centro},C_a)=(8.2104\text{E-}9)\cdot C_a+(-7.3181\text{E-}17)\cdot C_a^2+(2.1579\text{E-}25)\cdot C_a^3+(-1.5013\text{E-}34)\cdot C_a^4 \tag{6.32}$$

$$\gamma(a=0.2,V_{m,r}=20\,\text{m/s},C_a)=(8.6533\text{E-}5)\cdot C_a+(-5.7967\text{E-}9)\cdot C_a^2+(1.6967\text{E-}13)\cdot C_a^3+(-1.7333\text{E-}18)\cdot C_a^4 \tag{6.33}$$

$$\gamma(a=1,V_{m,r}=20\,\text{m/s},C_a)=(1.3149\text{E-}7)\cdot C_a+(-1.1765\text{E-}14)\cdot C_a^2+(3.2224\text{E-}22)\cdot C_a^3+(-2.5636\text{E-}30)\cdot C_a^4 \tag{6.34}$$

$$\gamma(a=3,V_{m,r}=20\,\text{m/s},C_a)=(4.4751\text{E-}15)\cdot C_a+(-4.4992\text{E-}30)\cdot C_a^2+(4.8504\text{E-}46)\cdot C_a^3+(-7.9368\text{E-}63)\cdot C_a^4 \tag{6.35}$$

When the desired system VPLF $\gamma^* = 50\%$, the viscous damping coefficient C_a with the damping exponent $a = 0.2, 1, 3$ can be designed as $C_{0.2} = 1.14\text{E}5$, $C_1 = 1.17\text{E}6$, $C_3 = 3.02\text{E}8$ under EI-Centro earthquake, and $C_{0.2} = 2.2\text{E}4$, $C_1 = 4.2\text{E}7$, $C_3 = 1\text{E}16$ under 20m/s mean wind speed excitation. The corresponding displacement vibrations at Storey7 are shown in Fig.6.10 under EI-Centro earthquake and in Fig.6.11 under 20m/s mean wind speed excitation. The system VPLFs can be evaluated from these simulations and the results are all $\gamma = 50\%$, which verify the effectiveness of the proposed additional fluid viscous dampers design approach on the system vibration control.

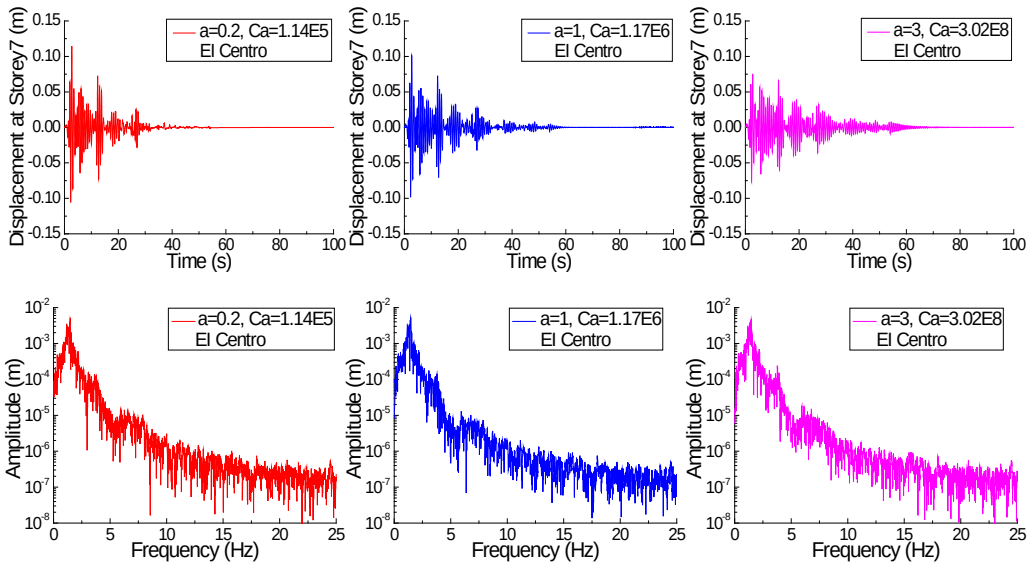

(a) when $C_{0.2} = 1.14\text{E}5$ (b) when $C_1 = 1.17\text{E}6$ (c) when $C_3 = 3.02\text{E}8$

Fig.6.10 Displacement vibration at Storey7 with VPLF $\gamma = 50\%$ under EI-Centro earthquake

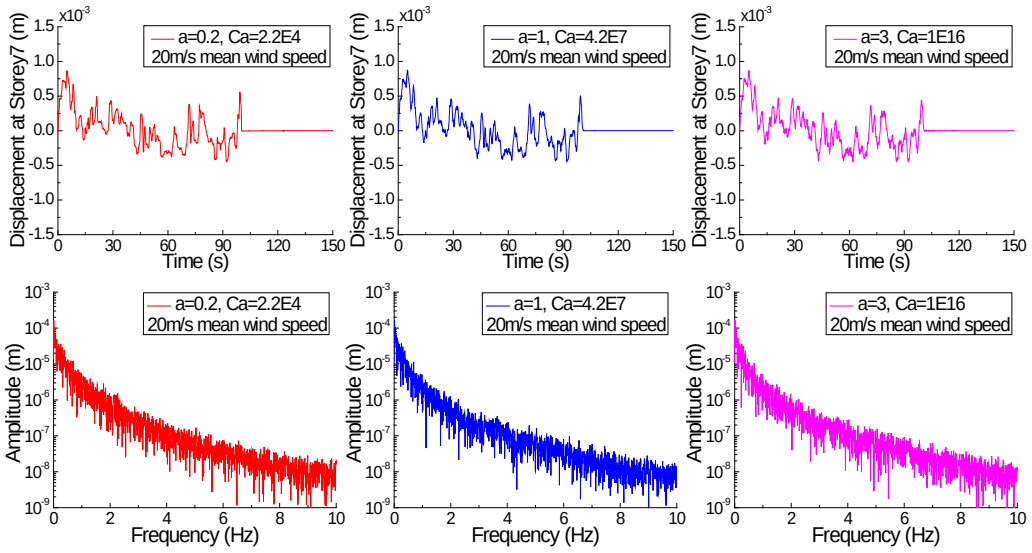

(a) when $C_{0.2} = 2.2\,\mathrm{E}\,4$ (b) when $C_1 = 4.2\,\mathrm{E}\,7$ (c) when $C_3 = 1\mathrm{E}16$

Fig.6.11 Displacement vibration at Storey7 with VPLF $\gamma = 50\%$ under $20\,\mathrm{m/s}$ mean wind speed excitation

Compared with the displacement vibration at Storey7 of the structure without fitted fluid viscous dampers as shown in Fig.6.8(a) and Fig.6.9(a), three types of fluid viscous dampers ($a<1$, $a=1$ and $a>1$) can all suppress the system displacement vibration at Storey7 with the same VPLF value $\gamma = 50\%$, that is, they have the same vibration control effects on the displacement at Storey7 under the considered seismic and wind loading excitations.

As introduced in Section 6.4.2.2, practical wind loading excitations on structural systems have turbulence. This implies that under the same mean wind speed $V_{m,r}(z)$ but different random phases ϕ_{ml}, the time histories of the wind force excitation are different. Six different time histories of the wind force excitations generated under the same $20\,\mathrm{m/s}$ mean wind speed as shown in Fig.6.12 (a)-(f) were considered to investigate how this difference can affect the system vibration control performance with the same additional fluid viscous dampers design. For this purpose, the system VPLFs of the displacement at Storey7 under the six different time histories of wind force excitations were evaluated for all the designs that have been achieved above. The results are listed in Table.6.3,

indicating that very similar VPLF values can be achieved even the time histories of wind force excitations are different, the differences are mainly due to that the random phases ϕ_{ml} are changed in each time history of the wind force excitations. These analysis results imply that the proposed design procedure is able to cover different scenarios of input loading excitations and reveal that the vibration control effects are statistically the same, which is very important for practical applications.

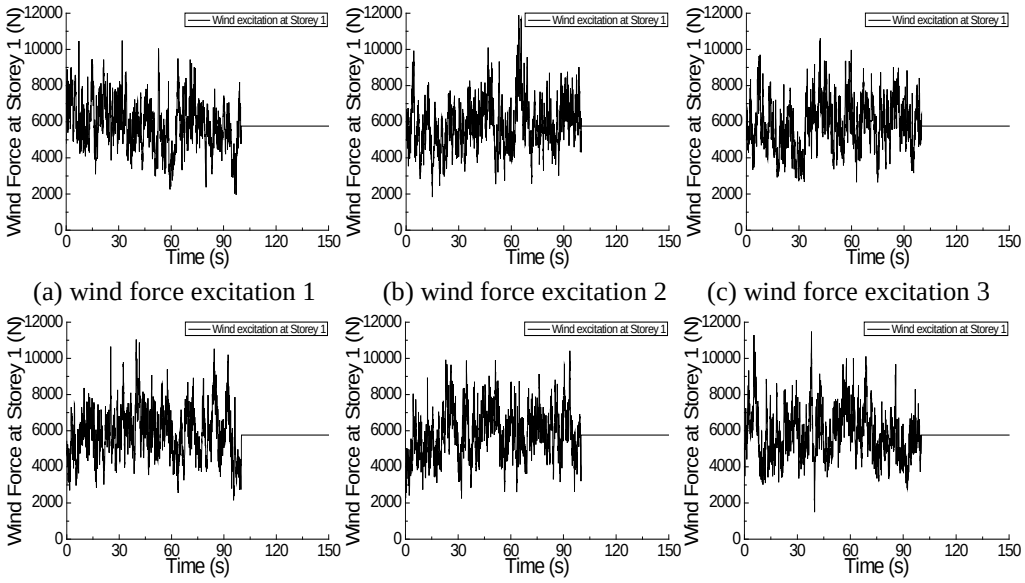

(a) wind force excitation 1 (b) wind force excitation 2 (c) wind force excitation 3

(d) wind force excitation 4 (e) wind force excitation 5 (f) wind force excitation 6

Fig.6.12 Wind force excitations at Storey1 under the same mean wind speed $V_{m,r}(z) = 20\,\text{m/s}$ but different random phases ϕ_{ml}

Table.6.3 VPLFs of the displacement at Storey7 with different types of fluid viscous dampers under the same wind mean speed but six different wind force excitation time histories

Wind force excitation Number	$C_1 = 4.2\,\text{E}\,7$	$C_{0.2} = 2.2\,\text{E}\,4$	$C_3 = 1\text{E}16$
1	$\gamma = 50\%$	$\gamma = 50\%$	$\gamma = 50\%$
2	$\gamma = 56.9\%$	$\gamma = 59.7\%$	$\gamma = 56.6\%$
3	$\gamma = 49.6\%$	$\gamma = 50.9\%$	$\gamma = 48.8\%$
4	$\gamma = 53.5\%$	$\gamma = 53.7\%$	$\gamma = 54.3\%$
5	$\gamma = 46.6\%$	$\gamma = 48.6\%$	$\gamma = 46.7\%$
6	$\gamma = 47.6\%$	$\gamma = 48.6\%$	$\gamma = 48.2\%$

In engineering practice, designs are normally made under typical loading conditions. But a desired situation is that these designs should also work well in situations when loadings change. Therefore, the designs achieved above were evaluated in different loading conditions to investigate how this important requirement can be met by the designs. The results are shown in Figs.6.13-6.16 and Table.6.4. Figs.6.13 and 6.14 show the displacement vibration responses at Storey7 of the 7-storey building structure with three different additional fluid viscous dampers designs when the structure is subjected to half and double of EI-Centro earthquake acceleration excitations, respectively. Figs.6.15 and 6.16 show the system vibration responses in the situations when the structure is subjected to 10m/s mean wind speed excitation and 40m/s mean wind speed excitation, respectively. Table.6.4 shows the VPLF values of the system displacement vibration response at Storey7 under different loadings and additional fluid viscous dampers designs.

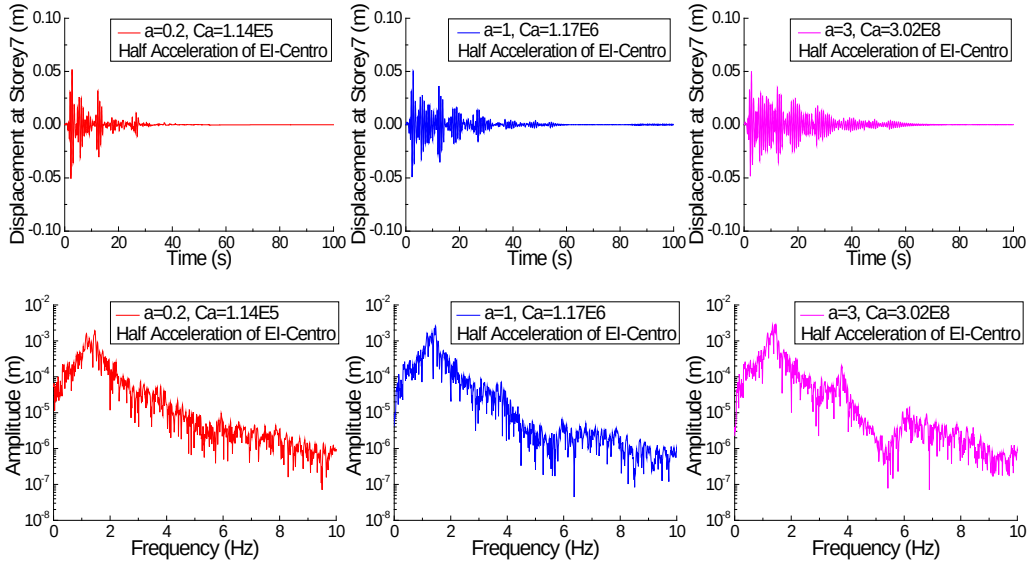

(a) when $C_{0.2} = 1.14\,\mathrm{E}\,5$ (b) when $C_1 = 1.17\,\mathrm{E}\,6$ (c) when $C_3 = 3.02\,\mathrm{E}\,8$

Fig.6.13 Displacement vibration at Storey7 under half of the EI-Centro earthquake acceleration

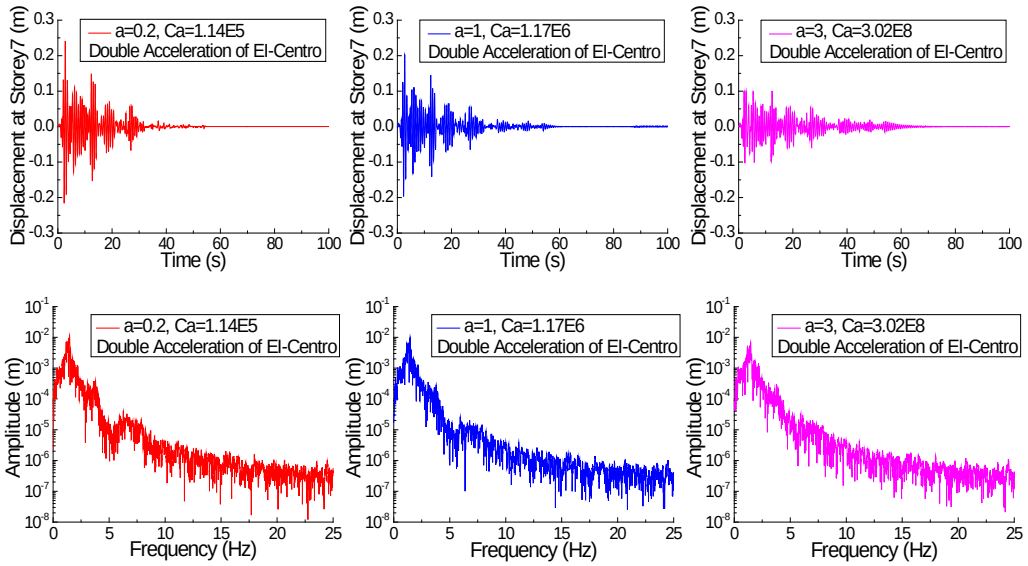

(a) when $C_{0.2}=1.14\,\mathrm{E}\,5$ (b) when $C_1=1.17\,\mathrm{E}\,6$ (c) when $C_3=3.02\,\mathrm{E}\,8$

Fig.6.14 Displacement vibration at Storey7 under double of the EI-Centro earthquake acceleration

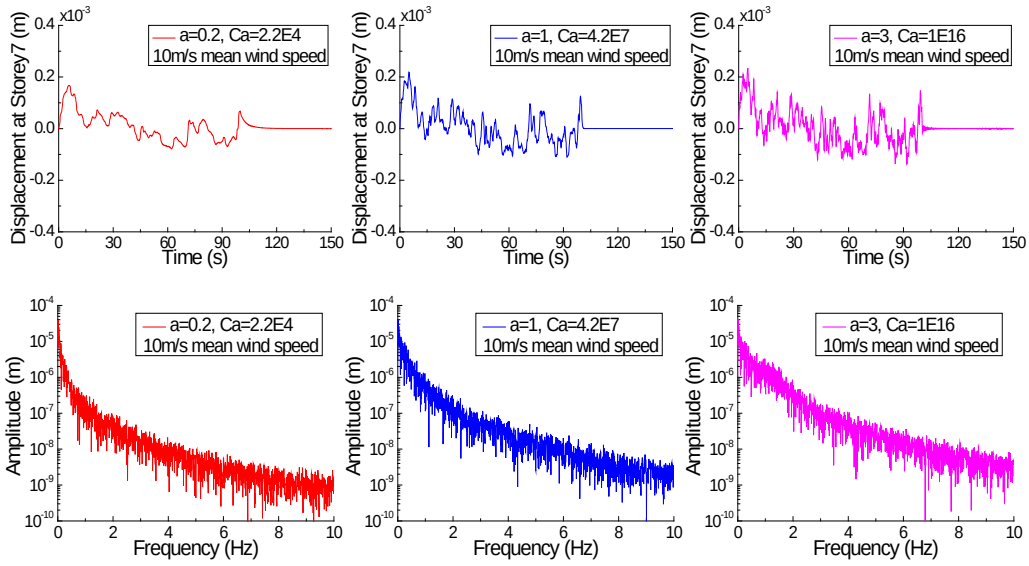

(a) when $C_{0.2}=2.2\,\mathrm{E}\,4$ (b) when $C_1=4.2\,\mathrm{E}\,7$ (c) when $C_3=1\mathrm{E}16$

Fig.6.15 Displacement vibration at Storey7 under $10\,\mathrm{m/s}$ mean wind speed excitation

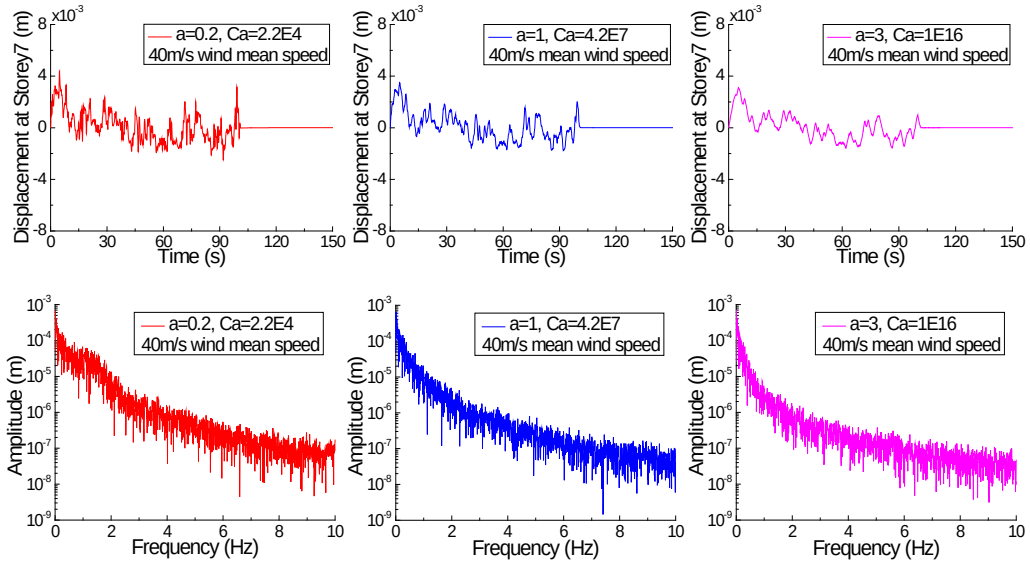

(a) when $C_{0.2}=2.2\,\mathrm{E}\,4$ (b) when $C_1=4.2\,\mathrm{E}\,7$ (c) when $C_3=1\mathrm{E}16$

Fig.6.16 Displacement vibration at Storey7 under 40 m/s mean wind speed excitation

Table.6.4 The VPLFs of the structural displacement response at Storey7 under different loadings and fluid viscous dampers designs

Viscous damping parameters	Half of EI-Centro earthquake Acceleration excitation	Double of EI-Centro earthquake Acceleration excitation
$a=0.2$, $C_{0.2}=1.14\,\mathrm{E}\,5$	$\gamma=63.8\%$	$\gamma=35.8\%$
$a=1$, $C_1=1.17\,\mathrm{E}\,6$	$\gamma=50\%$	$\gamma=50\%$
$a=3$, $C_3=3.02\,\mathrm{E}\,8$	$\gamma=24.8\%$	$\gamma=71.3\%$
Viscous damping parameters	10 m/s mean wind speed excitation	40 m/s mean wind speed excitation
$a=0.2$, $C_{0.2}=2.2\,\mathrm{E}\,4$	$\gamma=65.7\%$	$\gamma=41.8\%$
$a=1$, $C_1=4.2\,\mathrm{E}\,7$	$\gamma=50\%$	$\gamma=50\%$
$a=3$, $C_3=1\mathrm{E}16$	$\gamma=44.8\%$	$\gamma=58.9\%$

From the results in Figs.6.13-6.16 and Table.6.4, it can be observed that, in comparison with what can be achieved by the equivalent linear fluid viscous dampers design, additional nonlinear fluid viscous dampers with the damping exponent $a<1$ can dissipate more vibration energy and power under milder loading excitations, while additional nonlinear fluid viscous dampers with the damping exponent $a>1$ can dissipate more vibration energy and power under severer loading excitations. So, although nonlinear viscous damping devices with the damping exponent $a<1$ have been widely used in modern engineering systems, such as civil buildings and bridges, the corresponding vibration control designs may not be appropriate in different loading conditions which are severer than the considered loading condition for the design. So, the above results not only demonstrate the effectiveness of the proposed additional fluid viscous dampers design principle but also reveal that different nonlinear fluid viscous dampers designs based on the proposed principle should be used in different loading conditions so as to ensure the desired vibration control performance can always be achieved.

6.5 Conclusions

In this chapter, the VPLF concept is proposed to evaluate the effects of additional nonlinear fluid viscous dampers on the vibration control of engineering structural systems subjected to general excitations. The OFRF concept and associated techniques are applied to derive an OFRF based representation of the system VPLF, which reveals an explicit analytical relationship between a vibration system's VPLF and the parameter of nonlinear fluid viscous dampers fitted in the system. The result is then used to conduct nonlinear fluid viscous dampers design to achieve desired vibration control performance in different loading conditions. Simulation studies on a 7-storey building structure subject to seismic and wind loading excitations demonstrate

the effectiveness of the proposed nonlinear dampers design approach and reveal that

1) The increase of system stiffness as often used in practice may lead to the increase of the system output vibration response.

2) The VPLF provides a useful criterion for the system vibration control design and the OFRF based representation of the system VPLF can significantly facilitate the design to achieve a desired VPLF result.

3) Different types of additional fluid viscous dampers ($a<1$, $a=1$ and $a>1$) can achieve equivalent vibration control effects on a structural system in a considered loading condition but perform differently under milder and severer loading excitations. Therefore, different nonlinear fluid viscous dampers designs based on the proposed principle should be used in different loading conditions so as to ensure the desired vibration control performance can always be achieved.

These results significantly extend the OFRF concept based design to the design of additional nonlinear fluid viscous dampers for the vibration control of structural systems and provide a new fluid viscous dampers design methodology. These results have significant implications for the analysis and design of vibration systems in a wide range of practical applications.

Chapter 7

Additional Nonlinear Damping Device Designs for Structural Systems Described by Finite Element Model

In this chapter, the Output Frequency Response Function (OFRF) and Vibration Power Loss Factor (VPLF) concepts are applied for the design of additional nonlinear damping devices for the vibration control of structural systems, which are so complicated that Finite Element (FE) models have to be used for the system descriptions. The designs of additional fluid viscous dampers are conducted for the vibration control of multi-storey building structures under harmonic excitations and an offshore pylon structure under wind loading excitations. The results demonstrate the effectiveness of the OFRF and VPLF based design techniques. Moreover, the advantages of different types of fluid viscous dampers for the vibration control of structural systems in different loading conditions are discussed.

7.1 Introduction

In modern system designs, the Finite Element Method (FEM) has become an important tool for predicting and simulating the physical behaviors of complex engineering systems. Commercial Finite Element Analysis (FEA) programs have gained common acceptance among the engineers in industry, researchers at universities and government laboratories [191]. Especially for the dynamic analysis of nonlinear vibration systems, modern FEA programs have provided a variety of modeling and solving methods to consider the system nonlinearity in loading, geometric, material, contact and so on. The convenient and quick FE

simulation analysis has received more and more attentions from the engineers and designers and played an important role in the analysis and design of practical engineering systems.

Compared with practical engineering systems, the SDOD and MDOF vibration system equations used in previous chapters are the mathematical abstracts with simple dynamic expressions. Practical engineering systems always involve complex characteristics and the system behaviors are much more complicated. Traditional lumped parameter model descriptions [192] are difficult to be used to represent these complicated systems. However, with the rapid development of modern computation techniques and the widespread applications of flexible components, structural system analysis using FE models has received more and more attentions. The FE model analysis based structural system designs have achieved significant progresses towards improving system performance [45, 191, 193, 194].

In the areas of FE model analysis based designs for damping devices, Wang et al. [193] applied a FE model to analyze the vibration response of the Donghai Bridge in China under seismic excitations and studied the influences of additional fluid viscous dampers on the system vibration response. Their results revealed that, if appropriately designed, additional fluid viscous dampers can significantly improve the vibration performance of the civil bridge under seismic excitations. Shen et al. [45] established the 3D FE model for a high-rise steel structure and studied the effects of additional fluid viscous dampers on the structural vibration response under seismic and wind loading excitations. Their results showed that the vibration response of the structural system could be reduced by 10% under seismic excitations and 50% under wind loading excitations after introducing appropriately designed fluid viscous dampers.

This chapter is dedicated to the applications of the OFRF and VPLF concepts

based nonlinear system analysis and design approaches to study the effects and design the parameters of additional fluid viscous dampers for the vibration control of complicated structural systems described by FE model. Firstly, the displacement and force transmissibility of multi-storey building structures under harmonic excitations are evaluated using the OFRF based description. The results are compared with the FE simulations to verify the effectiveness of the application of the OFRF concept to describe the vibration transmissibility of more complicated engineering structural systems. Then, the displacement vibration responses of an offshore pylon structure under wind loading excitations are evaluated using the FE simulation analysis. The effects of different types of additional fluid viscous dampers on the vibration control of the structural system are studied. After that, the OFRF and VPLF concepts are applied to design the damping characteristic parameters of additional fluid viscous dampers in the offshore structure to achieve desired structural vibration response. The advantages of different types of fluid viscous dampers for the structural system vibration control in different loading conditions are also discussed. These results demonstrate that the OFRF and VPLF concepts based approaches have considerable significance in the analysis and design of additional damping devices for the vibration control of more complicated structural systems.

7.2 Finite Element Analysis

FE analysis was originally introduced by Turner in 1956 [195] for the analysis of aircraft structural systems. It’s a powerful computation technique for approximate solutions to a variety of practical engineering problems which have complex domains subjected to general boundary conditions [191]. FE models describe the practical systems by elements and specific points along the element boundaries, which are called “nodes”. FE analysis is an extension of derivative

and integral calculus and uses very large matrix arrays and mesh diagrams to calculate the stress, movement and forces on the nodes in the FE models, and to simulate the physical behaviors of practical systems.

With the development of modern computation techniques, the FE models have become more and more popular in the system analysis and design because of their simplicity and feasibility in practical applications. Many commercial FE analysis programs have been issued for different application fields, such as FLUENT for computational fluid dynamic analysis, ABAQUS for structural analysis, ADINA for solid-fluid interaction analysis, ANSYS for general engineering system analysis, and so on.

Up to now, many FE simulations have been studied and applied in the analysis and design of practical engineering structural systems, such as civil buildings, bridges, vehicle engines and so on, demonstrating good performance in engineering optimal analysis, vibration control design, structural safety protection and others [191, 196, 197]. Choi et al. [196] proposed an effective nonlinear analysis method for the earthquake response of soil-structure interaction systems based on the FE simulations. In their studies, the ANAYS program was used to obtain the nonlinear dynamic responses of complex structural systems in the time domain. Based on the FE simulation results, the effects of material nonlinearity and interface conditions on the system response to earthquake were discussed. Karagulle [197] applied the FE model in the active vibration control of smart structures, the results obtained by the Laplace transform and by the FE simulations were compared to verify the effectiveness of the FE model in the analysis and design of active control systems. Khot [198] studied the vibration responses of a two-degree-of-freedom spring-mass-damper system. The transfer function and state space model in physical coordinates of the same system were obtained by using the ANSYS program and the MATLAB program. The system output frequency responses obtained from the FE

simulations and the numerical simulations were compared and found to be in good agreement. In order to study the frequency domain characteristics of flexible systems, Kokkinos and Spyrakos [199] combined the Boundary Element Method (BEM) and the FE model to study the dynamic behaviors of flexible massive strip-foundations. Their results revealed that the new frequency domain BEM-FEM approach is more efficient and considerably faster than the traditional time domain methods in analyzing soil-structure interaction systems. Lee and Kim [200] applied the Signal Anomaly Index (SAI) to express the amount of changes in the shape of the system Frequency Response Functions (FRFs) and proposed a new structural damage identification and location technique based on the FE simulations. In their studies, a series of FE simulations of a civil bridge were performed to verify the effectiveness of the proposed approach in the analysis and design of nonlinear structural systems.

In this chapter, the ANSYS program is used to perform the FE simulations for nonlinearly damped structural systems. The ANSYS program has powerful solving capability in the system simulation and provides a variety of modeling and solving methods to consider the system nonlinearity in loading, geometric, material, contact and so on. A typical FE simulation analysis using the ANSYS program usually includes three main steps: model generation, solution and results review. In the model generation step, the geometric model of a practical system is created and the material properties are defined. Then the geometric model is meshed to generate the FE model of the practical system. In the solution step, the system boundary and loading conditions are specified in the FE model and the simulation study is conducted. In the results review step, the main works are to check the validity of the FE simulation and plot or list the simulation results.

According to the dynamic characteristics of practical engineering systems to be studied, three FE analysis methods are mainly used in the ANSYS program to

simulate the dynamic responses of structural systems under different loading excitations. These are harmonic response analysis, transient dynamic analysis and LS-DYNA explicit analysis.

Harmonic response analysis [191] is a technique used to determine the steady-state response of a system subjected to harmonic excitations. This FE analysis method calculates the system steady-state response at different frequencies and obtains a graph of the response quantity (such as displacement) versus frequency. Harmonic response analysis only considers the steady-state, forced vibrations of structural systems. It's a linear analysis approach, so the system nonlinearities, such as plasticity, is ignored [201] in the simulation.

Transient dynamic analysis (sometimes called “time-history analysis”) is a technique used to determine the dynamic response of a structural system subjected to non-cyclic transient excitations. The structural system’s inertial and damping effects are considered to be important in the simulation. This FE analysis method is often used to determine the time history of displacements, strains, stresses, and forces in a structural system induced by any combination of the static, transient, and harmonic excitations.

Different from the above two implicit FE analysis methods, LS-DYNA explicit analysis uses the explicit FE program and is designed for the transient dynamic analysis of highly nonlinear systems [202]. This FE analysis method is based on the explicit time integration and therefore it can greatly improve the simulation speed for complex systems with large deformation and nonlinearity [201]. LS-DYNA explicit analysis is originated from a "public domain" code named DYNA3D, which was developed at the Lawrence Livermore National Laboratory around the year 1976 [191]. It is a general purpose FE code particularly suitable to analyze the nonlinear responses of practical systems. With long time development, LS-DYNA explicit analysis has become a

powerful analysis and design tool for nonlinear systems in many different research fields and provided fast solutions for many practical problems, such as contact, large deformations, nonlinear materials, high frequency response phenomena and so on.

7.3 The OFRF based analysis of the vibration control effects of additional fluid viscous dampers on multi-storey building structures described by FE model

In order to confirm the effectiveness of the application of the OFRF concept in the analysis of structural systems described by FE model, the displacement vibration isolation and force vibration isolation of multi-storey building structures under harmonic excitations are analyzed using the ANSYS program. The OFRF based representations of the system transmissibility are evaluated and compared with the results from the FE model simulations. The effects of damping characteristic parameters and installation locations of additional fluid viscous dampers on the system transmissibility are investigated using the OFRF based approach.

7.3.1 FE models of multi-storey building structures

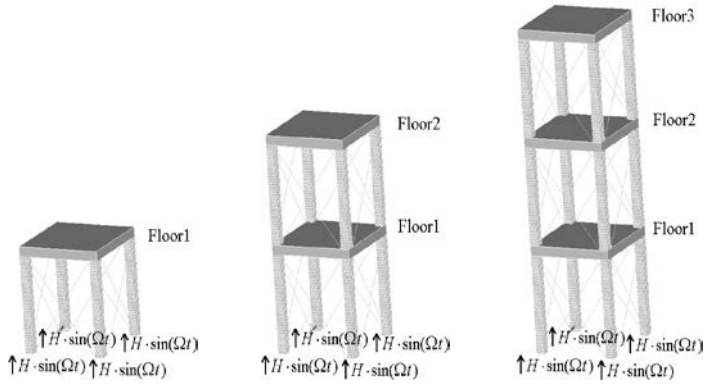

(a) 1-storey building (b) 2-storey building (c) 3-storey building

Fig. 7.1 FE models of multi-storey buildings for displacement vibration isolation analysis

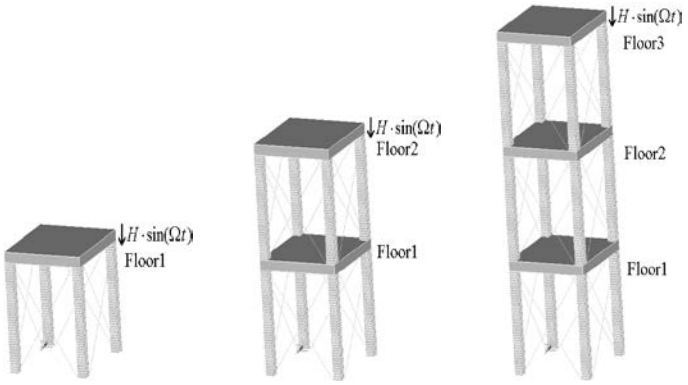

(a) 1-storey building (b) 2-storey building (c) 3-storey building

Fig. 7.2 FE models of multi-storey buildings for force vibration isolation analysis

Consider the FE models of 1, 2 and 3-storey building structures for displacement vibration isolation (DVI) analysis and force vibration isolation (FVI) analysis, respectively. The FE models of these structural systems are created using the ANSYS/LS-DYNA module as shown in Figs.7.1 and 7.2. Each support pillar of these models consists of 1250 flexible elements and the dimension is $40\times 40\times 400\,\text{mm}$. The flexible elements' material density $\rho_1 = 2000\,\text{kg/m}^3$ and elasticity modulus $EX = 10^6\,\text{P}_\text{a}$. The Poisson's ratios of all flexible materials are ignored in the FE simulations. The ceiling of each storey in these FE models is defined as a rigid board with the dimension $400\times 400\times 40\,\text{mm}$ and material density $\rho_2 = 2400\,\text{kg/m}^3$.

In the FE models for DVI analysis as shown in Fig.7.1, the foundation moves due to the harmonic displacement excitation

$$x_{\text{in}}(t) = H\sin(\Omega t) \tag{7.1}$$

in the vertical direction, where H represents the harmonic amplitude of the excitation; In the FE models for FVI analysis as shown in Fig.7.2, the harmonic force excitation

$$f_{\text{in}}(t) = H\sin(\Omega t) \tag{7.2}$$

is imposed on the top storey in the vertical direction. Eight identical additional fluid viscous dampers are cross-inserted on each floor to suppress the vibration

responses of structural systems. The damping force of these dampers is described by

$$F_{\mathrm{D}} = C_{n,a_n} \left| \dot{u}_r \right|^{a_n} \operatorname{sign}(\dot{u}_r) \tag{7.3}$$

where C_{n,a_n} and a_n, $n = 1, 2, 3$, represent the damping coefficient and exponent of the additional fluid viscous dampers on the n^{th} floor. $\dot{u}_r$ is the relative velocity between the two ends of the damper [33, 46, 50].

The element model of additional fluid viscous dampers is Combi165 explicit spring-damper element as shown in Fig.7.3, and the element model of the support pillars and ceilings of the structural systems is SOLID164 explicit 3D structural solid element as shown in Fig 7.4.

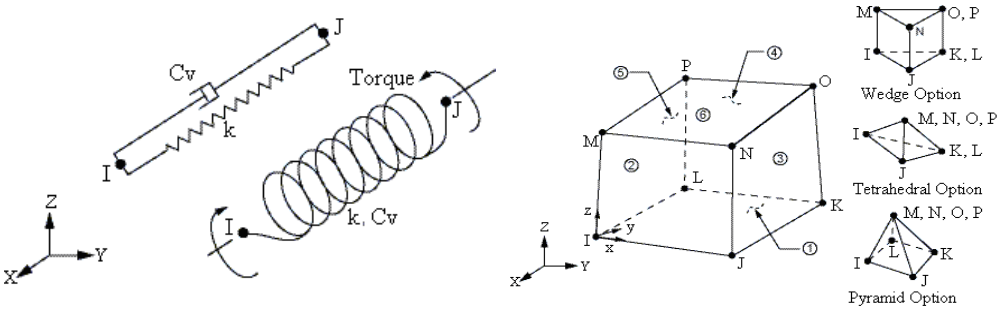

Fig.7.3 COMBI165 element in ANSYS program Fig.7.4 SOLID164 element in ANSYS program

COMBI165 [201] is a two-node, 1D explicit element and is only used in the explicit dynamic analyses. It's always used to model simple springs or dampers to simulate the vibration responses of complicated mechanisms. This element provides a variety of discrete element formulations that can be used to model complicated force-displacement relations.

SOLID164 element [201] is defined by eight nodes having the following DOF at each node: translations, velocities, and accelerations in the nodal x, y, and z directions. It's always used for the 3D modeling of solid structures [201].

7.3.2 Confirmation of the OFRF based representation of the structural vibration responses

In order to confirm the effectiveness of the application of the OFRF concept to represent the output frequency responses of multi-storey building structures described by FE models, the displacement transmissibility of the 1-storey and 2-storey building structures with additional fluid viscous dampers are evaluated using both the FE simulations and OFRF based evaluation method. The applied OFRF based representations for the displacement transmissibility of multi-story buildings take the following forms

$$DD(\omega) = \left|Y(j\omega)\right| \Big/ H = \left|R_0(\omega) + C_{\mathrm{vs}} R_1(\omega) + C_{\mathrm{vs}}^2 R_2(\omega) + C_{\mathrm{vs}}^3 R_3(\omega)\right|$$

for 1-storey building for DVI analysis (7.4)

$$DD_1(\omega) = \left|Y_1(j\omega)\right| \Big/ H = \left|\overline{R}_0(\omega) + \overline{C}_{\mathrm{vs}} \overline{R}_1(\omega) + \overline{C}_{\mathrm{vs}}^2 \overline{R}_2(\omega) + \overline{C}_{\mathrm{vs}}^3 \overline{R}_3(\omega)\right|$$

for Floor1 of 2-storey building for DVI analysis (7.5)

$$DD_2(\omega) = \left|Y_2(j\omega)\right| \Big/ H = \left|\widetilde{R}_0(\omega) + \widetilde{C}_{\mathrm{vs}} \widetilde{R}_1(\omega) + \widetilde{C}_{\mathrm{vs}}^2 \widetilde{R}_2(\omega) + \widetilde{C}_{\mathrm{vs}}^3 \widetilde{R}_3(\omega)\right|$$

for Floor2 of 2-storey building for DVI analysis (7.6)

where $DD(\omega)$, $DD_1(\omega)$ and $DD_2(\omega)$ are the system displacement transmissibility as introduced in Chapter 5; $Y(j\omega)$, $Y_1(j\omega)$ and $Y_2(j\omega)$ are the output frequency responses of the structural systems; C_{vs}, $\overline{C}_{\mathrm{vs}}$ and $\widetilde{C}_{\mathrm{vs}}$ are the damping coefficients of additional fluid viscous dampers; $R_i(\omega)$ ($\overline{R}_i(\omega)$ or $\widetilde{R}_i(\omega)$), $i = 0, 1, 2, 3$, are the functions of the system input spectrum, the frequency of interested ω and depend on all the system parameters apart from the damping coefficient C_{vs} ($\overline{C}_{\mathrm{vs}}$ or $\widetilde{C}_{\mathrm{vs}}$). In order to determine the OFRF based representations for the system transmissibility, the FE simulation studies are conducted with the damping coefficient C_{n,a_n} taking different $m \geq 4$ sets of non zero values for each given damping exponent a_n. For example, in order to determine the OFRF based representations of the

displacement transmissibility of 2-storey building for DVI analysis where the damping exponent of additional fluid viscous dampers $a_n = 0.2$, $n = 1$ or 2, the FE model of the structure is simulated with the same input excitations for all the cases where the damping coefficients of additional fluid viscous dampers are taken as $C_{n,a_n} = 0.2, 0.4, 0.6, 0.8$.

For the situations that the amplitude of harmonic input excitation $H = 10^{-4}$ m in Eq.(7.1), the comparisons between the displacement transmissibility obtained from the FE simulations and the OFRF based evaluation method are shown in Figs.7.5 to 7.10, where C_{mat} is the material damping coefficient defined in FE models of multi-storey building structures, C_{n,a_n} represents the damping coefficient of additional fluid viscous dampers fitted on the n^{th} floor $(n = 1, 2)$ and the damping exponent is taken as $a_n = 0.2$ or 3. For example, the displacement transmissibility $DD_1(\omega)$ and $DD_2(\omega)$ obtained from the FE simulations and from the OFRF based evaluation method are compared in Figs.7.7 and 7.9 in the case of $C_{n,a_n} = 0.5$.

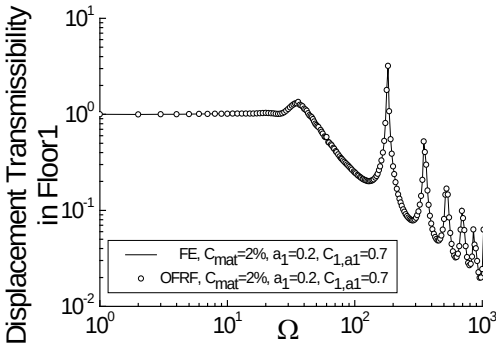

Fig.7.5 Displacement transmissibility on Floor1 of 1-storey building for DVI analysis when the damping exponent $a = 0.2$

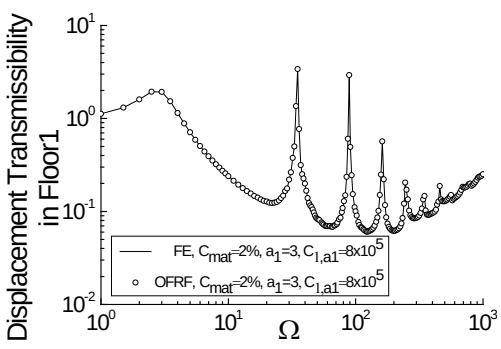

Fig.7.6 Displacement transmissibility on Floor1 of 1-storey building for DVI analysis when the damping exponent $a = 3$

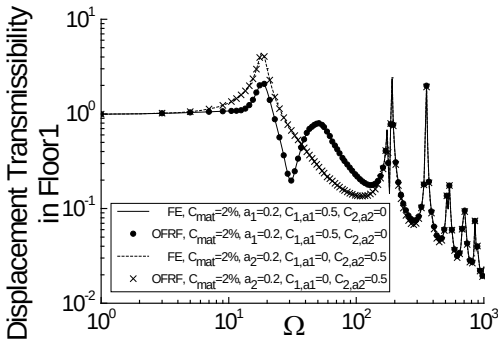

Fig.7.7 Displacement transmissibility on Floor1 of 2-storey building for DVI analysis when the damping exponent $a = 0.2$

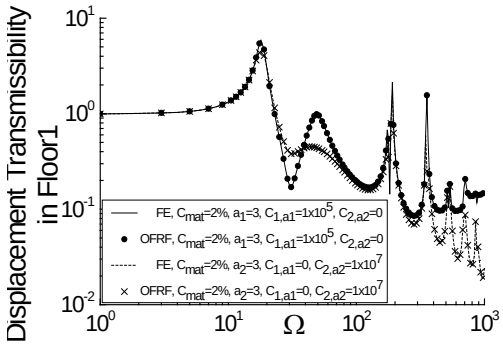

Fig.7.8 Displacement transmissibility on Floor1 of 2-storey building for DVI analysis when the damping exponent $a = 3$

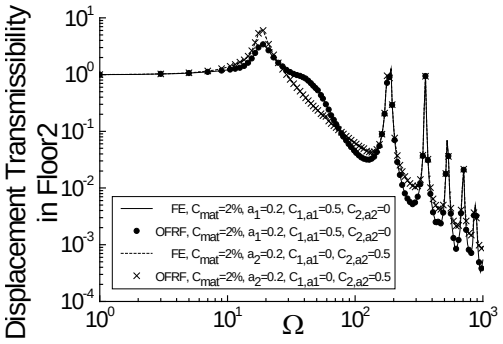

Fig.7.9 Displacement transmissibility on Floor2 of 2-storey building for DVI analysis when the damping exponent $a = 0.2$

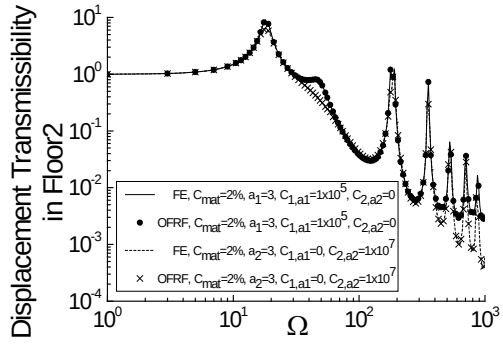

Fig.7.10 Displacement transmissibility on Floor2 of 2-storey building for DVI analysis when the damping exponent $a = 3$

In addition, in order to confirm the effectiveness of the OFRF based representation for both the damping coefficient and exponent to represent the system transmissibility, the force transmissibility $FF(\omega)$ of 1-storey building structure in Fig.7.2(a) are evaluated from both the FE simulations and OFRF based evaluation method at the system 1st resonant frequency. The results are shown in Figs.7.11 and 7.12 and the evaluation errors of the OFRF based approach is calculated in Fig.7.13. The OFRF representation for the system force transmissibility takes the following form

$$FF(\omega) = \left|Y_{force}(j\omega)\right| \Big/ H = \left|\sum_{m=0}^{N_1}\sum_{n=0}^{N_2} a_{vs}^{m} C_{vs}^{n} S_{m,n}(\omega)\right| \tag{7.7}$$

where the maximum powers of the damping exponent and coefficient

$N_1 = N_2 = 3$; $Y_{force}(j\omega)$ is the force output frequency response of the 1-storey building structure for FVI analysis; C_{vs} and a_{vs} are the damping coefficient and exponent of additional fluid viscous dampers; $S_{m,n}(\omega)$, $m,n = 0, 1, 2$, are the functions of the system input spectrum, the frequency of interest ω and depend on all the system parameters apart from the viscous damping coefficient C_{vs} and exponent a_{vs}.

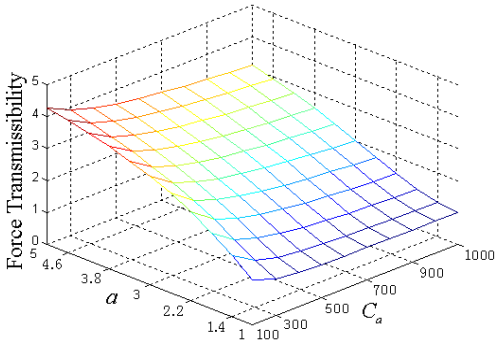

Fig.7.11 Force transmissibility at 1st resonant frequency of the FE model of 1-storey building for FVI analysis by the OFRF based method

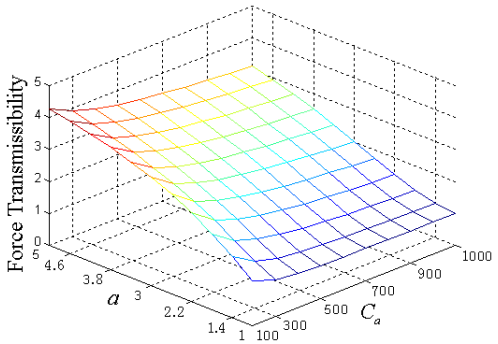

Fig.7.12 Force transmissibility at 1st resonant frequency of the FE model of 1-storey building for FVI analysis by FE simulations

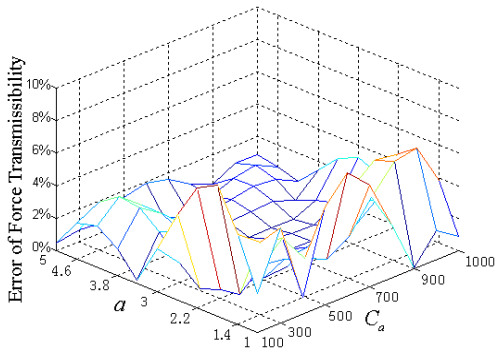

Fig.7.13 Errors of the force transmissibility by the OFRF based evaluation method

Because of the wave effects of flexible material elements in the FE model simulations, some peak values of the displacement transmissibility occur at the wave resonant frequencies in higher frequency region as shown in Figs.7.5 to 7.10. These have been theoretically confirmed by the "Long" –Rod and "Love" theories [178]. The displacement transmissibility of 1 and 2-storey buildings are more complicated than the displacement transmissibility of simplified MDOF systems discussed in Chapter 5. However, the results shown in Figs.7.5 to 7.13

clearly indicate an excellent agreement between the displacement and force transmissibility obtained from the FE simulations and the OFRF based evaluation method. These results confirm the effectiveness of the application of the OFRF concept in the analysis of more complicated structural systems. The small difference that can be observed are mainly due to the truncation error in the OFRF based evaluation method, which only considers up to power 3 of nonlinear damping parameters in the OFRF representations in Eqs.(7.4)-(7.7). The lower power of the nonlinear damping parameters will produce less accurate evaluation results. For example, when the maximum powers of the viscous damping exponent and coefficient $N_1 = N_2 = 2$ in Eq.(7.7) are considered, the force transmissibility of 1-storey building structure for FVI analysis in Fig.7.2(a) can be evaluated by the OFRF based method and the results are shown in Fig.7.14. The evaluation errors of the OFRF based approach in this case are shown in Fig.7.15.

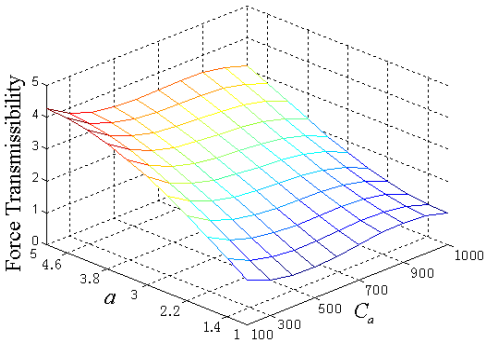

Fig.7.14 Force transmissibility at 1st resonant frequency of the FE model of 1-storey building for FVI analysis by the OFRF based method with the maximum powers $N_1 = N_2 = 2$

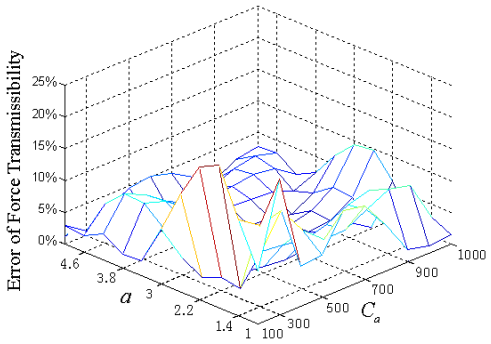

Fig.7.15 Errors of the force transmissibility by the OFRF based evaluation method with the maximum powers $N_1 = N_2 = 2$

Compared with traditional system design methods, the OFRF concept focuses on the relationship between the system output frequency response and the nonlinear system parameters. Even for the FE models of more complicated structural systems, the OFRF concept has shown its effectiveness when applied to represent the system output frequency response and to evaluate the system

transmissibility from the simulation data. By using the OFRF concept, the studies on the effects of nonlinear system parameters on the output frequency responses of complicated structural systems do not need to focus on the system structure and can be directly performed in an analytical representation. Therefore, the optimal design of nonlinear system parameters can be facilitated to achieve a desired output frequency response.

7.3.3 Effects of additional fluid viscous dampers on the system transmissibility

Using the OFRF based evaluation method, the effects of damping characteristic parameters and fitting locations of additional fluid viscous dampers on the system transmissibility of the multi-storey building structures described by FE models are studied and the results are provided in Figs.7.16 to 7.24, where the amplitudes of harmonic loading excitations are $H = 10^{-4}$ m for DVI analysis and $H = 100$ N for FVI analysis. a_i, $i = 1, 2, 3$, represents the damping exponent of additional fluid viscous damper on the i^{th} storey and $C_{i,ai}$ represents the damping coefficient.

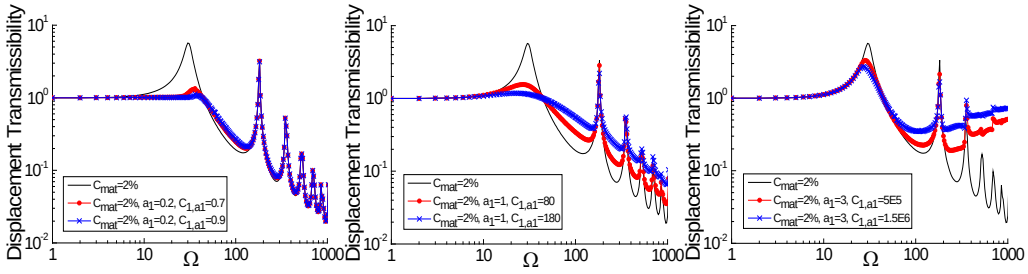

(a) $a_1 = 0.2 < 1$ (b) $a_1 = 1$ (c) $a_1 = 3 > 1$

Fig.7.16 Effects of fluid viscous dampers on $DD(\Omega)$ of 1-storey building for DVI analysis

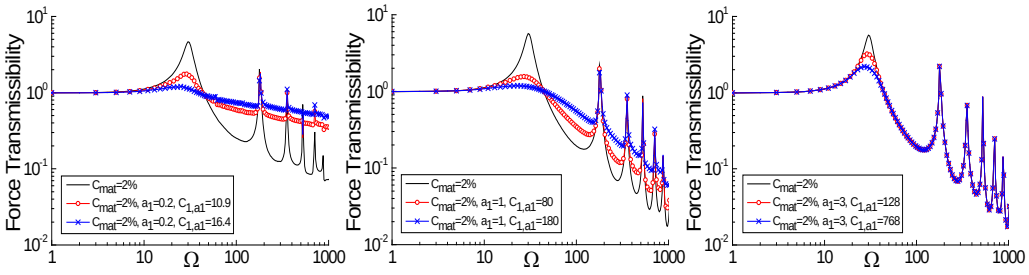

(a) $a_1 = 0.2 < 1$ (b) $a_1 = 1$ (c) $a_1 = 3 > 1$

Fig.7.17 Effects of fluid viscous dampers on $FF(\Omega)$ of 1-storey building for FVI analysis

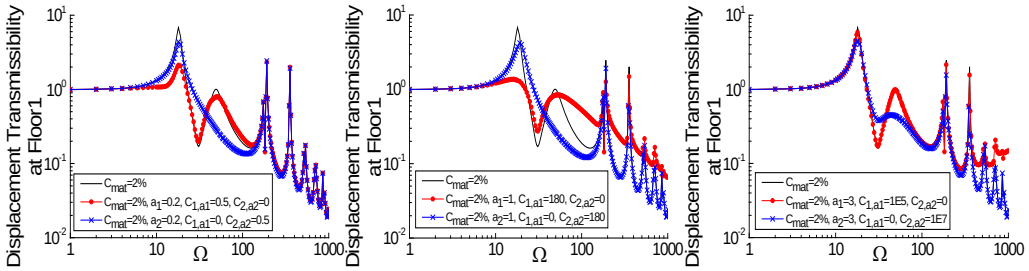

(a) $a_i = 0.2 < 1$, $i = 1$ or 2 (b) $a_i = 1$, $i = 1$ or 2 (c) $a_i = 3 > 1$, $i = 1$ or 2

Fig.7.18 Effects of fluid viscous dampers on $DD_1(\Omega)$ of 2-storey building for DVI analysis

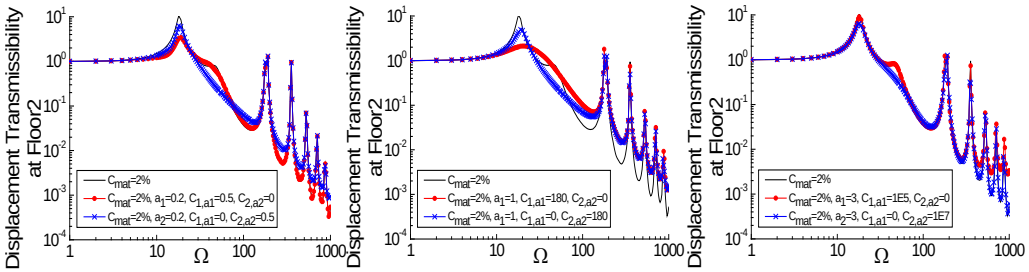

(a) $a_i = 0.2 < 1$, $i = 1$ or 2 (b) $a_i = 1$, $i = 1$ or 2 (c) $a_i = 3 > 1$, $i = 1$ or 2

Fig.7.19 Effects of fluid viscous dampers on $DD_2(\Omega)$ of 2-storey building for DVI analysis

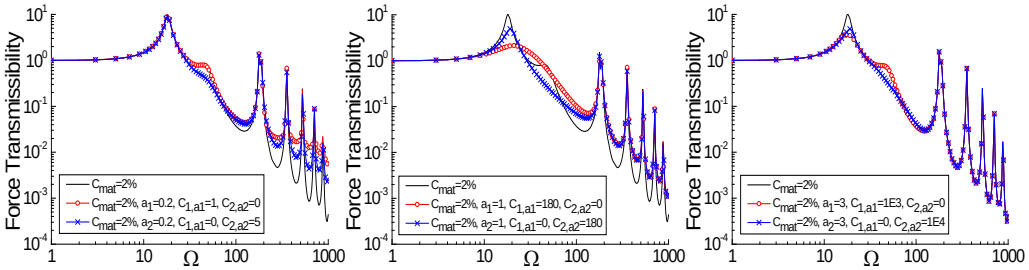

(a) $a_i = 0.2 < 1$, $i = 1$ or 2 (b) $a_i = 1$, $i = 1$ or 2 (c) $a_i = 3 > 1$, $i = 1$ or 2

Fig.7.20 Effects of fluid viscous dampers on $FF(\Omega)$ of 2-storey building for FVI analysis

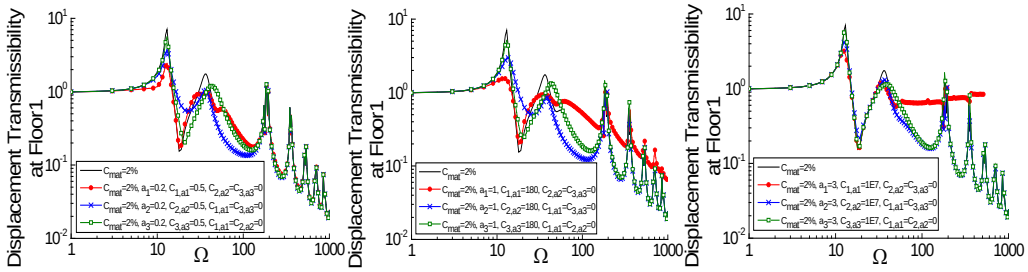

(a) $a_i = 0.2 < 1$, $i = 1, 2$ or 3 (b) $a_i = 1$, $i = 1, 2$ or 3 (c) $a_i = 3 > 1$, $i = 1, 2$ or 3

Fig.7.21 Effects of fluid viscous dampers on $DD_1(\Omega)$ of 3-storey building for DVI analysis

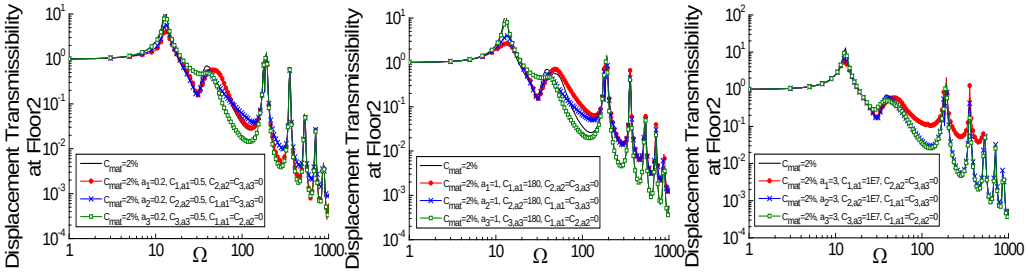

(a) $a_i = 0.2 < 1$, $i = 1, 2$ or 3 (b) $a_i = 1$, $i = 1, 2$ or 3 (c) $a_i = 3 > 1$, $i = 1, 2$ or 3

Fig.7.22 Effects of fluid viscous dampers on $DD_2(\Omega)$ of 3-storey building for DVI analysis

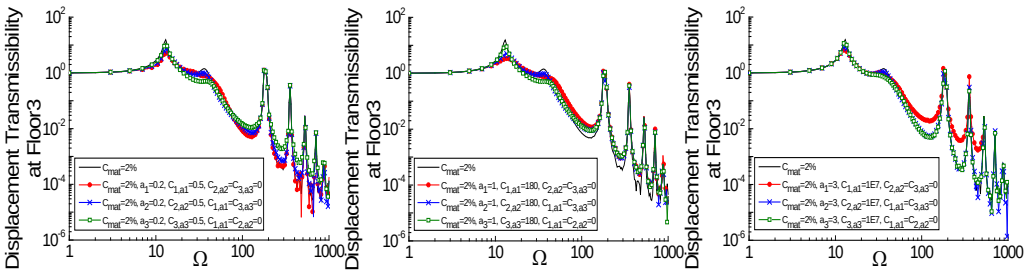

(a) $a_i = 0.2 < 1$, $i = 1, 2$ or 3 (b) $a_i = 1$, $i = 1, 2$ or 3 (c) $a_i = 3 > 1$, $i = 1, 2$ or 3

Fig.7.23 Effects of fluid viscous dampers on $DD_3(\Omega)$ of 3-storey building for DVI analysis

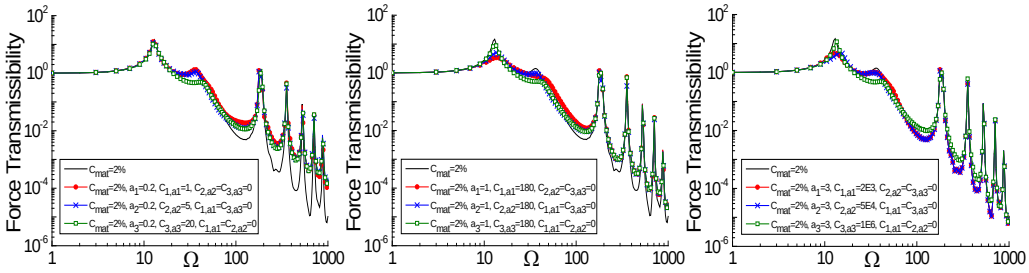

(a) $a_i = 0.2 < 1$, $i = 1, 2$ or 3 (b) $a_i = 1$, $i = 1, 2$ or 3 (c) $a_i = 3 > 1$, $i = 1, 2$ or 3

Fig.7.24 Effects of different types of fluid viscous dampers on $FF(\Omega)$ of 3-storey building for FVI analysis

Compare the results in Figs.7.16 to 7.24 with the corresponding results in

Chapter 5 where MDOF models were used to describe the building structures, it can be found that, apart from the peak values of the system transmissibility at the wave resonant frequencies over the higher frequency region, the effects of additional fluid viscous dampers on the displacement and force transmissibility revealed in here are all consistent with the conclusions achieved previously in Chapter 5. These results, therefore, further confirm the beneficial effects of additional nonlinear fluid viscous dampers on the vibration control of practical engineering structural systems.

7.4 Additional fluid viscous dampers design for an offshore pylon structure

7.4.1 Offshore pylon structure: FINO^3 research platform

In order to satisfy the increasing demands for energy and at the same time minimize negative effects on global environment, more and more next-generation energy technologies have focused on the renewable energy source, such as wind energy, ocean energy, solar energy and so on [203].

As one of the widely used energy, wind energy provides an environmental friendly renewable option for the energy generation [204] and is expected to play an increasingly important role in the future global energy supply [205]. Because of the good wind farm circumstance in the offshore environment, the renewable and pollution-free offshore wind energy industry has been considered as an important part of the next generation energy supply. However, compared with the well-developed industry on land, many new demands have occurred in the construction and operation of these offshore industries. Traditional wind power stations and wind turbine technologies need to be further developed and even completely redesigned for use in offshore areas.

Europe is the global leader in the wind energy [204]. In the Renewable Energy Sources Act (Erneuerbare-Energien-Gesetz, EEG), the German Federal Government specified that the share of renewable energy in gross electricity consumption is to be increased to at least 30% by 2020. In 2030 around half of Germany's electricity consumption should be covered by renewable energy. In order to achieve these targets, the potential of offshore wind energy generation should be utilized.

In order to maximize the wind energy utilization in the offshore environment, German Federal Government has built three offshore research platforms in the North Sea and Baltic Sea. The latest one is the FINO^3 (Forschungsplattformen in Nord und Ostsee – Nr.3), which is directly related to the FINO^1 (45km north of the island Borkum) and FINO^2 (40km northwest of the island Rügen) [206]. FINO^3 is located at $55^0$11.7'N/$007^0$9.5'E, approximately 80km west of the island of Sylt in the North Sea.

Fig.7.25 FINO^3 research platform

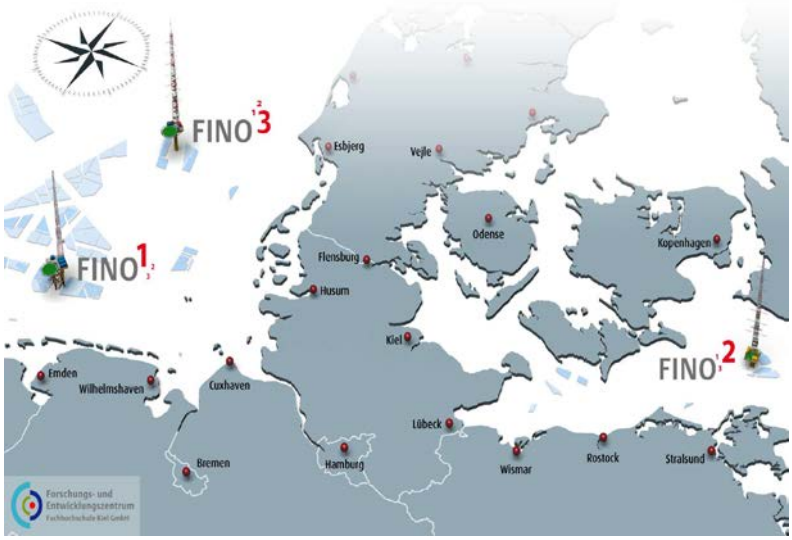

Fig.7.26 Locations of FINO$^{1-3}$

The objective of the FINO^3 project is to investigate boundary conditions for the realization of offshore wind farms at extreme distances from the coast. FINO^3 research platform will play a significant role in the development and expansion of offshore wind power generation.

In the present study, the vibration responses of the offshore pylon structure under wind loading excitations are simulated using the ANSYS program. In order to suppress the structural vibrations, additional fluid viscous dampers having the following characteristic

$$F_{\mathrm{D}} = C_a \left|\dot{u}_r\right|^a \operatorname{sign}(\dot{u}_r) \tag{7.8}$$

are installed inside the structure to dissipate the vibration energy. In Eq.(7.8), F_{D} is the damping force, $\dot{u}_r$ is the relative velocity between the two ends of the damper, C_a and a are the damping coefficient and exponent, respectively. Moreover, the design of additional fluid viscous dampers for the offshore pylon structure is conducted by using the OFRF approach and VPLF concept. The objective is to apply the OFRF based design approach to address the important offshore structure vibration control problems in order to provide a better solution to the challenging engineering problems in the offshore wind industry.

7.4.2 FE model of the FINO^3 pylon structure

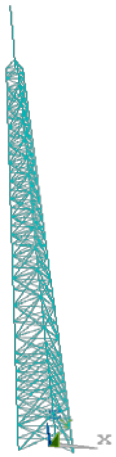

Fig.7.27 FE model of the pylon structure

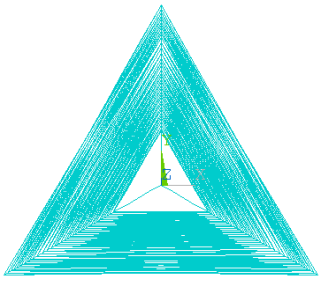

Fig.7.28 Top view of the pylon structure

Using the ANSYS program and the parameters of the offshore pylon structure provided by FINO^3 operator, the FE model of the pylon structure of FINO^3 is created as shown in Figs.7.27 and 7.28. The element model of steel pipes in the

pylon structure is PIPE16 as shown in Fig.7.29 and the element model of additional fluid viscous dampers fitted inside the structure is COMBIN37 as shown in Fig.7.30.

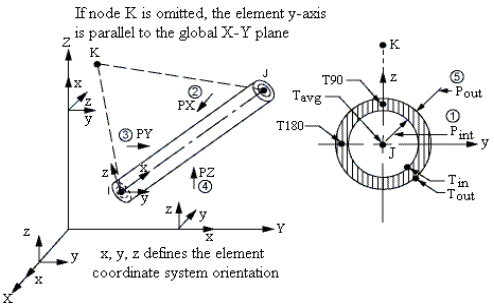

Fig.7.29 PIPE16 element

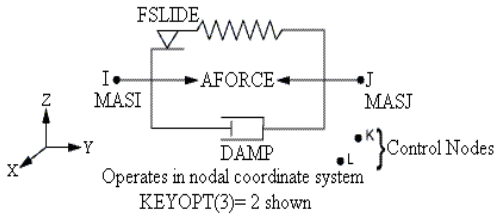

Fig.7.30 COMBIN37 element

PIPE16 [201] is a uni-axial element with tension-compression, torsion, and bending capabilities. This element has 6-DOF at two nodes: translations in the nodal x, y, and z directions and rotations about the nodal x, y, and z axes. PIPE16 element is usually used to model the pipes in practical engineering systems.

COMBIN37 [201] is a unidirectional element with the capability of turning on and off during an analysis. This element has 1-DOF at each node, either a translation in a nodal coordinate direction, rotation about a nodal coordinate axis, pressure, or temperature. This element has many applications in practical engineering systems, such as controlling heat flow as a function of temperature, controlling damping as a function of velocity, controlling flow resistance as a function of pressure, controlling friction as a function of displacement, etc..

Based on the FE simulation, the first modal frequency of the offshore pylon structure can be obtained as $f_1 = 1.0794(\mathrm{Hz})$. The system damping ratio is chosen as $\zeta = 3\%$ and defined in the form of Rayleigh damping in the ANSYS program. Because this FINO3 pylon structure is located in the offshore environment, the wind loading excitation is the most significant impact factor

for the safety and protection of this pylon structure. In order to study the effects of additional fluid viscous dampers on the system vibration response under wind loading excitations, the displacement vibration relative to the balance position under the mean wind speed loading at the top of the offshore pylon structure is defined as the system vibration response to be reduced. The wind loading excitations with $20\,\mathrm{m/s}$ meaning wind speed at the foundation are imposed along the pylon structure in the form of pressure loading. Additional fluid viscous dampers are installed inside the offshore pylon structure as shown in Fig.7.31, where the structure is divided to 17 floors and 6 identical fluid viscous dampers are installed on each floor as shown in Fig.7.32.

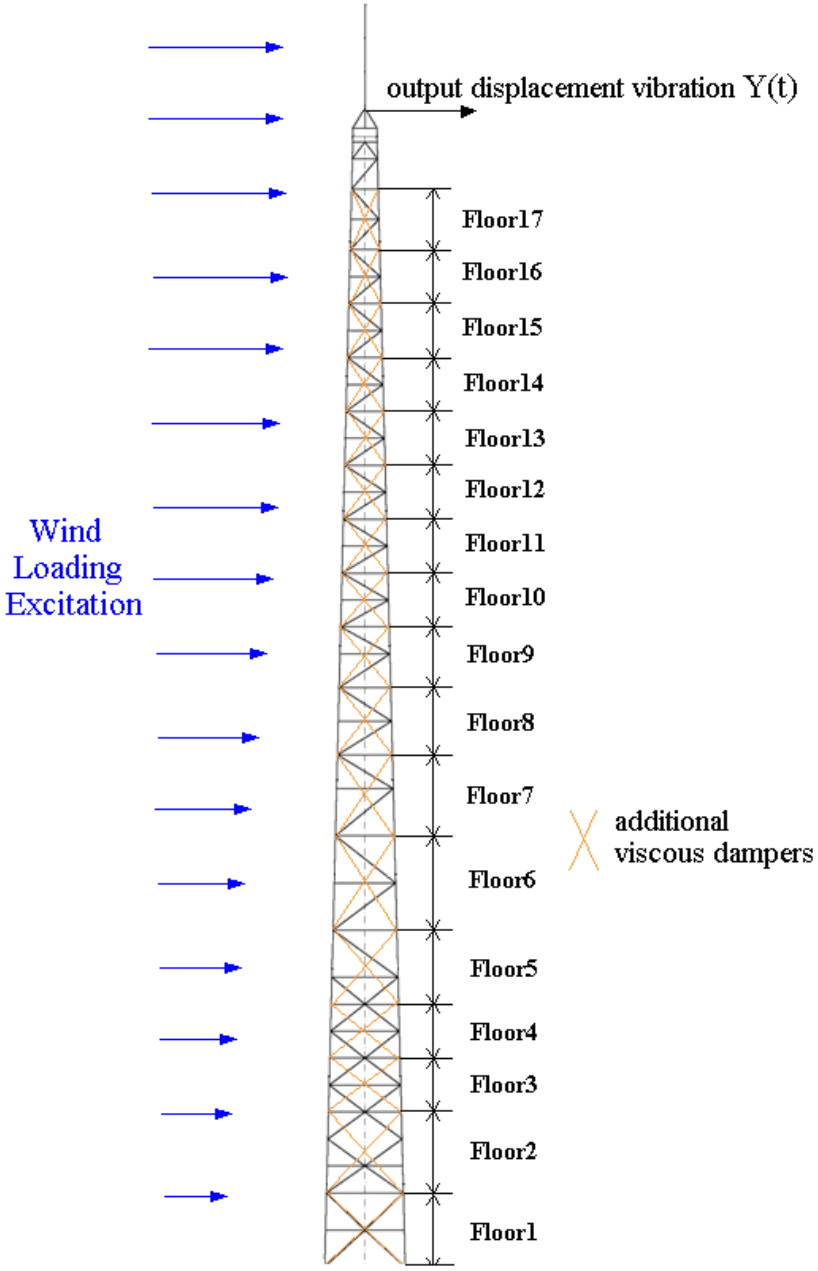

Fig.7.31 The offshore pylon structure of FINO[3] with fitted additional fluid viscous dampers

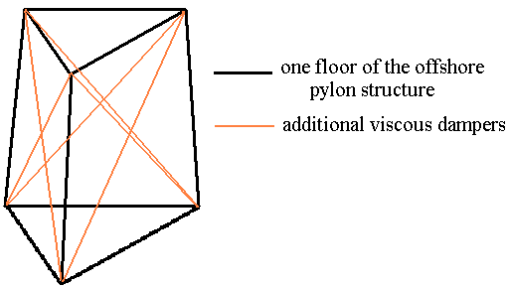

Fig.7.32 Additional fluid viscous dampers on one floor of the offshore pylon structure

7.4.3 Additional fluid viscous dampers design of the pylon structure

7.4.3.1 Determination of vibration power of the offshore pylon structure without fitted fluid viscous dampers

Following the computational process of the wind speed introduced in Section 6.4.2.2, the time history of 20 m/s mean wind speed at the foundation of the offshore pylon structure is calculated and shown in Fig.7.33. The Power Spectral Density (PSD) of this time history is evaluated as shown in Fig.7.34 to verify the validity of the computation.

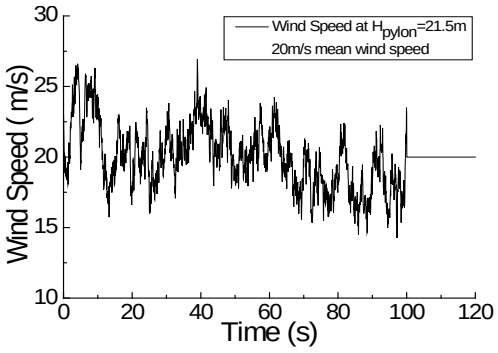

Fig.7.33 Time history of wind speed at foundation

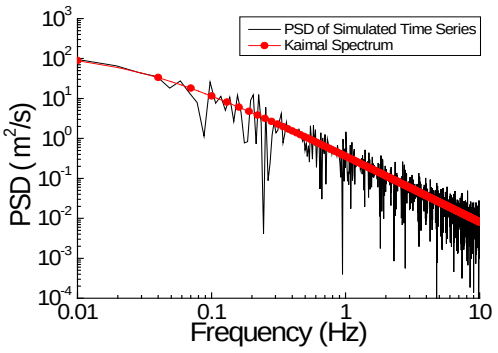

Fig.7.34 PSD of the simulated wind speed

Substituting the above time history of the wind speed into the FE model of the offshore pylon structure, the displacement vibration response of the structural system without fitted fluid viscous dampers can be simulated using the ANSYS program. Fig.7.35 shows the displacement vibration response of the offshore pylon structure under 20 m/s mean wind speed excitation and the FT of the result.

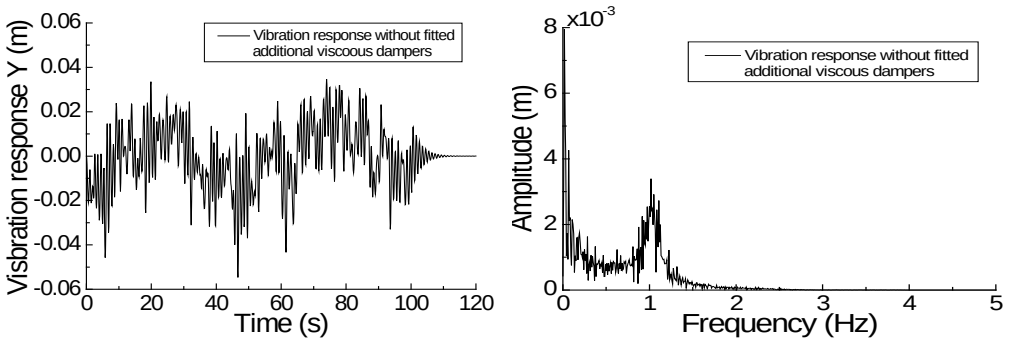

(a) Vibration response (b) FT of the vibration response of the offshore pylon structure

Fig.7.35 Vibration response of the pylon structure and its FT under 20 m/s mean wind speed

The power of this vibration response can be evaluated as $P_{\text{wind}} = 1.8529\text{E-}4(\text{m}^2)$.

7.4.3.2 Effects of the locations of additional fluid viscous dampers on the system VPLFs

In order to study the effects of additional fluid viscous dampers on the vibration control of the offshore pylon structure, the system displacement vibration responses under wind loading excitations are simulated using the transient dynamic analysis method in the ANSYS program. The effects of different locations of the fitted fluid viscous dampers on the structural vibration response are investigated by the FE model simulation analysis in the cases listed in Table.7.1.

Table 7.1 Cases for the locations and types of fitted fluid viscous dampers

	Types of fitted viscous dampers	Locations of dampers
Case1	Damping exponent $a = 0.3$, coefficient $C_{0.3} \in [0, 1\text{E}5]$	On all floors
Case2	Damping exponent $a = 1$, coefficient $C_1 \in [0, 1\text{E}8]$	On all floors

Case3	Damping exponent $a=1.5$, coefficient $C_{1.5} \in [0, 1\mathrm{E}10]$	On all floors
Case4	Damping exponent $a=0.3$, coefficient $C_{0.3}=1\mathrm{E}5$	On a single floor
Case5	Damping exponent $a=1$, coefficient $C_1=1\mathrm{E}8$	On a single floor
Case6	Damping exponent $a=1.5$, coefficient $C_{1.5}=1\mathrm{E}10$	On a single floor

In order to simplify the damping design, all fitted fluid viscous dampers are defined to have the same damping characteristics parameters. The system VPLFs with different fluid viscous dampers are calculated from the FE simulation results as shown in Fig.7.36 for Cases 1-3 and in Fig.7.37 for Cases 4-6.

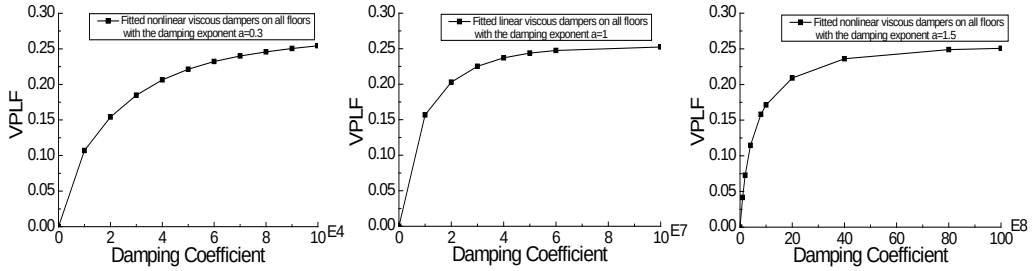

(a) VPLFs in Case1 (b) VPLFs in Case2 (c) VPLFs in Case3

Fig.7.36 VPLFs under different damping coefficients of additional dampers for Cases 1-3

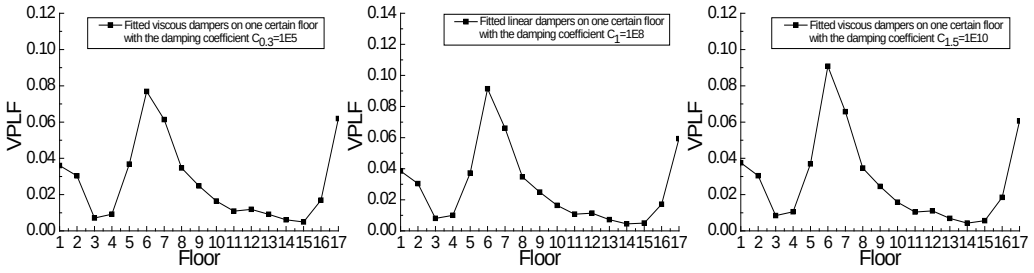

(a) VPLFs in Case4 (b) VPLFs in Case5 (c) VPLFs in Case6

Fig.7.37 VPLFs under different installation locations of additional dampers for Cases 4-6

From the VPLFs results in Figs.7.36 and 7.37, it can be found that the fitted

linear and nonlinear fluid viscous dampers can both suppress the displacement vibration response of the offshore pylon structure and the fluid viscous dampers with a larger value of the damping coefficient can produce better vibration control effect on the structural displacement vibration response. Especially, compared with fitted fluid viscous dampers on other floors, fitted fluid viscous dampers on Floor 1, 2, 5, 6, 7, 8 and 17 can obviously achieve better vibration control effects.

7.4.3.3 Design of the coefficient of additional fluid viscous dampers

Based on the above results, additional fluid viscous dampers are fitted on Floor 1, 2, 5, 6, 7, 8 and 17 for vibration control. According to the VPLF concept proposed in Chapter 6, the OFRF based representation for the system VPLF γ has the form

$$\gamma(C_a) = \sum_{i=1}^{2\overline{N}} C_a^i \rho_i \tag{7.9}$$

where C_a is the damping coefficient of additional fluid viscous dampers with a certain damping exponent a and $\overline{N}$ is the order of the OFRF representation. A higher order OFRF representation (a bigger value of $\overline{N}$) can achieve more accurate results but the computation will be more complicated and more simulation results are needed. The following system VPLF expression is used in the designs

$$\gamma(C_a) = \rho_1 C_a + \rho_2 C_a^2 + \rho_3 C_a^3 + \rho_4 C_a^4 \tag{7.10}$$

In order to work out the coefficients ρ_i, $i = 1, 2, 3, 4$, to determine the system VPLF expression in Eq.(7.10), $m = 10$ FE simulation studies are conducted where the offshore pylon structure is excited by the same wind loading excitation and the damping coefficients C_a of additional fluid viscous dampers take m different sets of non zero values with a certain damping exponents a.

The FE models of the offshore pylon structure with these dampers are simulated and the system VPLFs under these designs are evaluated from the FE simulation results as shown in Fig.7.38.

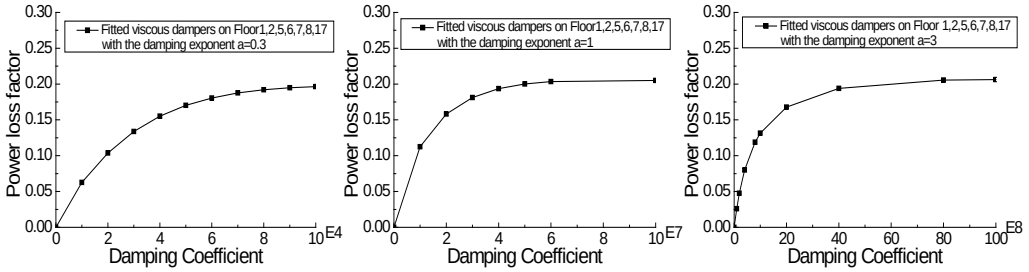

(a) $a = 0.3 < 1$ (b) $a = 1$ (c) $a = 1.5 > 1$

Fig.7.38 VPLFs with different damping coefficients of additional fluid viscous dampers

Using the system VPLFs obtained from the FE simulations in Fig.7.38, where three different types of fluid viscous dampers ($a = 0.2$, 1 and 1.5) are fitted in the structural system, the OFRF based representations for the VPLF of the pylon structure with different types of fluid viscous dampers can be respectively calculated as

$$\begin{aligned}\gamma(C_{0.2}) = {} & (7.1234\text{E-}6)C_{0.2} + (-1.1239\text{E-}10)C_{0.2}^2 \\ & + (9.0707\text{E-}16)C_{0.2}^3 + (-2.994\text{E-}21)C_{0.2}^4\end{aligned} \tag{7.11}$$

$$\begin{aligned}\gamma(C_1) = {} & (1.4331\text{E-}8)C_1 + (-4.0591\text{E-}16)C_1^2 \\ & + (5.0942\text{E-}24)C_1^3 + (-2.2634\text{E-}32)C_1^4\end{aligned} \tag{7.12}$$

$$\begin{aligned}\gamma(C_{1.5}) = {} & (1.8444\text{E-}10)C_{1.5} + (-5.9582\text{E-}20)C_{1.5}^2 \\ & + (7.5766\text{E-}30)C_{1.5}^3 + (-3.2573\text{E-}40)C_{1.5}^4\end{aligned} \tag{7.13}$$

Based on the system VPLF representations in Eqs.(7.11) to (7.13), when the system VPLF $\gamma = 15\%$ is to be achieved, $C_{0.3} = 3.8\text{E}4$, $C_1 = 1.8\text{E}7$, $C_{1.5} = 1.4\text{E}9$ should be designed as the corresponding damping coefficients of different types of fluid viscous dampers. By FE simulations, the displacement vibration responses of the offshore pylon structure with these designed fitted fluid viscous dampers and their FT can be shown in Figs.7.39 and 7.40.

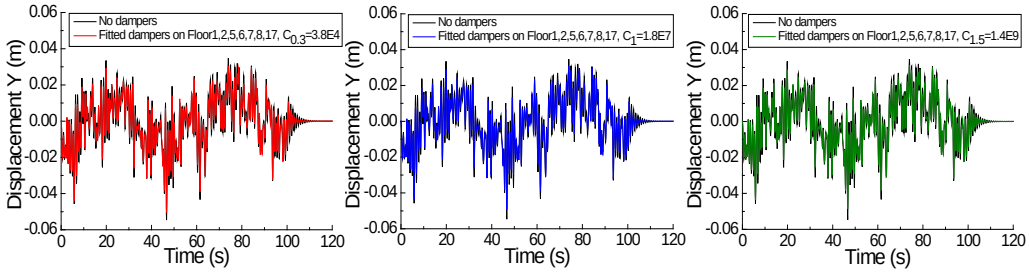

Fig.7.39 Vibration response of the offshore pylon structure with different types of fluid viscous dampers under 20 m/s mean wind speed excitation

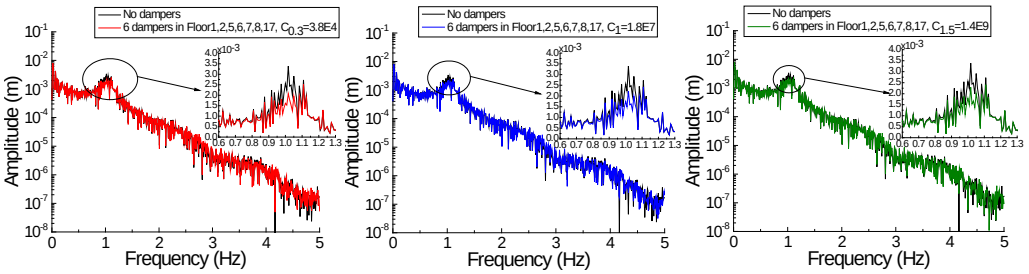

Fig.7.40 FT of the vibration response of the offshore pylon structure with different types of fluid viscous dampers under 20 m/s mean wind speed excitation

However, in the real offshore environment, the wind loading excitations on the structural systems change all the time. The system vibration control designs made in some typical loading conditions should also provide essential safety protection for the systems under some extreme loading excitations. In order to study the effects of different types of fluid viscous dampers on the vibration response of the pylon structure in different mean wind speed conditions, the system displacement vibration responses with the above additional fluid viscous dampers designs are evaluated from the FE simulation results in 10 m/s, 20 m/s and 40 m/s mean wind speed conditions. The results are listed in Table.7.2.

Table.7.2 VPLFs of the offshore pylon structure with different types of fluid viscous dampers under different mean wind speed conditions

Damping parameters	10 m/s mean wind speed	20 m/s mean wind speed	40 m/s mean wind speed
$a = 0.3$, $C_a = 3.8\mathrm{E}4$	20.04%	15%	8.16%

$a=1,\ C_a=1.8\mathrm{E}7$	15.15%	15%	15.07%
$a=1.5,\ C_a=1.4\mathrm{E}9$	11.23%	15%	18.14%

The results in Table.7.2 show that, in comparison with what can be achieved by the equivalent linear fluid viscous dampers design, nonlinear fluid viscous dampers with the damping exponent $a=0.3<1$ ($a=1.5>1$) can dissipate more vibration energy to protect the structural systems under milder (severer) loading exercitations.

The above results confirm the effectiveness of the application of the OFRF and VPLF concept in additional fluid viscous dampers design of more complicated offshore engineering systems described by FE models under general loading excitations. These results extend the application of the OFRF and VPLF concept to more complicated structural systems, and have significance for the practical engineering system design in a wide range of applications.

7.5 Conclusions

In this chapter, using the FE models of multi-storey building structures under harmonic excitations and the FE model of an offshore pylon structure under wind loading excitations, the effects of additional fluid viscous dampers on the suppression of vibration responses of complicated structural systems are studied. The additional fluid viscous dampers designs are achieved based on the OFRF and VPLF concepts. These results reveal that

1) The OFRF and VPLF concepts are confirmed to be effective for the analysis and design of more complicated engineering systems described by FE models. The OFRF concept can be used to directly evaluate the vibration transmissibility of these structural systems under harmonic excitations, and the VPLF concept

can be used to evaluate and design the vibration control effects of additional fluid viscous dampers on the vibration responses of complicated structural systems under general loading excitations.

2) In the vibration control design for complicated engineering systems, the additional fluid viscous dampers should be installed at proper locations in the structural systems and the damping characteristic parameters should be properly designed based on the considered loading conditions.

These results extend the applications of OFRF and VPLF concepts to more complicated structural systems and have significant implications for the analysis and design of vibration systems in a wide range of practical applications.

Chapter 8

Conclusions

Vibration control has significant implications for the safety and reliability of modern mechanical and civil engineering structural systems, especially in extreme loading conditions. In order to achieve desired structural vibration control performance, the linear frequency domain analysis and design methods have been widely studied and applied in engineering practice. The frequency domain approaches have provided intuitive and physically meaningful insights into the structural systems' dynamic behaviors and provided important theoretical foundation for the linear system design for vibration control purpose. However, these effective analysis and design approaches can not be easily extended to the nonlinear case. Conventional nonlinear system frequency analysis and design approaches often involve complicated mathematical computations and symbolic operations, and are therefore difficult to be applied in engineering practice.

This thesis has provided a comprehensive review of typical damping devices that have been widely applied in engineering practice, and introduced conventional nonlinear frequency domain analysis and design approaches. Then new analysis method and design procedure have been proposed to facilitate the study and design of SDOF viscously damped vibration systems subject to harmonic excitations. After that, based on the OFRF concept proposed at Sheffield, a frequency domain analysis and design approach has been developed to investigate the effects of nonlinear damping characteristic parameters on the transmissibility of MDOF viscously damped vibration systems subject to harmonic loading excitations and to design the parameters for a desired system vibration performance. Moreover, the new concept of VPLF has been proposed

to evaluate the vibration performance of MDOF systems subject to general loading excitations. This enables the derivation of the OFRF representation of the VPLF, which allows the design of the characteristic parameters of additional nonlinear viscous damping devices in MDOF structural systems to be readily achieved in general loading conditions. Finally, the proposed OFRF and VPLF based approaches have been applied to the analysis and design of additional viscous damping devices in more complex structural systems which are described by FE models to verify the performance of the analysis and design in more complicated situations.

The results in this thesis have demonstrated that appropriately designed nonlinear damping devices can achieve better vibration performance than linear damping devices. The proposed nonlinear frequency domain analysis and design approaches can be used to significantly facilitate the analysis of the behaviours of nonlinear viscously damped structural systems and the design of damping characteristic parameters in a wide range of practical applications.

8.1 Main Contributions of this thesis

The work in this thesis involves the development of significant nonlinear frequency domain analysis and design approaches for nonlinear viscously damped structural systems that can be represented by SDOF, MDOF and FE models and are subject to either harmonic or general loading excitations. The studies reveal the potential and demonstrate the significance of the application nonlinear damping devices in the vibration control of engineering structural systems. The main contributions of this thesis can be summarized as follows.

(1) Analysis and design of SDOF viscously damped vibration systems subject to harmonic excitations

Based on the Ritz-Galerkin method, a new method for the evaluation of the transmissibility of nonlinear SDOF viscously damped vibration systems under general harmonic excitations has been derived. The effects of damping characteristic parameters on the system transmissibility have been investigated. A three-step nonlinear damping system design procedure has been proposed to facilitate the viscous damping parameters design for a desired system vibration performance. The results reveal the potential of nonlinear viscous damping in the vibration control of SDOF viscously damped vibration systems subject to harmonic excitations, and provide important guidelines for the selection of the types and the design of the parameters of viscous damping devices in engineering practice.

(2) The OFRF based analysis and design of MDOF viscously damped vibration systems subject to harmonic excitations

The OFRF concept recently proposed at Sheffield has been applied to the analysis and design of viscously damped vibration systems which can be described by the anti-symmetric nonlinear differential equation model. The explicit analytical OFRF expression for the relationship between the system output frequency response and both the nonlinear viscous damping coefficient and exponent has been derived. Based on the OFRF representation, a frequency domain analysis and design approach has been developed to study the impact of additional nonlinear viscous damping devices on the vibration behaviours of MDOF viscously damped vibration systems subject to harmonic excitations. A four-step procedure is then proposed to facilitate the damping characteristic parameters design for a desired system vibration performance. The results have considerable significance for the analysis and design of nonlinear damping devices in a wide class of structural systems.

(3) Design of nonlinear damping devices for MDOF structural systems subject

to general loading excitations

In order to evaluate the effects of additional viscous damping devices on the vibration control of structural systems subjected to general loading excitations, a new concept called VPLF has been proposed. A novel OFRF and VPLF based approach for additional viscous damping design has then been proposed to achieve desired vibration performance in MDOF structural systems subject to general loading excitations. Numerical simulation studies on a MDOF civil building structure subject to seismic and wind loading excitations have demonstrated the effectiveness of the OFRF and VPLF based approach for nonlinear damping devices design. The results reveal the advantages of different types of viscous damping devices in the vibration control of structural systems and have significant implications for the design of the damping devices for the vibration control of MDOF structural systems under different loading excitations.

(4) Design of nonlinear damping devices for structural systems described by FE models and subject to harmonic and general loading excitations

The OFRF and VPLF based design approach has been applied to the design of additional viscous damping devices for the vibration control of structural systems, which are so complicated that FE models are used for the system description. The effects of damping characteristic parameters on the output frequency responses of these structural systems under harmonic and general loading excitations have been investigated. The results verify the effectiveness of the application of the proposed approaches to the design of additional fluid viscous dampers for the vibration control in more complicated structural systems.

8.2 Suggestions for further research

Although, in the present study, significant work has been done and many results have been achieved in the analysis of nonlinearly damped structural systems and in the design of the nonlinear damping devices, there are still many further issues yet to be addressed. These issues mainly involve the extension of the SODF system based evaluation approach to the MDOF systems, dealing with more complicated loading conditions, and experimental studies, which are discussed in more detail as follows.

(1) Although only the theoretical evaluation and design methods of SDOF viscously damped vibration systems subject to harmonic excitations are considered in Chapter 4, the principle of the Ritz-Galerkin method based evaluation and analysis approach can be applied to the analysis and design of MDOF and more complicated engineering systems. The related results can provide important guidelines and significant theoretical foundations for the analysis and design of the vibration control of MDOF structural systems. In order to extend the Ritz-Galerkin method based analysis and design approach to complicated structural systems, the issue of more involved mathematical computations needs be addressed.

(2) As mentioned in Chapter 5, one important issue with the OFRF concept is still to be further studied about how to determine the highest order used for the Volterra series representation of a nonlinear system’s output. Larger values of the order can produce more accurate results but the involved computation will be more complicated and more simulation or experimental data are needed. Moreover, for wider practical applications, the OFRF concept should be applied to more complicated nonlinear systems. In these cases, following the ideas in [114], different OFRF based representations need to be derived to reveal the link

between the system vibration responses and design parameters.

(3) By using the OFRF and VPLF based approach, the design of additional viscous damping devices can be achieved based on a considered loading excitation. But the real loading excitations are more complicated and may be stronger or weaker than the considered loading or even changing with time. A more comprehensive additional damping devices design methodology is still to be developed to address these challenges. Potential solutions to this issue could be to use the fully active damping devices, semi-active damping devices or combine the strengths of different types of nonlinear damping devices in the design to achieve an overall satisfactory vibration performance.

(4) Experimental tests need to be conducted to physically verify the effectiveness of the OFRF and VPLF based nonlinear frequency domain analysis and design approaches in the applications to practical mechanical and civil engineering systems.

The future work involves the further development of the nonlinear damping design methodologies. Different loading excitations will need to be collected from practical engineering systems and considered in the designs. Theoretical analysis, numerical simulation studies, and experimental tests will be conducted for the investigations. The final objective is to provide a more comprehensive nonlinear damping design approach for the vibration control of practical mechanical and civil engineering systems.

References

1. F. Sakai, S. Takaeda, and T. Tamaki. *Tuned liquid column damper-new type device for suppression of building vibrations.* Proceedings of International Conference on High-rise Buildings. 1989: 926-931.
2. X.J. Jing, Z.Q. Lang, S.A. Billings, and G.R. Tomlinson. *Frequency domain analysis for suppression of output vibration from periodic disturbance using nonlinearities.* Journal of Sound and Vibration. 2008. 314(3-5): 536-557.
3. D.P. Atherton. *Nonlinear control engineering.* Van Nostrand Reinhold Co., London & New York. 1975.
4. M. Krstic, P.V. Kokotovic, and I. Kanellakopoulos. *Nonlinear and adaptive control design.* John Wiley & Sons, Inc. 1995.
5. R.A. Ibrahim. *Recent advances in nonlinear passive vibration isolators.* Journal of Sound and Vibration. 2008. 314(3-5): 371-452.
6. S. Dyke, B.F. SpencerJr, M.K. Sain, and J.D. Carlson. *Modeling and control of magnetorheological dampers for seismic response reduction.* Smart Materials and Structures. 1996. 5(5): 565-575.
7. T. Haskett, B. Breukelman, J. Robinson, and J. Kottelenberg. *Tuned mass dampers under excessive structural excitation.* Report of the Motioneering Inc.
8. P.A. Irwin and B. Breukelman. *Recent applications of damping systems for wind response.* Proceedings of the Council on Tall Buildings and Urban Habitat World Congress, Melbourne, Australia. 2001: 645-655.
9. D. Lee and D.P. Taylor. *Viscous damper development and future trends.* The Structural Design of Tall Buildings. 2001. 10(5): 311-320.
10. R.J. McNamara, D.P. Taylor, and P. Duflot. *Fluid viscous dampers to reduce wind-induced vibrations in tall buildings.* Taylor Devices Inc., Technical Report. 2005.
11. D.P. Taylor and P. Duflot. *Fluid viscous dampers used for seismic energy dissipation in structures.* Taylor Devices Inc. Report. 2005.
12. A. Occhiuzzi. *Additional viscous dampers for civil structures: Analysis of design methods based on effective evaluation of modal damping ratios.* Engineering Structures. 2009. 31(5): 1093-1101.
13. S.H. Strogatz. *Nonlinear dynamics and chaos: With applications to physics, biology, chemistry, and engineering.* Westview Press. 1994.
14. J.S. Hwang and Y.S. Tseng. *Design formulations for supplemental viscous dampers to highway bridges.* Earthquake Engineering & Structural Dynamics. 2005. 34(13): 1627-1642.
15. H.K. Khalil and J.W. Grizzle. *Nonlinear systems.* Prentice-Hall Inc. 2002.
16. X.F. Wu. *Signal processing of nonlinear systems in the frequency domain.* University of Sheffield. PhD Dissertation. 2008.
17. C.E. Crede. *Vibration and shock isolation.* John Wiley, New York. 1951.
18. L.O. Chua and C.Y. Ng. *Frequency domain analysis of nonlinear systems: general theory.* IEE Journal on Electronic Circuits and Systems. 1979. 3(4): 165-185.

19. B.C. Kuo. *Automatic control systems.* Prentice Hall PTR Upper Saddle River, NJ, USA. 1981.
20. J.I. Soliman and E. Ismailzadeh. *Optimization of unidirectional viscous damped vibration isolation system.* Journal of Sound and Vibration. 1974. 36(4): 527-539.
21. C.T. Chen. *Linear system theory and design.* Oxford University Press, Inc. USA. 1998.
22. A.J. Krener and A. Isidori. *Linearization by output injection and nonlinear observers.* Systems & Control Letters. 1983. 3(1): 47-52.
23. D. Heeger. *Signals, linear Systems, and convolution.* Citeseer. 2000.
24. Z.Q. Lang, S.A. Billings, R. Yue, and J. Li. *Output frequency response function of nonlinear Volterra systems.* Automatica. 2007. 43(5): 805-816.
25. J.C. Snowdon. *Vibration isolation: use and characterization.* Journal of the Acoustical Society of America. 1979. 66: 1245-1279.
26. H.G. Lee, A. Arapostathis, and S.I. Marcus. *Linearization of discrete time nonlinear systems.* American Control Conference. 1987: 857-862.
27. J.M.T. Thompson and H.B. Stewart. *Nonlinear dynamics and chaos.* John Wiley & Sons Inc. 2002.
28. J. Guckenheimer and P. Holmes. *Nonlinear oscillations, dynamical systems and bifurcations of vector fields.* Springer. 1983.
29. X.J. Jing, Z.Q. Lang, and S.A. Billings. *Parametric characteristic analysis for generalized frequency response functions of nonlinear systems.* IEEE Transactions on Circuits and Systems. 2009. 28(5): 699-733.
30. X.J. Jing, Z.Q. Lang, and S.A. Billings. *Output frequency properties of nonlinear systems.* International Journal of Non-Linear Mechanics. 2010. 45(7): 681-690.
31. G. Duffing. *Forced oscillations in the presence of variable Eigen-Frequencies.* Vieweg, Braunshcweig. 1918.
32. B. Van Der Pol. *Forced oscillations in a circuit with non-linear resistance.* The London, Edinburgh, and Dublin Philosophical Magazine and Journal of Science. 1927. 3(13): 65-80.
33. B. Ravindra and A.K. Mallik. *Performance of nonlinear vibration isolators under harmonic excitation.* Journal of Sound and Vibration. 1994. 170(3): 325-337.
34. A.H. Nayfeh and D.T. Mook. *Nonlinear oscillations.* Wiley. 1995.
35. X.J. Jing, Z.Q. Lang, and S.A. Billings. *Mapping from parametric characteristics to generalized frequency response functions of non-linear systems.* International Journal of Control. 2008. 81(7): 1071-1088.
36. Z.Q. Lang and S.A. Billings. *Output frequency characteristics of nonlinear systems.* International Journal of Control. 1996. 64(6): 1049-1067.
37. N. Kryloff and N. Bogolyubov. *Introduction to non-linear mechanics.* Princeton University Press. 1947.
38. L.M. Delves and J.L. Mohamed. *Computational methods for integral equations.* Cambridge University Press. 1988.
39. M. Nakhla and J. Vlach. *A piecewise harmonic balance technique for determination of periodic response of nonlinear systems.* IEEE Transactions on Circuits and Systems. 1976. 23(2): 85-91.
40. D.A. George. *Continuous nonlinear systems.* MIT Research Laboratory of Electronics,

Technical Report 335. 1959.

41. X.J. Jing. *Frequency domain theory of nonlinear Volterra systems based on parametric characteristic analysis.* University of Sheffield. Phd Dissertation. 2008.
42. Z.Q. Lang and S.A. Billings. *Output frequencies of nonlinear systems.* International Journal of Control. 1997. 67(5): 713-730.
43. Z.K. Peng and Z.Q. Lang. *The effects of nonlinearity on the output frequency response of a passive engine mount.* Journal of Sound and Vibration. 2008. 318(1-2): 313-328.
44. S. Boyd and L. Chua. *Fading memory and the problem of approximating nonlinear operators with Volterra series.* IEEE Transactions on Circuits and Systems. 1985. 32(11): 1150-1161.
45. G.Q. Shen, H. Chen, Y.Q. Wang, and Y.J. Shi. *Analysis of viscous damper in high-rise steel structure on anti-seismic and wind resistance performance.* Journal of China University of Mining & Technology. 2007. 36(2).
46. J.S. Hwang. *Seismic design of structures with viscous dampers.* International Training Programs for Seismic Design of Building Structures. 2002.
47. Z.Q. Lang, X.J. Jing, S.A. Billings, G.R. Tomlinson, and Z.K. Peng. *Theoretical study of the effects of nonlinear viscous damping on vibration isolation of sdof systems.* Journal of Sound and Vibration. 2009. 323(1-2): 352-365.
48. C. Spelta, F. Previdi, S.M. Savaresi, G. Fraternale, and N. Gaudiano. *Control of magnetorheological dampers for vibration reduction in a washing machine.* Mechatronics. 2009. 19(3): 410-421.
49. W. Thomson. *Theory of vibration with applications.* Taylor & Francis. 2004.
50. J.E. Ruzicka. *Influence of damping in vibration isolation.* The Shock and Vibration Information Center. 1971.
51. C.W. De Silva. *Vibration damping, control, and design.* CRC Press. 2007.
52. J. Tao and C.M. Mak. *Effect of viscous damping on power transmissibility for the vibration isolation of building services equipment.* Applied Acoustics. 2006. 67(8): 733-742.
53. M.M. Haque, A.K.W. Ahmed, and S. Sankar. *Simulation of displacement sensitive non-linear dampers via integral formulation of damping force characterization.* Journal of Sound and Vibration. 1995. 187(1): 95-109.
54. P. Kytka, C. Ehmann, and R. Nordmann. *Active vibration damping of a flexible structure in hydrostatic bearings.*
55. Y.H. Lim, V.V. Varadan, and V.K. Varadan. *Closed loop finite element modeling of active structural damping in the frequency domain.* Smart Materials and Structures. 1997. 6: 161-168.
56. F. Ricciardelli, A.D. Pizzimenti, and M. Mattei. *Passive and active mass damper control of the response of tall buildings to wind gustiness.* Engineering Structures. 2003. 25(9): 1199-1209.
57. Y. Ribakov, J. Gluck, and A.M. Reinhorn. *Active viscous damping system for control of MDOF structures.* Earthquake Engineering & Structural Dynamics. 2001. 30(2): 195-212.
58. L. Su, G. Ahmadi, and I.G. Tadjbakhsh. *Comparative study of base isolation systems.* Journal of Engineering Mechanics. 1989. 115: 1976.

59. A. Abrishambaf and G. Ozay. *Effects of isolation damping and stiffness on the seismic behaviour of structures.* World Scientific and Engineering Academy and Society (WSEAS). 2010: 76-81.
60. H.C. Kwon, M.C. Kim, and I.W. Lee. *Vibration control of bridges under moving loads.* Computers & Structures. 1998. 66(4): 473-480.
61. C.S. Cai, W.J. Wu, and X.M. Shi. *Cable vibration reduction with a hung-on TMD system. part I: theoretical study.* Journal of Vibration and Control. 2006. 12(7): 801-814.
62. H.H. Lee, S.H. Wong, and R.S. Lee. *Response mitigation on the offshore floating platform system with tuned liquid column damper.* Ocean Engineering. 2006. 33(8-9): 1118-1142.
63. H. Kim and H. Adeli. *Wind-induced motion control of 76-story benchmark building using the hybrid damper-TLCD system.* Journal of Structural Engineering. 2005. 131: 1794-1802.
64. E. Suhir. *Dynamic response of a one-degree-of-freedom linear system to a shock load during drop tests: effect of viscous damping.* IEEE Transactions on Components, Packaging, and Manufacturing Technology. 1996. 19(3): 435-440.
65. M.D. Symans and M.C. Constantinou. *Passive fluid viscous damping systems for seismic energy dissipation.* Journal of Earthquake Technology. 1998. 35(4): 185-206.
66. N. Makris and S.P. Chang. *Effect of viscous, viscoplastic and friction damping on the response of seismic isolated structures.* Earthquake Engineering & Structural Dynamics. 2000. 29(1): 85-107.
67. B.C. Nakra. *Vibration control in machines and structures using viscoelastic damping.* Journal of Sound and Vibration. 1998. 211(3): 449-465.
68. H.N. Li and G. Li. *Experimental study of structure with "dual function" metallic dampers.* Engineering Structures. 2007. 29(8): 1917-1928.
69. J.M. Kelly. *A seismic base isolation: review and bibliography.* Soil Dynamics and Earthquake Engineering. 1986. 5(4): 202-216.
70. T.E. Kelly. *Base isolation of structures: Design guidelines.* Holmes Consulting Group Ltd. 2001.
71. S.H. Lee, S.S. Woo, S.H. Cho, and L. Chung. *Computation of optimal friction of tuned mass damper for controlling Base-Excited structures.* ICCES. 2008. 8: 115-120.
72. M.P. Singh, S. Singh, and L.M. Moreschi. *Tuned mass dampers for response control of torsional buildings.* Earthquake Engineering & Structural Dynamics. 2002. 31(4): 749-769.
73. S.V. Bakre and R.S. Jangid. *Optimum parameters of tuned mass damper for damped main system.* Structural Control and Health Monitoring. 2007. 14(3): 448-470.
74. P. Irwin, J. Kilpatrick, J. Robinson, and A. Frisque. *Wind and tall buildings: negatives and positives.* The Structural Design of Tall and Special Buildings. 2008. 17(5): 915-928.
75. J.P. Den Hartog. *Mechanical vibrations.* McGraw-Hill Book Company, Inc. 2007.
76. H. Kitamura, T. Fujita, T. Teramoto, and H. Kihara. *Design and analysis of a tower structure with a tuned mass damper.* Proceedings of 9th World Conference on Earthquake Engineering. 1988. 8: 415–20.

77. R. Rana and T.T. Soong. *Parametric study and simplified design of tuned mass dampers.* Engineering Structures. 1998. 20(3): 193-204.
78. Y.Y. Lin, C.M. Cheng, and C.H. Lee. *A tuned mass damper for suppressing the coupled flexural and torsional buffeting response of long-span bridges.* Engineering Structures. 2000. 22(9): 1195-1204.
79. C.L. Lee, Y.T. Chen, L.L. Chung, and Y.P. Wang. *Optimal design theories and applications of tuned mass dampers.* Engineering Structures. 2006. 28(1): 43-53.
80. S. Colwell and B. Basu. *Tuned liquid column dampers in offshore wind turbines for structural control.* Engineering Structures. 2009. 31(2): 358-368.
81. M. Reiterer and F. Ziegler. *Combined seismic activation of a SDOF-building with a passive TLCD attached.* 13th World Conference on Earthquake Engineering. 2004: 1-15.
82. A.J. Wilmink and J.F. Hengeveld. *Application of tuned liquid column dampers in wind turbines.* Proceedings of the European Wind Energy Conference. 2006.
83. S. Colwell and B. Basu. *Experimental and theoretical investigations of equivalent viscous damping of structures with TLCD for different fluids.* Journal of Structural Engineering. 2008: 154-164.
84. A. Teramura and O. Yoshida. *Development of vibration control system using U-shaped water tank.* 11th World Conference on Earthquake Engineering. 1996.
85. J.K. Vandiver and S. Mitome. *Effect of liquid storage tanks on the dynamic response of offshore platforms.* Applied Ocean Research. 1979. 1(2): 67-74.
86. Y.L. Xu and K.C.S. Kwok. *Control of along wind response of structures by mass and liquid dampers.* Journal of Engineering Mechanics. 1992.
87. D.P. Taylor and M.C. Constantinou. *Fluid dampers for applications of seismic energy dissipation and seismic isolation.* 11th World Conference on Earthquake Engineering. 1996.
88. http://www.lusas.com/.
89. http://www.staaleng.com/.
90. B. Ravindra and A.K. Mallik. *Hard Duffing-type vibration isolator with combined Coulomb and viscous damping.* International Journal of Non-Linear Mechanics. 1993. 28(4): 427-440.
91. B. Ravindra and A.K. Mallik. *Performance of non-linear vibration isolators under harmonic excitation.* Journal of Sound and Vibration. 1994. 170(3): 325-337.
92. B. Ravindra and A. Mallik. *Chaotic response of a harmonically excited mass on an isolator with non-linear stiffness and damping characteristics.* Journal of Sound and Vibration. 1995. 182(3): 345-353.
93. D.W. Look. *The seismic retrofit of historic buildings conference workbook.* Western Chapter of the Association for Preservation Technology. 1991.
94. T.T. Soong. *Full-scale Implementation of Viscoelastic Dampers.* 1998.
95. B. Samali and K.C.S. Kwok. *Use of viscoelastic dampers in reducing wind-and earthquake-induced motion of building structures.* Engineering Structures. 1995. 17(9): 639-654.
96. C.S. Tsai and H.H. Lee. *Applications of viscoelastic dampers to high-rise buildings.* Journal of structural engineering. 1993. 119(4): 1222-1233.

97. K.C. Chang, T.T. Soong, S.T. Oh, and M.L. Lai. *Seismic behavior of steel frame with added viscoelastic dampers.* Journal of Structural Engineering. 1995. 121: 1418-1426.

98. S.M.S. Alehashem, A. Keyhani, and H. Pourmohammad. *Behavior and performance of structures equipped with ADAS & TADAS dampers (a comparison with conventional structures).* The 14th World Conference on Earthquake Engineering. 2008.

99. T.T. Soong and G.F. Dargush. *Passive energy dissipation systems in structural engineering.* John Wiley & Sons, England. 1997.

100. J.M. Kelly, R.I. Skinner, and A.J. Heine. *Mechanisms of energy absorption in special devices for use in earthquake resistant structures.* Bulletin of N.Z. Society for Earthquake Engineering. 1972. 5: 63-88.

101. S.F. Stiemer, W.G. Godden, and J.M. Kelly. *Experimental behavior of a spatial piping system with steel energy absorbers subjected to a simulated differential seismic input.* Earthquake Engineering Research Center, University of California. 1981.

102. G. Chen and S.A. Eads. *Behavior and fatigue properties of metallic dampers for seismic retrofit of highway bridges.* Missouri Department of Transportation. 2005.

103. T.T. Soong and M.C. Costantinou. *Passive and active structural vibration control in civil engineering.* Springer. 1994.

104. M.C. Constantinou, P. Tsopelas, W. Hammel, and A.N. Sigaher. *Toggle-brace-damper seismic energy dissipation systems.* Journal of structural engineering. 2001. 127: 105.

105. H.B. Yun, F. Tasbighoo, S.F. Masri, J.P. Caffrey, R.W. Wolfe, N. Makris, and C. Black. *Comparison of modeling approaches for full-scale nonlinear viscous dampers.* Journal of Vibration and Control. 2008. 14(1-2): 51-76.

106. S. Infanti and M.G. Castellano. *Rion antirion bridge; design and full–scale testing of the seismic protection devices.* 13th World Conference on Earthquake Engineering. 2004.

107. R.J. McNamara, C.D. Huang, and V. Wan. *Viscous-Damper with motion amplification device for high rise building applications.* ASCE Structures Congress 2000. 2000.

108. *International application No.: PCT/US2008/053062.*

109. D. Karnopp. *Active and semi-active vibration isolation.* Journal of Mechanical Design. 1995: 177-185.

110. N. Jalili. *A comparative study and analysis of semi-active vibration-control systems.* Journal of Vibration and Acoustics. 2002. 124(4): 593-605.

111. P. Yang, J.M. Yang, and J.N. Ding. *Dynamic transmissibility of a complex nonlinear coupling isolator.* Tsinghua Science & Technology. 2006. 11(5): 538-542.

112. D.P. Mario, L. La Mendola, and G. Navarra. *Stochastic seismic analysis of structures with nonlinear viscous dampers.* Journal of Structural Engineering. 2007. 133: 1475-1478.

113. Z.K. Peng, Z.Q. Lang, X.J. Jing, S.A. Billings, G.R. Tomlinson, and L.Z. Guo. *The transmissibility of vibration isolators with a nonlinear antisymmetric damping characteristic.* Journal of Vibration and Acoustics. 2010. 132: 014501.

114. H. Laalej and Z.Q. Lang. *Numerical investigation of the effects of MR damper characteristic parameters on vibration isolation of SDOF systems under harmonic excitations.* Journal of Intelligent Material Systems and Structures. 2010. 21(5): 483-501.

115. L.R. Rabiner and B. Gold. *Theory and application of digital signal processing.* Englewood Cliffs, NJ, Prentice-Hall, Inc. 1975. 1.
116. B.P. Latni. *Signal processing and linear systems.* Berkeley Cambridge Press. 1998.
117. S.K. Mitra and Y. Kuo. *Digital signal processing: a computer-based approach.* McGraw-Hill College. 2001. 128.
118. M. Bellanger. *Digital processing of signals: theory and practice.* New York, Wiley-Interscience. 1984.
119. M. Schetzen. *The Volterra and Wiener theories of nonlinear systems.* John Wiley & Sons, Inc. 1980.
120. K. Worden and G.R. Tomlinson. *Nonlinearity in structural dynamics: detection, identification, and modelling.* Institute of Physics Publishing. 2001.
121. W.J. Liu and D.J. Ewins. *Transmissibility properties of MDOF systems.* Proceedings of the 16th IMAC. 1998. 2: 847-854.
122. N.M.M. Maia, J.M.M. Silva, and A.M.R. Ribeiro. *The transmissibility concept in multi-degree-of-freedom systems.* Mechanical Systems and Signal Processing. 2001. 15(1): 129-137.
123. G.E. Carlson. *Signal and linear system analysis.* John Wiley & Sons Ltd, England. 1998.
124. W.J. Rugh. *Nonlinear system theory: the Volterra/Wiener approach.* Johns Hopkings University Press. 1981.
125. A. Lapedes and R. Farber. *Nonlinear signal processing using neural networks: Prediction and system modelling.* Los Alamos National Laboratory, Technical Report. 1987.
126. O. Nelles. *Nonlinear system identification.* Springer. 2001.
127. A. Milanese. *Volterra series revisited, with applications in nonlinear structural dynamics and aeroelasticity.* Clarkson University, PhD Dissertation. 2009.
128. V. Volterra. *Theory of functionals and of integral and integro-differential equations.* Dover Publications, New York. 1959.
129. J.C. Peyton Jones. *Simplified computation of the Volterra frequency response functions of non-linear systems.* Mechanical Systems and Signal Processing. 2007. 21(3): 1452-1468.
130. S. Narayanan. *Application of Volterra series to intermodulation distortion analysis of transistor feedback amplifiers.* Circuit Theory, IEEE Transactions. 1970: 518 - 527.
131. S.A. Billings and J.C. Peyton Jones. *The interpretation of nonlinear frequency response functions.* International Journal of Control. 1990. 52(2): 319-346.
132. Z.K. Peng, Z.Q. Lang, and S.A. Billings. *Resonances and resonant frequencies for a class of nonlinear systems.* Journal of Sound and Vibration. 2007. 300(3-5): 993-1014.
133. A. Chatterjee. *Identification and parameter estimation of a bilinear oscillator using Volterra series with harmonic probing.* International Journal of Non-Linear Mechanics. 2010. 45(1): 12-20.
134. D. Mirri, G. Luculano, F. Filicori, G. Pasini, G. Vannini, and G. Gabriella. *A modified Volterra series approach for nonlinear dynamic systems modeling.* IEEE Transactions on Circuits and Systems. 2002. 49(8): 1118-1128.
135. F.J. Doyle, R.K. Pearson, and B.A. Ogunnaike. *Identification and control using Volterra*

models. Springer. 2002.

136. F.J. Doyle. *Nonlinear model-based control using second-order Volterra models.* Automatica. 1995. 31(5): 697-714.
137. S.K. Mitra and G.L. Sicuranza. *Nonlinear image processing.* Academic Press. 2001.
138. M. Landau and C.T. Leondes. *Volterra series synthesis of nonlinear stochastic tracking systems.* IEEE Transactions on Aerospace and Electronic Systems. 1975. 2: 245-265.
139. X.J. Jing, Z.Q. Lang, and S.A. Billings. *Output frequency response function-based analysis for nonlinear Volterra systems.* Mechanical Systems and Signal Processing. 2008. 22(1): 102-120.
140. S. Skogestad and I. Postlethwaite. *Multivariable feedback control: analysis and design.* John Wiley, New York. 1996.
141. E. Fridman and M. Gil. *A direct frequency domain approach to stability of linear systems with time-varying delays.* Proceedings of the 13th Mediterranean Conference on Control and Automation. 2005: 1544-1547.
142. A. Rahrooh and S. Shepard. *Identification of nonlinear systems using NARMAX model.* Nonlinear Analysis: Theory, Methods & Applications. 2009. 71(12): 1198-1202.
143. J.C. Peyton Jones and S.A. Billings. *Recursive algorithm for computing the frequency response of a class of non-linear difference equation models.* International Journal of Control. 1989. 50(5): 1925-1940.
144. A.V. Levy and A. Montalvo. *Comparison of multiplier and quasilinearization methods.* Industrial & Engineering Chemistry Process Design and Development. 1975. 14(4): 385-391.
145. J.A. Sanders, F. Verhulst, and J.A. Murdock. *Averaging methods in nonlinear dynamical systems.* Springer. 2007.
146. G.E.O. Giacaglia. *Perturbation methods in non-linear systems.* Springer. 1972.
147. A. Gelb and W.E.V. Velde. *Multiple-Input describing functions and nonlinear system design.* McGraw-Hill Book Co., New York, NY. 1968.
148. J.C. Luke. *A perturbation method for nonlinear dispersive wave problems.* Proceedings of the Royal Society of London. 1966: 403-412.
149. G.N. Jazar, A. Narimani, M.F. Golnaraghi, and D.A. Swanson. *Practical frequency and time optimal design of passive linear vibration isolation mounts.* Vehicle System Dynamics. 2003. 39(6): 437-466.
150. G.N. Jazar, R. Houim, A. Narimani, and M.F. Golnaraghi. *Frequency response and jump avoidance in a nonlinear passive engine mount.* Journal of Vibration and Control. 2006. 12(11): 1205-1237.
151. R.J. Gilmore and M.B. Steer. *Nonlinear circuit analysis using the method of harmonic balance—A review of the art. Part I. Introductory concepts.* International Journal of Microwave and Millimeter Wave Computer Aided Engineering. 1991. 1(1): 22-37.
152. H.G. Brachtendorf, G. Welsch, and R. Laur. *Fast simulation of the steady-state of circuits by the harmonic balance technique.* International Symposium on Circuits and Systems. 1995. 2: 1388-1391.
153. M.R. Belmont. *Generalized frequency response functions for systems with time varying coefficients.* Proceedings of the Institution of Mechanical Engineers. 1994. 208(33): 145-153.

154. B. Zhang, S.A. Billings, Z.Q. Lang, and G.R. Tomlinson. *Analytical description of the frequency response function of the generalized higher order Duffing oscillator model.* IEEE Transactions on Circuits and Systems. 2009. 56(1): 224-232.
155. L.M. Li and S.A. Billings. *Estimation of generalized frequency response functions for quadratically and cubically nonlinear systems.* Journal of Sound and Vibration. 2010. 330: 461-470.
156. A. Suzuki and J.K. Hedrick. *Nonlinear controller design by an inverse random input describing function method.* American Control Conference. 1985: 1236-1241.
157. J. Aracil and F. Gordillo. *Describing function method for stability analysis of PD and PI fuzzy controllers.* Fuzzy Sets and Systems. 2004. 143(2): 233-249.
158. S.N. Chandra, H. Hatwal, and A.K. Mallik. *Response of non-linear dissipative shock isolators.* Journal of Sound and Vibration. 1998. 214(4): 589-603.
159. A. Emadi. *Modeling of power electronic loads in ac distribution systems using the generalized state-space averaging method.* IEEE Transactions on Industrial Electronics. 2004. 51(5): 992-1000.
160. B. Raindra and A.K. Mallik. *Performance of nonlinear vibration isolator under harmonic excitation.* Journal of Sound and Vibration. 1994. 170(3): 325-337.
161. D.E. Adams. *Frequency domain ARX model and multi-harmonic frf estimators for non-linear dynamic systems.* Journal of Sound and Vibration. 2002. 250(5): 935-950.
162. S.W. Nam and E.J. Powers. *Application of higher order spectral analysis to cubically nonlinear system identification.* IEEE Transactions on Signal Processing. 1994. 42(7): 1746-1765.
163. J.S. Tao, G.R. Liu, and K.Y. Lam. *Design optimization of marine engine-mount system.* Journal of Sound and Vibration. 2000. 235(3): 477-494.
164. L.J. Tick. *The estimation of "transfer functions" of quadratic systems.* Technometrics. 1961. 3(4): 563-567.
165. Y.W. Lee and M. Schetzen. *Measurement of the Wiener kernels of a non- linear system by cross-correlation(Wiener kernels of nonlinear system based on cross- correlation techniques).* international Journal of Control. 1965. 2: 237-254.
166. J.S. Bendat. *Nonlinear system analysis and identification from random data.* John Wiley, New York. 1990. 392.
167. E. Bedrosian and S.O. Rice. *The output properties of Volterra systems (nonlinear systems with memory) driven by harmonic and Gaussian inputs.* Proceedings of the IEEE. 1971. 59(12): 1688-1707.
168. S.A. Billings and K.M. Tsang. *Spectral analysis for non-linear systems, Part I: Parametric non-linear spectral analysis.* Mechanical Systems and Signal Processing. 1989. 3(4): 319-339.
169. S.A. Billings and J.C. Peyton Jones. *Mapping non-linear integro-differential equations into the frequency domain.* International Journal of Control. 1990. 52(4): 863-879.
170. A.K. Swain and S.A. Billings. *Generalized frequency response function matrix for MIMO non-linear systems.* International Journal of Control. 2001. 74(8): 829-844.
171. Z.Q. Lang and S.A. Billings. *Energy transfer properties of non-linear systems in the frequency domain.* International Journal of Control. 2005. 78(5): 345-362.
172. A.K. SWain, D.T. Westwick, and E.J. Perreault. *Frequency domain identification of*

Hammerstein systems. Tencon 2009-2009 IEEE Region 10 Conference. 2009.

173. O.M. Boaghe, S.A. Billings, L.M. Li, P.J. Fleming, and J. Liu. *Time and frequency domain identification and analysis of a gas turbine engine.* Control Engineering Practice. 2002. 10(12): 1347-1356.
174. S. Caffery, J. Giacomin, and K. Worden. *A nonlinear model for automotive shock absorbers.* IOTAM Symposium on Identification of Mechanical System. Wuppertal, Germany. 1993.
175. Z.K. Peng, Z.Q. Lang, L. Zhao, S.A. Billings, and G.R. Tomlinson. *The force transmissibility of MDOF structures with a non-linear viscous damping device.* International Journal of Non-Linear Mechanics. 2011. 46: 1305-1314.
176. T.J. Johnson. *Analysis of dynamic transmissibility as a feature for structural damage detection.* Purdue University. Master Dissertation. 2002.
177. Z. Milovanovic, I. Kovacic, and M.J. Brennan. *On the displacement transmissibility of a base excited viscously damped nonlinear vibration isolator.* Journal of Vibration and Acoustics. 2009. 131: 054502.
178. J.C. Snowdon. *Vibration and shock in damped mechanical systems.* J. Wiley. 1968.
179. L.S. Chen, K. Qiu, and D.Y. Chen. *Research on continuous damping control improving force isolation of a SDOF mounting system.* Journal of Intelligent Material Systems and Structures. 2006. 17(4): 347-351.
180. H. Laalej, Z.Q. Lang, S. Daley, I. Zazas, S.A. Billings, and G.R. Tomlinson. *Application of non-linear damping to vibration isolation: an experimental study.* Nonlinear Dynamics. 2011: 1-13.
181. M.H. Stone. *The generalized Weierstrass approximation theorem.* Mathematics Magazine. 1948. 21(5): 237-254.
182. R.J. Allemang. *Vibrations: analytical and experimental modal analysis.* Structural Dynamics Research Laboratory, Department of Mechanical, Industrial and Nuclear Engineering, University of Cincinnati. 1998.
183. M.C. Constantinou, T.T. Soong, and G.F. Dargush. *Passive energy dissipation systems for structural design and retrofit.* Multidisciplinary Center for Earthquake Engineering Research. 1998.
184. S.H. Lee, K.W. Min, J.S. Hwang, and J. Kim. *Evaluation of equivalent damping ratio of a structure with added dampers.* Engineering Structures. 2004. 26(3): 335-346.
185. Parseval-des-Chênes and Marc-Antoine. *Mémoire sur les séries et sur l'intégration complète d'une équation aux différences partielles linéaire du second ordre, à coefficients constants.* Mémoires présentés à l'Institut des Sciences, Lettres et Arts, par divers savants, et lus dans ses assemblées. Sciences, mathématiques et physiques. 1806. 1: 638-648.
186. S. Adhikari. *Damping modelling using generalized proportional damping.* Journal of Sound and Vibration. 2006. 293(1-2): 156-170.
187. *Wind turbine generator systems - part 1: safety requirements international standard 61400-1 (Edition 3).* International Electrotechnical Commission. 2005.
188. T. Burton. *Wind energy handbook.* John Wiley & Sons Ltd, England. 2001.
189. A.G. Davenport. *The spectrum of horizontal gustiness near the ground in high winds.* Quarterly Journal of the Royal Meteorological Society. 1961. 87(372): 194-211.

190. M. Shinozuka and C.M. Jan. *Digital simulation of random processes and its applications.* Journal of Sound and Vibration. 1972. 25(1): 111-128.
191. E. Madenci and I. Guven. *The finite element method and applications in engineering using ANSYS.* Springer. 2006.
192. R.A. De Callafon. *Estimating parameters in a lumped parameter system with first principle modeling and dynamic experiments.* 13th IFAC Symposium on System Identification. 2003: 1613-1618.
193. Z.Q. Wang, S.D. Hu, and L.C. Fan. *Research on viscous damper parameters of Donghai Bridge.* China Journal of Highway and Transport. 2005. 18(3): 37-42.
194. K.T. Chau, C.Y. Shen, and X. Guo. *Nonlinear seismic soil-pile-structure interactions: Shaking table tests and FEM analyses.* Soil Dynamics and Earthquake Engineering. 2009. 29(2): 300-310.
195. M.J. Turner, R.W. Clough, H.C. Martin, and L.J. Topp. *Stiffness and deflection analysis of complex structures.* J. Aero. Sci. 1956. 23(9): 805-823.
196. J.S. Choi, J.S. Lee, and J.M. Kim. *Nonlinear earthquake response analysis of 2-D underground structures with soil-structure interaction including separation and sliding at interface.* 15th ASCE Engineering Mechanics Conference. 2002.
197. H. Karagülle, L. Malgaca, and H.F. Öktem. *Analysis of active vibration control in smart structures by ANSYS.* Smart Materials and Structures. 2004. 13: 661-667.
198. S.M. Khot and N.P. Yelve. *Modeling and response analysis of dynamic systems by using ANSYS© and MATLAB©.* Journal of Vibration and Control. 2010.
199. F.T. Kokkinos and C.C. Spyrakos. *Dynamic analysis of flexible strip-foundations in the frequency domain.* Computers & Structures. 1991. 39(5): 473-482.
200. J. Lee and S. Kim. *Structural damage detection in the frequency domain using neural networks.* Journal of Intelligent Material Systems and Structures. 2007. 18(8): 785-792.
201. *Release 11.0 documentation for ANSYS.* ANSYS, Inc. 2007.
202. Y.C. Liu. *ANSYS and LS-DYNA used for structural analysis.* International Journal of Computer Aided Engineering and Technology. 2008. 1(1): 31-44.
203. A. Carlson. *Energy system analysis of the inclusion of monetary values of environmental damage.* Biomass and Bioenergy. 2002. 22(3): 169-177.
204. G.M. Joselin Herbert, S. Iniyan, E. Sreevalsan, and S. Rajapandian. *A review of wind energy technologies.* Renewable and Sustainable Energy Reviews. 2007. 11(6): 1117-1145.
205. K.T. Fung, R.L. Scheffler, and J. Stolpe. *Wind energy-a utility perspective.* Power Apparatus and Systems, IEEE Transactions on Power Apparatus and Systems. 1981(3): 1176-1182.
206. *http://www.fino3.de.*